Regulatory processes in Aspergillus niger

Poulsen, Lars; Thykær, Jette; Eliasson Lantz, Anna

Publication date:
2012

Document Version
Early version, also known as pre-print

Technical University of Denmark

Regulatory processes in *Aspergillus niger*

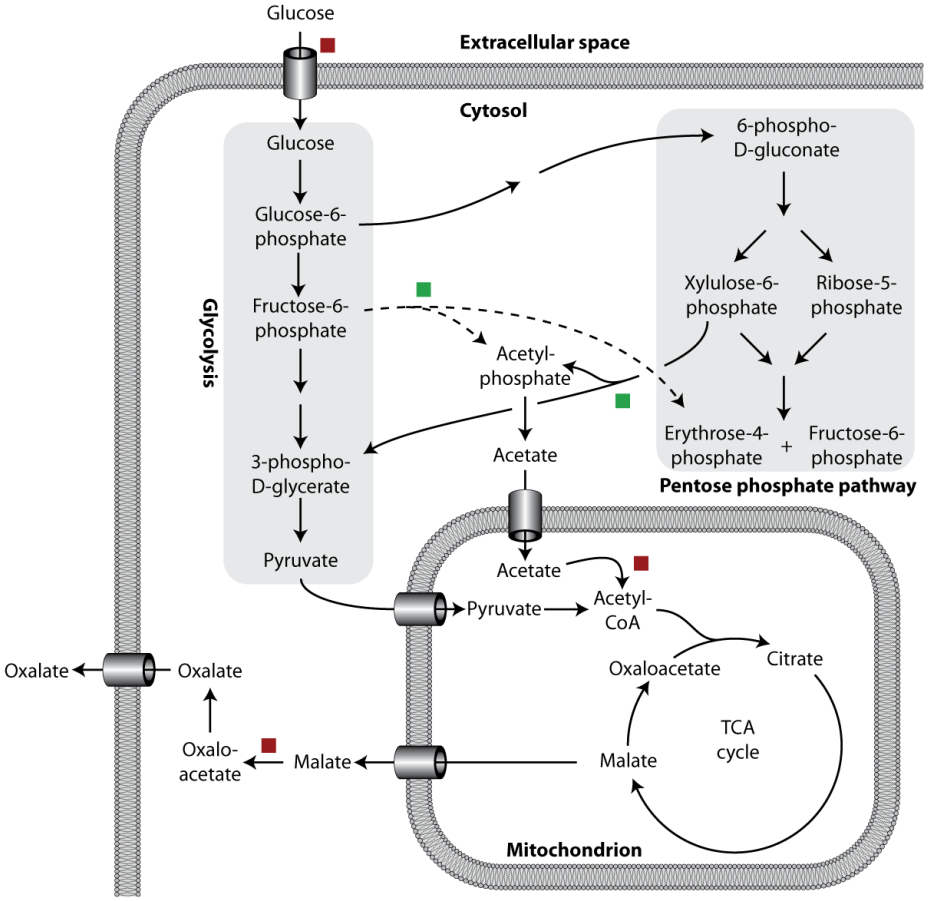

Lars Poulsen

Ph. D. Thesis

October 2012

Center for Microbial Biotechnology
Department of Systems Biology

Regulatory processes in *Aspergillus niger*

Ph. D. Thesis

Lars Poulsen

Department of Systems Biology

Technical university of university of Denmark

Supervisors

Assoc. Prof. Jette Thykær

Assoc. Prof. Anna E. Lantz

“The first step towards getting somewhere is to decide that you are not going to stay where you are.”

- John Pierpont Morgan

Summary

Filamentous fungi are extensively used in the fermentation industry for synthesis of numerous products. One of the most important, is the fungus *Aspergillus niger*, used industrially for production of organic acids, and homologous as well as heterologous enzymes. This fungus has numerous of advantages, including tolerance for low pH, which is important for acid production. Furthermore, it has the capability of metabolizing a wide variety of carbon sources, possesses an exceptional efficient protein secretion capacity, and three genome sequences are publicly available. However, *A. niger* have some disadvantages as well, those are byproduct formation, secretion of proteolytic enzymes and formation of mycotoxins. The aim of this project was to reduce these disadvantages, though investigating the regulatory processes.

The first objective was to study the regulatory events leading to *A. niger's* citric acid overflow metabolism. This was done with analysis of both transcriptome and proteome profiles, from cultivations in manganese limitation and manganese excess conditions. Beside already described responses, that were used to verify the experimental setup, identification of novel events was done. The most interesting was the strong down regulation of phosphoenolpyruvate carboxykinase (PEPCK) at manganese limited conditions that could be one of the main initiators for the citrate overflow metabolism.

To gain further insight into *A. niger's* metabolism, a new metabolic engineering tool, termed transcription factor modulation was developed. Using this approach, two novel mutants were isolated and formed the basis for the following studies.

Through knock out studies of putative trans-acting pH responding transcription factors, a mutant exhibiting an oxalate overproducing phenotype was identified and entitled Oxalic Acid repression Factor, OafA. This mutant was physiological characterized in details, using continues cultivation (chemostats), followed by transcriptional analysis. Two phosphoketolases were found to be down-regulated in the *ΔoafA* mutant and it was argued, that this was the main cause, for the increase oxalate formation.

From similar knock out studies, another mutant was identified and this strain was shown to be a protease mutant and the responsible transcription factor was entitled Protease Regulator B, PrtB. This was compared against the already described, protease deficient strain, *ΔprtT*. The physiological batch characterization showed that the *ΔprtT* strain had the lowest protease activity (fivefold reduced), but also featured excessive CO_2 yield, reduced growth rate and lower biomass yields. The *ΔprtB* strain had a close to twofold reduced levels of secreted proteases but with additional beneficial characteristics, as a lower oxalic

acid formation and wild type growth performance; it was therefore argued that this strain could be an attractive alternative to *ΔprtT*.

Finally, in order to characterize the formation of the carcinogenic mycotoxin fumonisin, a reporter strain of *A. niger* was constructed, where the promoter from the fumonisin synthase was fused to the green fluorescent protein. This strain was used together with the commercial large-scale nutrient profiling platform, Biolog Phenotype MicroArrays. Out of the 476 conditions tested, six compounds significantly induce fumonisin production, identified. These formed the basis for the subsequent examinations, which resulted in the identification of azelaic acid, a plant hormone and a very potent fumonisin inducer.

Dansk Resumé

Skimmelsvampe anvendes i stort omfang i fermenteringindustrien, til at producere en række forskellige produkter. En af de vigtigste er svampen *Aspergillus niger*, som anvendes til industriel produktion af organiske syrer og homologe samt heterologe proteiner. Denne svamp har en række fordele, heriblandt tolerance for lav pH, hvilket er vigtigt når den anvendes til produktion af organiske syrer. Ydermere, kan den metabolisere en bred vifte af kulstofsklider, udskille proteiner i store mængder samt der er tre offentlig tilgænglige genom sekvenser. Men *A. niger* har også ulemper, heribland dannelse af biprodukter, udskillelse af proteolytiske enzymer og dannelse af mykotoxiner. Målet med dette projekt er at reducere disse ulemper, via studier af de regulatoriske processer.

Det første mål var at undersøge de regulatoriske hændelser der forårsager citron syre overflow i *A. niger's* metabolisme. Dette blev udført via analyser af både transkriptom- og proteomprofiler, fra mangan begrænsede og mangan overskuds kultiveringer. Udover identifikation af allerede beskrevne processer, som blev anvendt til at verifice den eksperimentelle setup, blev nye og ukendte respons også identificeret. Det mest interessante af disse var en kraftige nedregulering af phosphoenolpyruvate carboxykinase (PEPCK) i de mangan begrænsede kulturer, som kunne være en af de primære igangsættere af citronsyre produktionen.

For at få en udvidet forståelse af *A. niger's* metabolisme, blev et nyt "metabolic engineering" værktøj udviklet, betegnet transkriptionsfaktor modulering. Med anvendelse af denne fremgangsmåde, blev to nye mutanter identificeret og disse dannede grundlaget for de efterfølgende undersøgelser.

Med "knock out" studier af formodet trans bindende pH reagerende transkriptionsfaktore, blev en transkriptionsmutant, der udviste en oxalsyre overproducerende fænotype, identificeret og efterfølgende navngivet Oxalic Acid repression Factor, OafA. Denne mutant blev fysiologisk karakteriseret vha. Kontinuerte gæringer (kemostater), efterfulgt af transkriptionsanalyse. To phophoketolaser blev fundet opreguleret i *ΔoafA* mutanten og derfor ansås dette respons at være den primære årsag, for den forøgede oxalsyre produktion.

Fra lignende "knock out" studier, blev en yderligere mutant identificeret og denne viste sig at være en protease deficient mutant. Den ansvarlige transkriptionsfaktor blev navngivet Protease Regulator B, PrtB. Denne blev sammenlignet med en allerede beskrevet protease deficient stamme, *ΔprtT*. Fysiologiske batch karakteriseringer, viste at *ΔprtT* stammen, havde den laveste protease aktivitet (femfold reduceret), men udviste også en forøget CO_2 produktion, reduceret vækst rate samt lavere biomasse udbytte. *ΔprtB*

stammens protease aktivitet var reduceret tofold, i forhold til vildtypen men udtrykte ydereligere fordelagtige karakteristika, så som lavere oxalsyre produktion samt vækst på vildtype niveau. Det blev derfor argumenteret for at denne stamme kunne være et attraktivt alternativ til *ΔprtT*.

Endeligt, for at karakterisere dannelsen af det kræftfremkaldende mykotoxin fumonisin, blev en rapportørstamme af *A. niger* konstrueret, hvor promotoren fra fumonisinsyntasen var fusioneret med det grønne fluorescerende protein. Denne stamme blev anvendt sammen med den kommercielle stor skala platform, "Biolog Phenotype MicroArrays". Ud af de 476 forhold undersøgt, fandtes seks stoffer der signifikant inducerer fumonisin produktionen. Disse dannede grundlaget for de efterfølgende undersøgelser, som resulterede i opdagelsen af azelaic syre, et plantehormer og en yderst potent fumonisin inducer.

Preface

The work presented in this thesis was performed between October 2009 and October 2012 at the Center for Microbial Biotechnology, Department of Systems Biology, Technical university of Denmark (DTU). The PhD study was a part of CMB's IVC (Ingeniør-Videnskabelige centre) supported by the Danish Resarch Council for Technology and Production. The work was supervised by associate professor Jette Thykær and associate professor Anna E. Lantz.

I wish to express my sincere gratitude to my supervisor Jette Thykær, I am thankful for the excellent supervision, guidance and daily scientific support. I will also like to thank Anna E. Lantz, my co-supervisor, for giving me the opportunity to carry out my Ph.D study at CMB and for her support and for the valuable scientific discussions.

Through Jette I came in touch with Scott E. Baker of the Pacific Northwest National Laboratories in Rihcland, WA, USA, who gave me the opportunity for a three month research stay. Here I met Ellen Panisko and Beth Hofstad that introduced me to the sample preparation required for proteome analysis. I am very grateful for getting to know you and despite our many differences, I will look back with smiles to our many conversations during our lunch and dinner dates.

Furthermore, I would like to thanks all my students, for their hard work and dedication. Especially Jens Christian Nielsen and Gerit Nymschefsky, that both showed a great personal drive and talent for making good research.

To all my CMB colleagues, I would like to thank you for making CMB a fun and stimulating place to work. I especially wish to thanks for following: Tina Johansen for excellent technical assistance and an incredible ability to solve problems, Martin Nielsen for hours of electrical assistance, especially during fermentations, Stig Rattleff for always providing peace, claim and candy, at the office, Simon Carlsen for your never ending spree of often funny "uncle humor" jokes, Paiman Khorsand-Jamal for all many Mexibar events and happy moments, Peter Knudsen, Tomas Strucko and Martin Schalén for improving the daily life CMB, Dorte M. Koefoed for the construction of two *A. niger* mutants and for forgiving me, injuring her, at Christmas party, Philippe Holt for his interesting views, Jakob B. Nielsen and Rasmus Frandsen for always having time, to more or less obscure scientific discussions, Mikael R. Andersen for helping with data analysis and for his work founding the basis to my project, Anne N. Johansen for always being helpful, Birgitte Karsbøl for our shared tea compassion, Kristian F. Nielsen for all the LC-MS analyses, Taja Andersen for always smiling and

learning my name is not Magnus, Aleksej Zelezniak for introducing me to the world of degtinė and Anna-Lena Heins for making the days at CMB better with great conversations and procrastinations.

Big Thanks to all my family and friends, who have giving their supported all through my Ph.D study and reminded me of the existences of the important things besides work. Especially thanks to Kasper, Christina and Julie!

Finally, I would like to thank my wife Lexy, for the all the love, patiences and understanding she has given me.

Publications

The results presented in this thesis have formed the basis for the following articles and manuscripts:

Poulsen L, Andersen MR, Lantz AE and Thykaer J. Identification of a transcription factor controlling pH-dependent organic acid response in *Aspergillus niger*. PLoS One 2012 (Accepted).

Poulsen L, Dai Z, Panisko EA, Lantz AE, Bruno KS, Daly DS, Nielsen J, Baker SE, Thykaer J. Transcriptome and proteome analysis of the correlation between citric acid formation and manganese limitation in *Aspergillus niger.* Appl Environ Microbiol (Submitted).

Poulsen L, Nielsen, JC, Lantz AE, Thykaer J. Identification and characterization of a transcription factor regulating extracellular proteolytic activity in Aspergillus niger. (Manuscript in preparation).

Poulsen L, Thykaer J, Nielsen, KF. Nutrient profiling reveals potent inducers of fumonisin biosynthesis in *Aspergillus niger*. (Manuscript in preparation).

Furthermore a minor contribution was given to the following article:

Andersen MR, Salazar MP, Schaap PJ, van de Vondervoort PJ, Culley D, Thykaer J, Frisvad JC, Nielsen KF, Albang R, Albermann K, Berka RM, Braus GH, Braus-Stromeyer SA, Corrochano LM, Dai Z, van Dijck PW, Hofmann G, Lasure LL, Magnuson JK, Menke H, Meijer M, Meijer SL, Nielsen JB, Nielsen ML, van Ooyen AJ, Pel HJ, **Poulsen L**, Samson RA, Stam H, Tsang A, van den Brink JM, Atkins A, Aerts A, Shapiro H, Pangilinan J, Salamov A, Lou Y, Lindquist E, Lucas S, Grimwood J, Grigoriev IV, Kubicek CP, Martinez D, van Peij NN, Roubos JA, Nielsen J, Baker SE. Comparative genomics of citric-acid-producing *Aspergillus niger* ATCC 1015 versus enzyme-producing CBS 513.88. Genome Res 21(6): 885-897.

Finally two patent applications are in preparation.

Abbreviations

2-DE Two-dimensional polyacrylamide gel electrophoresis

Bp Base pairs

BSA Bovine serum albumine

CDS coding sequences

CM Complex medium

Da Dalton

DAD diode array detector

EC Enzyme Commission

GC-MS Gas chromatography Mass spectrometry

GRAS Generally regarded as safe

HPLC High performance liquid chromatography

Kb Kilobases

MM Minimal medium

MS Mass spectrometry

PIM Protease induction medium

PPP Pentose phosphate pathway

RMA Robust multiarray average

TCA Tri carboxylic acid

TF Transcription factor

vvm Volume of gas per volume of liquid per minute

Nomenclature

μ Specific growth rate

Y_{SX} Specific yield of biomass on substrate

$Y_{S,Citrate}$ Specific yield of citrate on substrate

Y_{SCO2} Specific yield of CO_2 on substrate

$Y_{S,Gluconate}$ Specific yield of gluconate on substrate

Y_{SO} Specific oxygen consumption per substrate

$Y_{S,Oxalate}$ Specific yield of oxalate on substrate

Contents

List of tables

List of Figures

Chapter 1 Outline of the thesis

The aim of this project was to investigate the regulatory aspects of filamentous fungus *Aspergillus niger* to guide the improvement of this microorganism. The work covers a wide area of topics including, organic acid production, protease secretion and mycotoxin formation yet with the focus of industrial relevance.

The thesis was written in a monographic structure and to provide context for the work presented, a short outline will be given.

Chapter 2 provides a general introduction to *Aspergillus niger* and the industrial processes where this microorganism is applied. Furthermore the advances made with *A. niger,* improving the performance as a cell factory, are comprehensively reviewed.

Chapter 3 outlines the Systems Biology approaches and tools available for *A. niger* and highlights the individual advantages and disadvantages. The last part of this chapter includes the important aspects of biomass generation, to ensure quality data.

Chapter 4 presents a detailed examination of the citrate overflow metabolism. Using both transcriptomics and proteomics, the highly complex cellular responses that initiate citrate formation was uncovered. The study confirmed several events described in literature, together with novel finding, as down regulation of the gluconeogenesis and more.

Chapter 5 outlines the background behind transcription factor modulation and the strategy to locate transcription factors, applied as targets, in this metabolic engineering strategy. The thoughts and ideas presented in this chapter form the basis for the strategies applied in following two chapters.

Chapter 6 describes the identification of the transcription factor OafA and its meticulous characterization. Disruption of this transcriptions factor resulted in high levels of oxalic acid formation. Through transcriptional profiling links between the phosphoketolase pathway, the oxidative phosphorylation and oxalic acid overflow metabolism was discovered. Following the similar approach, chapter 7 focuses on protease secretion, in two protease mutants. The *ΔprtB* mutant, identified in this study, was assessed and compared to the previously descripted *ΔprtT* mutant. Pros and cons were identified for both strains; consequently, thoughts of industrial relevance are discussed.

In chapter 8, a systematic nutritional investigation of *A. niger's* fumonisin formation is presented. With the use of a reporter construct, a fascinating interacting between plants pathogen defense response and the fungus fumonisin formation was discovered.

Finally, chapter 9, contains conclusions and perspectives of the research presented in this thesis.

Two chapters was omitted from the thesis due to circumstances regarding patenting.

Chapter 2 Introduction to *Aspergillus*

Filamentous fungi have been extensively used as cell factories for a wide range of biotechnological products including enzymes, chemicals and food ingredients. The genus of *Aspergillus* has had substantial impact within biotechnology due to their many applications in food fermentation and biotechnological processes. This chapter will focus on the importance of Aspergilli in the biotech industry.

2.1 *Aspergillus* in biotechnology

From the beginning of biotechnology, dating millennia back, mankind has used microorganisms in various types of fermented food and beverages including beer, wine or bread without knowing of their existence (Bennett 1998). The use of Aspergilli in production processes was initiated more than two thousand years ago in Asia. Back then the production of the rice wine sake, by *A. oryzae* and the fermented soy sauces, shoyu and tamari, produced by *A. oryzae* and *A. tamari* are the earliest recorded (Machida 2002, Rokas 2009).

Not before the year 1894, did a well-defined process emerged, that can be classified as a modern industrial biotechnological production. The production of Takadiastase, an enzyme mixture with primarily an amylase activity by *A. oryzae.* This was followed with citric acid production by *A. niger* in 1917 (Currie 1917, Bodie et al. 1994). These early processes paved the way for an extensively expanding industry of biological derived products, where Aspergilli are still the dominating production platform. Ranging from organic acids in *A. niger* and *A. terreus* to cholesterol lowering statins in *A. terreus* to proteins and enzymes in a variety of different Aspergilli. Particularly, enzymes currently have a significant commercial interest, underlined by the increase in the market of 12 billion DKK from 1998 to 2011 (Adrio et al. 2005, Novozymes 2011).

Traditionally, *Aspergillus* has mainly been exploited for production of homologous enzymes (table 2.1). However, with the advances in systems biology coupled with enhanced genetic tools available, now permits the synthesis of industrially relevant amounts of various heterologous proteins, table 2.2.

Table 2.1 Examples of commercial homologous enzymes produced by *Aspergillus spp*. (A more comprehensive list can be found at the Association of Manufacturers and Formulators of Enzyme Products (AMFEP): http://www.amfep.org or the Enzyme Technical Association (ETA): http://enzymetechnicalassoc.org/)

Enzyme	Classification	Industry	Producer	Reference
Aminopeptidase	Protease	Cheese, baking, Soy production	*A. niger, A. oryzae, R. Ozyzae*	AMFEP, ETA
Celluase	Carbohydrase	Baking, Biofuel	*A. niger, A. aculeatus, Trichoderma spp.*	AMFEP
Glucose oxidase	Oxidoreductase	Baking, biosensors, Gluconic acid production	*A. niger*	(Wong et al. 2008)
Lipase triacylglycerol	Lipase	Cheese, detergents, biofuel	Various	(Olempska-Beer et al. 2006)
Phytase	Phosphatase	Animal feed supplement	*A. niger*	(Olempska-Beer et al. 2006)
ß-Glucanase	Carbohydrase	Brewing	*A. niger, A. aculeatus, Trichoderma spp.*	AMFEP

Table 2.2 Examples of heterologous proteins produced by *A. niger*, the most recent and detailed list of heterologous proteins produced by *Aspergillus* spp. Can be found by (Fleissner and Dersch 2010).

Enzyme	Classification	Industry	Origin	Reference
Laccase	Oxidase	Beer, Fruit juices	*Pycnoporus cinnabarinus*	(Record et al. 2002)
Interferon -α-2	Cytokine	Biopharmaceutical	*Homo sapiens*	(MacRae et al. 1993, Punt et al. 2002)
Lysozyme	Glycoside hydrolases	Biopharmaceutical, preservative	*Gallus gallus* (Chicken)	(Archer et al. 1990, Bohlin et al. 2006)
Prochymosin	Protease	Cheese, Baking	*Sus scrofa* (Porcine)	(Broekhuijsen et al. 1993, van den Brink et al. 2006)
Proteinase inhibitor	Inhibitor	Biopharmaceutical	*Homo sapiens*	(Mikosch et al. 1996)
Themostable Lipase	Lipase	Cheese, detergents, biofuel	*Thermomyces lanuginosus*	(Prathumpai et al. 2004)

Applying Aspergilli as protein cell factories carries numerous advantages compared to yeast and bacteria. *Aspergillus spp.* are able to utilize a wide range of carbon sources, including xylan and hemicellulose. In comparison to other eukaryotic expression systems, filamentous fungi possess an exceptional efficient

secretion capacity, enabling titers above 20 g/L of enzymes (Aunstrup 1984, Finkelstein 1987, Yoder et al. 2004). They have intron splicing and post translational machinery, allowing expression of proteins from multicellular eukaryotes. These features all combined, render the *Aspergillus* genus the most important fungi for commercial enzymes production.

A further illustration of Aspergilli being the most important producers of commercial enzymes, can be found in the number of processes being classified as Generally Recognized As Safe (GRAS) by the US Food and Drug Administration. Out of a total number of 53 GRAS status processes involving enzyme production preparation, the *Aspergillus* genus have 18 records whereas 11 of these belongs to *A. niger* (Food and Drug-Administration 2012).

As indicated above, *A. niger* is one of the most industrial important species within the genus of *Aspergillus*, consisting of more than 260 species (Samson and Varga 2009). The two major products from *A. niger* is the organic acid, citric acid and the enzyme glucoamylase.

2.1.1 Growth and morphology

Aspergillus belongs to the Phylum of fungi called Ascomycota and as most other species in this division, grows by apical filament elongation. The filamentous threadlike structures are named hyphae and developed from a single conidiospore (Wessels 1993). As the polarized hyphal elongation continues, branching eventually occurs, rendering the fungus the opportunity to explore the three dimensional space. The branching enables the fungus to search large areas in all direction for nutrients, a favorable feature, as nutrients often are scarce in its natural habitat, the soil. The branched network of hyphae is together termed mycelium.

Aspergillus spp. can produce specialized spore-bearing structures called conidiophores. The spores produced in these structures, named conidiospores, are characterized as asexual and allow a rapid propagation of the fungus (Etxebeste et al. 2010), figure 2. Reproduction can also occur sexually and involves the development of haploid ascospores, yet *A. niger* have not been observed in a telomorphic state (Crous et al. 2009).

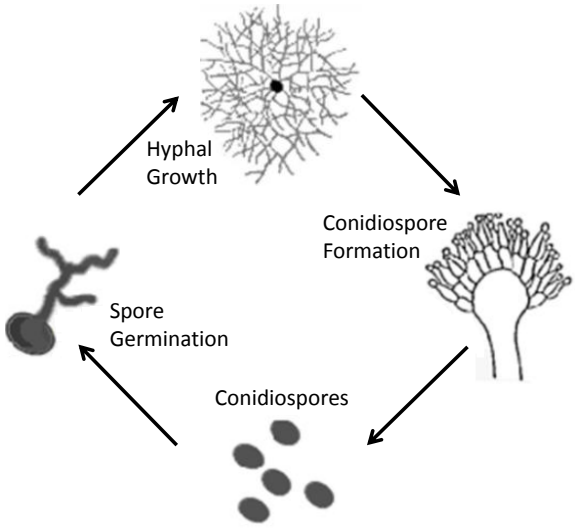

Figure 2.1 The life cycle of *A. niger*. Figure modified from Crous et al. (2009).

In submerged cultivations of filamentous fungi, the morphology can be described on two levels; macroscopic and microscopic (McIntyre et al. 2001). The macroscopic morphology describes the gross morphology including compact spherical from named pellet, free dispersed mycelia named filamentous and loose aggregates named clumps whereas the microscopic morphology describes the branch frequency, hyphae dimensions, segregation etc. For a visual description of the macromorphology see figure 2.2.

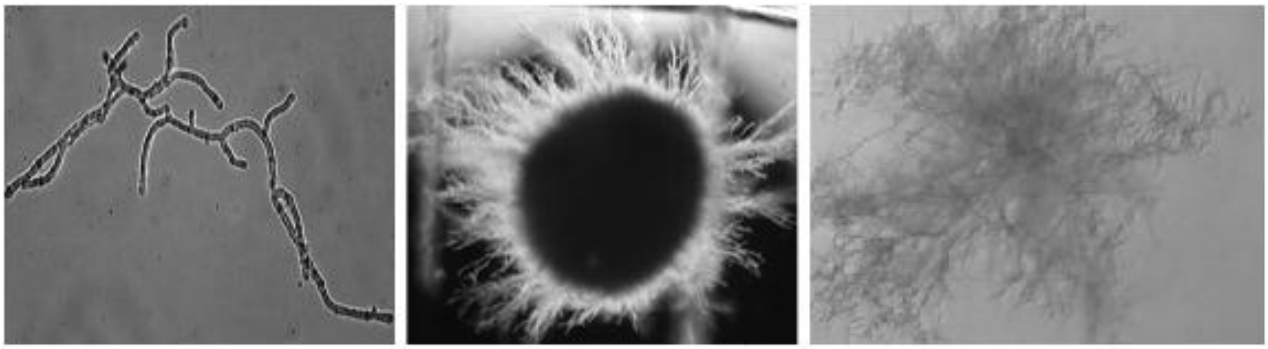

(A) (B) (C)

Figure 2.2 The microscopic morphology of *A. niger* in a submerged culture. (A) Free dispersed cells, (B) Pellets and (C) Clumps.

Determining the morphology is an interplay between many parameters including the pH value, the concentration of trace metals, especially manganese, the agitation- and aeration rate (Grimm et al. 2005, Papagianni 2007), but also the inoculum level (Papagianni and Mattey 2006) can influence the morphology.

Control of the morphology is vital to a production process since the morphology greatly influence parameters as, mass transfer and productivity. Where the pellet form is mainly used for the production of citric acid (Bodie et al. 1994), the dispersed filamentous morphology is beneficial producing extracellular proteins (Schrickx et al. 1993, Kelly et al. 2004).

2.1.2 Citric acid production

A. niger is very proficient in producing organic acids including citric acid. Citric acid is an important chemical due to its many applications; as acidifier, preservative and antioxidant in the food and beverage products. Citric acid has as well a strong affinity towards divalent charged metals, making it an excellent cleaning agent, as well as a SO_2 binder for smoke cleaning (Dutta et al. 1987).

Citric acid is a bulk, low value product and even with the increasing demands and rising costs of raw materials and energy, the price for citric acid in 2006 was in the range of $ 1.25-1.27 per kg. The annual output of citric acid worldwide, the same year, was predicted to 1.5 million tons (Graff 2007). This makes the industrial output of this compound greater than that of most other primary metabolites, derived by fermentation.

Citric acid was isolated for the first time in 1784, by German-Swedish chemist Carl Wilhelm Scheele, who crystallized it from lemon juice. The commercial production of citric acid was initiated in England 1826 and based of Italian lemons. With the increased value of citric acid as an item of commerce, a production was started in Italy and established a monopoly lasting to the end of the nineteenth century. To find alternative sources of citric acid, a chemical method using glycerol were invented by (Grimoux and Adams 1880). However, it was not economically competitive since the starting material costs exceeded the product value. In 1893, C. Wehmer discovered that a *Penicillium* mold could be used to produce citric acid from sugar. But since lemons at that time were readily available, this type of biological synthesis appeared unnecessary. Not until the First World War disrupted the Italian citrus exports, a demand for alternative sources emerged.

This resulted in the discovery of *A. niger's* ability to produce citric acid in 1917 by the American chemist J. Currie. He discovered when *A. niger* was cultured in media with low pH, high sugar and mineral salts, forming a substantial amount of citric acid. Prior to this finding, *A. niger* was only known to produce oxalic acid. The conversion of glucose to citric acid was vastly efficient and it led Currie together with Chas. Pfizer & co. inc. to start a large scale production, based on surface cultures. Advance in fermentation technology led to a process change, into submerged cultivation in the beginning of the 1950's. Leading to a reduced labor requiring process and resulting in an increased production rate (Bodie et al. 1994). Today, *A. niger* is

still the main cell factory for citric acid production and the yield has reached up to 95 kg citric acid per 100 kg of supplied carbohydrate (Karaffa and Kubicek 2003).

The low value of citric acid makes even minute yield improvements of a significant economic benefit. Traditionally, advances were achieved by mutagenesis and screening (Hjort 2005), but such improvements are not easily protected by patents. Consequently, secrecy is an important tool for the citric acid industry. This has made research in understanding the metabolic events coursing this intriguing and almost stoichiometric conversion of glucose into citric acid troublesome.

The first academic studies of *A. niger's* citric acid overflow metabolism emerged in the start 1950's (Damodaran and Rangachari 1951, Martin and Wilson 1951). Applying radiolabelled precursors led to the discovery that citric acid biosynthesis depended on the breakdown of carbon primary though glycolysis (Shu et al. 1954). An intriguing discovery made by Cleland and Johnson (1954), calculated that yields of citric acid was exceeding the theoretical yield, which is Y_{sp}=0.67 (cmole/cmole). The only way this can occur is, if the CO_2 released in the decarboxylation of 1 mole pyruvate is fixed by the pyruvate dehydrogenase and reused to form oxaloacetate from the second mole pyruvate. The reuse of CO_2 increases the theoretical yield to Y_{sp}= 0.80 (cmole/cmole). For a schematic representation, see figure 2.1. A further detailed description of the changes in the metabolism leading to the citric overflow metabolism can be found in chapter 4.

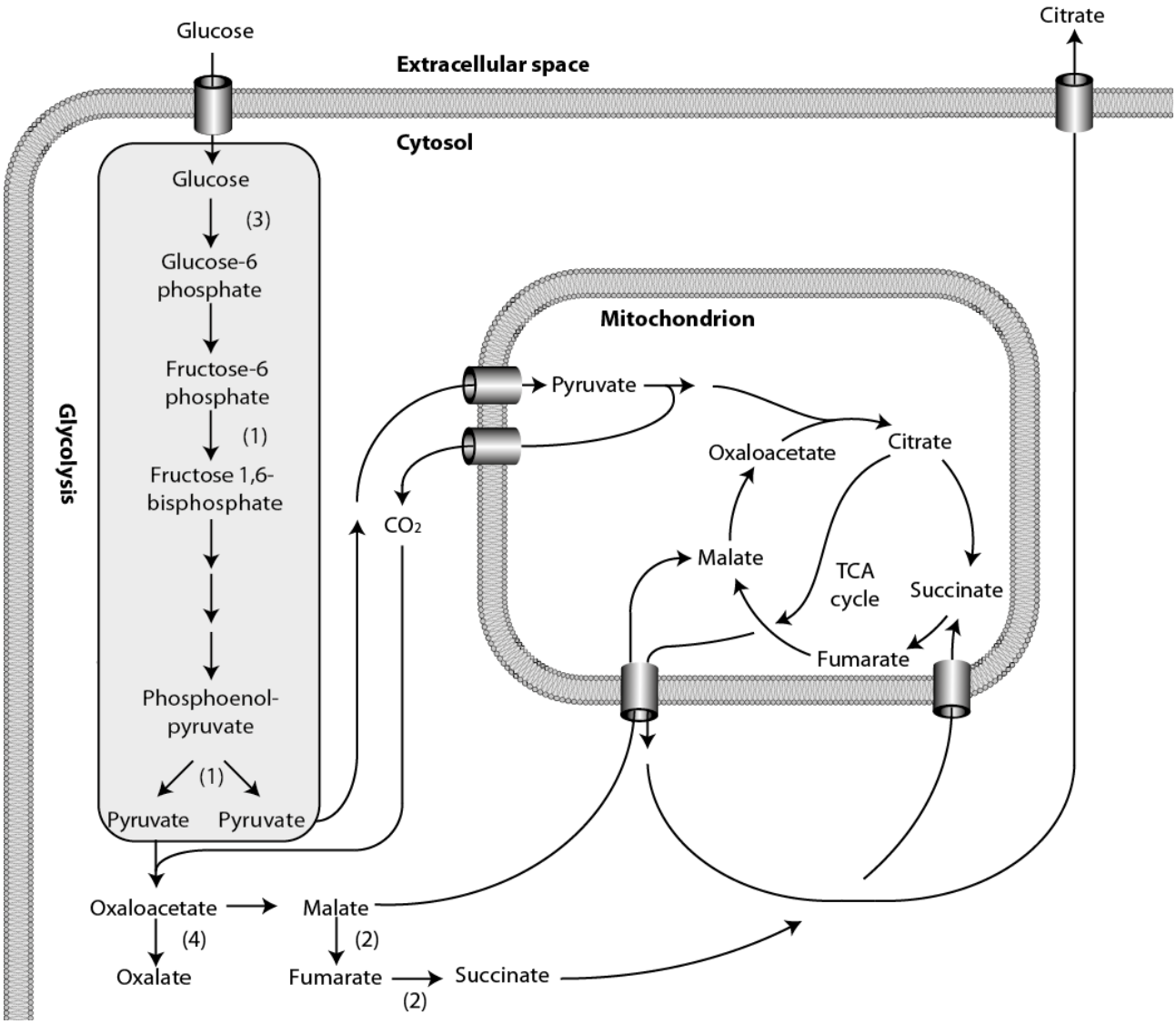

Figure 2.3 A schematic representation of the citrate metabolism in *A. niger*. The numbers in brackets refers to the order of appearance in the following text. (1) Phosphofructokinase and pyruvate kinase, (2) Fumarase and fumarate reductase, (3) Hexokinase, (4) Oxaloacetate acetylhydrolase.

Several academic studies to increase the rate and titer of citrate formation exist. They can be divided into two approaches, up regulating enzymes in the pathway increasing the flux towards citric acid or increasing citric acid production by elimination of byproducts, hence direct carbon towards citrate. An illustration of this, is found in the study by Ruijter et al. (1997), where phosphofructokinase and pyruvate kinase (figure 2.3.1) were overexpressed, 3 and 5 fold respectively. These two enzymes are involved in sugar uptake and were believed to be important steps in flux control (Kubicek et al. 1988, Kubicek-Pranz et al. 1990). The outcome was however disappointing since the overexpression did not influence the activity of other enzymes in the pathway, nor did it change intermediary metabolite levels. This outcome was supported by

calculations made by (Torres et al. 1996). Using biochemical system theory, it was calculated that at least seven glycolytic enzymes must be simultaneously up-regulated, to obtain an increased rate of citrate formation.

A more recent study was conducted by de Jongh and Nielsen (2008). Based on a metabolic flux balance model by (Guebel and Torres 2001), the citrate export from the mitrochondria was predicted to likely be rate limiting. The authors hypothesized that the principal mode of citrate export from the mitochondria, involved anti-port of cytosolic malate, hence inserting heterologous genes involved in this branch of TCA cycle, could increase citrate yield. By insertion of a fumarase and a fumarate reductase (figure 2.3.2) resulted in a strain that was able to produce citrate in presence of trace manganese concentrations. Manganese is a strong inhibitor of citrate overflow metabolism in *A. niger*. Additionally this strain had a significant increase yield coefficient of 0.9 (g Citrate /g glucose).

An example of eliminating byproducts is the of study by Arisan-Atac et al. (1996). This might be the first successful academic improvement of A. *niger*'s citrate production. By disruption of the gene encoding the trehalose-6-phosphate synthase, the authors managed to improve the rate of citric acid accumulation. This enzyme produces trehalose-6-phosphate, a strong inhibitor of hexokinase I and II (figure 2.3.3) (Blazquez et al. 1993) and the lack of this enzyme caused increased citric acid accumulation, especially in the early phase of the fermentation.

Following a similar strategy was the study by Ruijter et al. (1999). Oxalic acid produced by *A. niger* arises as an unwanted by-product, mainly due to decrease of yield of citric acid and that oxalate complicates recovery process. By disrupting of the oxaloacetate acetylhydrolase (figure 2.3.4), the enzyme that converts oxaloacetate into oxalate, the oxaloacetate acetylhydrolase deficient mutant produced citric acid up to pH 5 and was insensitive to manganese inhibition.

2.1.3 Glucoamylase production

As previously mentioned, the market for industrial enzymes has grown significantly in the last 10 years. Specifically, the starch degrading amylases has been one of the main triggers for the growth and this class of enzymes is now the largest market within the industrial enzymes (Kelly et al. 2009). All amylases are glycoside hydrolases but particularly the γ-amylase subclass also named glucoamylase (GA) is important. GA cleaves α(1-6) glycosidic linkages, as well as α(1-4) glycosidic linkages at the nonreducing end of amylose and amylopectin (Kumar and Satyanarayana 2009). This enzyme is used by the food industry for converting starch into glucose syrup and applied substantially in the production of first generation bioethanol. Before the 1960's this conversion was made by combining starch with dilute hydrochloric acid, followed by heating

under pressure. This chemical conversion had certain drawbacks as byproducts formation and salts from the neutralization. The change into the enzymatic process resulted in higher yield, higher degree of purity and facilitated crystallization of glucose (Kearsley and Dziedzic 1995).

Today, the enzymatic process typically consists of two steps, first the starch is liquefied using α-amylase converting the starch into lower-molecular-weight dextrins. These are then converted into monosaccharide glucose by GA. This enzymatic conversion of starch into glucose was the first large scale enzymatic process and still today the starch industry is the main user of enzymes (Hjort 2005).

Ironically one of reasons GA is produced in such large amount, is because it is a slow-acting enzyme, with a specific activity of 5.6 µmol/min/mg (free enzyme on maltodextrin, (Abraham et al. 2004)). This is orders of magnitude lower compared with α-amylase (Najafi and Deobagkar 2005). Consequently the enzyme needs a high dosing, and even under these conditions, dextrin to glucose conversion lasts up to 92 hours (Kumar and Satyanarayana 2009). Therefore efforts on optimizing the GA enzyme have been attempted.

The task of improving the enzyme temperature stability has been a major focus. GA from *A. niger* has an optimal temperature of 55°C–60°C. This pose a challenge, since the first step catalyzed by α-amylase, is operated at 105 °C where the enzyme operates very rapidly. To accommodate GA reduced thermostability, the reaction mixture has to be cooled which imposes a significant cost on the overall process. Multiple studies have been addressing the thermostability problem, by site-directed mutagenesis (Reilly et al. 1994, Chen et al. 1996, Allen et al. 1998, Liu and Wang 2003), but only minor improvements have been achieved. An interesting study by Wang et al. (2006) addressed the problem applying directed evolution and was able to increase the temperature optimum to 80 °C.

An alternative strategy is minding for themostable versions of GA from thermophilic organisms. Several studies can be found pursuing this approach (Ohnishi et al. 1992, Campos and Felix 1995, Li et al. 1998), yet none have been found to be superior to the traditional *A. niger* GA. A study by Nielsen et al. (2002) investigated a heterologous expressed thermostable glucoamylase from *Talaromyces emersonii*. The *T. emersonii* glucoamylase had a reduced Km towards the assayed substrates (3-5 fold) compared with the *A. niger* glucoamylase. Still the increased themostability resulted in the higher yield with *T. emersonii* GA using 3-fold lower protein concentration. It has to be noted that the two enzymes were evaluated at 65 °C, which is above the recommended 55 °C – 60 °C for *A. niger* GA (Abraham et al. 2004).

Besides optimizing the enzyme itself improvement in the yield of GA, in *A. niger* has been addressed in various studies. Increasing the amount of genetic copies of GA was done successfully by Wallis et al. (1999),

with 80 extra copies inserted into the genome. This resulted in eight fold increment of GA titer without a noteworthy change of the glycosylation pattern.

Morphology studies of the fungal cells made by (Wösten et al. 1991, Peberdy 1994) gave strong indication of protein secretion being localized at the hyphal tips. This discovery increased the commercial interest in the subject and several patents were filled. Mutation in the HbrA gene inducing hyperbranching and improving protein secretion (Turner et al. 2000). Another patent by (Akin et al. 2002) described truncation of the gene cotA, resulting in a compact morphology leading to incensement of the branching, as well as cessation of hyphal tip extension. More recent studies focus on morphology engineering mediated by physio-chemical methods. (Driouch et al. 2010) applied silicate microparticles, variating in size and concentration for a distinctive control of the morphology and achieve a fourfold higher concentration of glucoamylase. Wucherpfennig et al. (2011) used osmolality to control the morphology; however, this method has a strong negative effect on the germination time and growth rate.

2.1.4 Heterologous protein production

Glucoamylase and other homologous proteins are, in most cases, produced in one to two orders of magnitude higher than heterologous proteins (Braaksma and Punt 2008). Besides the previously mentioned advantages of using members of the *Aspergillus* family for protein production, disadvantages are present as well that surface especially when expressing a heterologous protein. These include transcription and translation control, mRNA stability, secretion, and extracellular degradation.

To circumvent the yield limiting factors, several strategies have been developed. They include classical yield improvement methods as manipulating promoter strength but also novel strategies, as amino acid terminal fusion. A schematic representation of targets for optimization and their correlation to central dogma can be found in figure 2.4.

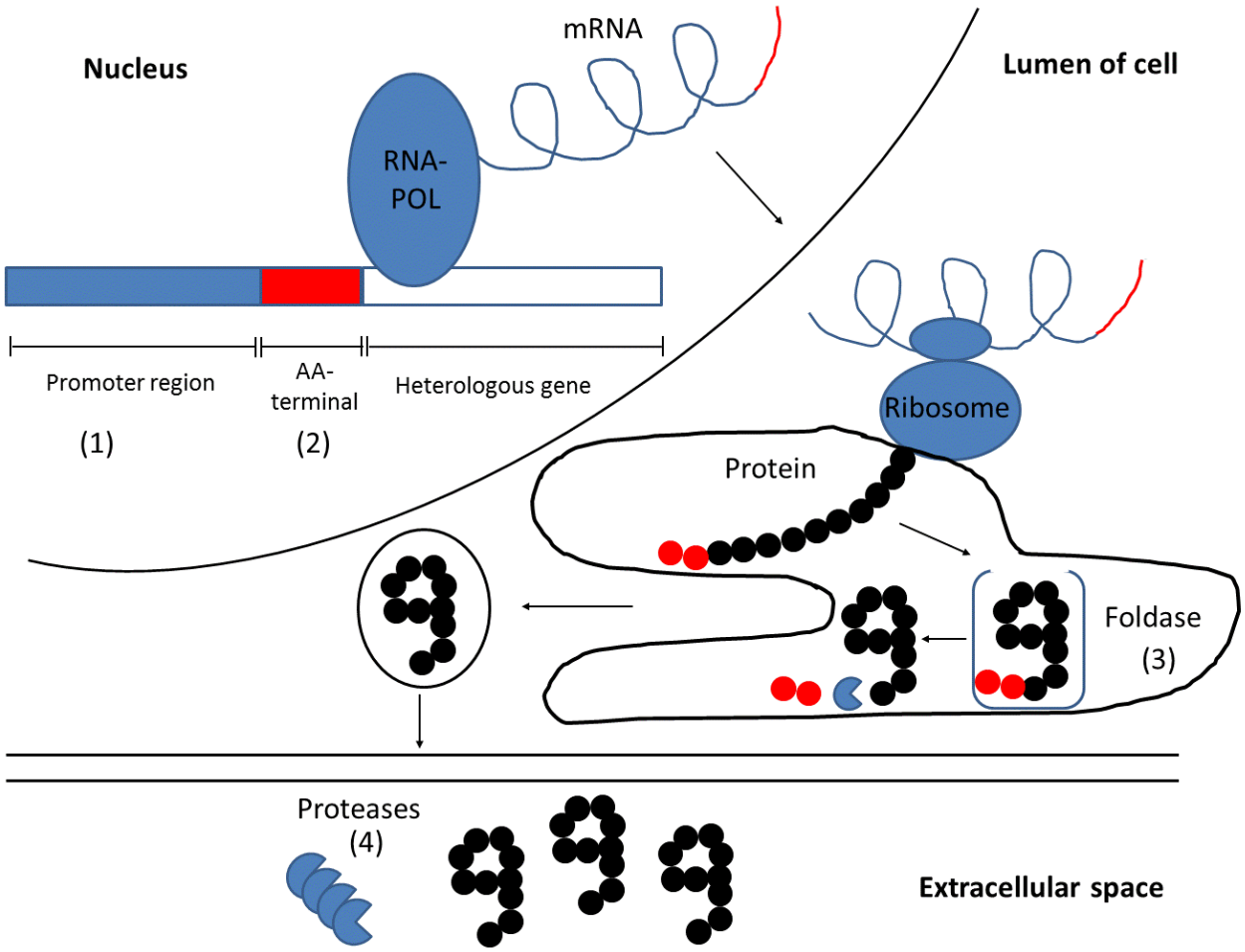

Figure 2.4 An overview of targets to manipulate in the central dogma to improve heterologous protein expression in *A. niger*. The numbers in brackets refers to the order of appearance in the following text.

The first challenge of heterologous protein production is expression. Typically the native promoter cannot be applied; therefore, a different promoter has to be selected (figure 2.4.1). The study by Moralejo et al. (1999) investigated this challenge of promoter selection. Four strong fungal promoters were assayed and more than a tenfold difference was observed of the promoters in between. The recent study by (Blumhoff et al. 2012) addressed the problem with a limited number of promoters for heterologous expression in fungi. Six novel constitutive promoters were characterized in *A. niger*, covering three orders of magnitude. Similar to prokaryotes, synthetic promoters have also been developed for fungi (Yaver and Nham 2003) as well as inducible promoters (Meyer et al. 2011).

The next challenge is the translation and folding of the heterologous protein. The main strategy for enhancing the processing is called amino-terminal fusion (figure 2.4.2). This technique employs the flanking sequences of highly expressed and secreted homologous protein e.g. glucoamylase, as a signal peptide (Ward et al. 1990) (Gouka et al. 1997b, Ward et al. 2004). The method of action has been proposed as

stabilization of the recombinant mRNA and facilitating the translocation of the heterologous protein into the secretory pathway. To release the heterologous protein from the signal peptide, a cleavage site for a protease is included. This is typically the serine proteinase KexB, located in the Golgi apparatus. A comprehensive review of this strategy as made by Gouka et al. (1997a).

An attractive technique for improving heterologous protein expression has shown to be the manipulation of regulatory proteins also known as transcription factors (TFs). Currently, two TFs have been described as particular beneficial.

High levels of protein expression require the cell to up-regulate the machinery responsible for protein folding and transport (figure 2.4.3). This is because otherwise unfolded protein would be targeted for degradation by the cell. This up-regulation is termed the unfolded protein response (UPR). To enhance the UPR, attempts on up regulating individual parts of UPR e.g. foldases and chaperones gene have been attempted. Although in some cases, this strategy has been reported successful, the outcome of this approach seems strongly dependent on the protein of interest, as reviewed by Conesa et al. (2001). The UPR pathway has been studied in details in *S. cerevisiae* and a transcription factor, HAC1, has been identified being the main responsible for regulation of the UPR pathway (Cox and Walter 1996, Mori et al. 1996, Welihinda et al. 1999). The ortholog to HAC1, *hacA* has later been identified in Aspergilli and overexpressed by (Valkonen et al. 2003). The study demonstrated that a 3 to 7-fold titer improvement could be reached with a constitutive expression of *hacA*. This study illustrates the significance of modulating TFs rather than by modulating single/few genes.

The last challenge when applying Aspergilli as protein cell factory is the secreted proteases (figure 2.4.4). Proteases are a general problem protein production, but they are more pronounced when producing heterologous proteins. (Braaksma and Punt 2008). *A. niger* have more than 150 genes encoding for proteases where 32 of these genes contain an export signal or have strong similarity to other secreted proteases, in other organisms. (Pel et al. 2007). Reducing the extracellular protease activity has been addressed by classical strain improvement (Mattern et al. 1992, Katz et al. 1996) and genetic engineering, targeting the aspergillopepsin protease family (van den Hombergh et al. 1997a, van den Hombergh et al. 1997b). Interestingly, a mutant obtained and described by Mattern et al. (1992) was later identified to be cause by a mutation in a gene encoding a TF named prtT (Hjort et al. 2000, Punt et al. 2008). The disruption of the prtT gene, reduced the total extracellular protease activity to 20% of the wild type.

2.2 Concluding remark

As illustrated in this chapter, *A. niger* is a versatile cell factory, that has been applied for close to a century. Initiated by *A. nigers* superior ability to produce citric acid and later also glucoamylase production, has established A. *niger* as one of the most significant production hosts of industrial biotechnology. Recently *A. niger* has also emerged as a heterologous protein production host. However, the titers of heterologous proteins are low compared with proteins from a homologous origin, leaving a potential for optimization. With the release of the genome sequence of *A. niger*, has enabled the possibility of applying Systems Biology approaches to pinpoint bottlenecks in the protein production machinery. Therefore, this is the main topic in chapter 3.

2.3 References

Abraham, T. E., J. R. Joseph, L. B. Bindhu and K. K. Jayakumar (2004). "Crosslinked enzyme crystals of glucoamylase as a potent catalyst for biotransformations." Carbohydr Res **339**(6): 1099-1104.

Adrio, J. L., A. L. Demain and J. Velasco (2005). Handbook of industrial mycology, 082475655X (hbk.) : [1]130.00082475655X (alk. paper).

Akin, A. R., E. A. Bodie, S. Burrow, N. S. Dunn-Coleman, G. Turner and M. Ward (2002). Regulatable growth of filamentous fungi. US7425450.

Allen, M. J., P. M. Coutinho and C. F. Ford (1998). "Stabilization of *Aspergillus awamori* glucoamylase by proline substitution and combining stabilizing mutations." Protein Engineering **11**(9): 783-788.

Archer, D. B., D. J. Jeenes, D. A. MacKenzie, G. Brightwell, N. Lambert, G. Lowe, S. E. Radford and C. M. Dobson (1990). "Hen egg white lysozyme expressed in, and secreted from, *Aspergillus niger* is correctly processed and folded." Biotechnology (N Y) **8**(8): 741-745.

Arisan-Atac, I., M. F. Wolschek and C. P. Kubicek (1996). "Trehalose-6-phosphate synthase A affects citrate accumulation by *Aspergillus niger* under conditions of high glycolytic flux." FEMS Microbiol Lett **140**(1): 77-83.

Aunstrup, K. (1984). "Enzyme technology, problems and possibilities." European Congress on Biotechnology **3**(4): 143-156.

Bennett, J. W. (1998). "Mycotechnology: the role of fungi in biotechnology." J Biotechnol **66**(2-3): 101-107.

Blazquez, M. A., R. Lagunas, C. Gancedo and J. M. Gancedo (1993). "Trehalose-6-phosphate, a new regulator of yeast glycolysis that inhibits hexokinases." FEBS Lett **329**(1-2): 51-54.

Blumhoff, M., M. G. Steiger, H. Marx, D. Mattanovich and M. Sauer (2012). "Six novel constitutive promoters for metabolic engineering of *Aspergillus niger*." Appl Microbiol Biotechnol.

Bodie, E. A., B. Bower, R. M. Berka and N. S. Dunn-Coleman (1994). "Economically important organic acid and enzyme products." Prog Ind Microbiol **29**: 561-602.

Bohlin, C., L. J. Jonsson, R. Roth and W. H. van Zyl (2006). "Heterologous expression of Trametes versicolor laccase in Pichia pastoris and *Aspergillus niger*." Appl Biochem Biotechnol **129-132**: 195-214.

Broekhuijsen, M. P., I. E. Mattern, R. Contreras, J. R. Kinghorn and C. A. van den Hondel (1993). "Secretion of heterologous proteins by *Aspergillus niger*: production of active human interleukin-6 in a protease-

deficient mutant by KEX2-like processing of a glucoamylase-hIL6 fusion protein." J Biotechnol **31**(2): 135-145.

Braaksma, M. and P. J. Punt (2008). *Aspergillus* as a cell factory for protein production: controlling protease activity in fungal production. The Aspergilli: Genomics, Medical Aspects, Biotechnology, and Research Methods, CRC Press**:** 441-455.

Campos, L. and C. R. Felix (1995). "Purification and Characterization of a Glucoamylase from Humicola grisea." Appl Environ Microbiol **61**(6): 2436-2438.

Chen, H.-m., Y. Li, T. Panda, F. U. Buehler, C. Ford and P. J. Reilly (1996). "Effect of replacing helical glycine residues with alanines on reversible and irreversible stability and production of *Aspergillus* awamori glucoamylase." Protein Engineering **9**(6): 499-505.

Cleland, W. W. and M. J. Johnson (1954). "Tracer experiments on the mechanism of citric acid formation by *Aspergillus niger*." J Biol Chem **208**(2): 679-689.

Conesa, A., P. J. Punt, N. van Luijk and C. A. van den Hondel (2001). "The secretion pathway in filamentous fungi: a biotechnological view." Fungal Genet Biol **33**(3): 155-171.

Cox, J. S. and P. Walter (1996). "A novel mechanism for regulating activity of a transcription factor that controls the unfolded protein response." Cell **87**(3): 391-404.

Crous, P. W., G. J. M. Verkley, J. Z. Groenewald and R. A. Samson (2009). Fungal Biodiversity, CBS-KNAW Biodiversity Centre Utrecht, 9070351773.

Currie, J. N. (1917). "The Citric acid fermentation of *Aspergillus niger*." J. Biol. Chem. **31**: 15-37.

Damodaran, M. and P. N. Rangachari (1951). "Carbohydrate metabolism in citric acid fermentation. I. The influence of inhibitors of glycolysis and respiration on citric acid formation by *Aspergillus niger*." Enzymologia **15**(2): 83-95.

de Jongh, W. A. and J. Nielsen (2008). "Enhanced citrate production through gene insertion in *Aspergillus niger*." Metab Eng **10**(2): 87-96.

Driouch, H., B. Sommer and C. Wittmann (2010). "Morphology engineering of *Aspergillus niger* for improved enzyme production." Biotechnol Bioeng **105**(6): 1058-1068.

Dutta, B. K., R. K. Basu, A. Pandit and P. Ray (1987). "Absorption of sulfur dioxide in citric acid-sodium citrate buffer solutions." Industrial & Engineering Chemistry Research **26**(7): 1291-1296.

Etxebeste, O., A. Garzia, E. A. Espeso and U. Ugalde (2010). "*Aspergillus* nidulans asexual development: making the most of cellular modules." Trends Microbiol **18**(12): 569-576.

Finkelstein, D. B. (1987). "Improvement of enzyme production in *Aspergillus*." Antonie Van Leeuwenhoek **53**(5): 349-352.

Fleissner, A. and P. Dersch (2010). "Expression and export: recombinant protein production systems for *Aspergillus*." Appl Microbiol Biotechnol **87**(4): 1255-1270.

Food and Drug-Administration (2012). GRAS Notice Inventory.

Gouka, R. J., P. J. Punt and C. A. van den Hondel (1997a). "Efficient production of secreted proteins by *Aspergillus*: progress, limitations and prospects." Appl Microbiol Biotechnol **47**(1): 1-11.

Gouka, R. J., P. J. Punt and C. A. van den Hondel (1997b). "Glucoamylase gene fusions alleviate limitations for protein production in *Aspergillus* awamori at the transcriptional and (post) translational levels." Appl Environ Microbiol **63**(2): 488-497.

Graff, G. (2007). "Citric acid prices to rise as increased demand tightens supply."

Grimm, L. H., S. Kelly, Volkerding, II, R. Krull and D. C. Hempel (2005). "Influence of mechanical stress and surface interaction on the aggregation of *Aspergillus niger* conidia." Biotechnol Bioeng **92**(7): 879-888.

Grimoux, E. and P. Adams (1880). "Synthese de lácide citrique." Seances. Acad. Sci **90**: 1252.

Guebel, D. V. and N. V. Torres (2001). "Optimization of the citric acid production by *Aspergillus niger* through a metabolic flux balance model." Electronic Journal of Biotechnology **4**.

Hjort, C. (2005). Production of Food Additives using Filamentous Fungi. Genetically Engineered Food: Methods and Detection. Weinheim, Wiley-VCH Verlag GmbH & Co. KGaA**:** 86-99.

Hjort, C., C. van den Hondel, P. J. Punt and F. H. Schuren (2000). Fungal transcriptional activators useful in methods for producing a polypeptide.

Karaffa, L. and C. P. Kubicek (2003). "*Aspergillus niger* citric acid accumulation: do we understand this well working black box?" Appl Microbiol Biotechnol **61**(3): 189-196.

Katz, M. E., P. K. Flynn, P. A. vanKuyk and B. F. Cheetham (1996). "Mutations affecting extracellular protease production in the filamentous fungus *Aspergillus* nidulans." Mol Gen Genet **250**(6): 715-724.

Kearsley, M. W. and S. Z. Dziedzic (1995). Handbook of starch hydrolysis products and their derivatives. London, Blackie Academic & Professional, 0751402699 : ¹65.00.

Kelly, R. M., L. Dijkhuizen and H. Leemhuis (2009). "Starch and alpha-glucan acting enzymes, modulating their properties by directed evolution." J Biotechnol **140**(3-4): 184-193.

Kelly, S., L. H. Grimm, J. Hengstler, E. Schultheis, R. Krull and D. C. Hempel (2004). "Agitation effects on submerged growth and product formation of *Aspergillus niger*." Bioprocess Biosyst Eng **26**(5): 315-323.

Kubicek-Pranz, E. M., M. Mozelt, M. Rohr and C. P. Kubicek (1990). "Changes in the concentration of fructose 2,6-bisphosphate in *Aspergillus niger* during stimulation of acidogenesis by elevated sucrose concentration." Biochim Biophys Acta **1033**(3): 250-255.

Kubicek, C. P., G. Schreferl-Kunar, W. Wohrer and M. Rohr (1988). "Evidence for a cytoplasmic pathway of oxalate biosynthesis in *Aspergillus niger*." Appl Environ Microbiol **54**(3): 633-637.

Kumar, P. and T. Satyanarayana (2009). "Microbial glucoamylases: characteristics and applications." Crit Rev Biotechnol **29**(3): 225-255.

Li, D.-C., Y.-J. Yang, Y.-L. Peng and C.-Y. Shen (1998). "Purification and characterization of extracellular glucoamylase from the thermophilic Thermomyces lanuginosus." Mycological Research **102**(05): 568-572.

Liu, H.-L. and W.-C. Wang (2003). "Protein engineering to improve the thermostability of glucoamylase from *Aspergillus* awamori based on molecular dynamics simulations." Protein Engineering **16**(1): 19-25.

Machida, M. (2002). "Progress of *Aspergillus* oryzae genomics." Adv Appl Microbiol **51**: 81-106.

MacRae, W. D., F. P. Buxton, D. I. Gwynne and R. W. Davies (1993). "Heterologous protein secretion directed by a repressible acid phosphatase system of *Aspergillus niger*." Gene **132**(2): 193-198.

Martin, S. M. and P. W. Wilson (1951). "Uptake of C14O2 by *Aspergillus niger* in the formation of citric acid." Arch Biochem Biophys **32**(1): 150-157.

Mattern, I. E., J. M. van Noort, P. van den Berg, D. B. Archer, I. N. Roberts and C. A. van den Hondel (1992). "Isolation and characterization of mutants of *Aspergillus niger* deficient in extracellular proteases." Mol Gen Genet **234**(2): 332-336.

McIntyre, M., C. Muller, J. Dynesen and J. Nielsen (2001). "Metabolic engineering of the morphology of *Aspergillus*." Adv Biochem Eng Biotechnol **73**: 103-128.

Meyer, V., F. Wanka, J. van Gent, M. Arentshorst, C. A. van den Hondel and A. F. Ram (2011). "Fungal gene expression on demand: an inducible, tunable, and metabolism-independent expression system for *Aspergillus niger*." Appl Environ Microbiol **77**(9): 2975-2983.

Mikosch, T., P. Klemm, H. G. Gassen, C. A. van den Hondel and M. Kemme (1996). "Secretion of active human mucus proteinase inhibitor by *Aspergillus niger* after KEX2-like processing of a glucoamylase-inhibitor fusion protein." J Biotechnol **52**(2): 97-106.

Moralejo, F. J., R. E. Cardoza, S. Gutierrez and J. F. Martin (1999). "Thaumatin production in *Aspergillus* awamori by use of expression cassettes with strong fungal promoters and high gene dosage." Appl Environ Microbiol **65**(3): 1168-1174.

Mori, K., T. Kawahara, H. Yoshida, H. Yanagi and T. Yura (1996). "Signalling from endoplasmic reticulum to nucleus: transcription factor with a basic-leucine zipper motif is required for the unfolded protein-response pathway." Genes Cells **1**(9): 803-817.

Najafi, M. F. and D. Deobagkar (2005). "Purification and characterization of an extracellular alpha-amylase from Bacillus subtilis AX20." Protein Expr Purif **41**(2): 349-354.

Nielsen, B. R., J. Lehmbeck and T. P. Frandsen (2002). "Cloning, heterologous expression, and enzymatic characterization of a thermostable glucoamylase from Talaromyces emersonii." Protein Expr Purif **26**(1): 1-8.

Novozymes (2011). "The Novozymes Report."

Ohnishi, H., H. Kitamura, T. Minowa, H. Sakai and T. Ohta (1992). "Molecular cloning of a glucoamylase gene from a thermophilic Clostridium and kinetics of the cloned enzyme." Eur J Biochem **207**(2): 413-418.

Olempska-Beer, Z. S., R. I. Merker, M. D. Ditto and M. J. DiNovi (2006). "Food-processing enzymes from recombinant microorganisms--a review." Regul Toxicol Pharmacol **45**(2): 144-158.

Papagianni, M. (2007). "Advances in citric acid fermentation by *Aspergillus niger*: biochemical aspects, membrane transport and modeling." Biotechnol Adv **25**(3): 244-263.

Papagianni, M. and M. Mattey (2006). "Morphological development of *Aspergillus niger* in submerged citric acid fermentation as a function of the spore inoculum level. Application of neural network and cluster analysis for characterization of mycelial morphology." Microb Cell Fact **5**: 3.

Peberdy, J. F. (1994). "Protein secretion in filamentous fungi--trying to understand a highly productive black box." Trends Biotechnol **12**(2): 50-57.

Pel, H. J., J. H. de Winde, D. B. Archer, P. S. Dyer, G. Hofmann, P. J. Schaap, G. Turner, R. P. de Vries, R. Albang, K. Albermann, M. R. Andersen, J. D. Bendtsen, J. A. Benen, M. van den Berg, S. Breestraat, M. X. Caddick, R. Contreras, M. Cornell, P. M. Coutinho, E. G. Danchin, A. J. Debets, P. Dekker, P. W. van Dijck, A. van Dijk, L. Dijkhuizen, A. J. Driessen, C. d'Enfert, S. Geysens, C. Goosen, G. S. Groot, P. W. de Groot, T. Guillemette, B. Henrissat, M. Herweijer, J. P. van den Hombergh, C. A. van den Hondel, R. T. van der Heijden, R. M. van der Kaaij, F. M. Klis, H. J. Kools, C. P. Kubicek, P. A. van Kuyk, J. Lauber, X. Lu, M. J. van der Maarel, R. Meulenberg, H. Menke, M. A. Mortimer, J. Nielsen, S. G. Oliver, M. Olsthoorn, K. Pal, N. N. van Peij, A. F. Ram, U. Rinas, J. A. Roubos, C. M. Sagt, M. Schmoll, J. Sun, D. Ussery, J. Varga, W. Vervecken, P. J. van de Vondervoort, H. Wedler, H. A. Wosten, A. P. Zeng, A. J. van Ooyen, J. Visser and H. Stam (2007). "Genome sequencing and analysis of the versatile cell factory *Aspergillus niger* CBS 513.88." Nat Biotechnol **25**(2): 221-231.

Prathumpai, W., S. J. Flitter, M. McIntyre and J. Nielsen (2004). "Lipase production by recombinant strains of *Aspergillus niger* expressing a lipase-encoding gene from Thermomyces lanuginosus." Appl Microbiol Biotechnol **65**(6): 714-719.

Punt, P. J., F. H. Schuren, J. Lehmbeck, T. Christensen, C. Hjort and C. A. van den Hondel (2008). "Characterization of the *Aspergillus niger* prtT, a unique regulator of extracellular protease encoding genes." Fungal Genet Biol **45**(12): 1591-1599.

Punt, P. J., N. van Biezen, A. Conesa, A. Albers, J. Mangnus and C. van den Hondel (2002). "Filamentous fungi as cell factories for heterologous protein production." Trends Biotechnol **20**(5): 200-206.

Record, E., P. J. Punt, M. Chamkha, M. Labat, C. A. van Den Hondel and M. Asther (2002). "Expression of the Pycnoporus cinnabarinus laccase gene in *Aspergillus niger* and characterization of the recombinant enzyme." Eur J Biochem **269**(2): 602-609.

Reilly, P. J., H.-M. Chen, U. Bakir and C. Ford (1994). "Increased thermostability of Asn182 → Ala mutant *Aspergillus* awamori glucoamylase." Biotechnology and Bioengineering **43**(1): 101-105.

Rokas, A. (2009). "The effect of domestication on the fungal proteome." Trends Genet **25**(2): 60-63.

Ruijter, G. J., H. Panneman and J. Visser (1997). "Overexpression of phosphofructokinase and pyruvate kinase in citric acid-producing *Aspergillus niger*." Biochim Biophys Acta **1334**(2-3): 317-326.

Ruijter, G. J., P. J. van de Vondervoort and J. Visser (1999). "Oxalic acid production by *Aspergillus niger:* an oxalate-non-producing mutant produces citric acid at pH 5 and in the presence of manganese." Microbiology **145 (Pt 9)**: 2569-2576.

Samson, R. A. and J. Varga (2009). "What is a species in *Aspergillus*?" Medical Mycology **47**(s1): S13-S20.

Schrickx, J. M., A. S. Krave, J. C. Verdoes, C. A. van den Hondel, A. H. Stouthamer and H. W. van Verseveld (1993). "Growth and product formation in chemostat and recycling cultures by *Aspergillus niger* N402 and a glucoamylase overproducing transformant, provided with multiple copies of the glaA gene." J Gen Microbiol **139**(11): 2801-2810.

Shu, P., A. Funk and A. C. Neish (1954). "Mechanism of citric acid formation from glucose by *Aspergillus niger*." Can J Biochem Physiol **32**(1): 68-80.

Torres, N. V., E. O. Voit and C. Gonzalez-Alcon (1996). "Optimization of nonlinear biotechnological processes with linear programming: Application to citric acid production by *Aspergillus niger*." Biotechnol Bioeng **49**(3): 247-258.

Turner, G., N. S. Dunn-Coleman, S. Pollerman and S. Memmott (2000). Hyphal Growth In Fungi. WO2005080420-A2.

Valkonen, M., M. Ward, H. Wang, M. Penttila and M. Saloheimo (2003). "Improvement of foreign-protein production in *Aspergillus niger* var. awamori by constitutive induction of the unfolded-protein response." Appl Environ Microbiol **69**(12): 6979-6986.

van den Brink, H. J., S. G. Petersen, H. Rahbek-Nielsen, K. Hellmuth and M. Harboe (2006). "Increased production of chymosin by glycosylation." J Biotechnol **125**(2): 304-310.

van den Hombergh, J. P., L. Fraissinet-Tachet, P. J. van de Vondervoort and J. Visser (1997a). "Production of the homologous pectin lyase B protein in six genetically defined protease-deficient *Aspergillus niger* mutant strains." Curr Genet **32**(1): 73-81.

van den Hombergh, J. P., M. D. Sollewijn Gelpke, P. J. van de Vondervoort, F. P. Buxton and J. Visser (1997b). "Disruption of three acid proteases in *Aspergillus niger*--effects on protease spectrum, intracellular proteolysis, and degradation of target proteins." Eur J Biochem **247**(2): 605-613.

Wallis, G. L., R. J. Swift, F. W. Hemming, A. P. Trinci and J. F. Peberdy (1999). "Glucoamylase overexpression and secretion in *Aspergillus niger*: analysis of glycosylation." Biochim Biophys Acta **1472**(3): 576-586.

Wang, Y., E. Fuchs, R. da Silva, A. McDaniel, J. Seibel and C. Ford (2006). "Improvement of *Aspergillus niger* Glucoamylase Thermostability by Directed Evolution." Starch - Stärke **58**(10): 501-508.

Ward, M., C. Lin, D. C. Victoria, B. P. Fox, J. A. Fox, D. L. Wong, H. J. Meerman, J. P. Pucci, R. B. Fong, M. H. Heng, N. Tsurushita, C. Gieswein, M. Park and H. Wang (2004). "Characterization of humanized antibodies secreted by *Aspergillus niger*." Appl Environ Microbiol **70**(5): 2567-2576.

Ward, M., L. J. Wilson, K. H. Kodama, M. W. Rey and R. M. Berka (1990). "Improved production of chymosin in *Aspergillus* by expression as a glucoamylase-chymosin fusion." Biotechnology (N Y) **8**(5): 435-440.

Welihinda, A. A., W. Tirasophon and R. J. Kaufman (1999). "The cellular response to protein misfolding in the endoplasmic reticulum." Gene Expr **7**(4-6): 293-300.

Wessels, J. G. (1993). "Fruiting in the higher fungi." Adv Microb Physiol **34**: 147-202.

Wong, C. M., K. H. Wong and X. D. Chen (2008). "Glucose oxidase: natural occurrence, function, properties and industrial applications." Appl Microbiol Biotechnol **78**(6): 927-938.

Wucherpfennig, T., T. Hestler and R. Krull (2011). "Morphology engineering--osmolality and its effect on *Aspergillus niger* morphology and productivity." Microb Cell Fact **10**: 58.

Wösten, H. A. B., S. M. Moukha, J. H. Sietsma and J. G. H. Wessels (1991). "Localization of growth and secretion of proteins in *Aspergillus niger*." Journal of General Microbiology **137**(8): 2017-2023.

Yaver, D. and P. Nham (2003). Promoter variants for expressing genes in a fungal cell.

Yoder, W. T., J. Lehmbeck and R. Borriss (2004). Heterologous expression and protein secretion in filamentous fungi. Advances in fungal biotechnology for industry, agriculture, and medicine, Kluver Academic**:** 201-219.

Chapter 3 Systems Biology approaches

Since the development of the first industrial processes, a major objective to maximize profit has sparked the desire for continuous process optimization. The same is applicable for biotechnological processes, yet with one major exception; the addition of the microorganism, thus challenging the optimization process multidimensionally, by creating almost infinite degrees of freedom. This challenge has typically been addressed by improving the microorganism through strain improvement programs, mediated by mutagenesis and followed by fermentation optimization (e.g. temperature, media composition, feed profile). This strategy poses several drawbacks; the changes obtained in the microorganism is unknown, hence optimizing the fermentation conditions to unspecified alterations can be troublesome, e.g. changed nutritional demand of the microorganism. Together with issues of strain instability, after several rounds of mutagenesis, and difficulties reaching above a certain titter (plateauing), this type of optimization is less desirable. The development of genetic engineering, metabolic engineering and "omic" methods, has enabled the possibility of selecting targets and performing precise genetic changes in the microorganism. To generate a background for those methods, which is also the basis of the research presented in this thesis, overviews of Systems Biology topics will be provided in this chapter.

As described in the previous chapter, the first defined process utilizing *A. niger* was initiated with Currie discovery in 1917. Throughout the many years, *A. niger* is still the main cell factory used for citrate production. This has been achieved through continuous advances in both fermentation technology and strain improvement, as outlined in chapter 2.

Before the 1980's, where the DNA mediated transformation was developed for Aspergilli (Ballance et al. 1983), the only technique for strain improvement, was classical strain improvement through mutagenesis and screening. It was a simple, empirical and in many cases, a powerful technique. However, the changes made were difficult to identify and interpret. With the development of molecular techniques, studies analyzing the role of individual cell components emerged, and efforts on strain improvement through genetic engineering, later paved the way for metabolic engineering, tracing the beginnings of a new field of research.

Metabolic engineering was first introduced by Bailey (1991) as, "the improvement of cellular activities by manipulation of enzymatic, transport and regulatory functions of the cell with the use of DNA recombinant technology." This technique, also referred as the metabolic engineering cycle, consisting of four steps and typically initiated by an analysis phase. The objective: to analyze the metabolic pathways of a

microorganism and determine the constraints and their effects on the production of desired compounds. These predicted changes can then be implemented into the strain by genetic engineering, constituting a synthesis phase. Followed by the characterization step where the results of the genetic alterations are examined *in vivo*. The last phase comprises analysis and evaluation of the data from the previous step. With the obtained knowledge the cycle can restart.

As indicated, metabolic engineering is a useful systematical method; however, due to cellular robustness, as a result of enzyme redundancies and complex regulatory circuits, often enable the cell to counteract the genetic modifications. For this reason application of Systems Biology approaches, have become increasingly popular in assisting in identifying targets for genetic engineering. Especially the increasing number of available genomes has enabled the shift, into integrating data from several "omics" techniques. Facilitating a holistic view on the cellular functions and aiding the target selection for strain improvement.

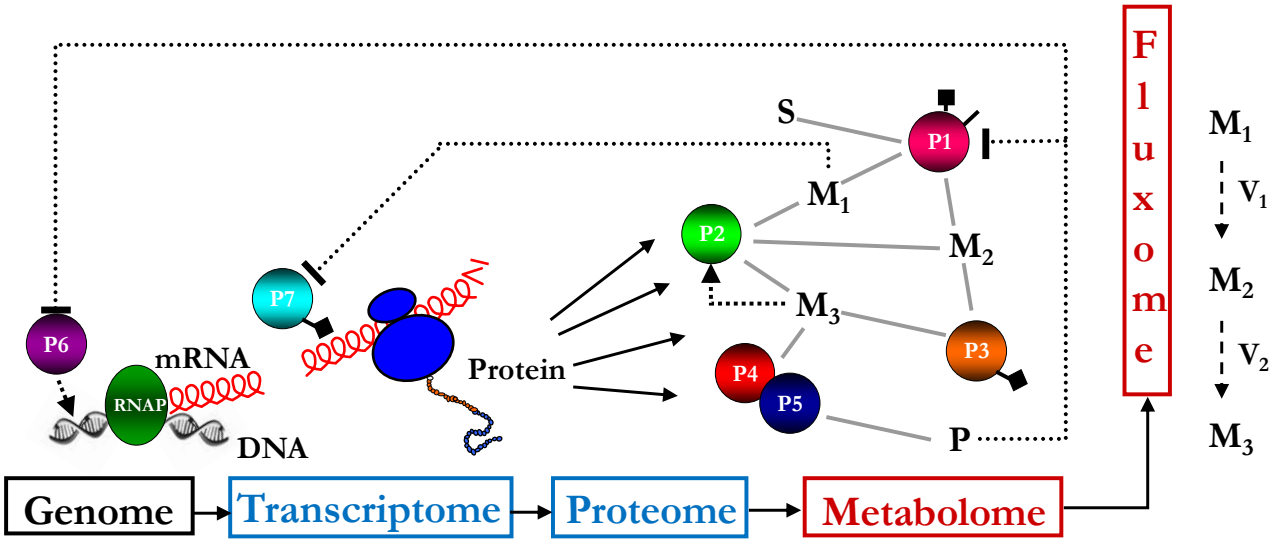

Figure 3.1 An overview of the central dogma and its connection to the "omics". Figure adapted from Jewett et al. (2005).

3.1 "omics" techniques

The following sections will present the different Systems Biology strategies and technologies that can be applied to *Aspergillus*.

3.1.1 Genome

Prior to having complete genome sequences, biological research projects were primarily focusing on a limited number of genes, or proteins. Genetic screens or biochemical strategies were applied to identify new genes and proteins involved in a biological process. Isolating and sequencing genes and proteins was a slow, laborious process. The advent of large-scale DNA sequencing fundamentally changed biological research.

The release of the first eukaryote genome, in 1996 of *S. cerevisiae* (Goffeau et al. 1996) initiated the genomic era for eukaryotes. Shortly after, the genome sequence of the multicellular organism Caenorhabditis elegans followed in 1998 (C. elegans Sequencing Consortium 1998), but still it took three more years for the first filamentous fungal genome to be published. At the beginning of 2001 the draft version of *N. crassa* genome was released and later the final version was published in 2003 (Galagan et al. 2003), followed by the release of the *A. nidulans* genome (Galagan et al. 2005).

Today, three *A. niger* genomes are publicly available (an outline can be found in table 3.1). The first sequence of an *A. niger* genome was completed already in the end of 2001, by the Dutch company DSM (DSM 2001). The strain was the CBS 518.88, a mutant isolated after mutagenesis and selection for improved glucoamylase production, an ancestor of currently used enzyme production strains. The access was however restricted to collaborators until 2007 (Pel et al. 2007). In 2005, the American company Integrated Genomics announced that they had completed sequencing the *A. niger* lab strain ATCC 9029 also named NRRL 3. Followed by the genome sequence of ATCC 1015 strain by The Joint Genome Institute, the wildtype strain used in the first patented citric acid process (Andersen et al. 2011).

Table 3.1 An overview of the completed whole genome sequence projects for *A. niger.* The list is compiled from the GOLD, Genomes OnLine Database (http://www.genomesonline.org).

Strain	Year of release	Scaffolds	Coverage	Size (Mb)	Predicted ORF
CBS 513.88	2001/2007	498	7.5X	33.9	14431
ATCC 9029	2005	9510	4X	N/A	N/A
ATCC 1015	2006	24	8.9X	34.9	11200

Currently two *A. niger* sequencing projects are in progress. Those are the ATCC 1015 derived strain ATCC 11414 and a wild type strain ATCC 64973 (GOLD, 2012).

3.1.2 Transcriptome

Transcriptomics is the study of mRNA expression levels on a genome wide basis. The increased availability of genome sequences for countless of organisms, has facilitated the application of DNA microarrays, as routinely applied tool, to study the transcriptome. This trend is illustrated in figure 3.2.

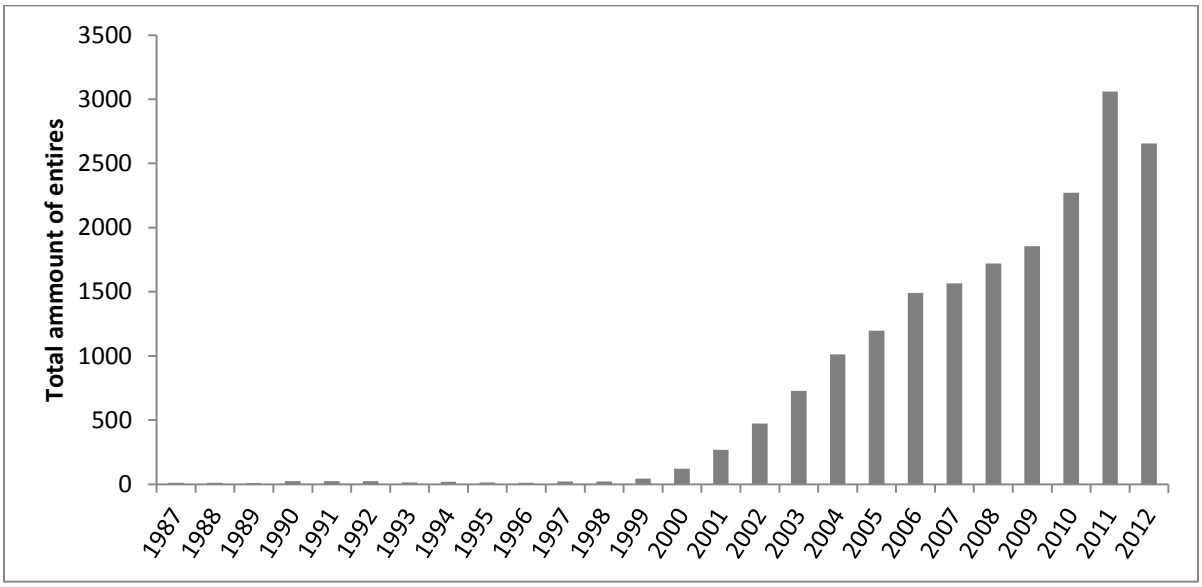

Figure 3.2 The quantity of indexed papers containing "DNA microarray", "transcription analysis" or "transcriptome" in the abstract within the PubMed database per year. In the period from 1970 to 1987 19 articles exists.

It is evident from figure 3.2 that there has been an exponential development in publications within this subject, from the mid 90's to 2003. A major focus during this period was the challenges connected to the technology and the statistical data handling. After many of these issues were solved, the focus has now shifted into applying the technology as a tool for assisting in solving biological questions. Today, more than 90 articles have been published, where the microarray technology has been applied within the *Aspergillus* genus, 19 of these include *A. niger*.

The microarray technology, the foundation of transcriptomics, evolved from Southern/Northern blotting techniques, where oligonucleotides were attached to a substrate and probed with a known DNA sequence. (Maskos and Southern 1992). Prior to this method, early arrays were made by spotting cDNAs onto filter paper. The arrays required a large sample volume and only allowed simultaneously monitoring of a few genes (Augenlicht and Kobrin 1982, Augenlicht et al. 1987). The first modern microarray analysis was presented by (Schena et al. 1995). Employing automatic robotic spotting of DNA, microarrays were

constructed and quantitative expressions of 45 *Arabidopsis thaliana* genes in two biological states were examined. First transcriptome study in *A. niger* was by MacKenzie et al. (2005). The UPR response (outlined in chapter 2) was examined under reductive stress induced by dithiothreitol (DTT), but it was concluded that DTT alone does not provide for specific induction of UPR genes.

Expression arrays are a powerful tool to identify the transcriptional regulation between two or more biological states. This was illustrated by the study of Salazar et al. (2009). Microarrays were applied to examine the transcriptional regulation of glycerol metabolism in Aspergilli. By comparing *A. niger*, *A. nidulans* and *A. oryzae*, a conserved response of 88 genes across the species was identified as being differentially expressed when utilizing glycerol as carbon sources. Other examples are outlined in chapter 4 and 6, where microarrays were used to identify the cellular response, causing acid overproduction, either induced by depletion of manganese or deleting of a pH responding transcription factor, respectively.

Identifying co-regulation can be a valuable technique to gain functional information of unknown genes, since genes that participate in the same pathway, often share similar expression profiles (Eisen et al. 1998, Chou et al. 2007). Identification of co-regulation can be done, using cluster algorithms on transcriptome data, yet a stronger method is by combining clustering with promoter analysis. First applied by Ideker et al. (2001), the method was used to identify the binding sites for the transcriptional activator Gal4 in *S. cerevisiae*. A similar strategy was applied in *A. niger* by Andersen et al. (2009) to investigate the ambient pHs effect on acid production. Applying clustering of transcription profiles, along with promoter analysis, resulted in identification of all six putative orthologous in the pacC/palABCFHI pathway. This is a conserved fungal signal-transduction and transcriptional-regulation system for pH sensing (MacCabe et al. 1996).

With a focus of cellular heterogeneity within an isogenic cell population de Bekker et al. (2011) developed a protocol for single cell transcriptome analysis of *A. niger* hyphae. The study demonstrated that hyphae experiencing identical environmental conditions are heterogeneous with respect to mRNA composition. The authors speculated whether single cell transcriptome analysis could be a necessary tool to provide an accurate understanding of the metabolic processes within a cell. The technique is still in its early phase but represents a new study area especially with great potential for investigating interactions as symbiotic/parasitic relationships.

The recent advances in high-throughput sequencing technology have enabled the possibility to shift from microarray based analysis into RNA sequencing (RNA-seq). Compared with microarrays, RNA-Seq could in theory identify all of the expressed transcripts of cells, as opposed to microarrays relying on *A priori* knowledge; hence, it cannot detect novel splicing variants and novel transcripts. In addition, RNA-Seq has

low background noise and high sensitivity combined with becoming increasingly cost-effective with the rapid advancements in the technology (Wang et al. 2009, Marguerat and Bahler 2010).

After genomics and transcriptomics, proteomics is considered the next step in the study of biological systems.

3.1.3 Proteome

Proteomics is a large-scale study of proteins encoded by ORFs in an organism, with special emphasis on physical and biochemical function. The term proteomics covers many aspects of protein analysis, including identification, quantification, characterization, post-translational modifications and cellular localization, recently reviewed by Kniemeyer (2011).

One of the drawbacks using transcriptomics is the lack of capturing post transcriptional regulation. This has been exemplified in several studies where scalability between mRNA and protein abundance is poor. Reviewed by de Hoog and Mann (2004) the authors stated, "*biological function is not carried out by the static genome but mainly by the dynamic population of proteins determined by an interplay of gene and protein regulation with extracellular influences"*. This makes proteomics an important tool to give a more complete picture of regulatory networks.

Proteins vary greatly in size, shape, isoelectric point, hydrophobicity and biological affinity. In addition to the diversity of physical properties, protein abundance in a proteome can range over six to twelve order of magnitude. Transcription factors may range from one to ten copies pr cell, while structural proteins may be present at 1,000,000 copies per cell (Ghaemmaghami et al. 2003). Compare to the transcriptome an organism's proteome is considerably more complicated. Alternative RNA splicing, RNA editing, proteolytic processing and posttranslational modifications dramatically increase the complexity of a cell's proteome (Modrek and Lee 2002, Zavolan et al. 2002).

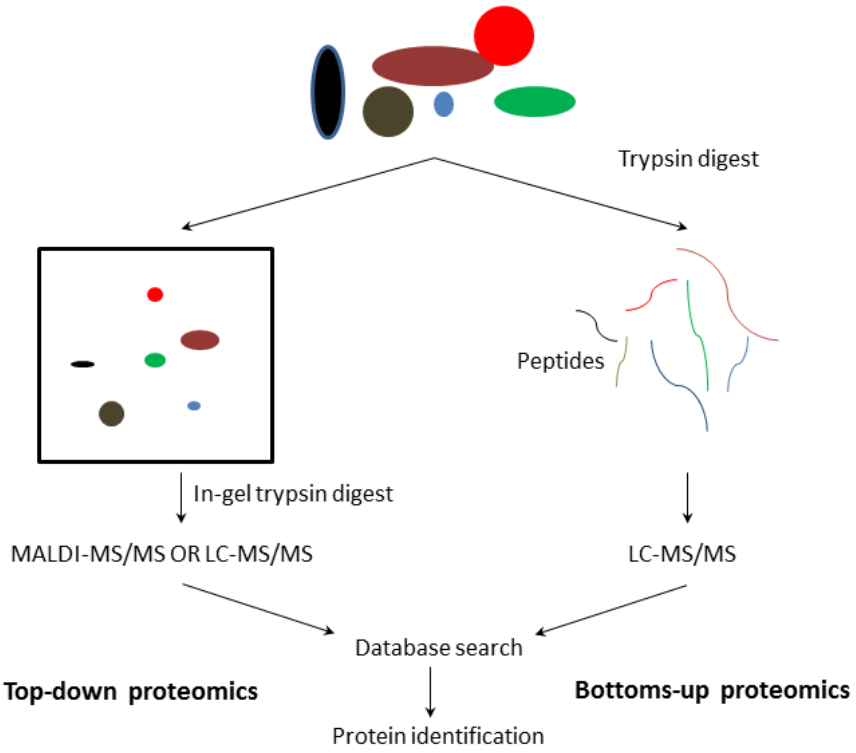

Figure 3.3 The two fundamental different approaches performing modern proteomics. A protein sample is fractionated by gel electrophoresis, termed top-down or digested by trypsin prior to analysis designated bottoms up.

Prior to available genome sequences, proteomics consisted virtually of only two-dimensional gel electrophoresis (2-DE), or top-down proteomics (figure 3.3). The method typically consists of isoelectric focusing of proteins in the first dimension, followed by separation of proteins according to their molecular mass in the second dimension. The proteins of interest could then be isolated and later sequenced using Edman sequencing, identifying one amino acid at the time (Niall 1973). First, applied to *A. nidulans* by Weatherbee (1985) to investigate the role of tubulin in fungal development. The 2D gels and Edman sequencing are slow and laborious techniques. However, with advances in multiplexing techniques designated as differential gel electrophoresis (DIGE), and improved protein sequencing techniques as Matrix-assisted laser desorption/ionization-Time of Flight (MALDI-TOF), the 2D gels is still today an important technique, as it allows studies of native proteins (top down).

The improvement in mass spectrometry (MS) and the availability of genome sequences, tandem-MS/MS for peptide and protein identification and quantification is now possible. Combined with liquid chromatography (LC), complex protein samples can be separated and analyzed and consequently avoiding the laborious 2-DE. Two fundamentally different methods exist. The first technique, termed shutgun proteomics is a bottoms up approach (figure 3.3), initially described by McCormack et al. (1997). This

method employs a sample preparation step, where the protein mixture is digested by a protease, typically trypsin, reducing the native proteins into peptides of 1-3 kDa. The treatment aids both the identification and the quantification, of the proteins. The sample is then separated using liquid chromatography, followed by tandem MS/MS. Next follows a crucial step of protein identification. An automated process using a database searching algorithm based on the DNA-predicted protein sequence. Lastly comes, the quantification step, which can be done with or without labels (e.g isotopic, Isobaric tag) and have recently been reviewed by Porteus et al. (2011). The shutgun method has become the workhorse in modern proteomics, with high throughput and automation. Therefore, this method was selected as the method of choice in chapter 4. Nevertheless, the bottom-up approach has distinct limitations in characterizing protein modifications, due to only a small fraction of peptides is recovered from digestion. This ultimately results in low percentage coverage of the protein sequence. In contrast to the shutgun approach, top-down MS analysis of intact proteins was demonstrated by Breuker et al.(2008). This has recently become possible with the newest generation of Fourier-transform mass spectrometer that has a unique high mass resolving power combined with high accuracy. However, this method still faces many technical challenges, as protein solubility compared with peptides, sensitivity, detection limits and the demand for high-end instrumentation making top-down MS in its early developmental stage (Zhang and Ge 2011).

A summary of the different proteomic techniques can be found in table 3.2.

Table 3.2 Proteomics strategies

Technique	Descriptions	Advances / Disadvances
2-DE	Two dimensional gel analysis of native proteins	Analysis on native proteins / Laborious, **high variance** due to gel to gel variation
DIGE	Two dimensional gel analysis with sample multiplexing of native proteins	Analysis on native proteins, **low variance** compared with 2-DE / Laborious
Shutgun-MS	LC-MS/MS analysis of trypsin digested proteins	Highly automated sample prep. and run, **low to moderate variance** dependent on method and equipment / Trypsin digestion necessary, only abundant peptides is identified
Top-down MS	LC-MS/MS analysis of native proteins	Highly automated sample prep. and run, **low variance** / Require state of the art equipment, protein solubility, emerging technique

Even with the development for sample preparation specific for filamentous fungi and compatible with LC-MS/MS (Kim et al. 2007), the majority of proteome studies in *Aspergillus* are based on 2-DE techniques. The challenges within the experimental procedures reflects the number of studies on *Aspergillus* using proteomics compared to transcriptomics yielding a factor of three fewer studies and for *A. niger* only four studies exist.

The first full proteome study in *A. niger* was conducted by Sorensen et al. (2009), where the full proteome was examined using 2-DE combined with MALDI. This was applied to uncover how fumonisin production by *A. niger* was influenced by starch and lactate addition. The study was performed on agar plates containing complex media, 59 spots were picked for identification, yet only 32 proteins (19 with putative annotation, 13 with predicted function) were identified. On this basis, the authors concluded that fumonisin production by *A. niger* was regulated by the pool of acetyl-CoA, a precursor for many secondary metabolites. Fumonisin production in *A. niger* is also the subject of chapter 8.

The work by Lu et al. (2010) presents a comprehensive study of *A. niger's* physiology growing in defined medium with xylose or maltose as carbon source, both in shake flasks and bioreactors. 2-D gels with MALDI-TOF were exploited for the intracellular proteome whereas a shotgun LC MS/MS method was used for extracellular proteome analysis. The choice of carbon source greatly affects the extracellular proteome, but has minor influence on the intracellular proteome. Lastly, the choice of cultivation had a profound effect on the intracellular proteome especially on the protein folding machinery.

The first LC-MS/MS whole cell lysate proteome study in *A. niger* is the one of Ferreira de Oliveira et al. (2010) where the effects of the xylose induction of cellulase and hemicellulase enzyme secretion was examined. 282 proteins were found only in the xylose induced samples. Within this subset an increase in small GTPases, known to be associated with polarized growth, exocytosis, and endocytosis was identified together with proteins related with the endoplasmic-reticulum-associated degradation.

3.1.4 Metabolomics and fluxomics

The metabolome refers to the complete set of small-molecule metabolites, including the primary and secondary metabolites, metabolic intermediates, and signaling molecules. The fluxome is referred to as the totality of all fluxes in a system.

Where transcriptomics and proteomics provide a measure of metabolic network capacities, metabolomics and fluxomics, deliver a measure of thermodynamic driving forces leading to a direct measure of the metabolic phenotype. However, the study of the full set of metabolites and fluxes is a complex task compared to transcriptomics and proteomics.

The central metabolomics challenge is that, no single extraction procedure works for all metabolites because conditions that stabilize one type of compound will destroy other types or interfere with their analysis. Consequently, a combination of several extraction protocols and analytical methods are required to separate and identify the metabolites. The complex nature of obtaining large scale quantitative metabolome data in *Aspergillus* are reflected in the few published studies. Of the 15 research articles, only one can be classified as a large scale, with more than 450 identified metabolites (Kouskoumvekaki et al. 2008). To circumvent the complexity of large scale metabolomics, metabolite profiling (Smedsgaard and Nielsen 2005), and reporter metabolite identification (Patil and Nielsen 2005) has been developed. Both approaches rely on identifying a subset of metabolites, to elucidate changes in parts of the metabolism (Vongsangnak et al. 2009).

Fluxomics carries similar issues of multiple extraction necessities, but the analytical part is most often performed solely by GC-MS. Fluxes are estimated indirectly and typically a measurement of the fate, by an isotopic label in various metabolite pools. To successfully perform these estimations, the requirement of an isotopic steady-state is of vital importance. Identical to metabolomics, very few research papers have been published within fluxome analysis in fungi. The study from Pedersen et al. (2000), flux analysis was applied to characterized an oxalic acid nonproducing strain of *A. niger*. The analysis revealed that, the lack of oxalate formation resulted in, increased flux through the Pentose Phosphate Pathway. David et al. (2005) applied fluxomics to examine creA influences of *A. nidulans* during growth on glucose and xylose. Deletion of the creA gene resulted in a 20% decrease in the flux through the oxidative part of the pentose-phosphate pathway on glucose; contrary, addition of xylose to the growth medium of the mutant led to an increase of about 40% in the activity of the oxidative part of the pentose-phosphate pathway. The few metabolomics and fluxomics studies, in fungi, underlines the high level of complexity for these two “omics” techniques; hence, neither metabolomics nor fluxome were applied in the research presented in this thesis.

As observed from figure 3.1, all “omics” are derived from the same biomass. Except genomics, which can be considered static, the remaining “omics” are highly dynamic and influenced by the environment the sample originates. Illustrated by single cell transcriptomics, cellular heterogeneity within an isogenic cell population is apparent. This signifies that the signals/data obtained is not from a single source, but rather an average

across the cells. Accordingly, controlling and minimizing the cellular heterogeneity is vital to ensure quality data and can be arrived by submerged cultivations.

3.2 Biomass preparation

Several methods, for generating biomass using submerged cultures exist. The most simple and fast technique is a shake flask cultivation, typically carried out in an Erlenmeyer flask equipped with a cotton stopper. The aeration in shake flasks is achieved by simple gas/liquid contact aided by rotary movement hence does not require any special equipment. However, this method has several distinct drawbacks. Active pH control is conventionally not possible in a shake flask, making the pH non constant. This can to some extend be counteracted by adding a buffer agent to the medium, yet in most cases not enough to keep the pH steady, especially when working with organisms producing acids. Another major drawback is the lack of bioprocess monitoring, as CO_2 production, an essential parameter to determine the biological state of the microorganism. This parameter cannot be measured due to the lack of active aeration of the culture, which also leads to the last major problem; a low oxygen transfer rate. The oxygen transfer rate is primarily dependent upon the volumetric mass transfer coefficient, k_La that in shake flaks is range of 30-60 h^{-1} (Gupta and Rao 2003). Compared to a bioreactor k_La values are in general a factor of 10-20 higher (Garcia-Ochoa and Gomez 2009). Changes in oxygen availability may lead to drastic effects on the metabolism, increasing cellular heterogeneities.

In contrast, a bioreactor offers a high level of monitoring and control of the growing culture. The reactor is aerated, stirred pH controlled and the off gas can be monitored. Operating a bioreactor is laborious task, but the data acquired is superior compared to those obtained from shake flasks. A bioreactor can be operated as batch, continuous or fed-batch mode. Especially the continuous mode, also termed a chemostat, is the gold standard within obtaining a homogenous biomass by reaching a steady state. A steady state is defined as a stable condition that does not change overtime and it is characterized by constant substrate and product concentrations. The steady state is obtained through a strict control of the growth rate. Hereby, it is possible to study the influence of a single operational parameter and with all other parameters kept constant, greatly lowers the variance between the samples.

One of the challenges in reaching a steady state is to have a homogenous cell culture, but unlike yeast and bacteria, filamentous fungi can have several growth morphologies, as described in chapter 2. The many parameters affecting the morphology, determine the possibility of reaching a steady state. An indication of the difficulties in applying chemostat cultivation for studying *A. niger,* can be found in the literature. Less

than 8 % of all cultivation studies of *A. niger* involve a chemostat (29/373), comparing to 20 % (397/1843) of *S. cerevisiae*. Further details regarding *A. niger* chemostat cultivations, can be found in chapter 6.

Special circumstances exist where a bioreactor cannot be applied, illustrated in chapter 4. As mentioned in chapter 2 manganese depletion is an initiator of the citrate overflow metabolism in *A. niger*. Consequently, examination of this response cannot to be conducted with contact to a metal surface due to manganese adsorption. A silanized glass surface is however unable to adsorb ions leaving shake flaks the only option to study this response.

The following chapter provides an in-depth analysis of the transcriptional and translational changes in *A. niger's* metabolism leading to the citrate overflow metabolism.

3.3 Reference

Andersen, M. R., L. Lehmann and J. Nielsen (2009). "Systemic analysis of the response of *Aspergillus niger* to ambient pH." Genome Biol **10**(5): R47.

Andersen, M. R., M. P. Salazar, P. J. Schaap, P. J. van de Vondervoort, D. Culley, J. Thykaer, J. C. Frisvad, K. F. Nielsen, R. Albang, K. Albermann, R. M. Berka, G. H. Braus, S. A. Braus-Stromeyer, L. M. Corrochano, Z. Dai, P. W. van Dijck, G. Hofmann, L. L. Lasure, J. K. Magnuson, H. Menke, M. Meijer, S. L. Meijer, J. B. Nielsen, M. L. Nielsen, A. J. van Ooyen, H. J. Pel, L. Poulsen, R. A. Samson, H. Stam, A. Tsang, J. M. van den Brink, A. Atkins, A. Aerts, H. Shapiro, J. Pangilinan, A. Salamov, Y. Lou, E. Lindquist, S. Lucas, J. Grimwood, I. V. Grigoriev, C. P. Kubicek, D. Martinez, N. N. van Peij, J. A. Roubos, J. Nielsen and S. E. Baker (2011). "Comparative genomics of citric-acid-producing *Aspergillus niger* ATCC 1015 versus enzyme-producing CBS 513.88." Genome Res **21**(6): 885-897.

Augenlicht, L. H. and D. Kobrin (1982). "Cloning and screening of sequences expressed in a mouse colon tumor." Cancer Res **42**(3): 1088-1093.

Augenlicht, L. H., M. Z. Wahrman, H. Halsey, L. Anderson, J. Taylor and M. Lipkin (1987). "Expression of cloned sequences in biopsies of human colonic tissue and in colonic carcinoma cells induced to differentiate in vitro." Cancer Res **47**(22): 6017-6021.

Bailey, J. E. (1991). "Toward a science of metabolic engineering." Science **252**(5013): 1668-1675.

Ballance, D. J., F. P. Buxton and G. Turner (1983). "Transformation of Aspergillus nidulans by the orotidine-5'-phosphate decarboxylase gene of Neurospora crassa." Biochemical and biophysical research communications **112**(1): 284-289.

Breuker, K., M. Jin, X. Han, H. Jiang and F. W. McLafferty (2008). "Top-Down Identification and Characterization of Biomolecules by Mass Spectrometry." Journal of the American Society for Mass Spectrometry **19**(8): 1045-1053.

Chou, J. W., T. Zhou, W. K. Kaufmann, R. S. Paules and P. R. Bushel (2007). "Extracting gene expression patterns and identifying co-expressed genes from microarray data reveals biologically responsive processes." BMC Bioinformatics **8**: 427.

Consortium, C. e. S. (1998). "Genome sequence of the nematode C. elegans: a platform for investigating biology." Science **282**(5396): 2012-2018.

David, H., A. M. Krogh, C. Roca, M. Åkesson and J. Nielsen (2005). "CreA influences the metabolic fluxes of Aspergillus nidulans during growth on glucose and xylose." Microbiology **151**(7): 2209-2221.

de Bekker, C., O. Bruning, M. J. Jonker, T. M. Breit and H. A. Wosten (2011). "Single cell transcriptomics of neighboring hyphae of *Aspergillus niger*." Genome Biol **12**(8): R71.

de Hoog, C. L. and M. Mann (2004). "Proteomics." Annu Rev Genomics Hum Genet **5**: 267-293.

DSM. (2001). "DSM determines DNA sequence of *Aspergillus niger* genome." from http://www.dsm.com/en_US/cworld/public/media/pages/press-releases/45_01_Aspergillus.jsp.

Eisen, M. B., P. T. Spellman, P. O. Brown and D. Botstein (1998). "Cluster analysis and display of genome-wide expression patterns." Proc Natl Acad Sci U S A **95**(25): 14863-14868.

Ferreira de Oliveira, J. M., M. W. van Passel, P. J. Schaap and L. H. de Graaff (2010). "Shotgun proteomics of *Aspergillus niger* microsomes upon D-xylose induction." Appl Environ Microbiol **76**(13): 4421-4429.

Galagan, J. E., S. E. Calvo, K. A. Borkovich, E. U. Selker, N. D. Read, D. Jaffe, W. FitzHugh, L. J. Ma, S. Smirnov, S. Purcell, B. Rehman, T. Elkins, R. Engels, S. Wang, C. B. Nielsen, J. Butler, M. Endrizzi, D. Qui, P. Ianakiev, D. Bell-Pedersen, M. A. Nelson, M. Werner-Washburne, C. P. Selitrennikoff, J. A. Kinsey, E. L. Braun, A. Zelter, U. Schulte, G. O. Kothe, G. Jedd, W. Mewes, C. Staben, E. Marcotte, D. Greenberg, A. Roy, K. Foley, J. Naylor, N. Stange-Thomann, R. Barrett, S. Gnerre, M. Kamal, M. Kamvysselis, E. Mauceli, C. Bielke, S. Rudd, D. Frishman, S. Krystofova, C. Rasmussen, R. L. Metzenberg, D. D. Perkins, S. Kroken, C. Cogoni, G. Macino, D. Catcheside, W. Li, R. J. Pratt, S. A. Osmani, C. P. DeSouza, L. Glass, M. J. Orbach, J. A. Berglund, R. Voelker, O. Yarden, M. Plamann, S. Seiler, J. Dunlap, A. Radford, R. Aramayo, D. O. Natvig, L. A. Alex, G. Mannhaupt, D. J. Ebbole, M. Freitag, I. Paulsen, M. S. Sachs, E. S. Lander, C. Nusbaum and B. Birren (2003). "The genome sequence of the filamentous fungus Neurospora crassa." Nature **422**(6934): 859-868.

Galagan, J. E., S. E. Calvo, C. Cuomo, L. J. Ma, J. R. Wortman, S. Batzoglou, S. I. Lee, M. Basturkmen, C. C. Spevak, J. Clutterbuck, V. Kapitonov, J. Jurka, C. Scazzocchio, M. Farman, J. Butler, S. Purcell, S. Harris, G. H. Braus, O. Draht, S. Busch, C. D'Enfert, C. Bouchier, G. H. Goldman, D. Bell-Pedersen, S. Griffiths-Jones, J. H. Doonan, J. Yu, K. Vienken, A. Pain, M. Freitag, E. U. Selker, D. B. Archer, M. A. Penalva, B. R. Oakley, M. Momany, T. Tanaka, T. Kumagai, K. Asai, M. Machida, W. C. Nierman, D. W. Denning, M. Caddick, M. Hynes, M. Paoletti, R. Fischer, B. Miller, P. Dyer, M. S. Sachs, S. A. Osmani and B. W. Birren (2005). "Sequencing of Aspergillus nidulans and comparative analysis with A. fumigatus and A. oryzae." Nature **438**(7071): 1105-1115.

Garcia-Ochoa, F. and E. Gomez (2009). "Bioreactor scale-up and oxygen transfer rate in microbial processes: An overview." Biotechnology Advances **27**(2): 153-176.

Ghaemmaghami, S., W. K. Huh, K. Bower, R. W. Howson, A. Belle, N. Dephoure, E. K. O'Shea and J. S. Weissman (2003). "Global analysis of protein expression in yeast." Nature **425**(6959): 737-741.

Goffeau, A., B. G. Barrell, H. Bussey, R. W. Davis, B. Dujon, H. Feldmann, F. Galibert, J. D. Hoheisel, C. Jacq, M. Johnston, E. J. Louis, H. W. Mewes, Y. Murakami, P. Philippsen, H. Tettelin and S. G. Oliver (1996). "Life with 6000 genes." Science **274**(5287): 546, 563-547.

Gupta, A. and G. Rao (2003). "A study of oxygen transfer in shake flasks using a non-invasive oxygen sensor." Biotechnology and Bioengineering **84**(3): 351-358.

Ideker, T., T. Galitski and L. Hood (2001). "A new approach to decoding life: systems biology." Annu Rev Genomics Hum Genet **2**: 343-372.

Jewett, M., A. Oliveira, K. Patil and J. Nielsen (2005). "The role of high-throughput transcriptome analysis in metabolic engineering." Biotechnology and Bioprocess Engineering **10**(5): 385-399.

Kim, Y., M. P. Nandakumar and M. R. Marten (2007). "Proteomics of filamentous fungi." Trends Biotechnol **25**(9): 395-400.

Kniemeyer, O. (2011). "Proteomics of eukaryotic microorganisms: The medically and biotechnologically important fungal genus Aspergillus." Proteomics **11**(15): 3232-3243.

Kouskoumvekaki, I., Z. Yang, S. O. Jonsdottir, L. Olsson and G. Panagiotou (2008). "Identification of biomarkers for genotyping Aspergilli using non-linear methods for clustering and classification." BMC Bioinformatics **9**: 59.

Lu, X., J. Sun, M. Nimtz, J. Wissing, A. P. Zeng and U. Rinas (2010). "The intra- and extracellular proteome of *Aspergillus niger* growing on defined medium with xylose or maltose as carbon substrate." Microb Cell Fact **9**: 23.

MacCabe, A. P., J. P. Van den Hombergh, J. Tilburn, H. N. Arst, Jr. and J. Visser (1996). "Identification, cloning and analysis of the *Aspergillus niger* gene pacC, a wide domain regulatory gene responsive to ambient pH." Mol Gen Genet **250**(3): 367-374.

MacKenzie, D. A., T. Guillemette, H. Al-Sheikh, A. J. Watson, D. J. Jeenes, P. Wongwathanarat, N. S. Dunn-Coleman, N. van Peij and D. B. Archer (2005). "UPR-independent dithiothreitol stress-induced genes in *Aspergillus niger*." Mol Genet Genomics **274**(4): 410-418.

Marguerat, S. and J. Bahler (2010). "RNA-seq: from technology to biology." Cell Mol Life Sci **67**(4): 569-579.

Maskos, U. and E. M. Southern (1992). "Oligonucleotide hybridizations on glass supports: a novel linker for oligonucleotide synthesis and hybridization properties of oligonucleotides synthesised in situ." Nucleic Acids Res **20**(7): 1679-1684.

McCormack, A. L., D. M. Schieltz, B. Goode, S. Yang, G. Barnes, D. Drubin and J. R. Yates, 3rd (1997). "Direct analysis and identification of proteins in mixtures by LC/MS/MS and database searching at the low-femtomole level." Anal Chem **69**(4): 767-776.

Modrek, B. and C. Lee (2002). "A genomic view of alternative splicing." Nat Genet **30**(1): 13-19.

Niall, H. D. (1973). "Automated Edman degradation: the protein sequenator." Methods Enzymol **27**: 942-1010.

Patil, K. R. and J. Nielsen (2005). "Uncovering transcriptional regulation of metabolism by using metabolic network topology." Proceedings of the National Academy of Sciences of the United States of America **102**(8): 2685-2689.

Pedersen, H., B. Christensen, C. Hjort and J. Nielsen (2000). "Construction and Characterization of an Oxalic Acid Nonproducing Strain of *Aspergillus niger*." Metabolic Engineering **2**(1): 34-41.

Pel, H. J., J. H. de Winde, D. B. Archer, P. S. Dyer, G. Hofmann, P. J. Schaap, G. Turner, R. P. de Vries, R. Albang, K. Albermann, M. R. Andersen, J. D. Bendtsen, J. A. Benen, M. van den Berg, S. Breestraat, M. X. Caddick, R. Contreras, M. Cornell, P. M. Coutinho, E. G. Danchin, A. J. Debets, P. Dekker, P. W. van Dijck, A. van Dijk, L. Dijkhuizen, A. J. Driessen, C. d'Enfert, S. Geysens, C. Goosen, G. S. Groot, P. W. de Groot, T. Guillemette, B. Henrissat, M. Herweijer, J. P. van den Hombergh, C. A. van den Hondel, R. T. van der Heijden, R. M. van der Kaaij, F. M. Klis, H. J. Kools, C. P. Kubicek, P. A. van Kuyk, J. Lauber, X. Lu, M. J. van der Maarel, R. Meulenberg, H. Menke, M. A. Mortimer, J. Nielsen, S. G. Oliver, M. Olsthoorn, K. Pal, N. N. van Peij, A. F. Ram, U. Rinas, J. A. Roubos, C. M. Sagt, M. Schmoll, J. Sun, D. Ussery, J. Varga, W. Vervecken, P. J. van de Vondervoort, H. Wedler, H. A. Wosten, A. P. Zeng, A. J. van Ooyen, J. Visser and H. Stam (2007). "Genome sequencing and analysis of the versatile cell factory *Aspergillus niger* CBS 513.88." Nat Biotechnol **25**(2): 221-231.

Porteus, B., C. Kocharunchitt, R. E. Nilsson, T. Ross and J. P. Bowman (2011). "Utility of gel-free, label-free shotgun proteomics approaches to investigate microorganisms." Appl Microbiol Biotechnol **90**(2): 407-416.

Salazar, M., W. Vongsangnak, G. Panagiotou, M. R. Andersen and J. Nielsen (2009). "Uncovering transcriptional regulation of glycerol metabolism in Aspergilli through genome-wide gene expression data analysis." Mol Genet Genomics **282**(6): 571-586.

Schena, M., D. Shalon, R. W. Davis and P. O. Brown (1995). "Quantitative monitoring of gene expression patterns with a complementary DNA microarray." Science **270**(5235): 467-470.

Smedsgaard, J. and J. Nielsen (2005). "Metabolite profiling of fungi and yeast: from phenotype to metabolome by MS and informatics." Journal of Experimental Botany **56**(410): 273-286.

Sorensen, B. S., M. R. Horsman, H. Vorum, B. Honore, J. Overgaard and J. Alsner (2009). "Proteins upregulated by mild and severe hypoxia in squamous cell carcinomas in vitro identified by proteomics." Radiother Oncol **92**(3): 443-449.

Vongsangnak, W., M. Salazar, K. Hansen and J. Nielsen (2009). "Genome-wide analysis of maltose utilization and regulation in aspergilli." Microbiology **155**(Pt 12): 3893-3902.

Wang, Z., M. Gerstein and M. Snyder (2009). "RNA-Seq: a revolutionary tool for transcriptomics." Nat Rev Genet **10**(1): 57-63.

Weatherbee, J. A., G. S. May, J. Gambino and N. R. Morris (1985). "Involvement of a particular species of beta-tubulin (beta 3) in conidial development in Aspergillus nidulans." The Journal of cell biology **101**(3): 706-711.

Zavolan, M., E. van Nimwegen and T. Gaasterland (2002). "Splice variation in mouse full-length cDNAs identified by mapping to the mouse genome." Genome Res **12**(9): 1377-1385.

Zhang, H. and Y. Ge (2011). "Comprehensive analysis of protein modifications by top-down mass spectrometry." Circ Cardiovasc Genet **4**(6): 711.

Chapter 4 Transcriptome and proteome analysis of the correlation between citric acid formation and manganese limitation in *Aspergillus niger*

Poulsen L, Dai Z, Panisko EA, Lantz AE, Bruno KS, Daly DS, Nielsen J, Baker SE, Thykaer J

4.1 Abstract

A. niger is well known for its capability to produce citrate in high amounts but despite much research on the mechanisms underlying citrate production, the details of the metabolic response causing citrate production has not been fully understood. Manganese is known to have an important effect on citrate production as manganese limited condition is a requirement to obtain high-level citrate formation. To identify the translational regulation causing citric acid overflow metabolism, we analyzed transcriptome and proteome data from cultivations in manganese limitation and manganese excess conditions. Beside three already described main responses, we identified two novel events. The first metabolic response was strong down regulation of phosphoenolpyruvate carboxykinase (PEPCK) at manganese limited conditions, which was later confirmed by *in vivo* experiments. Down regulation of the first step in the gluconeogenesis while maintaining a high activity through glycolysis leaves no alternative to regulate TCA intermediates than secreting citrate into the medium. Thus, citrate formation is the result of adjustment of the intracellular concentrations of TCA metabolites. The other novel observation was a strong down regulation of two cation transporters at manganese limited conditions. Based on these results, it was argued that shutdown of these two transporters makes the cell unable to maintain homeostasis thereby making secretion of citric acid beneficial.

4.2 Introduction

Citrate is the most intensively produced fungal bulk chemical, with a global production estimated to be above 1,600,000 tons/year in 2007 (Legisa and Mattey 2007). *Aspergillus niger* cultivations meet the largest part of this demand with a process that was first described and patented by Currie in 1917. Despite decades of research, only a limited part of the changes in the metabolism that leads to citric acid overflow metabolism is understood in detail. Three key metabolic events have been stated as being responsible for citric overflow metabolism [review 2007]:

- fast uptake of glucose
- unrestricted metabolic flow through glycolysis
- uncoupling NADH re-oxidation from proton pumping

Furthermore, initiation of overflow metabolism is related to limitation of certain trace metals including Zn^{2+}, Fe^{2+}, Cu^{2+} and especially Mn^{2+} (Shu and Johnson 1948).

Fast uptake of glucose is mediated by *A. niger* having two classes of glucose transporters, an active high affinity transporter (Km = 0.26 mmol) which is present in a wide range of carbon concentrations (Torres et al. 1996b) and a low affinity facilitated diffusion transporter (Km = 3.67 mmol) that is only expressed at high sugar concentration (Torres et al. 1996a). Together, these two transporters ensure a high glucose uptake which facilitates citrate overflow metabolism.

When citrate is being formed, the majority of carbon is being metabolized through the glycolytic pathway (Cleland and Johnson 1954) whereas the pentose phosphate pathway flux is low corresponding to a few percentages of the channeled carbon (Legiša and Mattey 1986). Glycolysis consists of 10 reactions where the steps catalyzed by hexokinase, phosphofructokinase and pyruvate kinase are of special interest as they are exergonic and considered having regulatory functions. The hexokinase mediated phosphorylation of glucose is the first committed step in glucose metabolism. The regulatory importance of hexokinase has been demonstrated both *in silico* (Torres 1994) and *in vitro* ((Schreferl-Kunar et al. 1989) and confirmed by biochemical characterization of the enzyme *in vivo* (Wolschek and Kubicek 1997, Panneman et al. 1998). The second control point is the phosphofructokinase, responsible for phosphorylating fructose-6-phosphate to fructose-1,6-bisphosphate. Before this point, the flux could revert and enter the pentose phosphate pathway and this step is therefore considered the first committed step in the glycolysis. Despite the importance of this regulatory step, it has been shown that glyceraldehyde 3-phosphate dehydrogenase is also of regulatory importance in *A. niger* when grown at high glucose concentrations ((Peksel et al. 2002). An interesting observation since the step catalyzed by glyceraldehyde 3-phosphate dehydrogenase is not

usually considered to have a regulatory function. Pyruvate kinase is the last enzyme of glycolysis converting phosphoenolpyruvate to pyruvate. This was earlier considered to be an important regulatory point in filamentous fungi based on studies in *Neurospora crassa* (Kapoor 1975) and *Mucor rouxii* (Terenzi et al. 1971). However, pyruvate kinase is not considered to have any important regulatory function in *A. niger* (Meixner-Monori et al. 1986).

A. niger have two distinct pathways for NADH reoxidation, one pathway coupled to the proton pumping NADH:ubiquinone oxidoreductase complex (complex 1) responsible for the oxidative phosphorylation and an alternative NADH reoxidation pathway not associated with proton pumping (Wallrath et al. 1992). The latter is found to be constitutive active, however only with 1% of the affinity to NADH compared complex 1 under normal physiological conditions. A connection between the alternative NADH reoxidation pathway and citrate formation has been hypothesized based on data from a high citrate yielding strain, which showed no activity of the complex 1 (Wallrath et al. 1991) and it is also supported by genome scale metabolic modeling (Andersen et al. 2008). In addition, deletion of complex 1 resulted in accumulation of intracellular citrate, but the mutant was not capable of secreting it into the extracellular medium (Schmidt et al. 1992, Promper et al. 1993). The conversion of glucose to citrate generates one mole of ATP and two moles of NADH, and in order to ensure a high citrate yield on glucose it is therefore important to ensure efficient removal of excess ATP and NADH reducing equivalents(Andersen et al. 2008).

The role of Mn^{2+} is especially interesting in terms of citric acid production, since limitation of this metal has been shown to be a key contributor for ensuring overflow metabolism towards citrate. The effect of Mn^{2+} has been subjected to several theories. One is that manganese limitation leads to an increase in protein degradation hence increased protein turnover (Ma et al. 1985, Schreferl et al. 1986). Dai et al (2004) confirmed that a number of genes involved in amino acid metabolism are differentially regulated by the depletion of Mn^{2+}. Protein breakdown under manganese limitation results in high intracellular NH_4^+ concentration and the increased intracellular concentration of NH_4^+ was argued to prevent citrate-mediated feedback inhibition of glucose catabolism maintaining a high glycolytic flux (Rohr and Kubicek 1981). However, Papagianni et al. (2005) subsequently showed that the intracellular concentration of NH_4^+ was not affected by protein degradation, since the ammonium ions were combined with glucose forming glucosamine (Papagianni et al. 2005). Citrate permease has also been assigned an important role in citrate production. This permease is responsible for the transport of citrate from the cytosol to the extracellular medium and is required to work against a strong gradient suggesting an ATP dependent process. A study made by (Netik et al. 1997) showed that this permease has a reciprocal regulation of citrate efflux and

uptake controlled by Mn^{2+}. This could imply that it is not the same permease that catalyzes both processes or as proposed by Glusker (1992) that the permease only can transport Mn^{2+} chelated citrate.

As outlined above, the metabolic foundation for citric acid production is of a complex nature and especially the role of manganese depletion is intriguing. In this study, transcriptional profiles of *A. niger* during growth at both Mn^{2+} limited and enriched conditions were characterized, focusing on the metabolic response associated with citric acid production. In addition, proteome analysis was carried out on the same sample material to investigate if the observed transcriptional response could be traced on the protein level.

4.3 Materials and Methods

4.3.1 Strains and spore preparation

A. niger strain (ATCC 11414), obtained from the American Type Culture Collection (12301 Parklawn Drive, Rockville, MD, 20852) was grown on potato dextrose agar plates (PDA) at 30°C for culture maintenance and spore preparation. Cultures were incubated for five days and the spores were harvested by washing with sterile 0.8% Tween 80 (polyoxyethylenesorbitan monooleate). Conidia were enumerated with a hemacytometer. Aliquots of the resulting spore suspension (1×10^9 spores/ml) were used to inoculate baffled-flask liquid cultures.

4.3.2 Media

The citric acid production (CAP) medium contained 140 g/l of glucose, 3.1 g/l NH_4NO_3, 0.15 g/l KH_2PO_4, 0.15 g/l NaCl, 2.2 g/l $MgSO_4 \cdot 7H_2O$, 6.6 mg/l $ZnSO_4 \cdot 7H_2O$, and 0.1 mg/l $FeCl_3$ adjusted to pH 2.0 with 4 M H_2SO_4. Cations were removed from the glucose solution by ion-exchange on Dowex 50W-X8, 100-200 mesh, H cation exchange resin (Fisher Scientific, Pittsburgh, PA) prior to adding the other nutrient components. Manganese concentration in the media was adjusted by the addition of appropriate volumes of a stock solution of $MnCl_2 \cdot 4H_2O$ (10 mM). The Mn^{2+} concentration in the media, before and after growth of *A. niger*, was determined using a Hewlett-Packard (HP) 4500 series inductively coupled plasma-mass spectrometry with sub-part per billion detection limit (ICP-MS, Agilent Technologies, Palo Alto, CA). The samples and manganese standard solutions were serially diluted with ultra-pure de-ionized water to optimal mass ranges before being injected into the ICP-MS for measurement. Three replicates of each sample and standard were measured. Concentrations of manganese in the samples were calculated based on the signal response of the manganese standards.

4.3.3 Culture methods

Glass baffled-flasks of 1000 ml were silanized with SigmaCote® (Sigma, St. Louis, MO) to minimize leaching of metals. To produce sufficient biomass for RNA and protein isolations, nine one-liter baffled-flasks containing 250 ml of CAP media with 10 ppb Mn^{2+} were used. Each flask was inoculated with 1×10^6 spores/ml and incubated for thirty hours at 30°C and 220 rpm to obtain large-amount biomass in pelleted morphology, then 1000 ppb Mn^{2+} was added to three of the flasks to induce filamentous growth and the same amount of H_2O was added into another three flasks for control. This procedure was replicated three times with the manganese induction of filamentous growth for one hour. Prior to harvest the biomass,

small aliquot was taken and observed under microscopy to examine the filamentous growth. The growth of fungal cultures was suspended by rapid cooling in an ice-water bath. The biomass was immediately separated from the culture supernatant by centrifugation for 10 minutes at 4^{o}C and 10,000 g. The biomass was transferred from 500 ml centrifugation bottles to 50 ml centrifugation tubes, washed with 50 ml ice-cold 50mM phosphate buffer, and centrifuged again at 9,000 g for 5 min. The biomass was immediately frozen in liquid N_2 for five minutes and stored at -80^{o}C.

4.3.4 RNA isolation

Total RNA was isolated from *A. niger* according to the modified acid-guanidinium isothiocyanate phenol-chloroform extraction method previously described (Chomczynski and Sacchi 1987; Dai, Hooker et al. 2000) and the total RNA concentration was quantified spectrophotometrically. Polyadenylated RNA was isolated from the total RNA with the Oligotex kit (QIAGEN, Valencia, Calif.).

4.3.5 Transcription analysis

Biotin-labeled cRNA was prepared from total RNA according to the Affymetrix GeneChip Expression Analysis Technical Manual (Aff, 2007) and subsequently hybridized to the 3AspergDTU GeneChip (Andersen et al. 2008). The cRNA was quantified spectrophotometrically and the quality was assessed using a BioAnalyzer. A GeneChip Fluidics Station FS-400 was applied for hybridization followed by scanning using a GeneChip Scanner 3000. The scanned probe array images (.DAT files) were converted into .CEL files using the GeneChip Operating Software (Affymetrix).

4.3.6 Analysis of transcription data

The analysis of the affymetrix CEL-data files was carried out accordingly to (Andersen et al. 2009) Data from the triplicates were statistically analyzed, and genes that are significantly regulated (Benjamini-Hochberg corrected Bayesian *P* values < 0.05) in pair-wise comparisons between two conditions were identified.

4.3.7 Proteome analysis

Liquid Chromatography and Mass Spectral Analysis

A 1 µl portion of each sample was then injected onto a Jupiter C18 resin reverse-phase column (5 µm particle size, 38 cm long, 150 µm inner diameter; Phenomenex, Torrance, CA). Triplicate injections were performed for each sample. The peptides were eluted at 2 µl/min with an Agilent (Santa Clara, CA) 1100

high-performance liquid chromatograph with solutions of 0.1% formic acid (solvent A) and 0.1% formic acid in 90% acetontirile (solvent B) using the following conditions:
0 to 15 min, isocratic at 100% solvent A; 15 to 20 min, linear gradient to 20% solvent B; 20 to 75 min, linear gradient to 50% solvent B: 75 to 80 min, linear gradient to 95% solvent B; isocratic at 95% solvent B. The column was reequilibrated in 100% solvent A for 40 min between sample injections. Eluted peptides were introduced into a LTQ mass spectrometer (Thermo Fisher, Waltham, MA) by electrospray ionization. Spectra were collected in a data-dependent mode, with the five most intense ions in each survey scan selected for collisional induced dissociation in subsequent scans.

Mass Spectral Data Analysis

Raw datasets were analyzed by the Sequest (Eng et al. 1994) program using a protein database created from the *Aspergillus niger* genome sequence (Andersen et al. 2011). Tryptic peptides with established scoring criteria (Wolters et al.) are represented in this work. Relative quantiation of proteins was determined by mixed-effects statistical modeling as previously described (Daly et al. 2008).

4.4 Results

Aspergillus niger cultures grown at Mn^{2+} limited conditions were pulsed with Mn^{2+} and the transcriptional response caused by Mn^{2+} addition was characterized by comparing the transcription profiles of samples taken before and after Mn^{2+} addition. In addition, the same biomass material was used for proteome analysis to investigate the correlation between the transcriptional and the proteinogenic response caused by Mn^{2+} addition. As described in the Materials and Methods section, the cultures were performed in triplicates and addition of water to a set of cultures was included as negative control. The experimental setup and an overview of the obtained results are presented in Figure 4.1

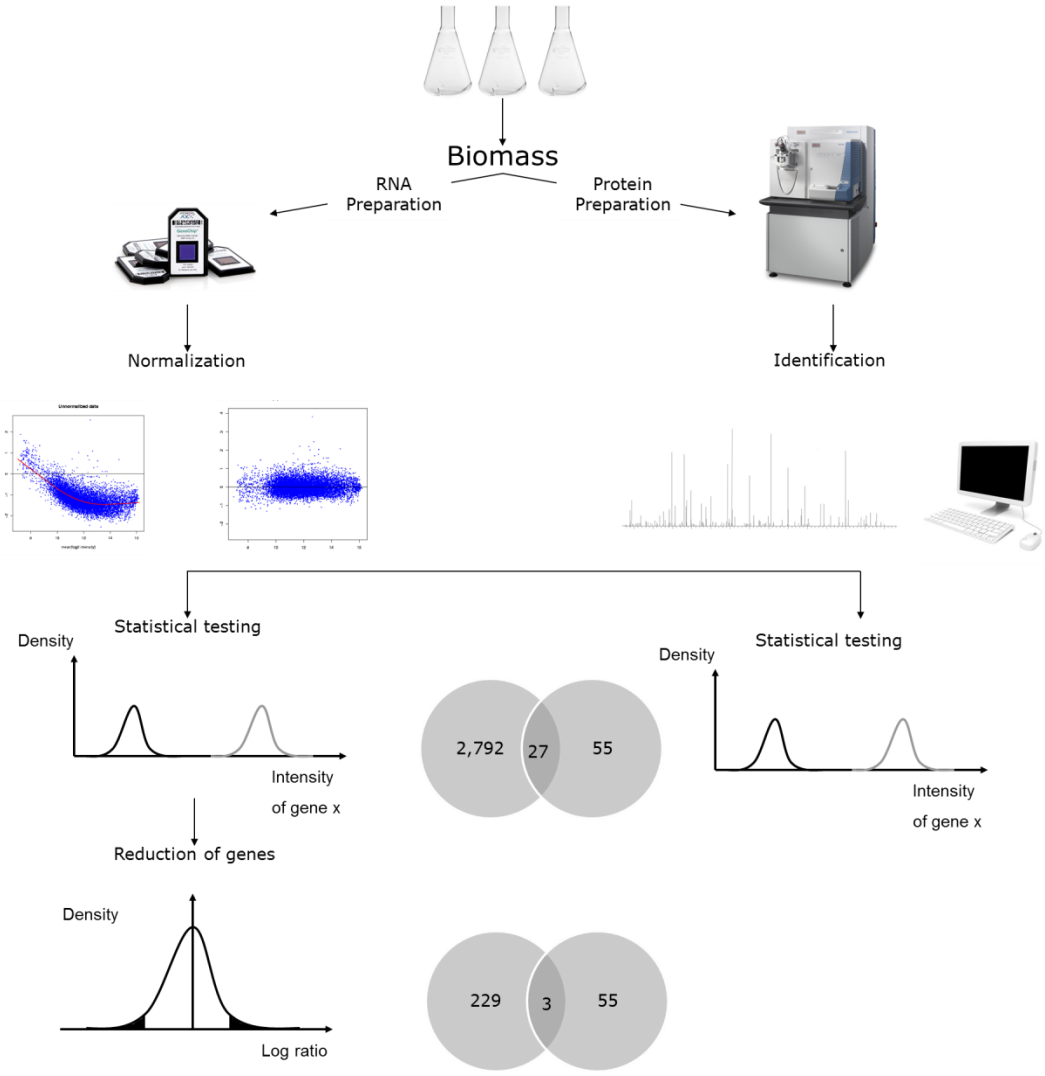

Figure 4.1 Overview of the experimental strategy and a summary of the obtain results from transcriptome and proteome analysis. The lower two Venn-diagrams show the level of overlap observed between the two applied methods.

4.4.1 Transcriptome analysis

The results of the transcriptional profiles identified a total number of 2,792 genes to be significant differentially expressed (p-value < 0.05) when adding Mn^{2+} to *A. niger* grown at Mn^{2+} limited conditions, which corresponds to approximately 25 % of the genome being affected (Appendix 1). Due to the experimental design and the possible elevated variance caused by this, a conservative fold change cut off was chosen. Based on the deviation of the log ratios, a fold change cut off was set to ±1.56 (95% confidence, σ=0.78) reducing the dataset to 229 genes, showing significantly change in expression level.

Examination of the genes responding to the manganese addition revealed that the majority of the genes (83%) were down regulated. A substantial fraction of the down regulated genes were predicted to be secreted proteins accounting for 28% of the total pool of down regulated genes. In this fraction the major activity can be categorized as catalytic and include genes coding for hydrolases, lipases and peptidases. In addition, down regulation of genes associated with secondary metabolite production including a non-ribosomal protein synthase, transferases, oxidases and a racemase were also detected. To obtain an overview of the metabolic response caused by the addition of Mn^{2+}, each of the 229 genes showing an altered expression level was investigated in further detail and a summary of this manual data analysis is presented in Table 4.1.

Table 4.1 Overview of the metabolic response and the genes involved

Part of metabolism involved	Genes involved (gene ID)	Reference
Protein degradation	56327, 139271	Ma el. al (1985), Schreferl et al (1986)
Fatty acid metabolism	56628, 45434, 45922, (211661)	Meixner et al. (1985), Kisser et al. (1980)
Glycolysis	200686, 186504	Cleland and Johnson (1954), Legiša and Mattey (1986)
Oxidative phosphorylation	205518, 204317	Wallrath (1991,1992)
Homeostasis	185327, 119984	Not described in literature
Glyconeogenesis	208685	Not described in literature

As outlined in Table 4.1, several of the observed transcriptional responses caused by Mn^{2+} addition to a limited Mn^{2+} culture have already been described in literature. However, the transcription data also revealed observations that have not previously been associated with the transition from Mn^{2+} limitation to

Mn^{2+} excess. Three genes were particularly interesting, highlighting homeostasis maintaining reactions in the mitochondria and increased gluconeogenetic activity as main metabolic responses to addition of Mn^{2+}.

During Mn^{2+} limited conditions and high glucose uptake rates, citrate is being produced as a result of overflow metabolism at the pyruvate note, Figure 2. When Mn^{2+} is introduced to the culture, the phosphoenolpyruvate carboxykinase (PEPCK) gene is up-regulated. PEPCK catalyzes the first irreversible step in the gluconeogenesis that converts oxaloacetate into phosphoenolpyruvate. Thus, the addition of Mn^{2+} causes a recycling of carbon through gluconeogenesis at the expense of citric acid production, illustrated in the metabolic chart in Figure 2.

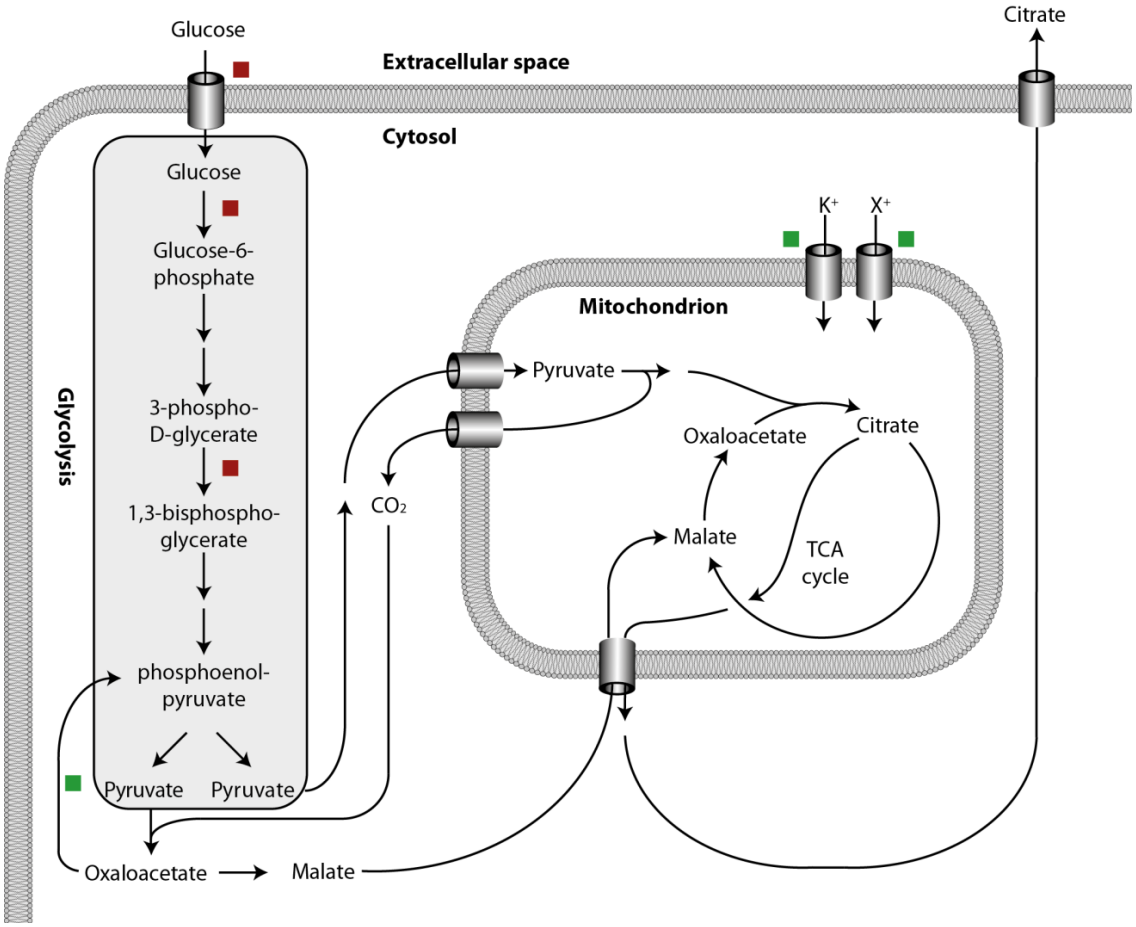

Table 4.2 Metabolic overview of the central metabolism leading to citrate formation at Mn2+ limited conditions. Up-regulation of hexokinase and glyceraldehyde 3-phosphate cause a high glucose uptake rate and unrestricted flow through glycolysis. The high glycolytic flux is argued to result in a large pool of pyruvate which enters is subjected to metabolization through the TCA cycle in the mitochondria. The simultaneous down-regulation of gluconeogenesis makes secretion of citrate favorable as a way of controlling/regulating the metabolic activity of the TCA cycle. The extract location of the two cation pumps, indicated in the figure, is unknown. However, due to the high malate/citrate

exchange, two acids having a minute charge difference, it is argued that this causes a reduced need for homeostasis maintaining reactions in the mitochondria.

From the results described above, it is evident that the C4-metabolites oxaloacetate and malate play important roles when switching from Mn^{2+} limited conditions to Mn^{2+} excess. It may be argued that PEPCK and thereby gluconeogenesis is repressed when Mn^{2+} is limited and citric acid is being produced and up-regulation of PEPCK associated with Mn^{2+} addition ensures that the C4-metabolites in the cytosol can be recycled through gluconeogenesis. To further investigate the importance of C4-metabolites and the influence of Mn^{2+} on the activity of the gluconeogenetic pathway, growth experiments using malate as the only carbon source in a Mn^{2+} limited- and excess environment were conducted. Malate is a gluconeogenic carbon source and requires PEPCK to be metabolized. *A. niger* was observed to germinate poorly on malate so to facilitate germination, 0.45 mM glucose was added to the culture medium. The results of these growth experiments with malate as the only carbon source showed growth in cultures where Mn^{2+} was in excess, whereas very limited growth was observed in Mn^{2+} limited cultures, corresponding to the small amount of glucose added (data not shown). Thus, these results supported the argument of a correlation between Mn^{2+} limitation and lack of PEPCK activity.

4.4.2 Proteome analysis

714 proteins were identified and out of these 53 proteins were found to be significantly regulated (Appendix 2). In this set of significant regulated proteins, 27 overlap with the original set of 2792 significant regulated genes identified in the transcription analysis. Those include down regulation of two proteasome components 20S and 26S, and a glycan synthase corresponding to increase protein degradation and altered cell wall composition. In addition proteins associated with secondary metabolism including dehydrogenases, a ligase, Acyl–CoA Synthetase and transferases were identified.

Interestingly two NADH-ubiquinone oxidoreductase, both associated with complex 1 was uniquely found in the proteome analysis. However, both proteins were found to respond in the opposite direction compared to the down regulation of the oxidative phosphorylation identified in the translational analysis and observed *in vivo*. This could be perceived as contradictory but in multicellular eukaryotes complex 1 consists of 45 NADH dehydrogenase subunits (Lodish 2003, Carroll et al. 2006) and if parts of these are regulated by a product feedback inhibition, a compensating response would be expected when the pathway is having a decreased activity.

Another unique response was a 3.4 times down regulation of an ABC transporter (ProteinID: 209700). ABC transporters utilize ATP to actively transport compounds. Since no other transporters are significantly regulated it could be hypothesized that this transporter might be a citrate permease.

Two proteins associated with regulation were likewise identified in the proteome analysis alone; one a protein phosphatase 2C (PPC2) and one a regulator with a U2AF domain responsible for pre-mRNA splicing. PPC2 is a heterotrimeric protein phosphatase with broad substrate specificity. PPC2 contains a conserved tripeptide Asp-Gly-His domain where the Asp residue is involved in the binding of manganese (Das et al. 1996). This binding is essential for signal transduction and lack of manganese as co-factor would diminish signal pathway.

4.5 Discussion

Comparing the results obtained in transcriptome and proteome analysis interestingly shows that the overlapping responses found using the two different methods is very limited. Three genes were identified by both methods as a result of the Mn^{2+} addition. This phenomena is often seen when comparing results from transcriptome and proteome profiles, as explained in details in chapter three . Furthermore the samples corresponding to the Mn^{2+} excess conditions were harvested only a few hours after the Mn^{2+} had been added. There was a clear shift in morphology (data not shown) and it was also obvious from the transcriptional data that this time frame was adequate to analyze the manganese shift from a transcriptional aspect. However, based on the results from the proteome analysis it may be argued that more time is needed to be able to characterize this shift in metabolism in more detail from a proteinogenic point of view.

Based on the results from the transcription analysis, the expression level of almost 25% of the genes in *A. niger* were significant affected when switching from Mn^{2+} limited to Mn^{2+} excess culture conditions. Mn^{2+} is an important cofactor for a broad range of enzymes classes (Campbell and Farrell 2003) and this was clearly demonstrated by the large amount of genes being affected by Mn^{2+}. The majority of the transcriptional response was down regulation of genes, which was anticipated since manganese depletion is known to cause severe stress to microbial cells (Barnett and Lilly 1966). Activity of the ABC multidrug transporter GeneID: 194639 have been associated with multidrug resistance in Aspergilli (de Waard et al. 2006, Morschhauser 2010). Since the function of this transporter is to ensure a proper intracellular environment it may be argued that the observed 2.4 fold down-regulation (Table 4.1) indicates an unfavorable intracellular environment at Mn^{2+} limited conditions.

As mentioned in the introduction three metabolic events are believed to be key contributors to the overflow metabolism, and all three events were identified in our analysis (Table 4.1). From the data it was observed that glyceraldehyde 3-phosphate dehydrogenase was down-regulated two fold when Mn^{2+} was added to the medium, which further substantiates the importance of this enzyme when the flux through the glycolysis is high and citrate is being formed. It should however be noted that the detected response is at the transcript level and has not been verified at the proteome level. In addition, deregulation of the glycolysis was observed as 1.6 fold down-regulation of the rco-3 monosaccharide transporter (GeneID: 200686) previously characterized as a high affinity transporter (Madi et al. 1997) together with a hexokinase both catalyzing exogenic reactions. Interestingly, this response appears to be a manganese initiated response that to our knowledge have not been reported previously. Whether this is due to manganese limitation itself or a secondary response from the overflow metabolism initiated from manganese limitation can only be speculative.

A two fold down-regulation of a putative ubiquitin-conjugating enzyme E2 was observed. Ubiquitination of proteins are the major system for proteasomal degradation in eukaryotic cells (palmer et al, 1994; Retis 1997; Tanaka and Chiba, 1998). An increase in uniquitination would give rise in protein degradation, a phenomenon observed in *A. niger* under Mn^{2+} deficiency (Ma et al. 1985, Schreferl et al. 1986). As described, the increased protein degradation results in higher glucosamine formation seen as a twofold down regulation of Glucosamine 6-phosphate synthetase (GeneID: 139271)

Down regulation of two genes associated with the glycolipid metabolism (GeneID: 56628, 45434) as well as one gene (GeneID: 45922) associated with fatty acid metabolism a response that can be correlated with shifting the saturated:unsaturated fatty acid ratio of the plasma membrane (Meixner et al. 1985), and altering the polysaccharide concentration of the cell wall and its morphology (Kisser et al. 1980). In this connection a two fold up regulation of the malic oxioreductase (GeneID: 211661) also referred to as malic enzyme, the enzyme responsible for the conversion of malate and NADP+ to pyruvate and NADPH was observed. NADPH have a vital role in anabolic reactions hence, it is an important factor controlling the extent of lipid accumulation by the supply of reducing equivalents.

As described in the introduction, conversion of glucose to citrate generates one mole of ATP and two moles of NADH, the two moles of NADH can subsequently be converted into two or more moles of ATP through the oxidative phosphorylation (Yoshida et al. 2001). Excess of ATP would repress a high glycolytic flux since ATP is a known inhibitor of both phosphofructokinase and pyruvate kinase (Campbell and Farrell 2003). It may therefore be argued that down-regulation of the oxidative phosphorylation is essential for citrate overflow metabolism. The down-regulation was detected as a two gene response, a NADH dehydrogenase

(GeneID: 205518) and H+ ATPase (GeneID: 204317), 1.9 and 1.6 fold up-regulated, correspondingly. In addition, no significant responses were found for alternative oxidases, which support the argument for the non-proton pumping oxidases being constitutively expressed.

Interestingly two cation transporters (GeneID: 185327, 119984) were subjected to a strong up regulation, 5.5 and 3.5 fold respectively. This could be interpreted as a lower demand of homeostasis maintaining reactions in the mitochondria since the minute differences in the charge between citrate / malate exchange. Contrary it could be hypothesized that the shutdown of these two transporters makes the cell unable to maintain homeostasis thereby making secretion of citrate beneficial.

An especially noteworthy observation was the strong up-regulation of PEPCK the first irreversible step in gluconeogenesis that converts oxaloacetate into phosphoenolpyruvate. PEPCK is especially important when utilizing non-carbohydrate carbon substrates as fatty acids, amino acids and TCA intermediates. This make gluconeogenesis an important regulatory step for converting TCA intermediates to hexose sugars. A high glucose uptake results in a high pool of pyruvate that enters the TCA. Based on the results presented above it may be argued that gluconeogenesis plays a role in regulating the concentration of TCA intermediates especially under high glycolytic flux ensuring a reconversion of C4-metabolites to C6-metabolite. However, the results presented here also demonstrated an essential role of Mn^{2+} in terms of PEPCK regulation. It is therefore hypothesized that Mn^{2+} limitation represses expression of PEPCK and thus prevents gluconeogenesis activity and combined with a high flux through glycolysis (overflow metabolism) secretion of citrate is the only way of controlling/regulating the metabolic activity of the TCA cycle. This Mn^{2+} dependency of PEPCK is supported by a recent study on a *Saccharomyces cerevisiae* PEPCK. The authors demonstrated that the yeast PEPCK needs Mn^{2+} as a co-factor to function (Sepulveda et al. 2010). Our hypothesis was further substantiated by the demonstration of Mn^{2+} facilitating growth on malate.

To summarize, the results of this study have indicated that gluconeogenesis plays a key role in citrate overflow metabolism. Furthermore, two cation pumps were found to be differentially regulated, and this led to the hypothesis that the secretion of citrate could be beneficial in terms of maintaining homeostasis. This response has already been described in literature but based on the results presented here, the responsible genes were identified. To summarize, the results of this study has brought new insight to the metabolic activity and the underlying regulation leading to citric acid formation in *A. niger*.

4.6 References

Andersen, M. R., L. Lehmann and J. Nielsen (2009). "Systemic analysis of the response of *Aspergillus niger* to ambient pH." Genome Biol **10**(5): R47.

Andersen, M. R., M. L. Nielsen and J. Nielsen (2008). "Metabolic model integration of the bibliome, genome, metabolome and reactome of *Aspergillus niger*." Mol Syst Biol **4**: 178.

Andersen, M. R., M. P. Salazar, P. J. Schaap, P. J. van de Vondervoort, D. Culley, J. Thykaer, J. C. Frisvad, K. F. Nielsen, R. Albang, K. Albermann, R. M. Berka, G. H. Braus, S. A. Braus-Stromeyer, L. M. Corrochano, Z. Dai, P. W. van Dijck, G. Hofmann, L. L. Lasure, J. K. Magnuson, H. Menke, M. Meijer, S. L. Meijer, J. B. Nielsen, M. L. Nielsen, A. J. van Ooyen, H. J. Pel, L. Poulsen, R. A. Samson, H. Stam, A. Tsang, J. M. van den Brink, A. Atkins, A. Aerts, H. Shapiro, J. Pangilinan, A. Salamov, Y. Lou, E. Lindquist, S. Lucas, J. Grimwood, I. V. Grigoriev, C. P. Kubicek, D. Martinez, N. N. van Peij, J. A. Roubos, J. Nielsen and S. E. Baker (2011). "Comparative genomics of citric-acid-producing *Aspergillus niger* ATCC 1015 versus enzyme-producing CBS 513.88." Genome Res **21**(6): 885-897.

Barnett, H. L. and V. G. Lilly (1966). "Manganese requirements and deficiency symptoms of some fungi." Mycologia **58**(4): 585-591.

Campbell, M. K. and S. O. Farrell (2003). Biochemistry. United States, Thomson-Brooks/Cole, 0030348498.

Carroll, J., I. M. Fearnley, J. M. Skehel, R. J. Shannon, J. Hirst and J. E. Walker (2006). "Bovine complex I is a complex of 45 different subunits." J Biol Chem **281**(43): 32724-32727.

Cleland, W. W. and M. J. Johnson (1954). "Tracer experiments on the mechanism of citric acid formation by *Aspergillus niger*." J Biol Chem **208**(2): 679-689.

Dai, Z., X. Mao, J. K. Magnuson and L. L. Lasure (2004). "Identification of genes associated with morphology in *Aspergillus niger* by using suppression subtractive hybridization." Appl Environ Microbiol **70**(4): 2474-2485.

Daly, D. S., K. K. Anderson, E. A. Panisko, S. O. Purvine, R. Fang, M. E. Monroe and S. E. Baker (2008). "Mixed-effects statistical model for comparative LC-MS proteomics studies." J Proteome Res **7**(3): 1209-1217.

Das, A. K., N. R. Helps, P. T. Cohen and D. Barford (1996). "Crystal structure of the protein serine/threonine phosphatase 2C at 2.0 A resolution." EMBO J **15**(24): 6798-6809.

de Waard, M. A., A. C. Andrade, K. Hayashi, H. J. Schoonbeek, I. Stergiopoulos and L. H. Zwiers (2006). "Impact of fungal drug transporters on fungicide sensitivity, multidrug resistance and virulence." Pest Manag Sci **62**(3): 195-207.

Eng, J. K., A. L. McCormack and J. R. Yates Iii (1994). "An approach to correlate tandem mass spectral data of peptides with amino acid sequences in a protein database." Journal of the American Society for Mass Spectrometry **5**(11): 976-989.

Glusker, J. P. (1992). "Structural aspects of citrate biochemistry." Curr Top Cell Regul **33**: 169-184.

Kapoor, M. (1975). "Subunit structure and some properties of pyruvate kinase of *Neurospora*." Can J Biochem **53**(2): 109-119.

Kisser, M., C. P. Kubicek and M. Röhr (1980). "Influence of manganese on morphology and cell wall composition of <i>*Aspergillus niger*</i> during citric acid fermentation." Archives of Microbiology **128**(1): 26-33.

Legisa, M. and M. Mattey (2007). "Changes in primary metabolism leading to citric acid overflow in *Aspergillus niger*." Biotechnol Lett **29**(2): 181-190.

Legiša, M. and M. Mattey (1986). "Glycerol as an initiator of citric acid accumulation in *Aspergillus niger*." Enzyme and Microbial Technology **8**(5): 258-259.

Lodish, H. F. (2003). Molecular cell biology. New York, W.H. Freeman and Company, 0716743663.

Ma, H., C. P. Kubicek and M. Rohr (1985). "Metabolic effects of manganese deficiency in *Aspergillus niger*: evidence for increased protein degradation." Arch Microbiol **141**(3): 266-268.

Madi, L., S. A. McBride, L. A. Bailey and D. J. Ebbole (1997). "rco-3, a gene involved in glucose transport and conidiation in *Neurospora crassa*." Genetics **146**(2): 499-508.

Meixner-Monori, B., C. P. Kubicek, W. Harrer, G. Schreferl and M. Rohr (1986). "NADP-specific isocitrate dehydrogenase from the citric acid-accumulating fungus *Aspergillus niger*." Biochem J **236**(2): 549-557.

Morschhauser, J. (2010). "Regulation of multidrug resistance in pathogenic fungi." Fungal Genet Biol **47**(2): 94-106.

Netik, A., N. V. Torres, J. M. Riol and C. P. Kubicek (1997). "Uptake and export of citric acid by *Aspergillus niger* is reciprocally regulated by manganese ions." Biochim Biophys Acta **1326**(2): 287-294.

Panneman, H., G. J. Ruijter, H. C. van den Broeck and J. Visser (1998). "Cloning and biochemical characterisation of *Aspergillus niger* hexokinase--the enzyme is strongly inhibited by physiological concentrations of trehalose 6-phosphate." Eur J Biochem **258**(1): 223-232.

Papagianni, M., F. Wayman and M. Mattey (2005). "Fate and role of ammonium ions during fermentation of citric acid by *Aspergillus niger*." Appl Environ Microbiol **71**(11): 7178-7186.

Peksel, A., N. V. Torres, J. Liu, G. Juneau and C. P. Kubicek (2002). "13C-NMR analysis of glucose metabolism during citric acid production by *Aspergillus niger*." Appl Microbiol Biotechnol **58**(2): 157-163.

Promper, C., R. Schneider and H. Weiss (1993). "The role of the proton-pumping and alternative respiratory chain NADH:ubiquinone oxidoreductases in overflow catabolism of *Aspergillus niger*." Eur J Biochem **216**(1): 223-230.

Rohr, M. and C. P. Kubicek (1981). " Regulatory aspects citric acid fermentation by *Aspergillus niger.*" Process Biochem **16**: 34-37.

Schmidt, M., J. Wallrath, A. Dörner and H. Weiss (1992). "Disturbed assemble of the respiratory chain NADH: ubiquinone reductase (complex I) in citric-acid-accumulating *Aspergillus niger* strain B 60." Applied Microbiology and Biotechnology **36**(5): 667-672.

Schreferl-Kunar, G., M. Grotz, M. Röhr and C. P. Kubicek (1989). "Increased citric acid production by mutants of *Aspergillus niger* with increased glycolytic capacity." FEMS Microbiology Letters **59**(3): 297-300.

Schreferl, G., C. P. Kubicek and M. Rohr (1986). "Inhibition of citric acid accumulation by manganese ions in *Aspergillus niger* mutants with reduced citrate control of phosphofructokinase." J Bacteriol **165**(3): 1019-1022.

Sepulveda, C., A. Poch, R. Espinoza and E. Cardemil (2010). "Electrostatic interactions play a significant role in the affinity of *Saccharomyces cerevisiae* phosphoenolpyruvate carboxykinase for Mn2+." Biochimie **92**(7): 814-819.

Shu, P. and M. J. Johnson (1948). "The Interdependence of Medium Constituents in Citric Acid Production by Submerged Fermentation." J Bacteriol **56**(5): 577-585.

Terenzi, H. F., E. Roselino and S. Passeron (1971). "Two types of pyruvate kinase in *Mucor rouxii*. Changes in the enzymatic pattern related to aerobic development." Eur J Biochem **18**(3): 342-350.

Torres, N. V. (1994). "Modeling approach to control of carbohydrate metabolism during citric acid accumulation by *Aspergillus niger*: I. Model definition and stability of the steady state." Biotechnology and Bioengineering **44**(1): 104-111.

Torres, N. V., J. M. Riol-Cimas, M. Wolschek and C. P. Kubicek (1996a). "Glucose transport by *Aspergillus niger*: the low-affinity carrier is only formed during growth on high glucose concentrations." Applied Microbiology and Biotechnology **44**(6): 790-794.

Torres, N. V., E. O. Voit and C. Gonzalez-Alcon (1996b). "Optimization of nonlinear biotechnological processes with linear programming: Application to citric acid production by *Aspergillus niger*." Biotechnol Bioeng **49**(3): 247-258.

Wallrath, J., M. Schmidt and H. Weiss (1991). "Concomitant loss of respiratory chain NADH: ubiquinone reductase (complex I) and citric acid accumulation in *Aspergillus niger*." Applied Microbiology and Biotechnology **36**(1): 76-81.

Wallrath, J., M. Schmidt and H. Weiss (1992). "Correlation between manganese-deficiency, loss of respiratory chain complex I activity and citric acid production in *Aspergillus niger*." Archives of Microbiology **158**(6): 435-438.

Wolschek, M. F. and C. P. Kubicek (1997). "The filamentous fungus *Aspergillus niger* contains two "differentially regulated" trehalose-6-phosphate synthase-encoding genes, tpsA and tpsB." J Biol Chem **272**(5): 2729-2735.

Yoshida, M., E. Muneyuki and T. Hisabori (2001). "ATP synthase--a marvellous rotary engine of the cell." Nat Rev Mol Cell Biol **2**(9): 669-677.

Chapter 5 Transcription factors modulation

The previous chapter demonstrated the strength of the "omics" techniques. Several decades of research had uncovered many events leading to the citrate overflow metabolism, yet novel insights, events, and connections were identified in the previous chapter. As presented, the citrate overflow metabolism was mediated by a complex response. Interestingly, it was followed by close to 100 differentially regulated transcription factors (TFs), unfortunately none of them were characterized. It could be speculated that manipulation of one/few of those TFs could initiate a similar overflow response without the necessity of manganese depletion. TFs have the potential of controlling multiple fluxes in an organism; hence manipulating expression of these proteins can provide an alternative tool for overcoming metabolic bottlenecks and/or tight regulation. Applying this strategy was the main purpose in chapters 6 and 7. Consequently, an introduction to TFs and the concepts of TF modulation will be discussed this chapter.

5.1.1 Transcription factors role in life

Controlling gene translation is central to both, tissue specific expressions, as well to the gene activity in the response to specific stimuli. Regulation primarily takes place at the level of transcription, yet occurring post transcriptionally as well (reviewed by Pezer et al. (2010)). Particularly in eukaryotes, the transcriptional regulation tends to involve combinatorial interactions between several proteins, which facilitate an integrated response to multiple conditions in the environment. Protein–protein interactions play a significant role in gene expression because they promote the formation of activator or inhibitory complexes, depending on their components and possible combinations (A schematic overview can be found in figure 3.1). TFs are a central subset of interacting proteins responsible for the control of gene expression. This makes TFs essential for the regulation of gene expression, hence they are found in all living organisms.

The mechanism of genetic regulation was first described by Jacob and Monod's (1961), study of the *lac* operon in *E. coli.* Followed by the discovery of the so called, cis-acting elements by Davidson et al. (1983). By inspecting the upstream regions of genes that co-regulated, the presence of short DNA sequences, sharing a high degree of similarity, was discovered. Integrating the information from 14 articles the authors were able to identify cis-acting elements in seven eukaryote organisms, regulating diverse biological responses covering amino acid depletion, heat shock response and glucocorticoid exposure. Nowadays it has become clear that these short DNA sequences act by binding TFs thus regulating the transcription of the gene either positively or negatively.

The abundance of TFs within an organism appears to be linked to the complexity of the organisms e.g. *E. coli* has 48 TFs (Blattner et al. 1997) *S. cerevisiae* 169 (Goffeau et al. 1996). In contrast, multi cellular organisms; *A. niger* has approximately 1000 TFs (Pel et al. 2007), *Arabidopsis thaliana* between 1500-1800 TFs (Arabidopsis Genome Initiative 2000) and *H. sapiens* approximately 2600 TFs (International Human Genome Sequencing Consortium 2004), yet more noteworthy is that the TF expansion strictly follows a power law, that in eukaryote is 1.23 whereas 1.98 is observed for prokaryotes, Figure 5.1. As a consequence, for larger genomes, each gene must be regulated by a larger number of TFs and/or each TF must be regulating a smaller set of genes (van Nimwegen 2003, Charoensawan et al. 2010).

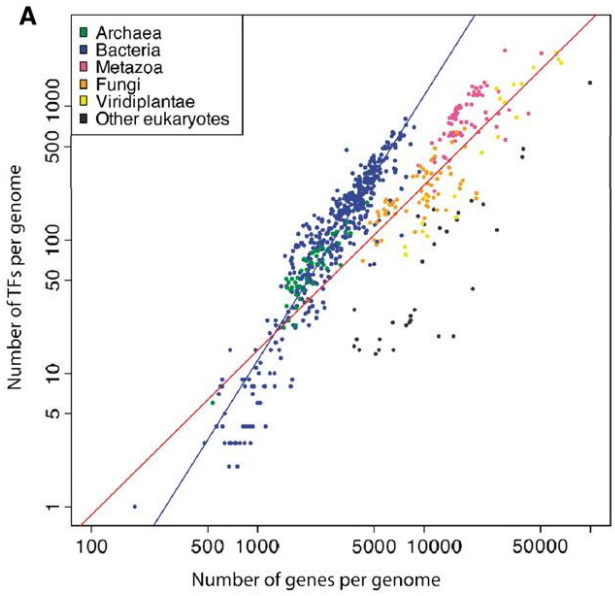

Figure 5.1 TF abundance against number of genes per genome on a double log scale. The colors are used to highlight genomes from different phylogenetic groups. The linear model fit for prokaryote (blue line) strictly follows a power law increase, with an exponent close to quadratic, $\alpha = 1.98$ with $R^2 = 0.87$. The TF increase in eukaryotes has a lower exponent (red line) as well as degree of correlation, $\alpha = 1.23$ $R^2 = 0.61$. Figure adapted from (Charoensawan et al. 2010).

Several hypotheses have been proposed to explain the existence of the power law relationship. One, is the hypothesis of Maslov et al. (2009). The author speculated from a metabolic network point of view, “When an organism evolve to explore a new environmental niche, a new set of TFs are required in order to monitor the new tasks necessary to adapt to different conditions. Meanwhile, some of the metabolic enzymes can be reused; hence, fewer new enzymes are required to regulate each new task”.

Regulatory networks typically involve a nested hierarchy structure, as exemplified in figure 5.2.

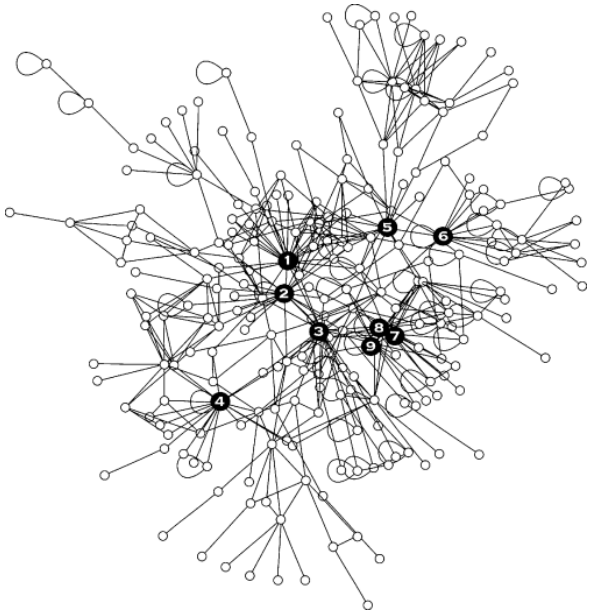

Figure 5.2 Human transcription factor network based on 230 interacting TFs. The numbered black filled nodes are the highest connected TFs also termed global TFs. Each circle represents a TF and a line, an interaction. The figure was modified from Rodriguez-Caso et al. (2005).

It is clear that most TFs are linked to only a few others, whereas a handful of the TFs have many connections. This may explain why the number of new tasks and their regulators increase faster than linearly with the number of genes encoding enzymes. This phenomenon ultimately facilitates exploitation of TFs in metabolic engineering, especially within organisms with large genomes.

5.1.2 Transcription factor modulation

The biggest challenge performing TFs modulation is that TFs is the abundant protein class in multicellular organisms, e.g. for *A. niger,* TFs constitutes 7-9 % of the total numbers predicted ORFs (Pel et al. 2007, Andersen et al. 2011). TFs, especially in non-model organisms, are a highly uncharacterized class of proteins. Out of *A. niger's* approximated 1000 TFs, only twelve TFs have been functional characterized, table 5.1.

Table 5.1 Overview of transcription factors characterized in *A. niger*.

Gene	Function	Reference
AcuA, AcuB	Acetyl-CoA synthetase regulators	(Sealy-Lewis and Fairhurst 1998)
AmyR	Amylolytic activator	(Tsukagoshi et al. 2001)
AraR	Arabinolytic regulator	(Battaglia et al. 2011)
AreA	Regulator of nitrogen metabolite repression	(MacCabe et al. 1998)
CpcA	Regulator of amino acid biosynthesis	(Wanke et al. 1997)
CreA	Carbon catabolite repressor	(Drysdale et al. 1993)
HacA	Regulator of the unfolded protein response	(Mulder et al. 2004)
InuR	Regulator of inulinolytic genes	(Yuan et al. 2008)
PrtT	Regulator of extracellular proteases	(Punt et al. 2008)
RlmA	Regulator of the cell well stress response	(Damveld et al. 2005)
XlnR	Xylanolytic regulator	(van Peij et al. 1998)

Many classification systems exist to describe TFs, including mechanism of action, regulatory function, or sequence homology (Heinemeyer et al. 1999, Brivanlou and Darnell 2002, Stegmaier et al. 2004). However, in this thesis, the simplified cis/trans grouping is applied. Cis-acting TFs are characterized by their local response and are often found in secondary metabolite clusters. On the other hand, the trans-acting TFs can affect genes on several chromosomes. To this category the highly connected TFs (global TFs) are found, as represented black circles on figure 5.2 and as well in this category, the lower connected TF (the white circles on figure 5.2). This group includes the TFs as HacA and PrtT (table 5.1), both found to be beneficial targets, for manipulation and applied in protein production.

TFs significance in cellular regulation makes this class of proteins, an attractive target to investigate. The challenge lies within locating the low connected trans-acting TFs. For instance, deleting a highly connected TF could be devastating to the cell resulting in a severe weakened or unviable phenotype. On the contrary, deleting a cis-acting TF possibly do not result in any altered phenotype. Attempting to solve this problem the following strategy was developed:

1. Locate a stimulus that affects the pathway of interest.
2. Cultivate in presence and absence of the stimuli.
3. Examine the transcriptiome and/or proteome.
4. Perform cluster analysis of all differential regulated genes/proteins.
5. Remove cis-acting TFs.
6. Remove TF subset that co-regulates with household genes.

Applying this approach increases the rate of success considerably, due to the elimination of the two much likely pitfalls, global TFs and cis-acting TFs. The following three chapters present the effectiveness of this strategy. Three TF mutants will be described, each with a phenotype posing a big potential for improving *A. niger* as a cell factory.

5.2 References

(2000). "Analysis of the genome sequence of the flowering plant *Arabidopsis thaliana*." Nature **408**(6814): 796-815.

(2004). "Finishing the euchromatic sequence of the human genome." Nature **431**(7011): 931-945.

Andersen, M. R., M. P. Salazar, P. J. Schaap, P. J. van de Vondervoort, D. Culley, J. Thykaer, J. C. Frisvad, K. F. Nielsen, R. Albang, K. Albermann, R. M. Berka, G. H. Braus, S. A. Braus-Stromeyer, L. M. Corrochano, Z. Dai, P. W. van Dijck, G. Hofmann, L. L. Lasure, J. K. Magnuson, H. Menke, M. Meijer, S. L. Meijer, J. B. Nielsen, M. L. Nielsen, A. J. van Ooyen, H. J. Pel, L. Poulsen, R. A. Samson, H. Stam, A. Tsang, J. M. van den Brink, A. Atkins, A. Aerts, H. Shapiro, J. Pangilinan, A. Salamov, Y. Lou, E. Lindquist, S. Lucas, J. Grimwood, I. V. Grigoriev, C. P. Kubicek, D. Martinez, N. N. van Peij, J. A. Roubos, J. Nielsen and S. E. Baker (2011). "Comparative genomics of citric-acid-producing *Aspergillus niger* ATCC 1015 versus enzyme-producing CBS 513.88." Genome Res **21**(6): 885-897.

Battaglia, E., S. F. Hansen, A. Leendertse, S. Madrid, H. Mulder, I. Nikolaev and R. P. de Vries (2011). "Regulation of pentose utilisation by AraR, but not XlnR, differs in *Aspergillus* nidulans and *Aspergillus niger*." Appl Microbiol Biotechnol **91**(2): 387-397.

Blattner, F. R., G. Plunkett, 3rd, C. A. Bloch, N. T. Perna, V. Burland, M. Riley, J. Collado-Vides, J. D. Glasner, C. K. Rode, G. F. Mayhew, J. Gregor, N. W. Davis, H. A. Kirkpatrick, M. A. Goeden, D. J. Rose, B. Mau and Y. Shao (1997). "The complete genome sequence of Escherichia coli K-12." Science **277**(5331): 1453-1462.

Brivanlou, A. H. and J. E. Darnell, Jr. (2002). "Signal transduction and the control of gene expression." Science **295**(5556): 813-818.

Charoensawan, V., D. Wilson and S. A. Teichmann (2010). "Genomic repertoires of DNA-binding transcription factors across the tree of life." Nucleic Acids Res **38**(21): 7364-7377.

Damveld, R. A., M. Arentshorst, A. Franken, P. A. vanKuyk, F. M. Klis, C. A. van den Hondel and A. F. Ram (2005). "The *Aspergillus niger* MADS-box transcription factor RlmA is required for cell wall reinforcement in response to cell wall stress." Mol Microbiol **58**(1): 305-319.

Davidson, E. H., H. T. Jacobs and R. J. Britten (1983). "Eukaryotic gene expression: Very short repeats and coordinate induction of genes." Nature **301**(5900): 468-470.

Drysdale, M. R., S. E. Kolze and J. M. Kelly (1993). "The *Aspergillus niger* carbon catabolite repressor encoding gene, creA." Gene **130**(2): 241-245.

Goffeau, A., B. G. Barrell, H. Bussey, R. W. Davis, B. Dujon, H. Feldmann, F. Galibert, J. D. Hoheisel, C. Jacq, M. Johnston, E. J. Louis, H. W. Mewes, Y. Murakami, P. Philippsen, H. Tettelin and S. G. Oliver (1996). "Life with 6000 genes." Science **274**(5287): 546, 563-547.

Heinemeyer, T., X. Chen, H. Karas, A. E. Kel, O. V. Kel, I. Liebich, T. Meinhardt, I. Reuter, F. Schacherer and E. Wingender (1999). "Expanding the TRANSFAC database towards an expert system of regulatory molecular mechanisms." Nucleic Acids Res **27**(1): 318-322.

Jacob, F. and J. Monod (1961). "Genetic regulatory mechanisms in the synthesis of proteins." J Mol Biol **3**: 318-356.

MacCabe, A. P., S. Vanhanen, M. D. Sollewign Gelpke, P. J. van de Vondervoort, H. N. Arst, Jr. and J. Visser (1998). "Identification, cloning and sequence of the *Aspergillus niger* areA wide domain regulatory gene controlling nitrogen utilisation." Biochim Biophys Acta **1396**(2): 163-168.

Maslov, S., S. Krishna, T. Y. Pang and K. Sneppen (2009). "Toolbox model of evolution of prokaryotic metabolic networks and their regulation." Proc Natl Acad Sci U S A **106**(24): 9743-9748.

Mulder, H. J., M. Saloheimo, M. Penttila and S. M. Madrid (2004). "The transcription factor HACA mediates the unfolded protein response in *Aspergillus niger*, and up-regulates its own transcription." Mol Genet Genomics **271**(2): 130-140.

Pel, H. J., J. H. de Winde, D. B. Archer, P. S. Dyer, G. Hofmann, P. J. Schaap, G. Turner, R. P. de Vries, R. Albang, K. Albermann, M. R. Andersen, J. D. Bendtsen, J. A. Benen, M. van den Berg, S. Breestraat, M. X. Caddick, R. Contreras, M. Cornell, P. M. Coutinho, E. G. Danchin, A. J. Debets, P. Dekker, P. W. van Dijck, A. van Dijk, L. Dijkhuizen, A. J. Driessen, C. d'Enfert, S. Geysens, C. Goosen, G. S. Groot, P. W. de Groot, T. Guillemette, B. Henrissat, M. Herweijer, J. P. van den Hombergh, C. A. van den Hondel, R. T. van der Heijden, R. M. van der Kaaij, F. M. Klis, H. J. Kools, C. P. Kubicek, P. A. van Kuyk, J. Lauber, X. Lu, M. J. van der Maarel, R. Meulenberg, H. Menke, M. A. Mortimer, J. Nielsen, S. G. Oliver, M. Olsthoorn, K. Pal, N. N. van Peij, A. F. Ram, U. Rinas, J. A. Roubos, C. M. Sagt, M. Schmoll, J. Sun, D. Ussery, J. Varga, W. Vervecken, P. J. van de Vondervoort, H. Wedler, H. A. Wosten, A. P. Zeng, A. J. van Ooyen, J. Visser and H. Stam (2007). "Genome sequencing and analysis of the versatile cell factory *Aspergillus niger* CBS 513.88." Nat Biotechnol **25**(2): 221-231.

Pezer, Z., J. Brajkovic, I. Feliciello and D. Ugarkovc (2010). "Satellite DNA-mediated effects on genome regulation." Genome Dyn **7**: 153-169.

Punt, P. J., F. H. Schuren, J. Lehmbeck, T. Christensen, C. Hjort and C. A. van den Hondel (2008). "Characterization of the *Aspergillus niger* prtT, a unique regulator of extracellular protease encoding genes." Fungal Genet Biol **45**(12): 1591-1599.

Rodriguez-Caso, C., M. A. Medina and R. V. Solé (2005). "Topology, tinkering and evolution of the human transcription factor network." FEBS Journal **272**(24): 6423-6434.

Sealy-Lewis, H. M. and V. Fairhurst (1998). "Isolation of mutants deficient in acetyl-CoA synthetase and a possible regulator of acetate induction in *Aspergillus niger*." Microbiology **144 (Pt 7)**: 1895-1900.

Stegmaier, P., A. E. Kel and E. Wingender (2004). "Systematic DNA-binding domain classification of transcription factors." Genome Inform **15**(2): 276-286.

Tsukagoshi, N., T. Kobayashi and M. Kato (2001). "Regulation of the amylolytic and (hemi-)cellulolytic genes in aspergilli." J Gen Appl Microbiol **47**(1): 1-19.

van Nimwegen, E. (2003). "Scaling laws in the functional content of genomes." Trends in Genetics **19**(9): 479-484.

van Peij, N. N., J. Visser and L. H. de Graaff (1998). "Isolation and analysis of xlnR, encoding a transcriptional activator co-ordinating xylanolytic expression in *Aspergillus niger*." Mol Microbiol **27**(1): 131-142.

Wanke, C., S. Eckert, G. Albrecht, W. van Hartingsveldt, P. J. Punt, C. A. van den Hondel and G. H. Braus (1997). "The *Aspergillus niger* GCN4 homologue, cpcA, is transcriptionally regulated and encodes an unusual leucine zipper." Mol Microbiol **23**(1): 23-33.

Yuan, X. L., J. A. Roubos, C. A. van den Hondel and A. F. Ram (2008). "Identification of InuR, a new Zn(II)2Cys6 transcriptional activator involved in the regulation of inulinolytic genes in *Aspergillus niger*." Mol Genet Genomics **279**(1): 11-26.

Chapter 6 Identification of a transcription factor controlling pH-dependent organic acid response in *Aspergillus niger*

Poulsen L, Andersen MR, Lantz AE, Thykaer J

6.1 Abstract

Acid formation in *Aspergilllus niger* is known to be subjected to tight regulation, and the acid production profiles are fine-tuned to respond to the ambient pH. Based on transcriptome data, putative trans-acting pH responding transcription factors were listed and through knock out studies a mutant exhibiting an oxalate overproducing phenotype was identified. The yield of oxalate was increased up to 158% compared to the wild type and the corresponding transcription factor was therefore entitled Oxalic Acid repression Factor, OafA. Detailed physiological characterization of the *ΔoafA* mutant, compared to the wild type, showed that both strains produced substantial amounts of gluconic acid, but the mutant strain was more efficient in the re-uptake of gluconic acid and converting it to oxalic acid, particularly at high pH (pH 5.0). Transcriptional profiles showed that 241 genes were differentially expressed due to the deletion of *oafA* and this supported the argument of OafA being a trans-acting transcription factor. Furthermore, expression of two phosphoketolases were down-regulated in the *ΔoafA* mutant, one of which has not previously been described in fungi. It was argued that the observed oxalate overproducing phenotype was a consequence of the efficient re-uptake of gluconic acid and thereby a higher flux through glycolysis. This results in a lower flux through the pentose phosphate pathway, demonstrated by the down-regulation of the phohsphoketolases. Finally, the physiological data, in terms of the specific oxygen consumption, indicated a connection between the oxidative phosphorylation and oxalate production and this was further substantiated through transcription analysis.

6.2 Introduction

Aspergillus niger is an industrially important organism, used as cell factory of a wide range of commercial enzymes as well as productions of million tons of citric acid (Baker 2006). Due to the significance of *A. niger* in the biotech industry, strain improvement is a key component in process optimization. Traditionally, it has been approached by genetic engineering of a single or few metabolic genes; however, this strategy struggles to overcome the superjacent regulation thus the outcome has frequently shown to be of limited success. Another strategy entails of direct manipulation of transcription factors (TFs), since these proteins have the potential of controlling several fluxes in an organism. Modulation of TFs as a strategy for metabolic engineering has been demonstrated by Schuurmans *et al.* 2008, where the authors deleted one TF and overexpressed another to improve ethanol production in *Saccharomyces cerevisiae (Schuurmans et al. 2008)*. A different approach is to use site directed mutagenesis on a TF, an approach that was applied to improve ethanol tolerance and production in *S. cerevisiae* (Alper et al. 2006). Both methods have been applied in prokaryotes as well as in unicellular eukaryotes, but to our knowledge have not been tested in multicellular eukaryotes. One explanation may be that the genome sequence for *S. cerevisiae* have been public available since 1996 (Goffeau et al. 1996), whereas the first filamentous fungal genome was released less than ten years ago, with the genome of *Neurospora crassa* being the earliest to be publically available (Galagan et al. 2003). Another challenge is the complexity of the regulatory networks caused by the large genomes in multicellular eukaryotes, illustrated by the number of increasing TF's with increasing genome size e.g. *E. coli* has 48 (McCue et al. 2002) whereas *A. niger* has approximately 1000 (Pel et al. 2007) and only a few of them have been functionally characterized.

Transcription factors can be grouped as cis- or trans-acting. Cis-acting TF's are characterized by their local response, inducing an entire cluster including the transcription factor itself as in the case of many secondary metabolite clusters (Milo et al. 2002, Schumann and Hertweck 2006, Nielsen et al. 2011). The other type of transcription factors, trans-acting, can regulate genes from a different region/chromosome of the genome than the region it was transcribed from itself as in the case of protease production, e.g. PrtT (Punt et al. 2008). This transcription factor, located on chromosome VI, controls proteases scattered throughout the genome, regulating the majority of the extracellular protease response in *A. niger.* Deleting *prtT* significantly lowers the protease activity without a noteworthy effect on the physiology of the fungus (Punt et al. 2008). Considering the nature of organic acid production by *A. niger* being highly dependent on pH of the culture medium (Heinrich and Rehm 1982, Ruijter et al. 1999), we hypothesize, that acid production is mediated through a trans-acting transcription factor response.

Based on transcriptome data from a previous study where *A. niger* was cultivated at three different pH's (Andersen et al. 2009), we identified a list of putative trans-acting pH responding transcription factors which formed the basis for sequential knockout studies. In the following screening process, particularly one mutant exhibited an elevated acidification of the media, which corresponded to increased oxalate production. The responsible transcription factor was therefore entitled OafA (oxalic acid repression factor). The deletion mutant, *ΔoafA,* and the reference strain, were subjected to detailed physiological characterization.

6.3 Materials and methods

6.3.1 Fungal strains

A. niger ATCC 1015 was used as wild type strain (obtained from the IBT collection as IBT 28639). The *ΔoafA* strain was generated from the ATCC 1015 strain. All strains were maintained as frozen spore suspensions at -80°C in 20% glycerol.

6.3.2 Media

Transformation medium: 182.2 g/L sorbitol, 10 g/L glucose monohydrate, 6 g/L $NaNO_3$, 0.52 g/L KCl, 0.52 g/L $MgSO_4 \cdot 7H_2O$, 1 mL/L of 1% thiamine solution, 1 mL/L trace element solution. Trace element solution: 22 g/L $ZnSO_4 \cdot 7\ H_2O$, 11 g/L H_3BO_3, 5 g/L $MnCl_2 \cdot 4\ H_2O$, 5 g/L $FeSO_4 \cdot 7\ H_2O$, 1.7 g/L $CoCl_2 \cdot 6\ H_2O$, 1.6 g/L $CuSO_4 \cdot 5\ H_2O$, 1.5 g/L $Na_2MoO_4 \cdot 2\ H_2O$, 50 g/L Na_4EDTA.

Czapek yeast extract (CYA) media: 30 g/L Sucrose, 5 g/L Yeast extract, 3 g/L $NaNO_3$, 1 g/L K_2HPO_4, 0.5 g/L $MgSO_4 \cdot 7\ H_2O$, 0.5 g/L KCl, 0.01 g/L $FeSO_4 \cdot 7H_2O$, 15 g/L Agar, 1 mL/L trace element solution. 0.4 g/L $CuSO_4 \cdot 5\ H_2O$, 0.04 g/L $Na_2B_2O_7 \cdot 10\ H_2O$, 0.8 g/L $FeSO_4 \cdot 7\ H_2O$, 0.8 g/L $MnSO_4 \cdot H_2O$, 0.8 g/L $Na_2MoO_4 \cdot 2\ H_2O$, 8.0 g/L $ZnSO_4 \cdot 7\ H_2O$. pH adjusted to 6.2 prior to autoclavation.

Minimal screenings medium: 10 g/L glucose monohydrate, 6 g/L $NaNO_3$, 0.52 g/L KCl, 0.52 g/L $MgSO_4 \cdot 7H_2O$, 1 mL/L of 1% thiamine solution, 1 mL/L trace element solution. Trace element solution: 22 g/L $ZnSO_4 \cdot 7\ H_2O$, 11 g/L H_3BO_3, 5 g/L $MnCl_2 \cdot 4\ H_2O$, 5 g/L $FeSO_4 \cdot 7\ H_2O$, 1.7 g/L $CoCl_2 \cdot 6\ H_2O$, 1.6 g/L $CuSO_4 \cdot 5\ H_2O$, 1.5 g/L $Na_2MoO_4 \cdot 2\ H_2O$, 50 g/L Na_4EDTA. As buffer 19.52 g/L 2-(N-morpholino)ethanesulfonic acid (MES) was used. pH adjusted to 6.0 prior to autoclavation.

Complex screening medium (Watman medium): 30 g/L Sucrose, 5 g/L Corn steep liquor, 2 g/L Yeast extract, 3 g/L Peptone, 2 g/L Glucose, 2 g/L $NaNO_3$, 1 g/L $K_2HPO_4 \cdot 3$ H2O, 0.5 g/L $MgSO_4 \cdot 7$ H2O, 0.05 g/L $FeSO_4 \cdot 7$ H2O, 0.2 g/L KCl, 1 mL/L Trace metal solution. Trace element solution: 22 g/L $ZnSO_4 \cdot 7\ H_2O$, 11 g/L H_3BO_3, 5 g/L $MnCl_2 \cdot 4\ H_2O$, 5 g/L $FeSO_4 \cdot 7\ H_2O$, 1.7 g/L $CoCl_2 \cdot 6\ H_2O$, 1.6 g/L $CuSO_4 \cdot 5\ H_2O$, 1.5 g/L $Na_2MoO_4 \cdot 2\ H_2O$, 50 g/L Na_4EDTA. As buffer 19.52 g/L 2-(N-morpholino)ethanesulfonic acid (MES) was used. pH adjusted to 6.0 prior to autoclavation.

Batch cultivation medium: 20 g/L glucose, 7.3 g/L $(NH_4)_2SO_4$, 1.5 g/L KH_2PO_4, 1.0 g/L $MgSO_4 \cdot 7\ H_2O$, 1.0 g/L NaCl, 0.1 g/L $CaCl_2$, 0.1 mL Antifoam 204 (sigma), 1 mL/L trace element solution. Trace element solution: 0.4 g/L $CuSO_4 \cdot 5\ H_2O$, 0.04 g/L $Na_2B_2O_7 \cdot 10\ H_2O$, 0.8 g/L $FeSO_4 \cdot 7\ H_2O$, 0.8 g/L $MnSO_4 \cdot H_2O$, 0.8 g/L $Na_2MoO_4 \cdot 2\ H_2O$, 8.0 g/L $ZnSO_4 \cdot 7\ H_2O$.

6.3.3 Preparation of inoculum

Conidia were propagated on CYA media plates and incubated for 5 to 7 days at 30°C before being harvested with 2 times 10 ml 0.9 % NaCl and filtered through miracloth and washed twice with 0.9 % NaCl. Fermentations were initiated by conidia inoculation to a final concentration of $2 \cdot 10^9$ spores/L

6.3.4 Target selection

A previous study (Andersen et al. 2009) identified 6228 genes which react significantly ($p<0.05$) to pH over three different conditions (pH. 2.5, 4.5, and 6.0). From this set of data, we examined all genes that react in a progressive manner over the values, either increasing or decreasing with pH, and extracted all predicted transcription factors in this set.

6.3.5 PCR amplification

All PCR reactions were carried out using the high fidelity Phusion polymerase from Finnzymes at standard conditions with HF-buffer.

6.3.6 Gene deletion

All DNA insertions into the *A. niger* genome were performed using protoplasts and PEG transformation. The deletion strains were constructed using PCR-generated bipartite gene targeting substrates (Nielsen et al. 2006). Each part of the bipartite substrate consisted of a targeting fragment and a marker fragment, all of which were amplified individually by PCR using the primer pairs presented in Table 1. Hygromycin phosphotransferase gene (hph) marker cassette was amplified from plasmid pCB10003 (McCluskey et al. 2010) as template DNA.

6.3.7 Oligonucleotide PCR primers

The oligonucleotides used for the strain construction of Δ*oafA*, can be found in Table 6.1.

Table 6.1 Primers used for deletion of *oafA* in *A. niger*. Lower-case letters indicate overlapping genetic elements used for fusion PCR.

Primer	Sequence
Upst_OAFA_F	TATGACGTGCGGGTATTCGAG
Upst_OAFA_R	gatccccgggaattgccatgTAACTTCAGTAGATCGCCCAGC
Dwst_OAFA_F	ggactgagtagcctgacatcTTAGCAGGGGCGAATAATGC
Dwst_OAFA_R	CGAATGAACAACAGCAGGATG
Upst_Hyg_F	catggcaattcccggggatcGCTGGAGCTAGTGGAGGTCA
Upst-HygR-N	CTGCTGCTCCATACAAGCCAACC
Dwst-HygF-N	GACATTGGGGAGTTCAGCGAGAG
Dwst-Hyg_R	gatgtcaggctactcagtccCGGTCGGCATCTACTCTATT

6.3.8 Southern blotting

1.5 µg genomic DNA was isolated and digested with appropriate restriction enzymes (SmaI and NdeI). Sequence information for restriction digest of the target loci was obtained from the *A. niger* ATCC 1015 genome sequence (Andersen et al. 2011) from the US Department of Energy Joint Genome Institute (http://genome.jgipsf.org/Aspni1/). Blotting was done according to standard methods (Sambrook and Russell 2001), using RapidHyb hybridization buffer (Amersham Pharmacia) for probing. The target locus was detected by probing with the labeledmarker gene PCR fragment. The probes were radioactively labeled with α-32P-dCTP by random priming using Rediprime II kit (GE Healthcare). For a graphical representation of the gene deletion strategy, see Figure 6.1.

6.3.8 Cultivations

Static cultivations

Fresh conidia were added to 8 mL of minimal- or complex screenings medium in a 50 mL sterile falcon tube (BD Biosciences) to a final concentration of $1 \cdot 10^3$ conidia/mL and incubated without agitation at 30 ^{o}C for 5 days. At the end of the experiment, samples for pH and HPLC-measurements were collected.

Batch cultivations

Batch cultivations were performed in 2 L Sartorius fermenters with a working volume of 1.5 L, equipped with two Rushton six-blade disc turbines. The bioreactor was sparged with air, and the concentrations of oxygen and carbon dioxide in the exhaust gas were measured in a gas analyzer (1311 Fast response Triple gas, Innova combined with multiplexer controller for Gas Analysis MUX100, B. Braun Biotech International (Melsungen, Germany)). The temperature was maintained at 30°C during the cultivation and pH was controlled by automatic addition of 2 M NaOH and 1 M HCl. Initial conditions in the bioreactor were pH: 3.0; stirring rate: 100 rpm; and aeration: 0.2 volumes of air per volume of fluid per minute (vvm). After germination, the stirring rate was gradually increased to 800 rpm and the air flow to 1 vvm. The pH was adjusted to 2.5 or 6.0 with addition of 2 M NaOH or 1 M HCl over 2 hours.

Chemostat cultivations

The chemostat cultivations were initiated as batch cultivations and in late exponential phase, supply of additional substrate through the feed was initiated. The feed medium was similar to the batch medium with the exception of the glucose concentration being 8 g/L. Pumps were controlled to a rate of 150 g/h (D = 0.1 h^{-1}). The first steady state, pH 2.5, was obtained after five residence times (50 hours), whereas the second steady state took place after three additional residence times (30 hours).

The pH shift to the second steady state was performed over five hours to avoid a morphological shift towards pellet formation.

6.3.9 Cell dry weight determination

The cell mass concentration on a dry weight basis was determined by the use of nitrocellulose filters with a pore size of 0.45 µm (Osmonics, Minnetonka, MN, USA). Initially, the filters were pre-dried in a microwave oven at 150 W for 20 min, and then weighed. A known weight of cell culture was filtered, and the residue was washed with distilled water. Finally, the filter was dried in the microwave at 150 W for 20 min and the dry weight was determined.

6.3.10 Quantification of extracellular metabolites

HPLC

For quantification of the extracellular metabolites, a culture sample was taken and immediately filtered through a 0.45 µm-pore-size nitrocellulose filter (Osmonics). The filtrate was frozen and kept at −20°C until analysis. Glucose, oxalate, citrate, gluconate, glycerol and acetate concentrations were detected and quantified by refractive index and UV using an Aminex HPX-87H cationic-exchange column (BioRad, Hercules, CA, USA) eluted at 35°C, with 5 mM H2SO4 at a flow rate of 0.6 mL min^{-1}.

Glucose assay

The applied HPLC method is unable to separate glucose and gluconate. Therefore, in samples where both glucose and gluconate were present, gluconate was quantified based on the UV-spectrum from the HPLC-analysis, whereas glucose was determined using a glucose enzymatic assay (Horiba ABX, Montpellier, France). This assay was based on NAD^+ through a coupled reaction with glucose-6-phosphate dehydrogenase and formation of NADH was determined spectrophotometrically by measuring the increase in absorbance at 340 nm.

6.3.11 Transcription analysis

Sampling

For gene expression analysis, mycelium was harvested at steady state by filtration through sterile Mira-Cloth (Calbiochem, San Diego, CA, USA). Liquid was quickly removed from the mycelium by squeezing, and it was then subsequently frozen in liquid nitrogen. Samples were stored at -80°C until RNA extraction.

Extraction of total RNA

Total RNA was extracted from 40 to 50 mg of frozen mycelium as described in (Andersen et al. 2009) and the quantity was determined using a Qubit 2.0 Fluorometer (Invitrogen). The total RNA was stored at -80°C until further processing.

cRNA and microarray

150 ng of total RNA in 1.5 µl was labeled according to the One Color Labeling for Expression Analysis, Quick Amp Low Input (QALI) version 6.5 May 2010 from Agilent Technologies. Yield and specific activity was determined on a NanoDrop ND-1000 and verified on Qubit 2.0. 1.65 µg labeled cRNA was fragmented at 60°C on a heating block and the cRNA was prepared for hybridization according to the QALI protocol.

100 µl sample was loaded on a 4 x 44 Agilent Gasket Slide situated in an Agilent Technologies hybridization chamber. The 4 x 44 Array was placed on top of the Gasket Slide. The Array was hybridized at 65°C for 17 hours in an Agilent Technologies Hybridization oven. The array was washed following the QALI protocol and scanned in a G2505C Agilent Technologies Micro Array Scanner.

Analysis of transcriptome data

The raw array signal was processed by first removing the background noise using the normexp method, and signal between arrays made comparable using the quantiles normalization method, as implemented in the Limma package (Smyth 2004) Multiple probe signals per gene were summarized into a gene-level expression index using Tukey's medianpolish (Irizarry et al. 2003).

Statistical analysis was applied to determine genes subject to differential transcriptional regulation. The limma package (Smyth 2004) was used to perform moderated *t* tests between sets of biological replicates from each pH level. Empiric Bayesian statistics were used to moderate the standard errors within each gene, and Benjamini-Hochberg's method (Benjamini and Hochberg 1995), to adjust for multitesting. A cut-off value of adjusted $P < 0.05$ was set to assess statistical significance.

6.3.12 Gene ontology enrichment analysis

Significantly regulated subsets of genes were examined for GO-term enrichment by using Cytoscape with BiNGO plugin (Maere et al. 2005). GO-term assignments were based on automatic annotation of the *A. niger* ATCC 1015 v3.0 gene models. The significance level was selected to $P < 0.05$ and calculated using hypergeometric testing with Benjamini & Hochberg correction.

6.4 Results

A. niger is known for its acid formation and recent studies have shown that a up to 6228 genes are influenced by ambient pH and the physiological response results in an acid production profile that ensures optimal acidification of the surrounding medium (Andersen et al. 2009). Based on these results, it was hypothesized that the acid formation response is mediated by trans-acting TFs , since the affected genes were scattered across the entire genome of *A. niger*. Further analysis of the data from (Andersen et al. 2009) resulted in a set of predicted transcription factors. The data was sorted into 17 clusters. In the largest cluster, which consisted of 2814 genes, a large number of housekeeping genes were identified. The main function of the genes in this cluster was considered to be growth or stress related and therefore not directly regulated by pH. Based on this, the cluster was excluded. In the resulting subset, now containing 3414 genes, the putative cis-acting transcription factors were predicted and removed. The predictions were performed using an in-house method based on their co-regulation with closely positioned biosynthetic clusters (data not shown). Finally, the trans acting transcription factors were ranked based on p-values.

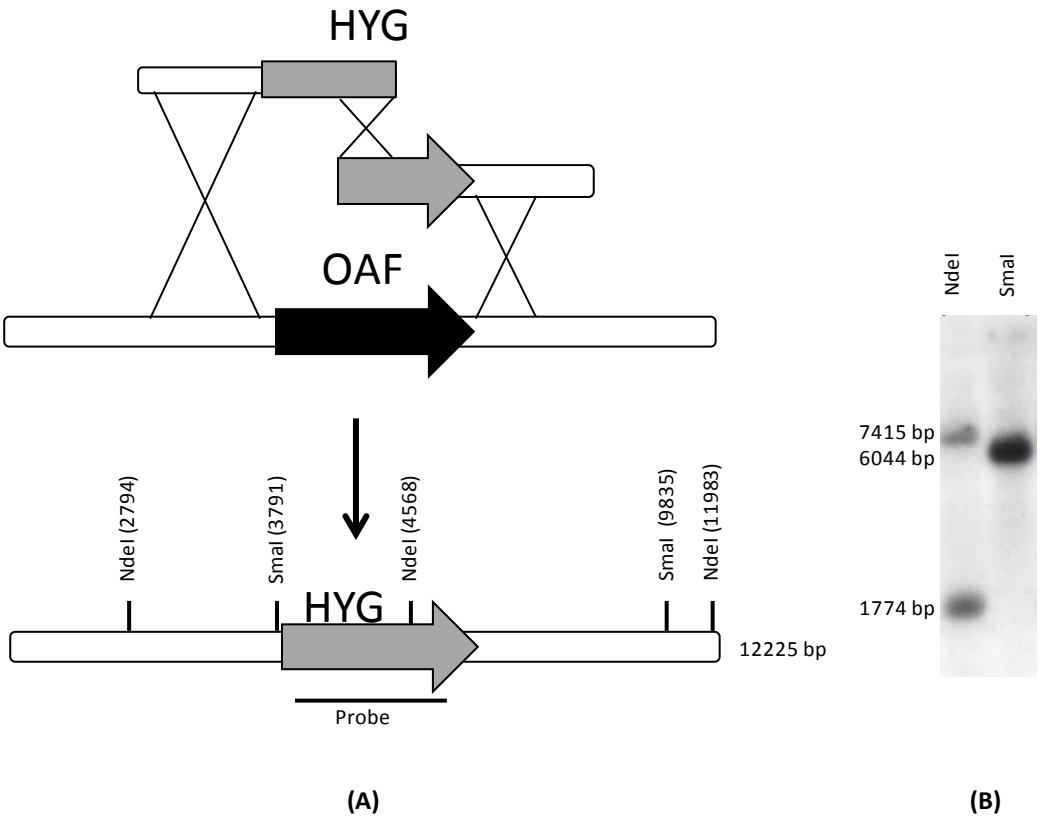

Figure 6.1 Graphical illustration of the gene deletion procedure exemplified with by insertion of hygromycin resistance marker into the *oafA* locus. (A) Bipartite substrate, locus and predicted resultant genomic locus. (B) Southern analysis of transformants for site specific integration of the construct. Genomic DNA was digested with either NdeI or SmaI. The position of the probe used is shown in (A).

The genes encoding the predicted TF's were individually deleted through a bipartite gene knockout approach (Nielsen et al. 2006) using hygromycin as dominant marker, Figure 6.1.A. The gene deletion was verified using PCR and resulting TF mutants were initially screened for an altered acid formation profile in static cultures (liquid cultures incubated without shaking). Three transformants per knockout were analyzed to ensure the phenotype was originated from a monogenetic effect. The assay simply relied on measurement of pH in the ambient medium. Particularly, one set of transformants showed an interesting phenotype as a significant decrease in pH was measured compared to the pH value in the wild type culture (data not shown). Subsequent HPLC analysis showed an increased oxalate formation, table 6.2. To validate for ectopic insertions, Southern analysis was carried out with a probe was designed so digestion with NdeI resulted in 2 bands of 1774 bp and 7415 bp respectively whereas SmaI digestion resulted in one band of 6044 bp. From the Southern blot, Figure 6.1.B, only correct sized bands were observed, thus the HygR cassette had been integrated at only at the right position in the genome of *A. niger* ATCC 1015. The corresponding transcription factor was entitled OafA (oxalic acid repression factor).

Table 6.2 Oxalate concentration in static cultures pH 6.0

	WT	***ΔoafA***		
		Transformatant A	Transformant B	Transformant C
	Oxalate g/L	Oxalate g/L	Oxalate g/L	Oxalate g/L
Minimal medium	1.15	2.78	2.72	2.34

6.4.1 Physiological characterization of the *ΔoafA*-strain

The constructed *ΔoafA* strain was subjected to detailed physiological characterization to explore the cellular performance of the oxalate overproducing strain from a quantitative perspective.

Batch cultures

The physiology of the wild type strain and the *ΔoafA* strain was compared in pH-controlled batch cultivations, in duplicates. *A. niger* has been reported to produce a range of different acids in high amounts at pH 6.0 (Ruijter et al. 1999, Andersen et al. 2009). Thus, by performing the batch cultures at this pH the acid profile together with the level of acid formation were challenged in the constructed *ΔoafA* strain.

Representative profiles of the biomass concentration, sugar concentration, carbon dioxide formation and acid formation during these batch cultivations are shown in Figure 6.2.

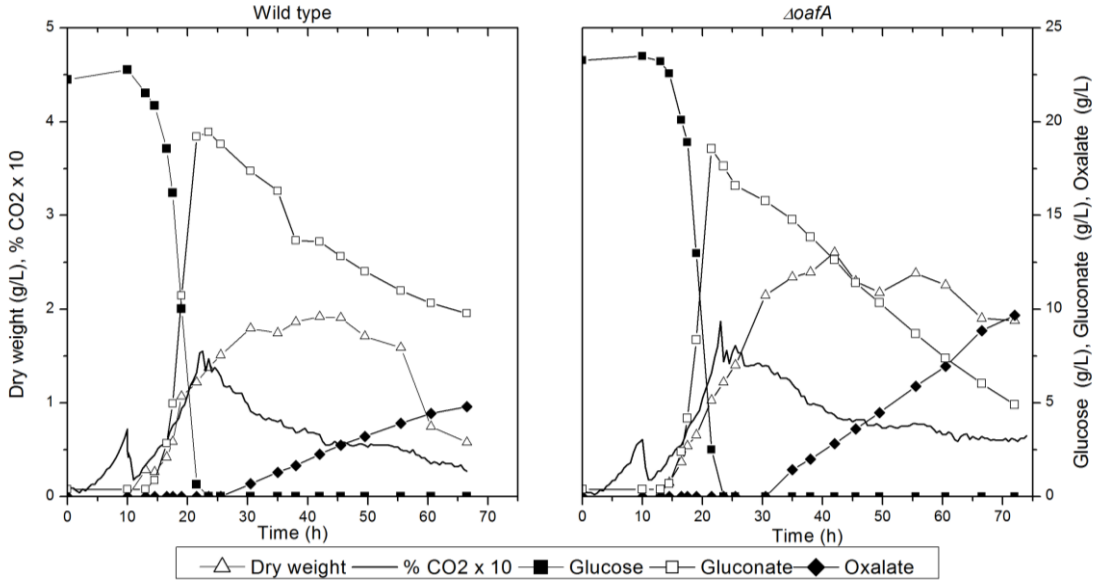

Figure 6.2 Representative profiles of the biomass concentration, sugar concentration, carbon dioxide formation and acid formation during batch cultivations at pH 6.0 with the WT-strain (left) and and the *ΔoafA* strain. The maximum specific growth rate was estimated trough a logarithmic plot of the biomass concentration as a function of time. Yield coefficients were calculated as overall yields based on the accumulated biomass or metabolite concentration in stationary phase related to the amount of consumed glucose. The volumetric oxalate formation rate was estimated as the slope of a linear regression of the oxalate titer as a function of time.

Characteristic for both the wild type and the *ΔoafA* strain was that the majority of glucose in the exponential growth phase was converted into gluconate and biomass, where gluconate formation accounted for approximately 90% of the carbon conversion. After complete utilization of glucose, gluconate was metabolized resulting in mainly oxalate formation, but citrate was also detected in both set of cultures, Figure 6.2. The maximum specific growth rates of the two strains were 0.23±0.02 h^{-1} and 0.25±0.02 h^{-1} for the WT and the *ΔoafA* strain respectively, so deleting *oafA* showed no effect on the growth rate. However, a notable difference was observed in the formation of oxalate as the yield of oxalate on glucose was increased by 87 % from 0.13 Cmol $Cmol^{-1}$ to 0.25 Cmol $Cmol^{-1}$ and the volumetric oxalate formation rate was doubled from 0.11±0.02 gOx $(L\ h)^{-1}$ in the WT to 0.22±0.00 gOx $(L\ h)^{-1}$ in the *ΔoafA* strain.

An interesting observation from the results of the batch cultivations was that acid production, except for gluconate formation, was mainly measured in stationary phase after glucose completion. From Figure 6.2 it

appears that during stationary phase the cells are converting gluconate to oxalate and oxalate formation is therefore decoupled from growth.

Characterization of *ΔoafA* in chemostat cultivations

To compare the acid production profiles of *ΔoafA* and the wild type during growth at both high and low pH, carbon limited chemostat cultivations were carried out. An important feature in the presented characterization was the application of chemostat cultures, as it can be difficult to obtain and maintain steady states working with filamentous fungi, because of the complex morphology of the cells (McIntyre and McNeil 1997). However, in this study steady states were obtained for both strains as well as for the two selected pH levels, Figure 6.3. The experimental setup was designed in a way that two steady states were obtained for each chemostat performed. An advantage of such a design is the possibility of attaining data from two distinct pH values using a single chemostat setup. Moreover, morphological issues such as pellet formation have been observed in transition from batch to chemostat at high pH (data not shown). To avoid pellet formation, the batch phase and the first steady state were at pH 2.5, whereas pH 5.0 was chosen for the second steady state, illustrated in Figure 6.3.

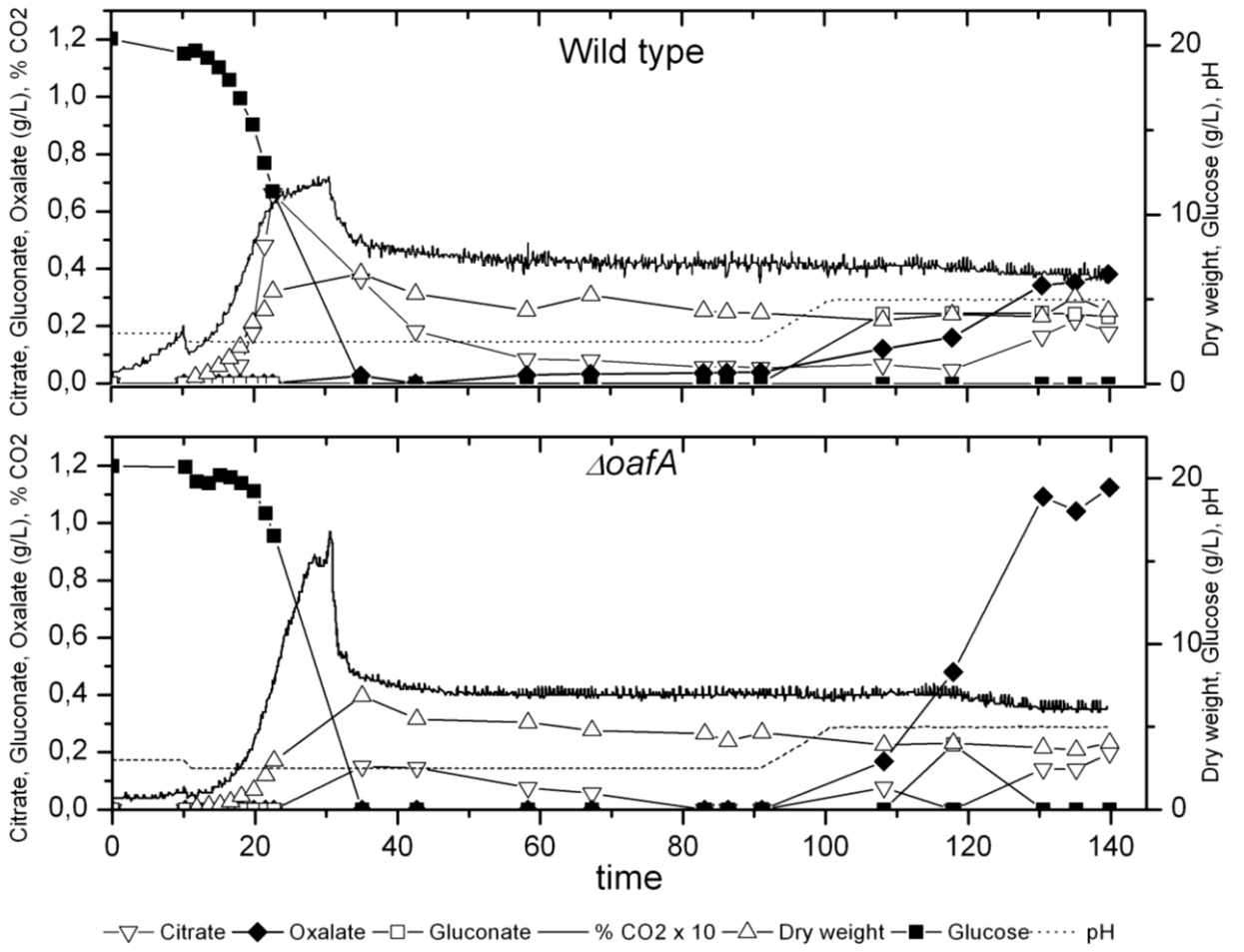

Figure 6.3 Representative profiles of chemostat cultivations for Wild type(top) and *ΔoafA*(bottom). Two steady states were obtained for each chemostat cultivation performed.

Figure 6.3 shows that for both strains, the main products in the exponential phase were biomass and CO_2 at comparable yields. However, low citrate production was observed in the wild type, a product not detected in *ΔoafA*. During the first steady state at pH 2.5, achieved at 73 h (5 retention times), the mutant had an unchanged product profile with identical quantities in comparison with the wild type. The second steady at state occurred at 126 hours, 3 retention times after pH change to pH 5.0. As it was evident in the high pH batch cultivation, *ΔoafA* had a highly increased oxalate formation (158 %) compared to WT, whereas both citrate and gluconate formation were reduced. A summary of growth and yield coefficients can be found in Table 6.3.

Table 6.3 Physiological coefficients from chemostat cultivations.

		Wild-type (Cmol/Cmol)	*ΔoafA* (Cmol/Cmol)	Difference
Batch phase ,pH 2.5	Y_{sx}	0.820 ± 0.026	0.803 ± 0.026	-2%
	$Y_{s,gluconate}$	0	0	0%
	$Y_{s,oxalate}$	0	0	0%
	$Y_{s,citrate}$	0.063 ± 0.027	0	-100%
	$Y_{s,CO2}$	0.225 ± 0.005	0.232 ± 0.007	3%
	Y_{so}	0.283 ± 0.05	0.282 ± 0.0 10	0%
Chemostat, pH 2.5	Y_{sx}	0.666 ± 0.019	0.685 ± 0.014	3%
	$Y_{s,gluconate}$	0	0	0%
	$Y_{s,oxalate}$	0	0	0%
	$Y_{s,citrate}$	0	0	0%
	$Y_{s,CO2}$	0.330 ± 0.002	0.313 ± 0.019	-5%
	Y_{so}	0.043 ± 0.004	0.036 ± 0.005	-16%
Chemostat, pH 5.0	Y_{sx}	0.679 ± 0.024	0.593 ± 0.005	-13%
	$Y_{s,gluconate}$	0.034 ± 0.003	0	-100%
	$Y_{s,oxalate}$	0.034 ± 0.004	0.088 ± 0.003	158%
	$Y_{s,citrate}$	0.017 ± 0.005	0.006 ± 0.011	-62%
	$Y_{s,CO2}$	0.335 ± 0.021	0.273 ± 0.032	-19%
	Y_{so}	0.046 ± 0.004	0.030 ± 0.004	-35%

From Table 6.3 it is apparent that the main different between the *ΔoafA* mutant and the wild type strain is increased oxalate formation in the *ΔoafA* mutant at the expense of gluconate, particularly in the second steady state at pH 5.0. The validity of the observed oxalate overproducing phenotype in the *ΔoafA* mutant is substantiated by the carbon balances, which closes for each distinctive phase.

The *ΔoafA* thus exhibits an oxalate overproducer phenotype at high pH in both the reported batch and chemostat culture, as well as in the initial screening. To investigate the transcriptional aspects of this phenotype and to obtain further insight to OafA's function as a transcription factor, biomass samples were

taken from all biological triplicates at steady state conditions (12 samples in total) and subjected to transcriptome analysis.

6.4.2 Transcriptome analysis

Data from the biological triplicates of the two strains at pH 2.5 and 5.0 were statistically analyzed, and genes that were significantly regulated (Benjamini-Hochberg corrected Bayesian P values < 0.05) in pair-wise comparisons between two strains were identified across pH. The raw data of the expression levels of all the *A. niger* gene analyzed are presented in the appendix 3 together with complete lists of the genes differentially expressed in the two strains at different pH's.

Comparing the wild type with the *oafA* mutant at the first steady state (pH 2.5), a notably low number of significantly regulated genes were identified. Seven genes with a significant change in expression level, where four have been annotated, were identified. They included: down-regulation of a putative lysophospholipase, a polyketide syntease and intriguingly oxaloacetate acetylhydrolase (*oahA*), the enzyme converting oxaloacetate to oxalate.

At pH 5.0, 241 genes were significant changed in expression levels, 121 genes being up-regulated and 120 being down-regulated. A Gene Ontology overrepresentation analysis on the subset of up-regulated genes revealed an enrichment of 19 genes (p-value $3.43 \cdot 10^{-4}$, cluster freq 19/64, genome freq. 818/6268) associated with transport processes and within this subset three of these putative transporters were annotated as hexose transporters.

Among the up-regulated genes, five TFs were found, where four were located next to putative secondary metabolite clusters. However, each TF showed a limited degree of co regulation with their nearby secondary metabolite cluster, predicted by an in-house method (data not shown). Additionally, two genes encoding for epigenic regulation, a RNA-dependent RNA polymerase (GeneID: 176277) and a histone acetyltransferase (GeneID: 53882) were also found to be up-regulated.

The phenotypic trait of the *ΔoafA* strain was shown to be a significant increase in oxalate formation. It was therefore surprising that the gene encoding *oahA* (oxalate dehydrogenase) was not up-regulated. Yet a slight up-regulation of a cytosolic malate dehydrogenase (MDH), the enzyme responsible for converting malate to oxaloacetate, was measured.

An ontology overrepresentation analysis on the subset of down-regulated genes showed an enrichment of 28 genes associated with oxidoreductase activity (p-value $1.58 \cdot 10^{-5}$, cluster freq 28/52, total freq

1300/6268). Two of these genes, a NADH-dehydrogenase and monooxygenase were associated with the oxidative phosphorylation. A catalase and a chloroperoxidase were additionally found down-regulated, a further indication of reduced oxidative phosphorylation.

In addition, down-regulation of two phosphoketolases were detected. GeneID 54814 contained zero introns, suggesting this gene might be of bacterial origin. GeneID 197387 contained six introns indicating that it has evolved within the eukaryote kingdom. An alignment of the two protein sequences showed 88 % query coverage and a max identity of 44 % suggesting that they are not homologs. Down-regulation of acetate kinase (206885) and an Acyl-CoA syntase (129581), both enzymes responsible for converting acetate-phosphate into acetyl-CoA, was observed as well.

6.5 Discussion

Deletion of a putative trans-acting transcription factor entitled oxalic acid repression factor, OafA, resulted in an oxalate overproducing strain. The physiology of the constructed strain was characterized in detail, in both batch and chemostat cultivations, and compared to wild type physiology. In addition, transcriptome analysis at steady state conditions at both high and low pH highlighted the transcriptional response caused by the deletion of *oafA*.

6.5.1 Differences in acid production

The physiological characterization of the *ΔoafA* mutant showed an altered organic acid production profile at high pH compared to the wild type strain. All of the acid yields were affected, but in particular the oxalate yield increased (Figure 6.2, Figure 6.3 and Table 6.3). In the batch cultures, glucose was converted to gluconate with a similar specific yield of approximately 90% in the exponential phase, but the *ΔoafA* strain showed an improved reuptake and conversion of gluconate to oxalate. In the chemostat cultivation at pH 5.0, no gluconate was detected for the mutant and the oxalate yield on glucose was increased. Based on these results it may be argued that gluconate was produced with a similar rate in the mutant and the wild type, but the increased reuptake of gluconate and conversion to oxalate, argued from the batch results, leads to a complete re-consumption of gluconate and therefore no detectable level of this acid. The citrate formation was in both cultivation types found to be reduced by approximately 60 %, however this was the least reproducible coefficient, hence it should be cautiously interpreted. An intriguing observation from the chemostat cultivations at pH 5.0 was the total acid yield, summarizing the yields of gluconate, citrate and oxalate on glucose, being similar for the two strains corresponding to 0.099 cmol cmol^{-1} for the wild type strain and 0.094 cmol cmol^{-1} for the *ΔoafA* mutant. This indicates that the capacity for acid

production is the same for the two strains under the defined conditions, but deletion of the oxalic acid repression factor ensures a more efficient conversion of gluconate to oxalate. The acid response of *A. niger* has been argued to be an evolutionary selection for efficient acidification of the environment and gluconate does not contribute to a noteworthy acidification compared to oxalate and citrate (Andersen et al. 2009). The conversion of glucose to gluconate is therefore considered an efficient way of rapidly make glucose unavailable for competing organisms (Ruijter et al. 1999, Andersen et al. 2009) thus, the constructed *ΔoafA* appears to be better at acidifying the ambient medium through efficient metabolization of gluconate.

6.5.2 Transcriptome analysis

The physiological characterization provided insight to the profile and quantitative aspects of acid production in the constructed *ΔoafA* mutant compared to the wild type strain. However, details on how the deletion of *ΔoafA* affected the central carbon metabolism were limited, which is of high relevance since the main metabolic response appears to be more efficient utilization of gluconate in the constructed strain. Therefore, transcriptional profiling across both strains and pH were performed. Transcriptome analysis was carried out on biological material from the chemostat cultures. Using this type of setup, pH and the strains were the only variables and running the experiments in triplicates ensured high reproducibility, Table 6.3. Furthermore, at steady state conditions in a carbon limited culture it is possible to mimic the conditions at glucose depletion and simultaneously obtain both acid formation and growth. This enables discrimination of even low-fold differences in expression and has been successfully applied earlier in *Aspergillus oryzae* (Muller et al. 2002).

The number of differentially expressed genes identified in the transcription analysis at pH 5.0 was 241. Considering that this response is caused by deletion of a single gene, *oafA*, it appears remarkable that one putative trans-acting TF is regulating this amount of genes. An explanation of the high number of affected genes could be the up-regulation of two genes connected to epigenetic regulation, especially a putative histone acetyltransferase. Epigenetic regulation has attracted attention in connection with secondary metabolite production (Reyes-Dominguez et al. 2010, Nutzmann et al. 2011), as it has been seen that certain secondary metabolism clusters are silent, but can be activated by deletion of the histone deacetylase HdaA, or inhibition of other fungal HDACs by trichostatin A (Shwab et al. 2007).

Oxaloacetate hydrolase encoded by *oahA* is an important enzyme in oxalate production, as it catalyzes the conversion of oxaloacetate to oxalate and acetate. It was therefore a surprising discovery that no change in expression level of *oahA* was measured at high pH in the *ΔoafA* mutant, since this strain was found to be an

oxalate overproducer. This indicates that *oahA* is either regulated after translation or *oahA* is not a rate-limiting step for oxalate formation. The latter appears to be more likely since the K_m value for OahA is 0.004 mM (Pedersen et al. 2000b) and K_m for malate dehydrogenase is 0.09 mM (Ma et al. 1981) and an up-regulation of a cytosolic malate dehydrogenase was observed at high pH. This enzyme has previously been shown to play a key role in acid production (de Jongh and Nielsen 2008), as over expression of malate dehydrogenase lead to increased citrate production as well as oxalate production. At low pH a significant down-regulation of *oahA* was measured, which was unexpected as the *oafA* mutant had an oxalic acid overproducing phenotype. However, as shown in Table 3 and supported by Ruijter et al. (1999), oxalate was not detected at low pH and that makes the observation less important with respect to the *oafA* phenotype at low pH.

Another interesting observation was the up-regulation of transporters in the *ΔoafA* mutant at high pH, particularly sugar permeases. This could explain the lack of gluconate in these chemostats, since the increased reuptake of gluconate could be mediated by the higher permease activity. Despite this higher permease activity, no genes coding for glycolytic enzymes were to be found differentially regulated. This is however a consequence of the chemostats being glucose limited and the glucose uptake cannot be affected by the higher permease activity.

6.5.3 The role of phosphoketolases in oxalate production

Deletion of *oafA* resulted in a metabolic shift in the central metabolism demonstrated by the down-regulation of both phosphoketolases (GeneID 54814 and 197387) in the *ΔoafA* mutant. Two types of phosphoketolases have been described in the literature. Type 1 (EC 4.1.2.9) catalyzes, in the presence of inorganic phosphate, an irreversible cleavage of D-xylulose-5-phosphate into acetyl phosphate and glyceraldehyde-3-phosphate. Type 2 (EC 4.1.2.22) also termed fructose-6-phosphate phosphoketolase catalyzes as well in presence of phosphate, an irreversible cleavage of D-fructose 6-phosphate into acetyl phosphate and D-erythrose 4-phosphate. The activity of type 1 phosphoketolases is well characterized in a wide range of bacterial species and recently indications of this activity were found in *Penicillium chrysogenum* (Thykaer and Nielsen 2007). Type 2 activity has only been described within a relative low number of bacteria with bifidobacterium being most predominant (Roopashri and Varadaraj 2009).

An interesting finding in relation to geneID 197387 was that the open reading frame (ORF) of this gene was located next to the ORF of an acetate kinase. The close linkage of the ORFs of phosphoketolase and acetate kinase is found in many bacteria (Ingram-Smith et al. 2006), and this argues for geneID 197387 being a D-

xylulose 5-phosphate phosphoketolase. Which type geneID 54814 is encoding, can only be speculative since the only annotated gene in the vicinity is a hypothetical dehydrogenase with an interpro id suggesting a glucose/ribitol dehydrogenase activity.

The product in common for the two phosphoketolase enzymes is acetyl-phosphate that can be converted to acetyl-CoA through two enzymatic steps catalyzed by acetate-kinase and acetyl-CoA synthase, respectively. Together with the two genes encoding the phosphoketolases, the genes encoding acetate-kinase and acetyl-CoA synthase were also down-regulated in the *ΔoafA* mutant. The metabolic response caused by the deletion of *oafA* is presented in Figure 6.4. As a consequence of the down regulation of the phosphoketolases, the acetate-kinase and the acetyl-CoA synthase, the cytosolic pool of acetyl-phosphate and the mitochondrial acetate pool must be reduced. To compensate for this, a larger fraction mitochondrial AcCoA must originate from pyruvate, which requires a higher flux through glycolysis. This argument is supported by the reported correlation between the glycolytic flux and the pool size of acetyl-CoA (Sorensen et al. 2009). It was observed that addition of lactate, led to an increased pool of AcCoA, which caused an up-regulation of the rate-limiting enzyme of the pentose phosphate pathway (PP pathway), Glucose-6-phosphate dehydrogenase (Sorensen et al. 2009). In addition, increased flux through glycolysis has earlier been associated with increased organic acid production. In citrate overflow metabolism, the majority of the citrate produced originates from the glycolytic pathway (Cleland and Johnson 1954, Legiša and Mattey 1986). However, based on the transcriptional profiling of the *ΔoafA* mutant, none of the genes encoding glycolytic enzymes were up-regulated. As described earlier, an up-regulation of sugar permeases were argued to mediate an increased reuptake of gluconate in the *ΔoafA* mutant compared to the wild type strain. Furthermore, since the cultures were carried out as glucose limited chemostats, the glucose uptake rate was fixed but the reuptake of gluconate by the mutant strain could result in a higher amount of carbon metabolized through the glycolysis without a significant up-regulation of the glycolytic genes, subsequently leading to the observed overproduction of oxalate.

In continuation of the proposed higher flux through glycolysis, the measured down-regulation of the two phosphoketolase genes indicate a lower flux through the pentose phosphate pathway in the *oafA* mutant compared to the wild type strain. The primary outcome of the PP-pathway is generation of reducing equivalents in the form of NADPH, used mainly in reductive biosynthesis reactions *e.g.* amino acid biosynthesis. A reduced flux through the PP-pathway would therefore result in a lower biomass yield and this further substantiates the argument of a lower PP-pathway in the *oafA* mutant, as the biomass yield, Y_{SX}; in the *ΔoafA* strain was reduced compared to Y_{SX} of the wild type. Finally, in the reverse study where *oahA* was deleted in *A. niger* eliminating oxalic acid production, an increase in the PP-pathway flux of 10%

was detected (Pedersen et al. 2000a, Pedersen et al. 2000b). Whether this was due to an up-regulation of the phosphoketolases can only be speculative since neither transcription profiles nor enzyme activities of these two enzymes were measured. Based on the results of the transcriptional profiles and the physiological characterizations of the *oafA* mutant and the wild type strain, it is argued that the increased oxalate formation in the *oafA* mutant is a consequence of an effective re-uptake of gluconate and thereby a higher flux through glycolysis resulting in a lower flux through the PP-pathway, demonstrated by down-regulation of the two phosphoketolases.

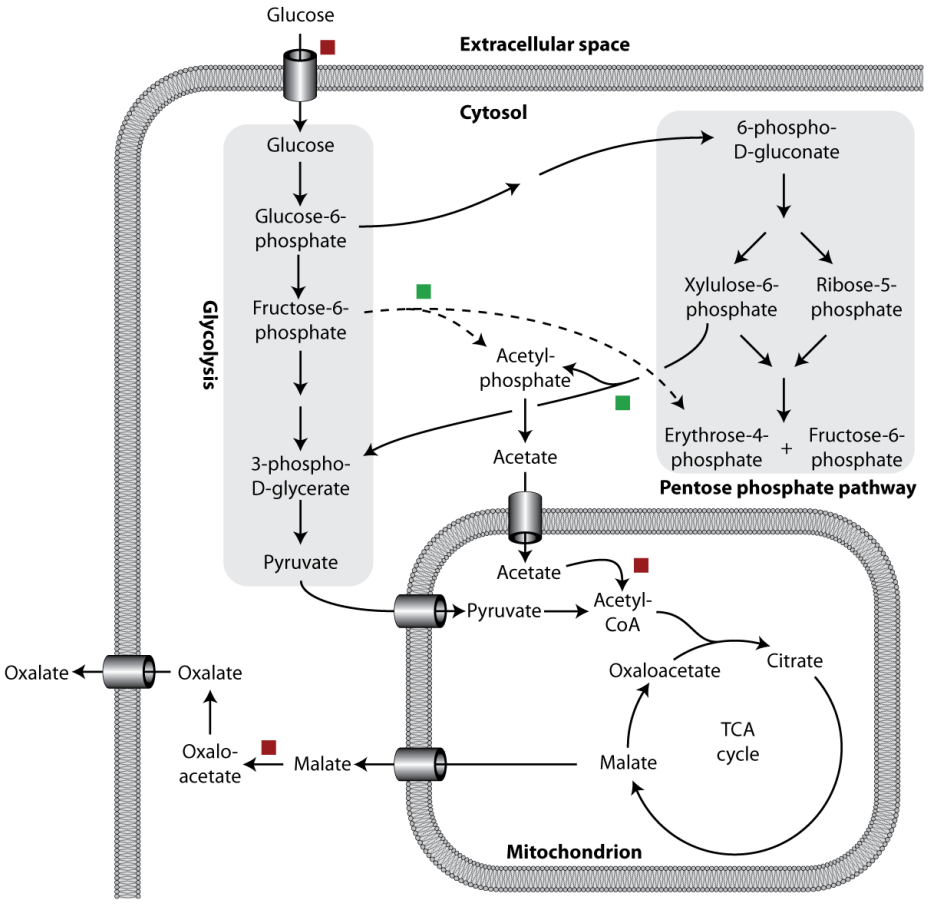

Figure 6.4 Metabolic map illustrating the response of central carbon metabolism caused by the *oafA* deletion. A red box indicates up-regulation of a gene encoding an enzyme catalyzing this reaction. Green box indicates down-regulation. The dotted line indicates fructose-6-phosphate phosphoketolase, a reaction not previously described within the fungal kingdom.

6.5.4 Oxidative phosphorylation

The oxidative phosphorylation is responsible for the major ATP generation during aerobic metabolism by coupling reoxidation of NADH to ATP synthesis. In the *ΔoafA* strain, down-regulation of the oxidative

phosphorylation was observed both physiologically by a 35 % decrease in oxygen consumption pr cmol glucose (Y_{SO}) and transcriptionally as down-regulation of a NADH dehydrogenase and monooxygenase both with ubiquinone binding. The decreased activity of the oxidative phosphoylation is further supported by the down-regulation of genes encoding a catalase and a chloroperoxidase. These enzymes are highly conserved in organisms exposed to oxygen and aid removal of reactive oxygen species that is an inevitable byproduct of the cytochrome c oxidase complex. To our knowledge a connection between oxidative phosphorylation and oxalate production has not been described, however the mutant response presented here provides indications of such a connection.

6.6 Conclusion

From the results described above it is concluded that OafA is a trans-acting transcription factor since deletion of the responsible gene resulted in 241 genes being differently expressed compared to the wild type strain. In addition, OafA's function as a transcription factor was further underlined by the altered acid production profile in the *ΔoafA* mutant strain, with focus on the mutant being an oxalate overproducing strain.

Through transcription analysis, reduced phosphoketolase activity together with increased reuptake of gluconate were identified as being the main players in the metabolic response, resulting in the observed oxalate overproducing phenotype of the *ΔoafA* strain. Furthermore, the oxidative phosphorylation was down-regulated in the oafA mutant and this indicates an interesting correlation between the oxidative phosphorylation and organic acid formation.

6.7 Acknowledgements

The students Julie Philip and Katherina Garcia Vanegas are acknowledged for their part in the experimental work.

6.8 References

Alper, H., J. Moxley, E. Nevoigt, G. R. Fink and G. Stephanopoulos (2006). "Engineering yeast transcription machinery for improved ethanol tolerance and production." Science **314**(5805): 1565-1568.

Andersen, M. R., L. Lehmann and J. Nielsen (2009). "Systemic analysis of the response of *Aspergillus niger* to ambient pH." Genome Biol **10**(5): R47.

Andersen, M. R., M. P. Salazar, P. J. Schaap, P. J. van de Vondervoort, D. Culley, J. Thykaer, J. C. Frisvad, K. F. Nielsen, R. Albang, K. Albermann, R. M. Berka, G. H. Braus, S. A. Braus-Stromeyer, L. M. Corrochano, Z. Dai, P. W. van Dijck, G. Hofmann, L. L. Lasure, J. K. Magnuson, H. Menke, M. Meijer, S. L. Meijer, J. B. Nielsen, M. L. Nielsen, A. J. van Ooyen, H. J. Pel, L. Poulsen, R. A. Samson, H. Stam, A. Tsang, J. M. van den Brink, A. Atkins, A. Aerts, H. Shapiro, J. Pangilinan, A. Salamov, Y. Lou, E. Lindquist, S. Lucas, J. Grimwood, I. V. Grigoriev, C. P. Kubicek, D. Martinez, N. N. van Peij, J. A. Roubos, J. Nielsen and S. E. Baker (2011). "Comparative genomics of citric-acid-producing *Aspergillus niger* ATCC 1015 versus enzyme-producing CBS 513.88." Genome Res **21**(6): 885-897.

Baker, S. E. (2006). "*Aspergillus niger* genomics: past, present and into the future." Med Mycol **44 Suppl 1**: S17-21.

Benjamini, Y. and Y. Hochberg (1995). "Controlling the False Discovery Rate: A Practical and Powerful Approach to Multiple Testing." Journal of the Royal Statistical Society. Series B (Methodological) **57**(1): 289-300.

Cleland, W. W. and M. J. Johnson (1954). "Tracer experiments on the mechanism of citric acid formation by *Aspergillus niger*." J Biol Chem **208**(2): 679-689.

de Jongh, W. A. and J. Nielsen (2008). "Enhanced citrate production through gene insertion in *Aspergillus niger*." Metab Eng **10**(2): 87-96.

Galagan, J. E., S. E. Calvo, K. A. Borkovich, E. U. Selker, N. D. Read, D. Jaffe, W. FitzHugh, L. J. Ma, S. Smirnov, S. Purcell, B. Rehman, T. Elkins, R. Engels, S. Wang, C. B. Nielsen, J. Butler, M. Endrizzi, D. Qui, P. Ianakiev, D. Bell-Pedersen, M. A. Nelson, M. Werner-Washburne, C. P. Selitrennikoff, J. A. Kinsey, E. L. Braun, A. Zelter, U. Schulte, G. O. Kothe, G. Jedd, W. Mewes, C. Staben, E. Marcotte, D. Greenberg, A. Roy, K. Foley, J. Naylor, N. Stange-Thomann, R. Barrett, S. Gnerre, M. Kamal, M. Kamvysselis, E. Mauceli, C. Bielke, S. Rudd, D. Frishman, S. Krystofova, C. Rasmussen, R. L. Metzenberg, D. D. Perkins, S. Kroken, C. Cogoni, G. Macino, D. Catcheside, W. Li, R. J. Pratt, S. A. Osmani, C. P. DeSouza, L. Glass, M. J. Orbach, J. A. Berglund, R. Voelker, O. Yarden, M. Plamann, S. Seiler, J. Dunlap, A. Radford, R. Aramayo, D. O. Natvig, L. A. Alex, G. Mannhaupt, D. J. Ebbole, M. Freitag, I. Paulsen, M. S. Sachs, E. S. Lander, C. Nusbaum and B. Birren (2003). "The genome sequence of the filamentous fungus Neurospora crassa." Nature **422**(6934): 859-868.

Goffeau, A., B. G. Barrell, H. Bussey, R. W. Davis, B. Dujon, H. Feldmann, F. Galibert, J. D. Hoheisel, C. Jacq, M. Johnston, E. J. Louis, H. W. Mewes, Y. Murakami, P. Philippsen, H. Tettelin and S. G. Oliver (1996). "Life with 6000 genes." Science **274**(5287): 546, 563-547.

Heinrich, M. and H. J. Rehm (1982). "Formation of gluconic acid at low pH-values by free and immobilized *Aspergillus niger* cells during citric acid fermentation." Applied Microbiology and Biotechnology **15**(2): 88-92.

Ingram-Smith, C., S. R. Martin and K. S. Smith (2006). "Acetate kinase: not just a bacterial enzyme." Trends Microbiol **14**(6): 249-253.

Irizarry, R. A., B. M. Bolstad, F. Collin, L. M. Cope, B. Hobbs and T. P. Speed (2003). "Summaries of Affymetrix GeneChip probe level data." Nucleic Acids Res **31**(4): e15.

Legiša, M. and M. Mattey (1986). "Glycerol as an initiator of citric acid accumulation in *Aspergillus niger*." Enzyme and Microbial Technology **8**(5): 258-259.

Ma, H., C. P. Kubicek and M. Röhr (1981). "Malate dehydrogenase isoenzymes in *Aspergillus niger*." FEMS Microbiology Letters **12**(2): 147-151.

Maere, S., K. Heymans and M. Kuiper (2005). "BiNGO: a Cytoscape plugin to assess overrepresentation of gene ontology categories in biological networks." Bioinformatics **21**(16): 3448-3449.

McCluskey, K., A. Wiest and M. Plamann (2010). "The Fungal Genetics Stock Center: a repository for 50 years of fungal genetics research." J Biosci **35**(1): 119-126.

McCue, L. A., W. Thompson, C. S. Carmack and C. E. Lawrence (2002). "Factors influencing the identification of transcription factor binding sites by cross-species comparison." Genome Res **12**(10): 1523-1532.

McIntyre, M. and B. McNeil (1997). "Effect of carbon dioxide on morphology and product synthesis in chemostat cultures of *Aspergillus niger* A60." Enzyme and Microbial Technology **21**(7): 479-483.

Milo, R., S. Shen-Orr, S. Itzkovitz, N. Kashtan, D. Chklovskii and U. Alon (2002). "Network motifs: simple building blocks of complex networks." Science **298**(5594): 824-827.

Muller, C., M. McIntyre, K. Hansen and J. Nielsen (2002). "Metabolic engineering of the morphology of *Aspergillus oryzae* by altering chitin synthesis." Appl Environ Microbiol **68**(4): 1827-1836.

Nielsen, M. L., L. Albertsen, G. Lettier, J. B. Nielsen and U. H. Mortensen (2006). "Efficient PCR-based gene targeting with a recyclable marker for *Aspergillus nidulans*." Fungal Genet Biol **43**(1): 54-64.

Nielsen, M. L., J. B. Nielsen, C. Rank, M. L. Klejnstrup, D. K. Holm, K. H. Brogaard, B. G. Hansen, J. C. Frisvad, T. O. Larsen and U. H. Mortensen (2011). "A genome-wide polyketide synthase deletion library uncovers

novel genetic links to polyketides and meroterpenoids in *Aspergillus nidulans*." FEMS Microbiol Lett **321**(2): 157-166.

Nutzmann, H. W., Y. Reyes-Dominguez, K. Scherlach, V. Schroeckh, F. Horn, A. Gacek, J. Schumann, C. Hertweck, J. Strauss and A. A. Brakhage (2011). "Bacteria-induced natural product formation in the fungus *Aspergillus nidulans* requires Saga/Ada-mediated histone acetylation." Proc Natl Acad Sci U S A **108**(34): 14282-14287.

Pedersen, H., B. Christensen, C. Hjort and J. Nielsen (2000a). "Construction and Characterization of an Oxalic Acid Nonproducing Strain of *Aspergillus niger*." Metabolic Engineering **2**(1): 34-41.

Pedersen, H., C. Hjort and J. Nielsen (2000b). "Cloning and characterization of oah, the gene encoding oxaloacetate hydrolase in *Aspergillus niger*." Mol Gen Genet **263**(2): 281-286.

Pel, H. J., J. H. de Winde, D. B. Archer, P. S. Dyer, G. Hofmann, P. J. Schaap, G. Turner, R. P. de Vries, R. Albang, K. Albermann, M. R. Andersen, J. D. Bendtsen, J. A. Benen, M. van den Berg, S. Breestraat, M. X. Caddick, R. Contreras, M. Cornell, P. M. Coutinho, E. G. Danchin, A. J. Debets, P. Dekker, P. W. van Dijck, A. van Dijk, L. Dijkhuizen, A. J. Driessen, C. d'Enfert, S. Geysens, C. Goosen, G. S. Groot, P. W. de Groot, T. Guillemette, B. Henrissat, M. Herweijer, J. P. van den Hombergh, C. A. van den Hondel, R. T. van der Heijden, R. M. van der Kaaij, F. M. Klis, H. J. Kools, C. P. Kubicek, P. A. van Kuyk, J. Lauber, X. Lu, M. J. van der Maarel, R. Meulenberg, H. Menke, M. A. Mortimer, J. Nielsen, S. G. Oliver, M. Olsthoorn, K. Pal, N. N. van Peij, A. F. Ram, U. Rinas, J. A. Roubos, C. M. Sagt, M. Schmoll, J. Sun, D. Ussery, J. Varga, W. Vervecken, P. J. van de Vondervoort, H. Wedler, H. A. Wosten, A. P. Zeng, A. J. van Ooyen, J. Visser and H. Stam (2007). "Genome sequencing and analysis of the versatile cell factory *Aspergillus niger* CBS 513.88." Nat Biotechnol **25**(2): 221-231.

Punt, P. J., F. H. Schuren, J. Lehmbeck, T. Christensen, C. Hjort and C. A. van den Hondel (2008). "Characterization of the *Aspergillus niger* prtT, a unique regulator of extracellular protease encoding genes." Fungal Genet Biol **45**(12): 1591-1599.

Reyes-Dominguez, Y., J. W. Bok, H. Berger, E. K. Shwab, A. Basheer, A. Gallmetzer, C. Scazzocchio, N. Keller and J. Strauss (2010). "Heterochromatic marks are associated with the repression of secondary metabolism clusters in *Aspergillus nidulans*." Mol Microbiol **76**(6): 1376-1386.

Roopashri, A. N. and M. C. Varadaraj (2009). "Molecular characterization of native isolates of lactic acid bacteria, bifidobacteria and yeasts for beneficial attributes." Appl Microbiol Biotechnol **83**(6): 1115-1126.

Ruijter, G. J., P. J. van de Vondervoort and J. Visser (1999). "Oxalic acid production by *Aspergillus niger:* an oxalate-non-producing mutant produces citric acid at pH 5 and in the presence of manganese." Microbiology **145 (Pt 9)**: 2569-2576.

Sambrook, J. and D. W. Russell (2001). Molecular cloning : a laboratory manual. Cold Spring Harbor, N.Y., Cold Spring Harbor Laboratory Press, 0879695773 (paper)

Schumann, J. and C. Hertweck (2006). "Advances in cloning, functional analysis and heterologous expression of fungal polyketide synthase genes." J Biotechnol **124**(4): 690-703.

Schuurmans, J. M., S. L. Rossell, A. van Tuijl, B. M. Bakker, K. J. Hellingwerf and M. J. Teixeira de Mattos (2008). "Effect of hxk2 deletion and HAP4 overexpression on fermentative capacity in *Saccharomyces cerevisiae*." FEMS Yeast Res **8**(2): 195-203.

Shwab, E. K., J. W. Bok, M. Tribus, J. Galehr, S. Graessle and N. P. Keller (2007). "Histone deacetylase activity regulates chemical diversity in *Aspergillus*." Eukaryot Cell **6**(9): 1656-1664.

Smyth, G. K. (2004). "Linear models and empirical bayes methods for assessing differential expression in microarray experiments." Stat Appl Genet Mol Biol **3**: Article3.

Sorensen, L. M., R. Lametsch, M. R. Andersen, P. V. Nielsen and J. C. Frisvad (2009). "Proteome analysis of *Aspergillus niger*: lactate added in starch-containing medium can increase production of the mycotoxin fumonisin B2 by modifying acetyl-CoA metabolism." BMC Microbiol **9**: 255.

Thykaer, J. and J. Nielsen (2007). "Evidence, through C13-labelling analysis, of phosphoketolase activity in fungi." Process Biochemistry **42**(7): 1050-1055.

Chapter 7 Identification and characterization of a transcription factor regulating extracellular proteolytic activity in *Aspergillus niger*

Poulsen L, Nielsen, JC., Lantz AE. and Thykaer J

7.1 Abstract

Aspergillus niger is widely used in the biotechnological industry, as it possess the ability to secrete proteins in high titters. The yield of protein can be significantly reduced by proteolytic degradation, as a result of secreted fungal proteases during cultivation. Based on transcriptome data, putative trans-acting, pH responding transcription factors were identified and through knock out studies, a mutant exhibiting a reduced extracellular protease activity was identified. The gene of the responsible transcription factor was entitled protease regulator B (prtB). The prtB mutant strain (*ΔprtB)* was benchmarked against the well described protease deficient strain, *ΔprtT*. The extracellular proteolytic activity was examined in three different media, featuring different levels of protease induction.

The *ΔprtT* strain showed superior to *ΔprtB* in respect to reduced protease activity. Compared to the wild type, the *ΔprtB* strain's secreted protease activity was nearly twofold reduced whereas the *ΔprtT* strain's extracellular proteolytic activity was fivefold reduced. However, the *ΔprtT* strain had a higher CO_2 yield on substrate (44 % increased) and a lower biomass yield coefficient compared to the wild type and *ΔprtB*. Additionally, the *ΔprtB* strain had a threefold reduction of oxalate formation compared to wild type and *ΔprtT*. The results from the study showed that the *ΔprtB* strain holds potential as a future protein production host in the biotechnological industry.

7.2 Introduction

The *Aspergillus* family, in particular *A. niger*, is widely applied as host for protein production. One of the challenges using e.g. *A. niger* as production organism, is the formation and secretion of proteolytic enzymes, that are produced simultaneously with the protein of interest. The proteases are a general problem because they degrade the product and the problem is even more pronounced in production of heterologous proteins due to the foreign origin of the produced protein. Consequently, homologous proteins are in most cases produced in one to two orders of magnitude higher than heterologous proteins (Braaksma and Punt 2008). The challenge with protease formation in *A. niger* is underlined by more than 150 genes encoding for proteases being identified in this fungus (Edens et al. 2005), where 32 of these genes contain an export signal or have strong similarity to other secreted proteases in other organisms (Pel et al. 2007). This indicates a complex regulation of the proteolytic system, which renders the fungus with the ability to adapt to a wide range of environmental conditions, including pH and temperature variations.

The protease problem has been addressed by construction of protease deficient strains, which resulted in reduced protease secretion (van den Hombergh et al. 1997a, van den Hombergh et al. 1997b). Another strategy could be to target the regulation of the proteases by alteration of transcription factors (TF), as described in chapter 5.

Only one TF regulating extracellular protease activity have so far been identified in *A. niger*, designated *prtT.* Initially Mattern et al. (1992) identified a protease mutant, AB1.13, obtained by applying UV mutagenesis. The location of the mutation was later identified by Braaksma & Punt (2008), to be within the prtT gene. The regulatory protein PrtT is a member of the Zn(II)2Cys6 TF family and orthologs have been identified in several *Aspergilli* as well in *P. chrysogenum* (Punt et al. 2008, Sharon et al. 2009) ; however, no similar protein has been found in *A. nidulans*. PrtT has been identified to positively regulate multiple extracellular proteases at the post-translational level. Expression of four out of seven investigated protease genes was shown to be regulated by Δ*prtT* and activity studies have shown Δ*prtT* to have 20 % of the activity of the wild type at pH 4.5 (Connelly & Brody 2004).

Based on the TF modulation strategy described in chapter 6, we identified a novel TF, designated prtB (protease regulator B), found to positively regulate extracellular protease activity. In order to benchmark the *ΔprtB* mutant, a *ΔprtT* mutant strain was also constructed and applied as a protease deficient reference strain, in the present study.

7.3 Materials and methods

7.3.1 Fungal strains

A. niger ATCC 1015 was selected as reference strain in the present study (obtained from the IBT collection as IBT 28639). The *ΔprtT* and *ΔprtB* strains were generated from the ATCC 1015 strain. All strains were maintained as frozen spore suspensions at -80°C in 20% glycerol.

7.3.2 Media

Transformation medium: 182.2 g/L sorbitol, 10 g/L glucose monohydrate, 6 g/L $NaNO_3$, 0.52 g/L KCl, 0.52 g/L $MgSO_4 \cdot 7H_2O$, 1 mL/L of 1% thiamine solution, 1 mL/L trace element solution. Trace element solution: 22 g/L $ZnSO_4 \cdot 7\ H_2O$, 11 g/L H_3BO_3, 5 g/L $MnCl_2 \cdot 4\ H_2O$, 5 g/L $FeSO_4 \cdot 7\ H_2O$, 1.7 g/L $CoCl_2 \cdot 6\ H_2O$, 1.6 g/L $CuSO_4 \cdot 5\ H_2O$, 1.5 g/L $Na_2MoO_4 \cdot 2\ H_2O$, 50 g/L Na_4EDTA.

Czapek yeast extract (CYA) media: 30 g/L Sucrose, 5 g/L Yeast extract, 3 g/L $NaNO_3$, 1 g/L K_2HPO_4, 0.5 g/L $MgSO_4 \cdot 7\ H_2O$, 0.5 g/L KCl, 0.01 g/L $FeSO_4 \cdot 7H_2O$, 15 g/L Agar, 1 mL/L trace element solution. 0.4 g/L $CuSO_4 \cdot 5\ H_2O$, 0.04 g/L $Na_2B_2O_7 \cdot 10\ H_2O$, 0.8 g/L $FeSO_4 \cdot 7\ H_2O$, 0.8 g/L $MnSO_4 \cdot H_2O$, 0.8 g/L $Na_2MoO_4 \cdot 2\ H_2O$, 8.0 g/L $ZnSO_4 \cdot 7\ H_2O$. pH adjusted to 6.2 prior to autoclavation.

Minimal medium: 20 g/L glucose, 7.3 g/L $(NH_4)_2SO_4$, 1.5 g/L KH_2PO_4, 1.0 g/L $MgSO_4 \cdot 7\ H_2O$, 1.0 g/L NaCl, 0.1 g/L $CaCl_2$, 0.1 mL Antifoam 204 (sigma), 1 mL/L trace element solution. Trace element solution: 0.4 g/L $CuSO_4 \cdot 5\ H_2O$, 0.04 g/L $Na_2B_2O_7 \cdot 10\ H_2O$, 0.8 g/L $FeSO_4 \cdot 7\ H_2O$, 0.8 g/L $MnSO_4 \cdot H_2O$, 0.8 g/L $Na_2MoO_4 \cdot 2\ H_2O$, 8.0 g/L $ZnSO_4 \cdot 7\ H_2O$. For screening, 19.52 g/L 2-(N-morpholino)ethanesulfonic acid (MES) was added. pH adjusted to 6.0 prior to autoclavation.

Complex medium (Watman medium): 30 g/L Sucrose, 5 g/L Corn steep liquor, 2 g/L Yeast extract, 3 g/L Peptone, 2 g/L Glucose, 2 g/L $NaNO_3$, 1 g/L $K_2HPO_4 \cdot 3$ H2O, 0.5 g/L $MgSO_4 \cdot 7$ H2O, 0.05 g/L $FeSO_4 \cdot 7$ H2O, 0.2 g/L KCl, 1 mL/L Trace metal solution. Trace element solution: 22 g/L $ZnSO_4 \cdot 7\ H_2O$, 11 g/L H_3BO_3, 5 g/L $MnCl_2 \cdot 4\ H_2O$, 5 g/L $FeSO_4 \cdot 7\ H_2O$, 1.7 g/L $CoCl_2 \cdot 6\ H_2O$, 1.6 g/L $CuSO_4 \cdot 5\ H_2O$, 1.5 g/L $Na_2MoO_4 \cdot 2\ H_2O$, 50 g/L Na_4EDTA. As buffer 19.52 g/L 2-(N-morpholino)ethanesulfonic acid (MES) was used. pH adjusted to 6.0 prior to autoclavation.

Protease induction medium (PIM), was prepared as described by van den Hombergh et al. (1995).

7.3.3 Preparation of inoculum

Conidia were propagated on CYA media plates and incubated for 5 to 7 days at 30°C before being harvested with 2 times 10 ml 0.9 % NaCl and filtered through miracloth and washed twice with 0.9 % NaCl. Fermentations were initiated by conidia inoculation to a final concentration of 2×10^9 spores/L

7.3.4 Target selection

The target selection was performed analogue to chapter 6.

7.3.5 PCR amplification

All PCR reactions were carried out using the high fidelity Phusion polymerase from Finnzymes at standard conditions with HF-buffer.

7.3.6 Gene deletion

All DNA insertions into the *A. niger* genome were performed using protoplasts and PEG transformation. The deletion strains were constructed using PCR-generated bipartite gene targeting substrates (Nielsen et al. 2006). Each part of the bipartite substrate consisted of a targeting fragment and a marker fragment, all of which were amplified individually by PCR using the primer pairs presented in Table 7.1. Hygromycin phosphotransferase gene (hph) marker cassette amplified from plasmid pCB10003 (McCluskey et al. 2010) as template DNA.

7.3.7 Oligonucleotide PCR primers

The oligonucleotides used for the strain construction of Δ*prtT* and Δ*prtB* can be found in table 7.1.

Table 7.1 Primers used for deletion of *prtT* in *A. niger*. Lower-case letters indicate overlapping genetic elements used for fusion PCR.

Primer	Sequence
prtt_up_F	CGGCGATCATGTGTCTACAAA
prtt_up_R	gatccccgggaattgccatgTCCACATTGATGGTCAGGCA
prtt_dw_F	ggactgagtagcctgacatcTCGGGTTGGAAAGGACATGA
prtt_dw_R	CGCAAAGGCTACAATGGCA
HYG_up_F	catggcaattcccggggatcGCTGGAGCTAGTGGAGGTCA
HYG_up_R	CTGCTGCTCCATACAAGCCAACC
HYG_dw_F	GACATTGGGGAGTTCAGCGAGAG
HYG_dw_R	gatgtcaggctactcagtccCGGTCGGCATCTACTCTATT

7.3.8 Southern blotting

1.5µg genomic DNA was isolated and digested with appropriate restriction enzymes (SmaI and NdeI). Sequence information for restriction digest of the target loci was obtained from the *A. niger* ATCC 1015 genome sequence (Andersen et al. 2011) from the US Department of Energy Joint Genome Institute (http://genome.jgipsf.org/Aspni1/). Blotting was done according to standard methods (Sambrook and Russell 2001), using RapidHyb hybridization buffer (Amersham Pharmacia) for probing. The target locus was detected by probing with the labeled upstream target gene PCR fragment. The probes were radioactively labeled with α-32P-dCTP by random priming using Rediprime II kit (GE Healthcare). For a graphical representation of the gene deletion strategy, see figure 6.1 in chapter 6.

7.3.9 Cultivations

Static cultivations

Fresh conidia were added to 8 mL of minimal- or complex screenings medium in a 50 mL sterile falcon tube (BD Biosciences) to a final concentration of $1*10^3$ conidia/mL and incubated without agitation at 30 ^oC for 5 days. At the end of the experiment, samples for pH and HPLC were collected.

Batch cultivations

Batch cultivations were performed in 1 L Braun fermenters with a working volume of 0.8 L, equipped with two Rushton six-blade disc turbines. The bioreactor was sparged with air, and the concentrations of oxygen

and carbon dioxide in the exhaust gas were measured in a gas analyzer (1311 Fast response Triple gas, Innova combined with multiplexer controller for Gas Analysis MUX100, B. Braun Biotech International (Melsungen, Germany)). The temperature was maintained at 30°C during the cultivation and pH was controlled by automatic addition of 2 M NaOH and 1 M HCl. For inoculation of the bioreactor, the pH was adjusted to 3.0; stirring rate: 100 rpm; and aeration: 0.2 volumes of air per volume of fluid per minute (vvm). After germination, the stirring rate was increased to 800 rpm and the air flow to 1 vvm. The pH was adjusted to 2.5 or 6.0 with addition of 2 M NaOH or 1 M HCl over 2 hours.

7.3.10 Cell dry weight determination

The cell mass concentration on a dry weight basis was determined by the use of nitrocellulose filters with a pore size of 0.45 µm (Osmonics, Minnetonka, MN, USA). Initially, the filters were pre-dried in a microwave oven at 150 W for 20 min, and then weighed. A known weight of cell culture was filtered, and the residue was washed with distilled water. Finally, the filter was dried in the microwave at 150 W for 20 min and the dry weight was determined.

7.3.11 Quantification of extracellular metabolites

HPLC

For quantification of the extracellular metabolites, a culture sample was taken and immediately filtered through a 0.45 µm-pore-size nitrocellulose filter (Osmonics). The filtrate was frozen and kept at −20°C until analysis. Glucose, oxalate, citrate, gluconate, glycerol and acetate concentrations were detected and quantified by refractive index and UV using an Aminex HPX-87H cationic-exchange column (BioRad, Hercules, CA, USA) eluted at 35°C, with 5 mM H2SO4 at a flow rate of 0.6 mL min^{-1}.

Glucose assay

Enzymatic glucose assay was performed using an enzymatic glucose kit (ABX Pentra, Glucose HK CP) to determine the glucose concentration in the PIM media where HPLC quantification was not possible. Samples were processed as described by the manufacturer and absorbance was kinetically measured for 10 minutes at 360 nm, using a Biotek Synergy 2 plate reader. The assay was based on NAD^+ through a coupled reaction with glucose-6-phosphate dehydrogenase and formation of NADH was determined spectrophotometrically by measuring the increase in absorbance at 340 nm.

7.3.12 Protein analysis

Protein quantification

Protein content was quantified using Bradford assay. Pierce Bradord assay kit was applied and performed as described by the manufacturer. Absorbance was measured at 600 nm, using a Biotek Synergy 2 plate reader.

Protease assay

Protease activity was determined by a modified procedure of Megazyme azocasein assay. Samples and 2.5 % azocasein diluted in 100 mM sodium acetate, pH 4.5, were preheated to reaction temperature (30$_o$C). 50 µL of preheated 2.5 % azocasein was added to same volume of sample. The reaction mixture was vortexed, incubated for 2 hours, and terminated by the addition of 1 mL 5 % trichloroaceticacid (w/v). Samples were kept on ice for 20 minutes and precipitated by centrifugation at 13,000 g at 4$_o$C for 8 minutes. After centrifugation 200 µL of the supernatant were mixed with 50 µL 1.6 M NaOH to a final concentration of 0.1 M NaOH, and absorbance were measured at 420 nm using a Biotek Synergy 2 plate reader.

Acetone Precipitation

Prior to SDS-page, the samples were concentrated by acetone precipitation. A sample volume were mixed with -20^{o}C acetone, in the proportion 1:4. The reaction mixture were kept at -20^{o}C for 1 hour, followed by centrifugation at 20,000 g in 10 minutes at 4^{o}C. The supernatant were discarded, and the remaining acetone evaporated for 30 minutes at room temperature. The precipitate was resuspended in 20 mM Tris buffer, pH 7.5.

SDS-page

The samples were separated on SDS-PAGE, using a commercial pre-cast gel, NuPAGE Novex®, 4-12% Bis-Tris, 1.0-mm thick. The gel was placed in a Xcell Surelock Mini-Cell and performed as described by the manufacturer.

7.4 Results and discussion

7.4.1 Strain construction

Several deletion mutants where constructed through a bipartite gene knockout approach, using hygromycin as dominant marker. The deletion where verified by PCR and checked for ectopic insertions by Southern analysis.

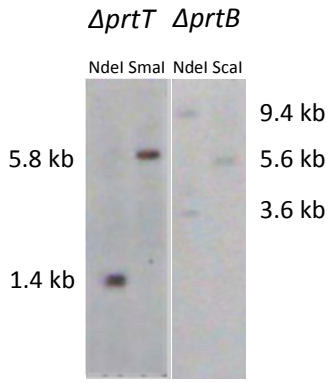

Figure 7.1 Southern analysis of transformants for site specific integration of the construct. Genomic DNA was digested with NdeI or SmaI in the case of *ΔprtT* and NdeI or ScaI, in the case of *ΔprtB.*

The Southern analysis was carried out with a similar strategy, as described in chapter 6. A correct insertion for the *ΔprtT* strain was designed so; digestion with NdeI resulted in one band of 1.4 kb, whereas SmaI digestion results in one band of 5.8 kb. Similarly for a the *ΔprtB* strain, digestion with NdeI resulted in two bands of 1.4 kb and 5.8 kb respectively, whereas ScaI digestion resulted in one band of 5.6 kb. Figure 7.1, only correct sized bands were observed, thus the HygR cassette had been integrated at only at the right position, in the genome of *A. niger* ATCC 1015.

7.4.2 Screening

Secretion of proteases are affected by many environmental parameters including, the source, the type and concentrations of carbon and nitrogen (Jarai and Buxton 1994, Gordon et al. 2000, Braaksma and Punt 2008). To characterize the strains protease secretion, in a profound manner, three liquid growth media were selected, comprised of diverse media compositions. A minimal medium (MM), a complete rich medium (CM) and a protease induction media (PIM), a minimal medium supplemented 3 % (w/v) wheat bran. The initial screening phase only included the MM and CM. All protease activities were based on the azocasein assay and given as a normalized value based on the wild type protease activity in the referred media.

The resulting TF mutants were initially screened for a reduced protease activity in static cultures (liquid cultures incubated without shaking). The mutants were compared to the reference and the *ΔprtT* strain by relative protease activity and total protein content in the ambient medium. Of the constructed mutants particularly one strain, entitled *ΔprtB*, had reduced protease activity. This strain maintained a similar total protein concentration, as of references, indicating this was not a secretion deficient strain, table 7.2.

Table 7.2 Total protein concentration and overall protease activity form in minimal media (MM) and complex media (CM), pH 6.0.

	WT		***ΔprtT***		***ΔprtB***	
	MM	CM	MM	CM	MM	CM
Total protein (mg/L)	65.2	177.6	62.4	182.9	56.4	166.0
Relative protease activity	100%	100%	16%	21%	41%	35%

ΔprtT had the lowest relative protease activity, roughly a fivefold reduction compared to the wild type activity. Similarly, the *ΔprtB* mutant protease activity was reduced to 35% of that wildtype activity. To further examine and characterize the extracellular proteolytic activity in the *ΔprtB* mutant, batch cultivations were performed.

7.4.3 Physiological characterization

The constructed *ΔprtB* strain was subjected to detailed physiological characterization and compared with the wild type and the *ΔprtT* strain.

Representative profiles of the biomass concentration, sugar concentration, carbon dioxide and protease secretion during these batch cultivations are shown in Figure 7.2. In addition, the estimated physiological parameters are presented in Table 7.3

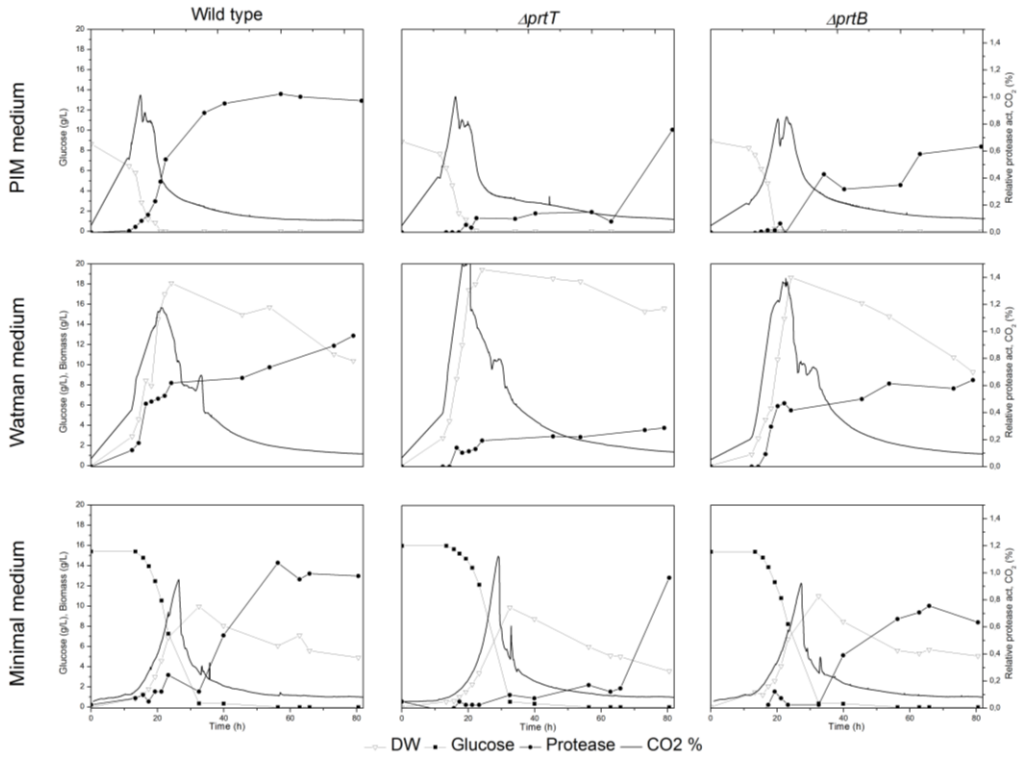

Figure 7.2 Representative cultivation profiles of biomass concentration, sugar concentration, carbon dioxide formation and relative protease activity during batch cultivations at pH 4.5 for the wild type-strain (left), *ΔprtT* (middle) and the *ΔprtB* strain (right).

As presented in figure 7.2, both deletion strains were able to grow similarly to the wild type in all three mediums. The induction of the extracellular proteases followed as well a comparable pattern, of glucose depletion initiating the activity. The correlation between protease secretion and carbon catabolite repression (CCR) has been investigated in *A. nidulans*, where disruption in the CCR regulatory gene *creA*, resulted in increased levels of extracellular protease activity (Katz et al. 2008). Orthologs of this gene are present in other *Aspergilli*, including *A. niger* (Drysdale et al. 1993).

Table 7.3 Physiological coefficients from the batch cultivations at pH 4.5.

		WT	*ΔprtT*	*ΔprtB*
PIM	µmax (h^{-1})*	0.18 ± 0.00	0.18 ± 0.02	0.20 ± 0.00
	Y_{SX} (cmole/cmole)	N/A	N/A	N/A
	Y_{SCO2}(cmole/cmole)	N/A	N/A	N/A
	$Y_{SX,overall}$(cmole/cmole)	N/A	N/A	N/A
CM	µmax (h^{-1})	0.22 ± 0.01	0.23 ± 0.01	0.25 ± 0.02
	Y_{SX} (cmole/cmole)	N/A	N/A	N/A
	Y_{SCO2}(cmole/cmole)	N/A	N/A	N/A
	$Y_{SX,overall}$(cmole/cmole)	N/A	N/A	N/A
MM	µmax (h^{-1})	0.22 ± 0.02	0.20 ± 0.00	0.23 ± 0.01
	Y_{SX} (cmole/cmole)	0.84 ± 0.12	0.82 ± 0.10	0.85 ± 0.10
	Y_{SCO2}(cmole/cmole)	0.24 ± 0.01	0.34 ±0.06	0.22 ± 0.03
	$Y_{SX,overall}$(cmole/cmole)	0.71 ± 0.08	0.64 ± 0.09	0.74 ± 0.12

Values are shown as average ± standard deviation of two biological replicates. Yield coefficients are based on measured values at mid-exponential phase and the overall coefficients are based on values measured at the end of the cultivation. * Due to wheat bran particles precluded dry weight measurement, the growth rate in the PIM media was estimated applying the rate of CO_2 generation. Using the r_{CO2} measurement and assuming a similar central carbon metabolism, r_{CO2} can give an estimate for the growth rate.

From table 7.3, no considerable changes between the strains growth rates (<12 % difference) were observed in PIM and CM. For the MM cultivations, the wild type and *ΔprtB* grew with similar rates, while the growth rate of ΔprtT was 10-13 % reduced. Notable was the 42 % increased CO_2 generation of *ΔprtT* in MM. A similar trend, for *ΔprtT*, was also observed in the CM for the *ΔprtT* strain. A consequence of the The increased CO2 generation was a reduction of 10% in, reduced the overall biomass yield in MM with 10 %. Differences were also seen in oxalic acid formation. For *ΔprtB* the highest concentration observed of this acid was 0.5 g/L and compared to the wild type and the *ΔprtT* stains, this was a more than threefold reduction (data no shown).

From the physiological characterization, it was apparent that the *ΔprtB* strain had beneficial features for being a host for protein production. The performance in the bioreactors was close to the wild type, with a couple of exceptions. Oxalic acid can cause problems in the downstream processing due to formation of precipitates with metal ions, hence lower yields of this acid is a particular beneficial feature for *ΔprtB*. Interestingly, the *ΔprtT*-mutant showed a higher yield of CO_2 on substrate compared to both the wild type

and the *ΔprtB* strains. This observation has not been described in literature and public available data on quantitative physiology of the *ΔprtT* strain is limited. However, the role of PrtT in the human pathogen *A. fumigatus* has been investigated (Hagag et al. 2012). Using microarray analysis on biomass obtained from shake flasks cultures, the authors compared the transcriptome of a *ΔprtT* mutant with a wild type strain. Beside identification of an expected decreased protease expression, expression of genes involved in iron uptake and four cytochrome c oxidases was considerably decreased in the *ΔprtT* mutant. Iron and cytochrome c oxidases are important parts of the oxidative phosphorylation. These findings could be an indication of this pathway being down-regulated and as described in chapter 4, such response would initiate a decoupled reoxidation of NADH, resulting in lower ATP yield. This would increase CO_2 generation and the reduced biomass yield.

7.4.4 Proteolytic Characterization

To examine and compare the strains, the maximum protease activities were estimated and can be found in table 7.4.

Table 7.4 Relative maximum protease activity expressed relative to the WT protease activity of 100 %.

		Relative max. protease act. (% of WT)	Relative max. biomass specific protease act. (% of WT)
	MM	20.5 ± 3.5	22.5
ΔprtT	CM	27.8 ± 3.7	28.7
	PIM	30.2 ± 4.9	N/A
	MM	65.4 ± 6.2	53.2
ΔprtB	CM	68.2 ± 1.6	69.2
	PIM	71.8 ± 4.3	N/A

The relative maximum protease activity is given as the max protease activity, normalized to the max wild type protease activity. The relative maximum specific protease activity is given analog to relative max. protease act. however, the max activities have been divided with the biomass concentration prior to wild type normalization.

It is clear, from table 7.4, that *ΔprtT* is superior in respect to low protease activity, close to a fivefold reduction of the wild type activity. This corresponds well, with the activity, reported by Connelly and Brody (2010) and obtained in the ATCC 9029 strain background. The *ΔprtB* strain had a 2.5 fold higher protease activity, compared to the *ΔprtT* strain; however, this was still a significantly lower activity, compared to the wild type level. Especially in the MM, the *ΔprtB* strain, expressed approximately half of the protease activity

compared to the wild type. It should however be noted, that in the end of some of the cultivations, the protease activity suddenly raised e.g. Δ*prtT* in minimal media, Figure 7.2. These values were neglected from the calculated values of table 7.4, as it was assumed to be caused by autolysis of mycelia, hence release of intracellular proteases into the medium.

7.4.5 Protein profile

To investigate changes in the extracellular protein composition of the three strains, the protein profile was examined by SDS-PAGE analysis of the fermentation broth. All samples were from the mid stationary phase (40-45 hours).

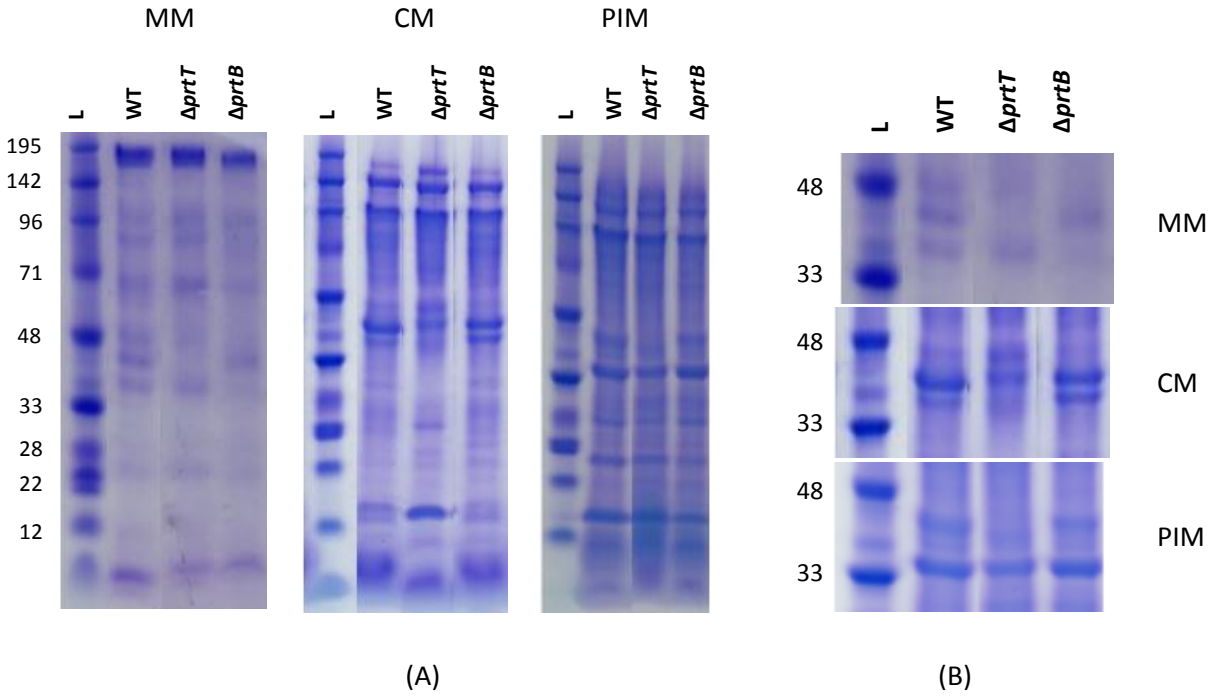

Figure 7.3: (A) SDS-PAGE of mid stationary phase samples. The figure is compiled from the full SDS-PAGE gels. 'L' is the ladder and the weight of the protein fragments are marked to the left, given in kDa. **(B)** Magnification of the 33-48 kDa area. Only qualitative comparing can be performed, as the sample loads were not normalized. Full pictures can be found in appendix 4.

As presented in figure 7.3.A, the protein content varies greatly, dependent on the composition of medium the strains were cultured in. The protein content of the MM samples was considerably lower, compared to the CM and PIM samples. Yet, by close examinations of figure 7.3.B, differences can still be observed. From the MM samples, the wild-type contains three bands whereas the extracellular samples from *ΔprtT* and *ΔprtB* cultures contain one and two bands respectively. In the samples of remaining media, only *ΔprtT*

differs considerably. Especially the PIM sample from *ΔprtT*, a 43-45 kDa band was missing. A similar observation was made by Mattern et al. (1992) and by applying western blotting the missing band was identified the protease pepA (Punt et al. 2008). It is therefore argued, that a disruption of prtT, independent on strain background, results in lack of pepA.

The observations from figure 7.3, correlates well with the protease activities found table 7.3. In the *ΔprtB* sample from the MM had the lowest relative protease activity and in the PIM and CM the differences compared to the wild type was less apparent.

The results obtained this study are summarized in table 7.5.

Table 7.5 Summary of the data obtain throughout this study

	μmax	**Ysx**	**Protease activity**	**Biproducts**
Wild type	+ + +	+ + +	+ + +	+ + +
ΔprtT	+ +	+ +	+	+ + +
ΔprtB	+ + +	+ + +	+ +	+

The ideal *A. niger* host, for protein production, should have the lowest possible extracellular protease activity and byproduct formation coupled with, wild type performance formation rate and yield of biomass. From table 7.5, none of the deletion strains fulfill the all these criteria. The *ΔprtT* strain secreted low amount of proteases but featured lower biomass yield, increase CO_2 production and a slightly decreased growth rate. Contrary *ΔprtB* had reduced extracellular protease activity yet, not as low as *ΔprtT*; however, this strain had additional beneficial characteristics, as a lower oxalic acid formation as well as wild type performance on maximum growth rate and yield of biomass formation.

7.5 Conclusion

In perspective as potential protein cell factories, different characteristics were proved by both strains, favorable and unfavorable features. It is therefore impossible, with the data from this study, to favor one strain over the other. Especially with regard to industrial relevance, a product specific evaluation is needed.

Finally, these results were obtained in the ATCC 1015 strain background. The similar reported protease activity obtained by *ΔprtT* in ATCC 9029 strain background indicates, that the obtained result from *ΔprtB* could possibly be directly transferred to other *A. niger* strain backgrounds.

7.6 References

Andersen, M. R., M. P. Salazar, P. J. Schaap, P. J. van de Vondervoort, D. Culley, J. Thykaer, J. C. Frisvad, K. F. Nielsen, R. Albang, K. Albermann, R. M. Berka, G. H. Braus, S. A. Braus-Stromeyer, L. M. Corrochano, Z. Dai, P. W. van Dijck, G. Hofmann, L. L. Lasure, J. K. Magnuson, H. Menke, M. Meijer, S. L. Meijer, J. B. Nielsen, M. L. Nielsen, A. J. van Ooyen, H. J. Pel, L. Poulsen, R. A. Samson, H. Stam, A. Tsang, J. M. van den Brink, A. Atkins, A. Aerts, H. Shapiro, J. Pangilinan, A. Salamov, Y. Lou, E. Lindquist, S. Lucas, J. Grimwood, I. V. Grigoriev, C. P. Kubicek, D. Martinez, N. N. van Peij, J. A. Roubos, J. Nielsen and S. E. Baker (2011). "Comparative genomics of citric-acid-producing *Aspergillus niger* ATCC 1015 versus enzyme-producing CBS 513.88." Genome Res **21**(6): 885-897.

Braaksma, M. and P. J. Punt (2008). *Aspergillus* as a cell factory for protein production: controlling protease activity in fungal production. The Aspergilli: Genomics, Medical Aspects, Biotechnology, and Research Methods, CRC Press**:** 441-455.

Drysdale, M. R., S. E. Kolze and J. M. Kelly (1993). "The *Aspergillus niger* carbon catabolite repressor encoding gene, creA." Gene **130**(2): 241-245.

Edens, L., A. Van Dijk, P. Krubasik, K. Albermann, A. Stock, E. Kimpel, S. Klugbauer, C. Wagner, A. Fritz, W. Von Gustedt, O. Heinrich, D. Maier, F. Spreafico, U. Folkers, S. Hopper, W. Kemmner, P. Tan, J. Stiebler and R. Albang (2005). Novel genes encoding proteolytic enzymes: US7323327.

Gordon, C. L., V. Khalaj, A. F. Ram, D. B. Archer, J. L. Brookman, A. P. Trinci, D. J. Jeenes, J. H. Doonan, B. Wells, P. J. Punt, C. A. van den Hondel and G. D. Robson (2000). "Glucoamylase::green fluorescent protein fusions to monitor protein secretion in *Aspergillus niger*." Microbiology **146 (Pt 2)**: 415-426.

Hagag, S., P. Kubitschek-Barreira, G. W. Neves, D. Amar, W. Nierman, I. Shalit, R. Shamir, L. Lopes-Bezerra and N. Osherov (2012). "Transcriptional and proteomic analysis of the *Aspergillus* fumigatus DeltaprtT protease-deficient mutant." PLoS One **7**(4): e33604.

Jarai, G. and F. Buxton (1994). "Nitrogen, carbon, and pH regulation of extracellular acidic proteases of *Aspergillus niger*." Curr Genet **26**(3): 238-244.

Katz, M. E., S. M. Bernardo and B. F. Cheetham (2008). "The interaction of induction, repression and starvation in the regulation of extracellular proteases in *Aspergillus* nidulans: evidence for a role for CreA in the response to carbon starvation." Curr Genet **54**(1): 47-55.

Mattern, I. E., J. M. van Noort, P. van den Berg, D. B. Archer, I. N. Roberts and C. A. van den Hondel (1992). "Isolation and characterization of mutants of *Aspergillus niger* deficient in extracellular proteases." Mol Gen Genet **234**(2): 332-336.

McCluskey, K., A. Wiest and M. Plamann (2010). "The Fungal Genetics Stock Center: a repository for 50 years of fungal genetics research." J Biosci **35**(1): 119-126.

Nielsen, M. L., L. Albertsen, G. Lettier, J. B. Nielsen and U. H. Mortensen (2006). "Efficient PCR-based gene targeting with a recyclable marker for *Aspergillus nidulans*." Fungal Genet Biol **43**(1): 54-64.

Pel, H. J., J. H. de Winde, D. B. Archer, P. S. Dyer, G. Hofmann, P. J. Schaap, G. Turner, R. P. de Vries, R. Albang, K. Albermann, M. R. Andersen, J. D. Bendtsen, J. A. Benen, M. van den Berg, S. Breestraat, M. X. Caddick, R. Contreras, M. Cornell, P. M. Coutinho, E. G. Danchin, A. J. Debets, P. Dekker, P. W. van Dijck, A. van Dijk, L. Dijkhuizen, A. J. Driessen, C. d'Enfert, S. Geysens, C. Goosen, G. S. Groot, P. W. de Groot, T. Guillemette, B. Henrissat, M. Herweijer, J. P. van den Hombergh, C. A. van den Hondel, R. T. van der Heijden, R. M. van der Kaaij, F. M. Klis, H. J. Kools, C. P. Kubicek, P. A. van Kuyk, J. Lauber, X. Lu, M. J. van der Maarel, R. Meulenberg, H. Menke, M. A. Mortimer, J. Nielsen, S. G. Oliver, M. Olsthoorn, K. Pal, N. N. van Peij, A. F. Ram, U. Rinas, J. A. Roubos, C. M. Sagt, M. Schmoll, J. Sun, D. Ussery, J. Varga, W. Vervecken, P. J. van de Vondervoort, H. Wedler, H. A. Wosten, A. P. Zeng, A. J. van Ooyen, J. Visser and H. Stam (2007). "Genome sequencing and analysis of the versatile cell factory *Aspergillus niger* CBS 513.88." Nat Biotechnol **25**(2): 221-231.

Punt, P. J., F. H. Schuren, J. Lehmbeck, T. Christensen, C. Hjort and C. A. van den Hondel (2008). "Characterization of the *Aspergillus niger* prtT, a unique regulator of extracellular protease encoding genes." Fungal Genet Biol **45**(12): 1591-1599.

Sambrook, J. and D. W. Russell (2001). Molecular cloning : a laboratory manual. Cold Spring Harbor, N.Y., Cold Spring Harbor Laboratory Press, 0879695773 (paper)

0879695765 (cloth).

Sharon, H., S. Hagag and N. Osherov (2009). "Transcription factor PrtT controls expression of multiple secreted proteases in the human pathogenic mold *Aspergillus* fumigatus." Infect Immun **77**(9): 4051-4060.

van den Hombergh, J. P., L. Fraissinet-Tachet, P. J. van de Vondervoort and J. Visser (1997a). "Production of the homologous pectin lyase B protein in six genetically defined protease-deficient *Aspergillus niger* mutant strains." Curr Genet **32**(1): 73-81.

van den Hombergh, J. P., M. D. Sollewijn Gelpke, P. J. van de Vondervoort, F. P. Buxton and J. Visser (1997b). "Disruption of three acid proteases in *Aspergillus niger*--effects on protease spectrum, intracellular proteolysis, and degradation of target proteins." Eur J Biochem **247**(2): 605-613.

van den Hombergh, J. P., P. J. van de Vondervoort, N. C. van der Heijden and J. Visser (1995). "New protease mutants in *Aspergillus niger* result in strongly reduced in vitro degradation of target proteins; genetical and biochemical characterization of seven complementation groups." Curr Genet **28**(4): 299-308.

Chapter 8 Nutrient profiling reveals potent inducers of fumonisin biosynthesis in *Aspergillus niger*

Poulsen L., Thykaer J. and Nielsen, KF.

8.1 Abstract

Aspergillus niger is one of the most important and widely applied cell factories. The recent discovery of the fumonisin gene cluster, in *A. nigers* genome, was for many surprising, since fumonsins had not previously been detected in the species. To investigate this conundrum, a reporter strain of *A. niger* was constructed, where the promoter from the fumonisin synthase was fused to the green fluorescent protein. This strain was screened using 476 Biolog nutrient profiling conditions showing that six compounds significantly induce fumonisin production. These compounds formed the basis for an expanded investigation, targeting the central metabolism and melanin synthesis. It was discovered that the fumonisin synthesis takes place in the vesicle of the conidiophore and requires activation of compounds that enter the metabolism through the glycolysis. Inhibitors (4 of 5 tested) of the enzyme tyrosinase, an important enzymatic step for melanin synthesis, also induced fumonisin. The strongest fumonisin inducer was the tyrosinase inhibitor and plant hormone, azelaic acid that increased fumonisin production 64 fold. Finally, based on fluorescence microscopy, we propose that fumonisin production only take place within the conidiophore (thus requiring sporulation)

8.2 Introduction

Aspergillus niger is one of the most important industrial organisms as it has a high growth rate, can tolerate very low pH, and performs well in fermenters. Currently *A. niger* is used extensively for industrial production of organic acids (Kubicek et al. 1985, Karaffa and Kubicek 2003, Goldberg et al. 2006) and extracellular enzymes (Olempska-Beer et al. 2006, Fleissner and Dersch 2010), where many processes has gained GRAS status, as described in chapter 2. Since it has intron splicing and post translational machinery it is widely applied for heterologous production of proteins (chapter 2), as well as being considered a good candidate for production of secondary metabolites (Hofmann et al. 2009, Nielsen et al. 2009). Three *A. niger* full genomes are publically available, and analysis of these genomes revealed presence of the gene cluster of the carcinogenic fumonisins later shown to be responsible for formation of fumonisins B_2, B_4, and B_6 but not B_1 (Mansson et al. 2010, Frisvad et al. 2011). Interestingly only one of the three, CBS 513.88, harbours an entire functional ochratoxin A gene cluster (Frisvad et al. 2011).

Despite the historical use of *A. niger* in industry, it appears intriguing that formation of fumonisins in this species was not reported before the release of the genome sequences, as a large fraction of the strains are capable of producing the toxins (Frisvad et al. 2011). Most likely fumonisins are not produced under submerged conditions, and it has not been detected it in industrial *A. niger* products nor samples from fermenters (Nielsen, KF. unpublished results). However, recently fumonsins production was observed under special submerged conditions, called retentostate (Jørgensen et al. 2011). Contrary to traditional batch and chemostat cultures, in this retentostate setup, conidia formation was observed. We therefore speculate that fumonisin production is linked to the conidiophore formation. Furthermore fumonisin production also seem to be collated with slightly osmolytic stress (Mogensen et al. 2009).

The role of fumonisin is still obscure. Fusaria strains producing high amounts of the toxins are found more frequently in infected tissue (Sánchez-Rangel and Plasencia 2010) and fumonisins induces leaf lesions and disease in maize seedlings and that severity of symptom is clearly correlated to the quantity of produced fumonisins (Glenn et al. 2008, Sánchez-Rangel and Plasencia 2010). Even though fumonisin production is not absolute required for strains to infect plants, the fumonisins seem to promote the infection rate (Desjardins et al. 2007).

To systematically investigate chemical inducers of fumonisin production, a GFP-fumonisin reporter strain was constructed. This was inspired by to the study of (Gardiner et al. 2009), conducted in *Fusarium graminearum* identifying inducers of trichothecenes production. In the reporter strain, the GFP production

was controlled by the FUM promoter. With this strain, fumonisin production was mapped at 476 different conditions using the Biolog nutritional profiling system, and investigated the inducing compounds and conditions on solid media.

8.3 Material and methods

8.3.1 Fungal strains

A. niger ATCC 1015 was used as wild type reference strain (obtained from the IBT collection as IBT 28639). The fumonisin reporter strain was generated from the ATCC 1015 strain. Both strains were maintained as frozen spore suspensions at -80°C in 20% glycerol.

8.3.2 Oligonucleotide PCR primers

The oligonucleotides used for the strain construction of fumonisin reporter strain, can be found in Table 1.

Table 8.1 Primers used for construction of the vector. Lower-case letters indicate overlapping genetic elements used for fusion PCR and bold letters represent the restriction sites.

Primer	Sequence
pFum1-F_kasI	ATAGTTAGG**GGCGCC**AGCTGGGTGACGATGGACAC
pFum1-R	gtacactgcggtctatccacGGTGAGCGGGCGAGCGATA
eGFP-F	gtggatagaccgcagtgtacATGGTGAGCAAGGGCGAGGA
GFP-R_hindIII	CATTAACG**AAGCTT**TTACTTGTACAGCTCGTCCA
CHK-pFUM-F	CGCCAGCCGATAGTGTCGAT
CHK-pFUM-R	TTGATGCCGTTCTTCTGCTTG
S-probe_F	CGACGCAGAGGATGATGATG
S-probe_R	TATATCCTTAGTGGTGCCGCT

8.3.3 Vector construction

The fumonisin promoter-GFP fusion vector was constructed by PCR using primers to the FUM promoter, pFUM1-F and pFUM1-R and to eGFP using the primers eGFP-F and eGFP-R. The PCR construct consisted of 2.0 kb of FUM promoter amplified from *A. niger* ATCC 1015 and eGFP from (Toews et al. 2004). Fragments were amplified with Phusion DNA polymerase from Finnzymes (Espoo, Finland) at standard conditions with HF-buffer. Fragments were gel purified and fused using the external primers. The PCR product was digested with KasI and HindII, and ligated into the pAN7-1 vector, digested with the same restriction enzymes. The vector contained the hygromycin phosphotransferase gene under the *Aspergillus nidulans* TrpC promoter and terminator (Punt et al. 1987). A schematic overview of the vector construction is presented in Figure 8.1.

8.3.4 Transformation

DNA insertion into the *A. niger* genome was performed using protoplasts and standard PEG transformation. The wild type strain was transformed with an integrative vector and the transformations were initially verified by PCR using the primers, CHK-pFUM-F and CHK-pFUM-R.

8.3.5 Southern blotting

To examine for ectopic insertions, southern analysis was carried out. Genomic DNA, 1.5 µg, was isolated and digested with BamHI. Sequence information for restriction digest of the target loci was obtained from the *A. niger* ATCC 1015 genome sequence (Andersen et al. 2011) from the US Department of Energy Joint Genome Institute (http://genome.jgipsf.org/Aspni1/). Blotting was done according to standard methods (Sambrook and Russell 2001). The target locus was detected by probing with the labeled upstream target PCR fragment, generated using the primers, s-probe-F and s-probe-R. The probes were labeled with Biotin using the Biotin DecaLabel DNA Labeling Kit (Thermo Fisher Scientific (formerly Fermentas), Slangerup Denmark) and visualized using the Biotin Chromogenic Detection Kit (Thermo Fisher Scientific (formerly Fermentas), Slangerup Denmark). For a graphical representation of the gene deletion strategy, see Figure 8.1.

8.3.6 Fluorescence microscopy and imaging

Tape slides for microscopy were prepared as described by (Samson 2002). Images were captured with a cooled Orca-ER CCD camera (Hamamatsu, Japan) mounted on a Zeiss Axioplan II microscope (Carl Zeiss, Thornwood, NY. All images were captured at a 10-fold magnification.

8.3.7 Growth experiments

Biolog plate screening and measurements

Five sets of Phenotype Microarrays (PM) were purchased from Biolog (Hayward, CA); Two carbon arrays (PM1 and PM2A), one nitrogen array (PM3), one combined phosphorus and sulfur array (PM4A) and an osmolyte array (PM9). The array designs can be found at the manufacturer homepage: http://www.biolog.com/pdf/PM1-PM10.pdf.

100 uL of FF-IF Biolog media was added to the arrays. Growth media was added supplements accordingly to Biolog protocol “PM Procedures for Filamentous Fungi”. The inoculum was prepared from 4 day old Czapek yeast autolysate (CYA) plates. Conidia were harvested with 0.9 %NaCl, washed twice and the concentration was estimated using a hemocytometer. Media was inoculated to obtain a final concentration of 1000

conidia / mL. Cultures were incubated in a Cytomat 2C450-LIN ToS, Thermo Scientific attached to a Biotek Synergy Mx Monochromator-Based Multi-Mode Microplate Reader. Each hour the growth was estimated by the optical density (600nm) and the GFP determined by fluorescence with excitation at 485/20 nm and emission at 520/25 nm.

All time depended data collected from the Biolog arrays were collated into MATLAB R2009b. The individual conditions, T=0 values, were subtracted each well and integrated using the MATLAB function "cumtrapz". The output of this function, the cumulative integral value (refer to as the area under curve or AUC), formed the basis for the comparison.
To evaluate significant fumonisin promoter activation, the standard deviation of the GFP AUC data distribution was computed applying the STDEV function in Microsoft Excel 2007.

Agar plate

All plate experiments were prepared from a minimal base medium containing: 7.3 g/L (NH4)2SO4, 1.5 g/L KH2PO4, 1.0 g/L MgSO4·7H2O, 1.0 g/L NaCl, 0.1 g/L CaCl2·2H2O, 15 g/L agar and 1 mL/L trace element solution. Trace element solution composition: 7.2 g/L ZnSO4·7H2O, 0.3 g/L NiCl2·6H2O, 6.9 g/L FeSO4·7H2O, 3.5 g/L MnCl2·4H2O, and 1.3 g/L CuSO4·5H2O. The carbon sources were added after autoclaving into a final concentration of 0.50 cmole/L. IBT 28639 was incubated for 7 days at 30°C as three point inoculations and then three plugs (6 mm inner diameter) were taken from each plate (Nielsen et al. 2009).

8.3.8 Chemical analysis of *A. niger* cultures

From the PM arrays 100 µL solid culture was extracted in a 2-mL Eppendorf tube with 300 µL methanol:water (3:1 v/v) for 30 min in a ultra-sonication bath. The samples were and centrifuged for 12 min @ 20000 G, and 120 µL were transferred to a vial fitting the UHPLC-TOFMS autosampler.
From agar plates, extraction was made by taking 3 6-mm ID plugs and extracting with 400 uL of Methanol:H_20 (3:1 v/v) placed in an ultrasonication bath for 30 min, and centrifuged at 20000 g for 12 min *(9)*.

Ultra high Performance Chromatography-time of flight mass spectrometry (UHPLC-TOFMS) was performed on a maXis G3 quadrupole time of flight mass spectrometer (Bruker Daltonics, Bremen, Germany) equipped with an electrospray (ESI) ion source. The MS was coupled to an Ultimate 3000 UHPLC system (Dionex,

Sunnyvale, CA). Separation of extracts (0.1 µL from PM plates and 1 µL from agar plates) was performed at 40 ºC on a 100 mm × 2.1 mm ID, 2.6 µm Kinetex C_{18} column (Phenomenex, Torrance, CA) using a linear water-acetonitrile gradient (both buffered with 20 mM formic acid) at a flow of 0.4 mL/min starting from 10% acetonitrile and increased to 100% in 10 minutes, keeping this for 3 minutes. MS analyses were performed in ESI^+ using a data acquisition range of m/z 100-1000, a resolution of 40 000 FMWH and calibrated using sodium formate automatically infused prior to each analytical run, providing a mass accuracy of less than 1.2 ppm. Extracted ion chromatograms of the $[M+H]^+$ ions (± m/z 0.001) for the target compounds were constructed using the TargetAnalysis 1.2 software (Bruker Daltonics) which also was used to verify the identity of the targets via: i) retention time ± 0.1 min, ii) isotope pattern (SigmaFit <30), and iii) mass accuracy better than 1.2 ppm.

Fumonisins B_1, B_2 and B_3 standards, were obtained from RomerLabs (Tulln, Austria) as certified solutions, while fumonisins B_4 and B_6 were available from previous studies (Mansson et al. 2010). The limit of detection for fumonisin B_2 and B_4 was <2 ng/cm^2 (s/n 5).

8.4 Results and discussion

8.4.1 Strain construction

Ten transformants were examined for the correct insertion into the fumonisin locus using PCR. Two confirmed transformants were selected, single conidia were isolated and Southern analysis revealed that no etopic inserts were present, figure 8.1.

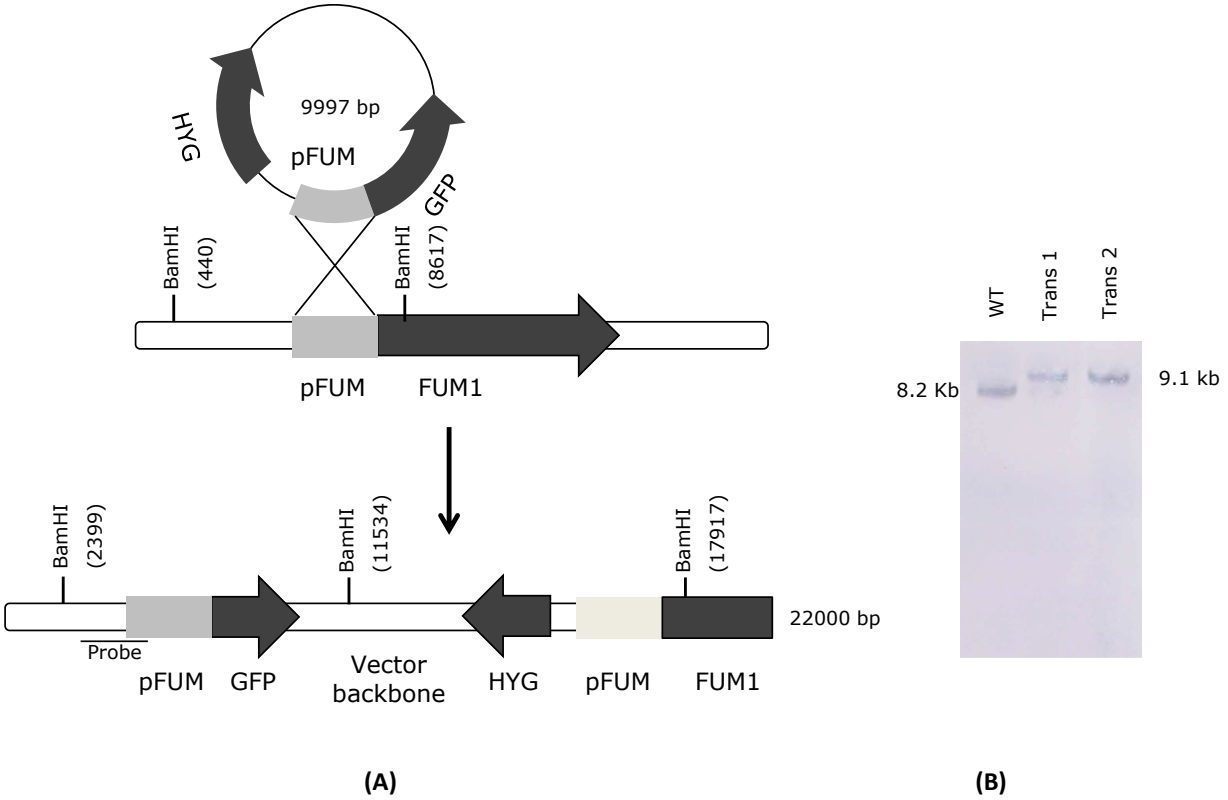

Figure 8.1 (A) Graphical illustration of the vector insertion procedure into the fumonisin synthase locus and predicted resultant genomic locus. (B) Southern analysis of wild type and the transformants for site specific integration of the construct. Genomic DNA was digested with BamHI. The position of the probe used is shown in (A).

8.4.2 Verification of the correlation between fumonisin and GFP in reporter strain

To examining the validity of GFP based prediction obtained from the fumonisin reporter strain, 60 cultures were selected across the plates; PM1, PM2 and PM9, and the produced fumonisins quantified using UHPLC-TOFMS. Unfortunately the concentration of fumonisin in all samples from PM1 and PM2 were under the UHPLC-TOFMS detection limit, due to high interference caused by polymers (presumable the gelefying agent) from the commercial Biolog FF media thus could only 0.1 µL sample could be injected. This lead to 35 samples where fumonisin and GFP production could be compared (Figure 8.2).

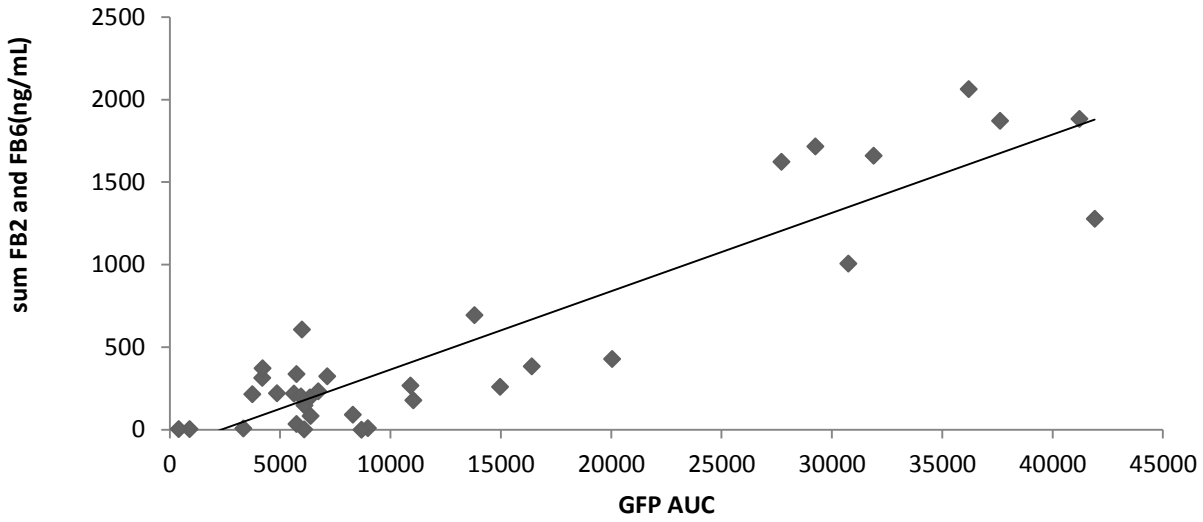

Figure 8.2 Dose response curve from 35 exacts.

From figure 2 it could deduced that the reporter strain provide a correct estimation of the fumonisin yield, a GFP AUC signal of 10.000 corresponding to 364.5 ng/mL.

8.4.3 Localization of fumonisin production

Tape slides investigated under fluorescence microscope showed a substantial fluorescent signal, which was strictly centred within the vesicle of the conidiophore (Figure 8.3). The GFP signal, on tape slides from 1, 2 and 3 day old cultures revealed that the expression was initiated in the near proximity to the vesicle of the conidiophore, for then to proceed into the vesicle. The signal centred and persisted throughout the majority of the experiment. At third day, the GFP expression finalized, fainted from the conidiophore and diffused into the hyphae. All three stages can be observed on figure 8.3.B

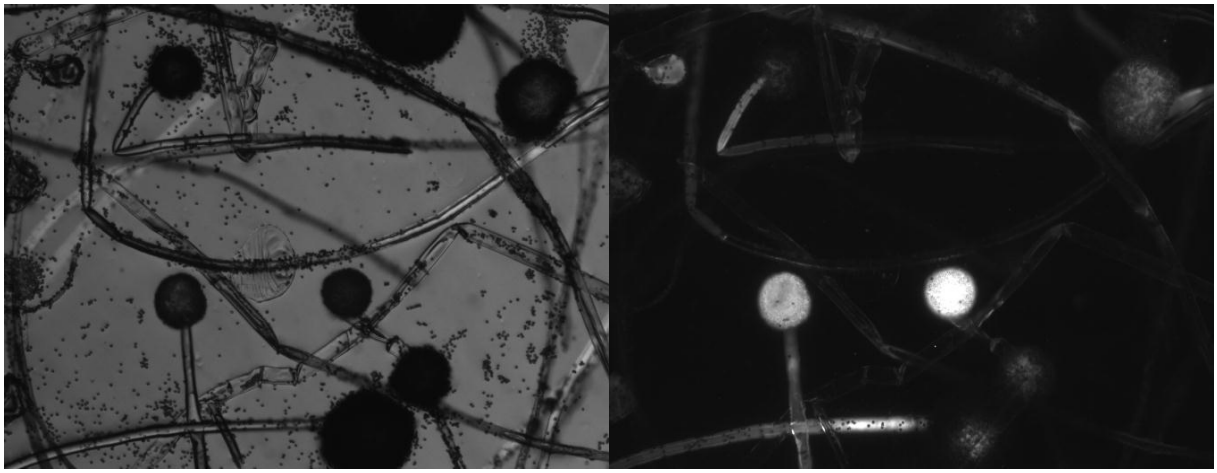

(A) (B)

Figure 8.3 Day 2 Tape slides from the reporter strain on glucose minimal media agar supplemented 5 % (w/v) NaCl. (A) Bright field at 10X magnification. (B) GFP signal from the same position.

8.4.3 Nutritionally profiling of fumonisin production

The results of the Biolog PM plates were used to evaluate induction of the fumonisin promoter. As cut-off value, a three time the standard deviation of σ=716 (PM1-4) and σ=9710 (PM9) was chosen. The osmolyte array (PM9) was evaluated individually, since the fluorescent signal as well as the optical density signal was order of magnitudes larger, compared to the PM1-PM4 plates.

Ten carbon based compounds were found to significantly activate the fumonisin promoter. Those were, lyxose, glucose, ribose, trehalose, threonine and alanine from the PM1 plate and arbutin, dihydroxyacetone, 2-deoxy-D-ribose and glucosamine from the PM2 array. Surprisingly, none of the nitrogen, phosphor or sulphur source induced the fumonisin promoter, as presented in figure 4.

Based on the data collected from the PM9 plate, a total of eleven osmolyte conditions were found to significantly induced fumonisin. All of these were sodium lactate from a concentration of 2-12 %. Interestingly even high concentrations of sodium lactate, did not appear to affect the growth considerably (<11% reduction), observed by the measured optical densities all being in the range of 225-275, Figure 8.4 right.

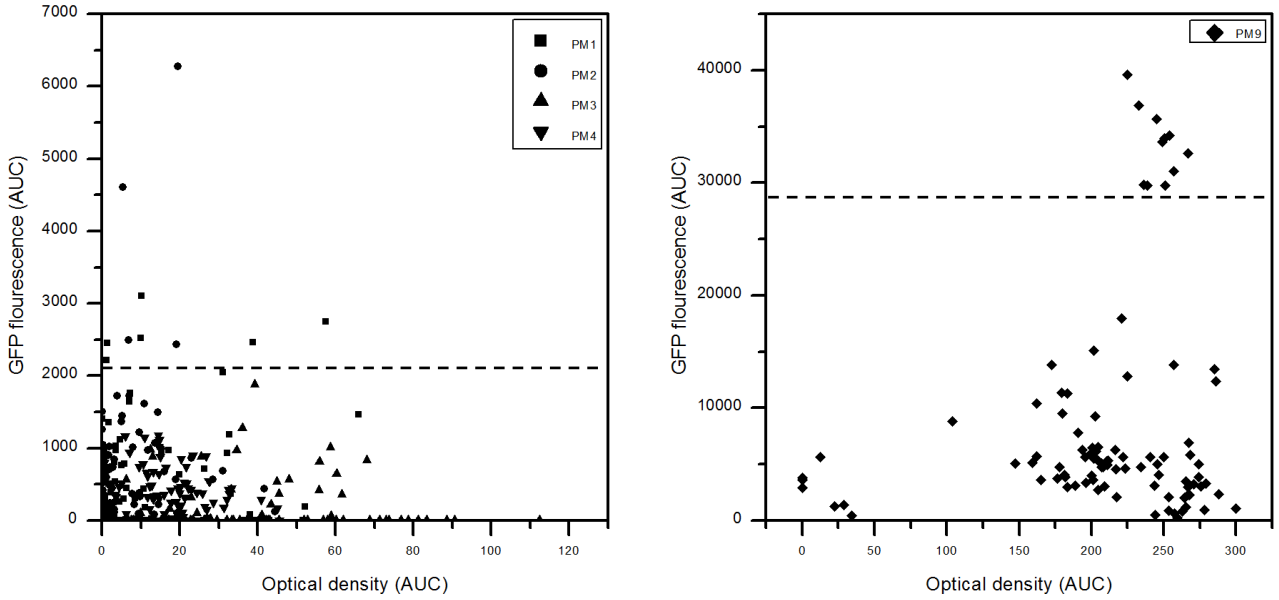

Figure 8.4 Left: The effect of Carbon (PM1-2), nitrogen (PM3), phorphor and sulfur (PM4) sources on growth and fumonisins induction. Right: The effect of osmolyte sources (PM9) on growth and fumonisin induction. The black line indicates the threshold of significance, 99 % confidence. Complete dataset can be found in appendix 5.

Interesting, only few of the surveyed osmolytes, inhibited *A. niger* biomass yield (OD AUC). Those were known fungal growth inhibitors, sodium benzoate > 20 mM and sodium nitrite > 10 mM (Clausen and Yang 2004).

From figure 8.4, most of the compounds that supports growth, fails to induce fumonisin production. This verifies that fumonisin production is not directly coupled to growth but rather needs an initiation by sporulation and subsequent an inductive carbon source. This proposition was further supported by observing the fumonisin promoter activation together with growth over time (figure 8.5). The promoter activation initiates when growth have reached end of the exponential phase.

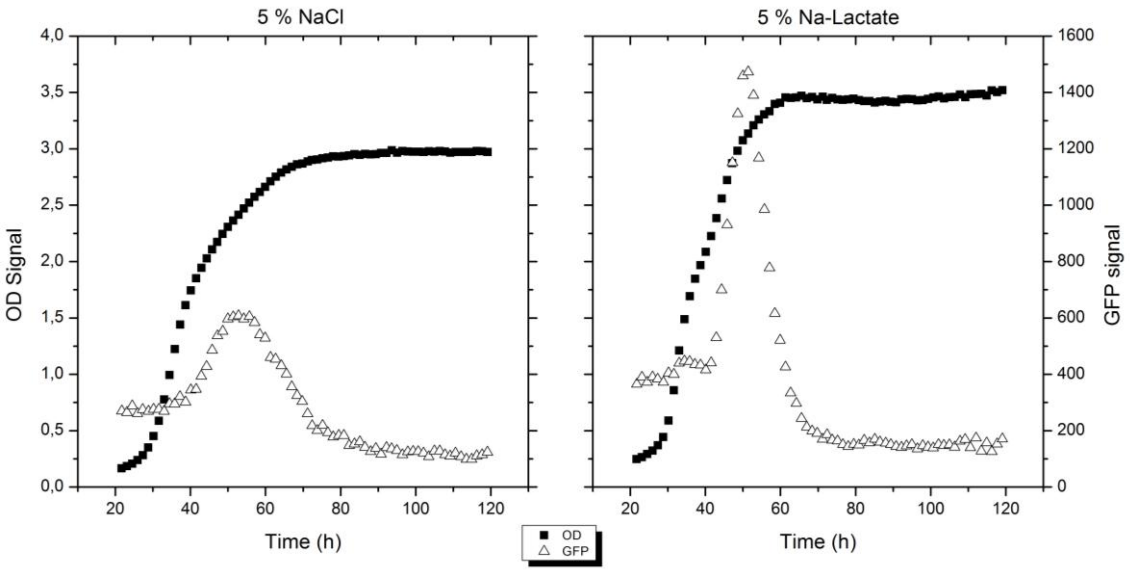

Figure 8.5 Raw data of fumonisin induction and growth over time.

From figure 8.5, it is evident that fumonisin induction, for both conditions, was induced in the late exponential phase, starting at around 42 hours. Since lacate can be metabolized by A. niger, a diauxic shift, in the growth curve, was apparent from the condition.

Based on the screening results derived from the Biolog plates, ten conditions were selected for further evaluation. Defined minimal media plates were produced of the conditions, from the carbon plates, forecasted to induce fumonisin production.

Table 8.2 A comparison between the predicted fumonisin titer (GFP AUC) in the small scale biolog plates and the fumonisin concentration produced on defined agar plates.

	GFP AUC (PM plates)	ng/mL (Agar plates)	sporulation
Arbutin	6278 ± 2453	1106±203	+++
Dihydroxyacetone	4603 ± 245	345±225	+++
Lyxose	3109	0±0	-
Glucose	2750	200±18.7	+++
Ribose	2518	0±0	-
2-deoxy-D-ribose	2490 ± 1520	0±0	-
Trehalose	2465	1119±318	+++
Threonine	2455	0±0	-
Glucosamine	2432 ± 1204	10±0	++
Alanine	2219	550±215	(+)

+++	High degree of sporulation
+	Low degree of sporulation, only few conidia present
-	No sporulation visible

From table 8.2, no clear correlation was found, between the predicted fumonisin productions from the PM plates, compared with the titers obtained in minimal media. Out of the ten assayed conditions, six of these induced fumonisin production in *A. niger*. Notable was, that the remaining false positives, failed to sporulate. This can be explained by variations in medium compositions, as trace elements and vitamins, between the commercial PM plates and defined solid media plates. Moreover the carbon plates' (PM1 and PM2) nitrogen source is unknown, as well as the exact amount of compound, added into the PM plates. Biolog only disclose the concentration range. The carbon sources in PM1 and PM2 are in the 5–50 mM range and the nitrogen sources in PM3 are in the 2–20 mM range (Bochner et al. 2001). The results underline the power of the Biolog nutritionally profiling system, as an efficient screenings tool; therefore, the interpretation of the data should only be seen an indicative.

Still six conditions (Table 8.2) still gave fumonisin production, with the glycosylated hydroquinone arbutin and the disaccharide trehalose being the strongest inducers.

8.4.5 Investigating fumonisin inducers

To examine the events leading to fumonisin induction in *A. niger* and to understand the molecular subjacent mechanisms, further experimentation were performed on numerous defined minimal media plates. Based on the hypothesis, that fumonisin production is initiated upon formation of conidiophores and subsequently regulated by: i) The entry point into the central metabolism: ii) the anomeric position of glycosidic bond in carbohydrates; iii) Biological inducers; and finally iv) Melanin inhibitors.

The first category focused on glucose and the glycolysis. Glucose and fructose formed similar quantities of biomass (Appendix 5) yet glucose had a GFP AUC signal of 2750 where fructose had 190. Similarly lyxose and ribose, both compounds that enter the metabolism through the pentose phosphate pathway did not give rise to fumonisin induction. This led to the hypothesis, that glucose is a key metabolite in fumonisin production.

The results from table 8.3 clearly support this hypothesis of glucose being a key metabolite in fumonisin synthesis. Utilizing fructose yielded in 5 fold less fumonisin compared with utilization of glucose.

To investigate how compounds metabolised through the PP-pathway, the experiment was expanded with plates containing ribose, xylose and lyxose, Tabel 8.3. Based on these results it appears that compounds entering the central metabolism through the Pentose Phosphate pathway repress fumonisin production.

The second experimental series was centred on the glycosidic bonds and their stereochemistry of the anomeric position in disaccharide. Trehalose, maltose and cellobiose are all disaccharides composed of glucose residues but a great difference in AUC fluorescence was observed. The only chemical difference is the glycosidic linkage. Trehalose is α(1→1), maltose is linked with an α(1→4) and cellobiose is a β(1→4). The origin of these compounds in nature varies. Maltose originates from starch typically found in living plants and used as an energy storage, cellobiose originates from cellulose, a structural component of the cell wall in plants and trehalose is accumulated by a wide variety of organisms including fungal spores where it is believed mainly to act as a carbon storage utilized doing germination (Thevelein 1984). Hence understanding which type of glycosidic linkages induces fumonisins formation could give hints to niches where *A. niger* naturally produce fumonisin.

It was evident that the orientation of the glycosidic linkage had some influence on fumonisin titers. Particularly, trehalose resulted in a 5.5 fold increase in fumonisin titer. Trehalose titers are typically high in fungal spores, it could therefore be speculated that a connection between induction of fumonisin, conidia formation and trehalose metabolism exists. Fumonisin production was not affected by cellulosic

breakdown since growth on maltose and cellobiose generated similar amounts of fumonisin. However, interestingly both maltose and cellobiose caused a twofold higher fumonisin titer, compared with pure glucose.

The third category of experiments, attempted to comprehend biological inducers. From table 8.2, the compounds confirmed to significantly induce fumonisin formation included dihydroxyacetone and alanine. These are C3 compounds that are both able to enter the glycolysis by one enzymatic step (dihydroxyacetone kinase and alanine aminotransferase). This supported the hypothesis suggested by Sorensen et al. (2009), that an increased pyruvate pool increases the fumonisin production. Being a biological inducer, lactate was also included since it can be converted into pyruvate by lactate dehydrogenase. The biological inducers were examined in both glucose and xylose background to elucidate induction under both repressing (xylose) and non-repressing (glucose) conditions.

The results in the third set of experiments confirmed the hypothesis that compounds entering into the glycolysis through a single or a few number of steps induces fumonisin production. The number of enzymatic steps required to synthesise pyruvate appears to determine the effect of induction. Comparing glycerol that requires eight enzymatic steps with dihydroxyacetone requiring seven, it is evident that dihydroxyacetone is a stronger inducer of fumonisin production. Likewise by observing fumonisin formation with addition of alanine or lactate that only entail one enzymatic step, they are superior to dihydroxyacetone.

Arbutin is a glycoside that inhibits the enzyme tyrosinase, an oxidase and the rate limiting step in production of melanin. This makes arbutin and other tyrosinase inhibiting compounds especially interesting since the fumonisin synthesis is localized in the same compartment as melanin production. To assess the connection between melanin production and fumonisin, kojic acid, azelaic acid and hydroquirone all belonging to a class of tyrosinase inhibitors (Parvez et al. 2007, Bandyopadhyay 2009) were examined. Glucosamine have also been shown to inhibit melanin by inhibiting the activation of tyrosinase (Bissett 2006), thus also included.

The last and final set assayed compounds, all supposed to target melanin production showed great potential. Arbutin had a great inducer potential, yielding a 10.5 fold increase in fumonisin titre but azelaic acid was the strongest overall inducer found in this study, with fumonisin titres of 0.8-1.2 g/L yielding a more than 64 fold increase.

Azelaic acid besides being a tyrosinase inhibitor, is also a plant hormone, part of plants systemic acquired resistance (SAR) response (Shah 2009). SAR is an inducible defence mechanism, activated as response to a

local infection with a pathogen (Vlot et al. 2008). SAR results in enhanced resistance against subsequent patogen attack. Azelaic acid primes SAR therefore we found it fascinating that this compound, applied as a defence mechanism appears to be exploited by *A. nigers* fumonisin response. The results from all plate experiments were summarized in table 8.3.

Table 8.3 Fumonisin production in minimal medium. The last column "In biolog" is the predicted fumonisin production from the Biolog nutritional profiling experiments.

Compound	Fumonisin	Std	In Biolog
Experiment 1	ng/mL		
Glucose (****)	200	18,7	2750
Fructose (**)	36	9,9	190
Xylose (****)	ND	0,0	0
Sorbitol (**)	15	1,1	0
Experiment 2			
Sucrose (**)	40	15,5	82
Maltose (**)	443	185,0	710
Cellobiose (****)	269	167,3	1765
Experiment 3			
Glycerol + glucose (**)	1551	157,9	N/A
Dyhydoxyacetone + glucose (***)	2004	937,4	N/A
Alanine + glucose (***)	4541	327,0	N/A
Lactate + glucose (**)	2859	966	N/A
Glycerol + xylose (**)	123	24,8	N/A
Dyhydoxyacetone + xylose (**)	783	78,9	N/A
Alanine + xylose (**)	1202	343.2	N/A
Lactate + xylose (**)	801	144,3	N/A
Experiment 4			
Arbutin + glucose (****)	2104	592,0	N/A
Hydroquirone + glucose (**)	0	0,0	N/A
Kojic acid + glucose (***)	458	37,9	N/A
Glucosamine + glucose (**)	465	95,4	N/A
Azelaic acid + glucose (****)	12818	1015,4	N/A
Azelaic acid + xylose (**)	7871	424,9	N/A

Numbers of replicates are indicated with stars

A. niger is generally viewed as post-harvest pathogen, causing decay of fresh and dried fruits and certain vegetables, nuts, coffee, and cereals (Varga et al. 2004, Perrone et al. 2007). Fumonisin occurrences have been detected in most of these food items (Mogensen et al. 2010, Palencia et al. 2010, Knudsen et al. 2011). Interestingly, arbutin are found in wheat, coffee, tea, onion, corn cereal and red wine (Deisinger et al. 1996), where azelaic acid have been found in wheat, oat and grape stones (Sun and Sun 2001, Kim et al. 2006, Verardo et al. 2011). *A. niger* can attack grapes even when they are still attached on the vine itself, the presence of azelaic acid in grape stone could be an explaining for an evolved inducer response towards degradation of grapes.

In contrary, it could be that this response was not evolved in *A. niger* but in *Fusarium verticillioides*, a plant pathogen, and believed to be the ancestral origin of *A. nigers* fumonisin gene cluster (Khaldi and Wolfe 2011). *F. verticillioides* can initiate a SAR response during an attack (Savitch et al. 2007, Endah et al. 2008); hence, exposure to azelaic acid would occur. It could be speculated that azelaic acid are a fumonisin inducer in *F. verticillioides*, but further investigation is required to document this statement.

8.5 Conclusion and future perspectives

In conclusion, using a constructed reporter strain, fumonisin production was found to take place in the conidiophores. This implies, that applying *A. niger* as cell factory in submerged cultivations, should not give rise for concerns toward fumonisin formation.

Additionally we discovered a link between fumonisin production and melanin synthesis. The exact motivation for this connection can only remain speculative; however, both compounds are polyketides hence rely on similar intermediates.

A fascinating relationship between plants SAR response and fumonisin induction was also discovered. Since *A. niger* is not generally regarded as a plant pathogen this could support the hypothesis of the fumonisin cluster was transferred from an ancestral *F. verticillioides*. A diverse group of compounds have been implicated as SAR signals and speculations of redundancies have been proposed (Dempsey and Klessig 2012). Consequently, it might be speculated that disruption of the azelaic acid pathway in plants, could lower fumonisin production in a fungal attack.

Lastly, the fumonisin promoter's strict conidiophore activation might be applied in metabolic engineering. This promoter could be particular beneficial to apply for characterization of secondary metabolite clusters since the application of this promoter would assure expression and localization in the same compartment. Additionally the promoter is repressed by xylose and activated by glucose and fine-tuning can be performed by addition of e.g. salts.

8.6 References

Andersen, M. R., M. P. Salazar, P. J. Schaap, P. J. van de Vondervoort, D. Culley, J. Thykaer, J. C. Frisvad, K. F. Nielsen, R. Albang, K. Albermann, R. M. Berka, G. H. Braus, S. A. Braus-Stromeyer, L. M. Corrochano, Z. Dai, P. W. van Dijck, G. Hofmann, L. L. Lasure, J. K. Magnuson, H. Menke, M. Meijer, S. L. Meijer, J. B. Nielsen, M. L. Nielsen, A. J. van Ooyen, H. J. Pel, L. Poulsen, R. A. Samson, H. Stam, A. Tsang, J. M. van den Brink, A. Atkins, A. Aerts, H. Shapiro, J. Pangilinan, A. Salamov, Y. Lou, E. Lindquist, S. Lucas, J. Grimwood, I. V. Grigoriev, C. P. Kubicek, D. Martinez, N. N. van Peij, J. A. Roubos, J. Nielsen and S. E. Baker (2011). "Comparative genomics of citric-acid-producing *Aspergillus niger* ATCC 1015 versus enzyme-producing CBS 513.88." Genome Res **21**(6): 885-897.

Bandyopadhyay, D. (2009). "Topical treatment of melasma." Indian J Dermatol **54**(4): 303-309.

Bissett, D. L. (2006). "Glucosamine: an ingredient with skin and other benefits." J Cosmet Dermatol **5**(4): 309-315.

Clausen, C. A. and V. W. Yang (2004). "Curbing indoor mold growth with mold inhibitors." Proceedings from the Woodframe Housing Durability and Disaster Issues Conference: 303-306.

Deisinger, P. J., T. S. Hill and J. C. English (1996). "Human exposure to naturally occurring hydroquinone." J Toxicol Environ Health **47**(1): 31-46.

Dempsey, D. A. and D. F. Klessig (2012). "SOS - too many signals for systemic acquired resistance?" Trends Plant Sci **17**(9): 538-545.

Desjardins, A. E., M. Busman, M. Muhitch and R. H. Proctor (2007). "Complementary host–pathogen genetic analyses of the role of fumonisins in the Zea mays–Gibberella moniliformis interaction." Physiological and Molecular Plant Pathology **70**(4–6): 149-160.

Endah, R., G. Beyene, A. Kiggundu, N. van den Berg, U. Schluter, K. Kunert and R. Chikwamba (2008). "Elicitor and Fusarium-induced expression of NPR1-like genes in banana." Plant Physiol Biochem **46**(11): 1007-1014.

Fleissner, A. and P. Dersch (2010). "Expression and export: recombinant protein production systems for *Aspergillus*." Appl Microbiol Biotechnol **87**(4): 1255-1270.

Frisvad, J. C., T. O. Larsen, U. Thrane, M. Meijer, J. Varga, R. A. Samson and K. F. Nielsen (2011). "Fumonisin and ochratoxin production in industrial *Aspergillus niger* strains." PLoS One **6**(8): e23496.

Gardiner, D. M., K. Kazan and J. M. Manners (2009). "Nutrient profiling reveals potent inducers of trichothecene biosynthesis in Fusarium graminearum." Fungal Genet Biol **46**(8): 604-613.

Glenn, A. E., N. C. Zitomer, A. M. Zimeri, L. D. Williams, R. T. Riley and R. H. Proctor (2008). "Transformation-mediated complementation of a FUM gene cluster deletion in Fusarium verticillioides restores both fumonisin production and pathogenicity on maize seedlings." Mol Plant Microbe Interact **21**(1): 87-97.

Goldberg, I., J. S. Rokem and O. Pines (2006). "Organic acids: old metabolites, new themes." Journal of Chemical Technology & Biotechnology **81**(10): 1601-1611.

Hofmann, G., A. Diano and J. Nielsen (2009). "Recombinant bacterial hemoglobin alters metabolism of *Aspergillus niger*." Metab Eng **11**(1): 8-12.

Jørgensen, T. R., K. F. Nielsen, M. Arentshorst, J. Park, C. A. van den Hondel, J. C. Frisvad and A. F. Ram (2011). "Submerged conidiation and product formation of *Aspergillus niger* at low specific growth rates is affected in aerial developmental mutants." Applied and Environmental Microbiology.

Karaffa, L. and C. P. Kubicek (2003). "*Aspergillus niger* citric acid accumulation: do we understand this well working black box?" Appl Microbiol Biotechnol **61**(3): 189-196.

Khaldi, N. and K. H. Wolfe (2011). "Evolutionary Origins of the Fumonisin Secondary Metabolite Gene Cluster in Fusarium verticillioides and *Aspergillus niger*." Int J Evol Biol **2011**: 423821.

Kim, S.-Y., S.-M. Jeong, W.-P. Park, K. C. Nam, D. U. Ahn and S.-C. Lee (2006). "Effect of heating conditions of grape seeds on the antioxidant activity of grape seed extracts." Food Chemistry **97**(3): 472-479.

Knudsen, P. B., J. M. Mogensen, T. O. Larsen and K. F. Nielsen (2011). "Occurrence of fumonisins B(2) and B(4) in retail raisins." J Agric Food Chem **59**(2): 772-776.

Kubicek, C. P., M. Röhr and H. J. Rehm (1985). "Citric Acid Fermentation." Critical Reviews in Biotechnology **3**(4): 331-373.

Mansson, M., M. L. Klejnstrup, R. K. Phipps, K. F. Nielsen, J. C. Frisvad, C. H. Gotfredsen and T. O. Larsen (2010). "Isolation and NMR characterization of fumonisin B2 and a new fumonisin B6 from *Aspergillus niger*." J Agric Food Chem **58**(2): 949-953.

Mogensen, J. M., T. O. Larsen and K. F. Nielsen (2010). "Widespread occurrence of the mycotoxin fumonisin b(2) in wine." J Agric Food Chem **58**(8): 4853-4857.

Mogensen, J. M., K. F. Nielsen, R. A. Samson, J. C. Frisvad and U. Thrane (2009). "Effect of temperature and water activity on the production of fumonisins by *Aspergillus niger* and different Fusarium species." BMC Microbiol **9**: 281.

Nielsen, K. F., J. M. Mogensen, M. Johansen, T. O. Larsen and J. C. Frisvad (2009). "Review of secondary metabolites and mycotoxins from the *Aspergillus niger* group." Anal Bioanal Chem **395**(5): 1225-1242.

Olempska-Beer, Z. S., R. I. Merker, M. D. Ditto and M. J. DiNovi (2006). "Food-processing enzymes from recombinant microorganisms--a review." Regul Toxicol Pharmacol **45**(2): 144-158.

Palencia, E. R., D. M. Hinton and C. W. Bacon (2010). "The black *Aspergillus* species of maize and peanuts and their potential for mycotoxin production." Toxins (Basel) **2**(4): 399-416.

Parvez, S., M. Kang, H. S. Chung and H. Bae (2007). "Naturally occurring tyrosinase inhibitors: mechanism and applications in skin health, cosmetics and agriculture industries." Phytother Res **21**(9): 805-816.

Perrone, G., A. Susca, G. Cozzi, K. Ehrlich, J. Varga, J. C. Frisvad, M. Meijer, P. Noonim, W. Mahakarnchanakul and R. A. Samson (2007). "Biodiversity of *Aspergillus* species in some important agricultural products." Stud Mycol **59**: 53-66.

Punt, P. J., R. P. Oliver, M. A. Dingemanse, P. H. Pouwels and C. A. van den Hondel (1987). "Transformation of *Aspergillus* based on the hygromycin B resistance marker from Escherichia coli." Gene **56**(1): 117-124.

Sambrook, J. and D. W. Russell (2001). Molecular cloning : a laboratory manual. Cold Spring Harbor, N.Y., Cold Spring Harbor Laboratory Press, 0879695773 (paper)

0879695765 (cloth).

Samson, R. A. (2002). Introduction to food- and airborne fungi. Utrecht, Centraalbureau voor Schimmelcultures, 9070351420.

Sánchez-Rangel, D. and J. Plasencia (2010). "The role of sphinganine analog mycotoxins on the virulence of plant pathogenic fungi." Toxin Reviews **29**(3-4): 73-86.

Savitch, L. V., R. Subramaniam, G. C. Allard and J. Singh (2007). "The GLK1 'regulon' encodes disease defense related proteins and confers resistance to Fusarium graminearum in Arabidopsis." Biochemical and biophysical research communications **359**(2): 234-238.

Shah, J. (2009). "Plants under attack: systemic signals in defence." Curr Opin Plant Biol **12**(4): 459-464.

Sorensen, L. M., R. Lametsch, M. R. Andersen, P. V. Nielsen and J. C. Frisvad (2009). "Proteome analysis of *Aspergillus niger*: lactate added in starch-containing medium can increase production of the mycotoxin fumonisin B2 by modifying acetyl-CoA metabolism." BMC Microbiol **9**: 255.

Sun, R. C. and X. F. Sun (2001). "Identification and quantitation of lipophilic extractives from wheat straw." Industrial Crops and Products **14**(1): 51-64.

Thevelein, J. M. (1984). "Regulation of trehalose mobilization in fungi." Microbiol Rev **48**(1): 42-59.

Toews, M. W., J. Warmbold, S. Konzack, P. Rischitor, D. Veith, K. Vienken, C. Vinuesa, H. Wei and R. Fischer (2004). "Establishment of mRFP1 as a fluorescent marker in *Aspergillus* nidulans and construction of expression vectors for high-throughput protein tagging using recombination in vitro (GATEWAY)." Curr Genet **45**(6): 383-389.

Varga, J., Á. Juhász, F. Kevei and Z. Kozakiewicz (2004). "Molecular Diversity of Agriculturally Important <i>*Aspergillus*</i> Species." European Journal of Plant Pathology **110**(5): 627-640.

Verardo, V., C. Serea, R. Segal and M. F. Caboni (2011). "Free and bound minor polar compounds in oats: Different extraction methods and analytical determinations." Journal of Cereal Science **54**(2): 211-217.

Vlot, A. C., D. F. Klessig and S. W. Park (2008). "Systemic acquired resistance: the elusive signal(s)." Curr Opin Plant Biol **11**(4): 436-442.

Chapter 9 Conclusion

”All things are difficult before they are easy.”

- Dr. Thomas Fuller

The focus of this thesis has been to study *A. niger* in the different industrial aspects of where this fungus is applied. From in depth examinations of citrate and oxalate overflow metabolisms, to characterization of protease secretion mutants and nutritional investigation of the fumonisin biosynthesis, a wide range of topics have been covered. Some of the main contributions in this thesis include; the tool of transcription factor modulation, how to select the targets and the novel mutants obtained using this method. The idea of TF modulation were developed and tested only in *A. niger;* yet, the scope of this metabolic engineering method, is not limited to this species but may aid improving other eukaryote cell factories.

All the individual studies present interesting findings. The examination of the citrate overflow metabolism using a systems biology approach revealed, among other novel findings that the gluconeogenesis was significantly down regulated, during citrate overflow metabolism. Similarly, the study of oxalic acid overproducer mutant, *ΔoafA,* exposed that down regulation of the phosphoketolase pathway in *A. niger* caused evaluated oxalate formation.

A new protease deficient strain, *ΔprtB,* a candidate for heterologous protein production, was also presented. The strain was compared to the previously described *ΔprtT* protease mutant. The study demonstrated some of the difficulties in altering regulatory networks. Indeed the *ΔprtT* strain had the lowest protease activity (fivefold reduced) but at the expense of excessive CO_2 yield, reduced growth rate and lower biomass yields. Contrary, the *ΔprtB* had a close to twofold reduced levels of secreted proteases but combined with additional beneficial characteristics, as a lower oxalic acid formation and wild type growth performance; this strain could be an attractive alternative to *ΔprtT*.

The relatively new awareness concerning fumonisins from *A. niger,* was studied using a constructed reporter strain combined with large-scale nutrient profiling. The obtained data formed basis for the subsequent examinations, which resulted in the identification of azelaic acid, a plant hormone and a very potent fumonisin inducer. Plants use this compound as a signal for pathogen attacks (SAR) and that *A. niger* may have evolved such response, is remarkable. However, the perspective is far greater than just the

knowledge of this inducer. Redundancies have been proposed in the plants SAR response; hence, the possibility of disrupting the azelaic acid the biosynthesis pathway in the plants, perhaps reduces the fumonisin formation in infected plants.

The work in this thesis has generated new tools, strains, knowledge and fresh hypothesis, than can be applied to improve *A. niger* as a cell factory, presently and in the future.

Appendix 1 Significantly expressed genes of Chapter 4

JGI ID	Fold Change	P. Value	Annotation
49896	**-2,2738**	**1,23E-05**	Mandelate racemase
141873	**-2,1679**	**0,0004528**	Carbon-nitrogen hydrolase
209161	**-1,3204**	**0,0004528**	Major facilitator superfamily
134351	**-1,3085**	**0,0005023**	-
206339	**-1,8959**	**0,0005023**	Haem peroxidase, plant/fungal/bacterial
186371	**-1,4043**	**0,0005258**	-
187103	**-1,1618**	**0,0005258**	-
190396	**-1,2345**	**0,0005258**	-
191642	**-2,0426**	**0,0005258**	-
191756	**-1,8294**	**0,0005258**	-
194603	**-3,3021**	**0,0005258**	-
194767	**-1,3009**	**0,0005258**	-
36015	**-1,8662**	**0,0005258**	-
37328	**-2,1644**	**0,0005258**	-
39611	**-1,2827**	**0,0005258**	-
40159	**-2,1881**	**0,0005258**	-
45100	**-0,9521**	**0,0005258**	-
46007	**-1,9794**	**0,0005258**	-
52342	**-1,6384**	**0,0005258**	-
180131	**-1,5721**	**0,0005258**	Abl interactor ABI-1, contains SH3 domain
38370	**-1,5412**	**0,0005258**	AMP-dependent synthetase and ligase
204301	**-1,8448**	**0,0005258**	candidate 1,3-beta-glucanosyltransferase
179634	**-1,265**	**0,0005258**	Cytochrome P450
214803	**-2,0779**	**0,0005258**	Cytochrome P450
40956	**-2,7523**	**0,0005258**	Cytochrome P450
49535	**-1,1247**	**0,0005258**	FMN-dependent alpha-hydroxy acid dehydrogenase
48710	**-2,2769**	**0,0005258**	Glutathione-dependent formaldehyde-activating, GFA
55161	**-1,1639**	**0,0005258**	Hypothetical Alpha/beta hydrolase. Involded in aromatic compound metabolism
54699	**-1,1964**	**0,0005258**	Hypothetical amidase
212098	**-1,1157**	**0,0005258**	Hypothetical CAP20-like protein
42043	**-1,676**	**0,0005258**	Hypothetical dihydrolipoamide dehydrogenase; EC 1.8.1.4
51812	**-1,5737**	**0,0005258**	Hypothetical D-lactate dehydrogenase
49063	**-2,1075**	**0,0005258**	Hypothetical fatty acid omega-hydroxylase

50817	**-1,5947**	**0,0005258**	Hypothetical hexokinase; EC 2.7.1.1; phosphorylation of glucose and fructose
41753	**-2,4577**	**0,0005258**	Hypothetical protein. Contains 6 predicted transmembrane domains
212718	**-1,5918**	**0,0005258**	Hypothetical protein. PFam suggests Oligopeptide transporter activity. 12 transmembrane domains are predicted
214017	**-1,6325**	**0,0005258**	MEKK and related serine/threonine protein kinases
35714	**-1,328**	**0,0005258**	N-acetyltransferase activity
52038	**-1,3149**	**0,0005258**	related to D-amino acid oxidase of Fusarium solani
55835	**-1,3368**	**0,0005258**	related to voltage-gated calcium channel
211983	**-1,5472**	**0,0005258**	Serine/threonine protein kinase
121906	**-0,9025**	**0,0005258**	Vacuolar sorting protein VPS36
122060	**-1,3104**	**0,0005258**	#N/A
126829	**-2,1122**	**0,0005258**	#N/A
40951	**-1,2123**	**0,0005258**	#N/A
45304	**-1,7834**	**0,0005459**	related to alpha-amylase; glycoside hydrolase, family 13
54445	**-1,6839**	**0,0005459**	#N/A
184284	**-1,2597**	**0,0005478**	Serine/threonine protein kinase
120939	**-1,5389**	**0,0005538**	-
174977	**-0,9377**	**0,0005538**	-
201412	**-1,6615**	**0,0005538**	-
43220	**-1,1217**	**0,0005538**	-
53243	**-1,7266**	**0,0005538**	-
53909	**-1,5427**	**0,0005538**	-
191914	**-1,0781**	**0,0005538**	Acyl-CoA dehydrogenase,
209231	**-1,1709**	**0,0005538**	Aldo/keto reductase
201415	**-1,0926**	**0,0005538**	beta-1,6-N-acetylglucosaminyltransferase, contains WSC domain
47739	**-0,9718**	**0,0005538**	Cell cycle-associated protein Mob1-1
185495	**-1,3727**	**0,0005538**	endoribonuclease
185082	**-1,3925**	**0,0005538**	Fungal transcriptional regulatory protein
200314	**-1,4248**	**0,0005538**	Glutathione S-transferase
135787	**-1,2168**	**0,0005538**	hypothetical lipolytic enzyme
174348	**-1,3166**	**0,0005538**	Hypothetical protein with an ubiquitin-activating enzyme repeat
54451	**-1,3395**	**0,0005538**	Hypothetical. Interpro: UTP-glucose-1-phosphate uridylyltransferase
183237	**-2,1252**	**0,0005538**	Hypothetical. Major facilitator superfamily, Monocarboxylate transporter
188030	**-1,3059**	**0,0005538**	Major facilitator superfamily
206955	**-1,1139**	**0,0005538**	Transthyretin and related proteins
45622	**-1,1408**	**0,0005598**	-

45623	**-1,6772**	**0,0005598**	-
173936	**-1,4331**	**0,0005613**	-
36674	**-2,9398**	**0,0005613**	-
207936	**-1,0336**	**0,0005613**	D-isomer specific 2-hydroxyacid dehydrogenase
40935	**-0,7948**	**0,0005613**	hypothetical prolyl aminopeptidase
43044	**-1,4679**	**0,0005613**	Hypothetical protein. Is very likely associated with degradation of aromatic compounds based on Pfam and protein similarity
174831	**-1,0402**	**0,0005613**	Ribonuclease T2
44755	**-1,5914**	**0,0005743**	-
183926	**-1,6416**	**0,0005743**	hypothetical class II aldolase/adducin domain protein
210508	**-1,0572**	**0,0005743**	Hypothetical L-kynurenine hydrolase
51134	**-2,1155**	**0,0005743**	putative transmembrane GH family 47 mannosyl-oligosaccharide 1,2-alpha-mannosidase
204464	**-1,7988**	**0,0005841**	Hypothetical protein. Contains a putative BAR domain.
38352	**-1,8385**	**0,0005863**	-
46081	**-2,372**	**0,0005863**	-
176911	**-1,0412**	**0,0005898**	-
37965	**-0,9469**	**0,0005898**	-
40551	**-1,2142**	**0,0005898**	-
52903	**-1,2628**	**0,0005898**	-
56923	**-1,9051**	**0,0005898**	-
133702	**-1,267**	**0,0005898**	Esterase/lipase/thioesterase
42613	**-1,757**	**0,0005898**	Esterase/lipase/thioesterase
57197	**-1,502**	**0,0005898**	Glutathione-dependent formaldehyde-activating, GFA
194170	**-1,4533**	**0,0005898**	Hypothetical flavoprotein monooxygenase. HMMPfam indicates acitivity towards hydroxylation of aromatic rings.
43537	**-1,5168**	**0,0005898**	hypothetical protein; Interpro desc: Peptidase M24 & Histone H4
35566	**-1,847**	**0,0005898**	Short-chain dehydrogenase/reductase
42211	**-1,3018**	**0,0005898**	#N/A
174284	**-1,8772**	**0,0006091**	-
196241	**-1,1602**	**0,0006091**	-
44921	**-2,1521**	**0,0006091**	-
54952	**-0,7546**	**0,0006091**	-
188462	**-1,0104**	**0,0006091**	Acyltransferase
195962	**-1,1283**	**0,0006091**	Amino acid transporters
193010	**-2,2165**	**0,0006091**	Ferric reductase-like transmembrane component
45434	**-1,6506**	**0,0006091**	Glycerol kinase (glcA).
40917	**-2,3718**	**0,0006091**	Predicted mechanosensitive ion channel

205706	**-1,2941**	**0,0006091**	Protein kinase
46465	**-1,1933**	**0,0006091**	Taurine catabolism dioxygenase
48103	**-1,2175**	**0,0006091**	WD40 repeat-containing protein
207853	**-1,6681**	**0,0006146**	Predicted dehydrogenase
56498	**-1,0454**	**0,0006239**	Isoflavone reductase
54141	**-1,2079**	**0,0006296**	Ankyrin
54896	**-1,5023**	**0,0006392**	-
52941	**-1,0946**	**0,0006546**	-
170261	**-1,8713**	**0,0006546**	Permease of the major facilitator superfamily
55640	**-0,9085**	**0,0006613**	#N/A
170355	**-0,9255**	**0,0006677**	-
174765	**-0,8971**	**0,0006677**	-
189793	**-2,279**	**0,0006677**	-
193892	**-1,3985**	**0,0006677**	-
208209	**-1,1453**	**0,0006677**	-
208583	**-1,7478**	**0,0006677**	-
212116	**-1,2989**	**0,0006677**	-
212997	**-1,6972**	**0,0006677**	-
49515	**-1,3363**	**0,0006677**	-
54373	**-1,1354**	**0,0006677**	-
55190	**-1,7319**	**0,0006677**	-
57315	**-2,2728**	**0,0006677**	-
46065	**-2,2902**	**0,0006677**	(xghA) endo-xylogalacturonase A
205909	**-1,0286**	**0,0006677**	ABC transporter associated with fumonisin-like biosyntehetic gene cluster
38000	**-1,3481**	**0,0006677**	Acetoacetyl-CoA synthase
41388	**-1,1411**	**0,0006677**	Actin regulatory proteins
187366	**-1,6851**	**0,0006677**	AMP-binding enzyme
55052	**-1,0004**	**0,0006677**	Fungal specific transcription factor
134540	**-1,4823**	**0,0006677**	Fungal transcriptional regulatory protein, N-terminal
210306	**-2,0791**	**0,0006677**	Hypothetical aspartic protease
214353	**-1,8502**	**0,0006677**	Nucleolar GTPase/ATPase p130
55671	**-2,1914**	**0,0006677**	Oxoprolinase
120873	**-0,8724**	**0,0006677**	Sec1-like protein
214360	**-1,4719**	**0,0006677**	Xanthine dehydrogenase
177954	**-2,3293**	**0,0006677**	#N/A
120104	**-1,5027**	**0,0006723**	candidate beta-N-acetylglucosaminidase
134658	**-0,9025**	**0,0006723**	Hypothetical 3-methyladenine DNA glycosidase
40218	**-2,8797**	**0,0006723**	hypothetical aspartic protease
187510	**-1,3224**	**0,0006723**	hypothetical O-methylsterigmatocystin oxidoreductase (OMST oxidoreductase) (Cytochrome P450 64) [Aspergillus flavus]
51857	**-0,8321**	**0,0006921**	-

52306	**-1,5947**	**0,0006949**	-
210988	**-2,4544**	**0,0006949**	candidate cell wall protein
35964	**-1,7483**	**0,0006949**	Chitin synthase
121560	**-0,9943**	**0,0006991**	Hypothetical ribonuclease CAF1
202949	**-2,7102**	**0,0007127**	Hypothetical. Has similarity to beta-1,6-N-acetylglucosaminyltransferase (KOG), contains WSC domain
209195	**-0,8623**	**0,0007127**	Peptidase
211015	**-0,9873**	**0,0007324**	#N/A
45408	**-1,268**	**0,000737**	-
214825	**-2,3878**	**0,000737**	Glycosyl transferase, group 1
210522	**-1,0094**	**0,0007381**	-
205471	**-1,5067**	**0,0007413**	putative Xaa-Pro dipeptidase
57436	**-1,8213**	**0,0007416**	xynA, xylanase A. extracellular GH family 11 endo-1,4-beta-xylanase
134561	**-0,8354**	**0,0007458**	-
203625	**-1,4444**	**0,0007458**	-
142717	**-1,3179**	**0,0007458**	Carbohydrate kinase
181179	**-2,0516**	**0,0007458**	Catechol dioxygenase, N-terminal
183355	**-1,9061**	**0,0007458**	Histidine acid phosphatase
120372	**-0,9729**	**0,0007458**	Phosphoinositide-specific phospholipase C (PLC)
52590	**-1,156**	**0,0007458**	putative alpha-1,3-glucanase, family 71
127307	**-1,6725**	**0,0007458**	#N/A
214611	**-1,512**	**0,0007576**	candidate multidrug resistance ABC transporter
197631	**-1,0749**	**0,0007605**	-
45270	**-0,7174**	**0,0007605**	-
55763	**-1,0291**	**0,0007605**	(manA) Mannose-6-phosphate isomerase (EC 5.3.1.8)
53523	**-1,1693**	**0,0007605**	Dihydroxy-acid and 6-phosphogluconate dehydratase
54585	**-1,3733**	**0,0007605**	DSBA oxidoreductase
211163	**-1,8673**	**0,0007605**	endo-rhamnogalacturonase
48268	**-0,9551**	**0,0007605**	Hypothetical aminotransferase. FPrintScan queries indicates aromatic amino acid activity
43594	**-2,1947**	**0,0007605**	Hypothetical. SignalP suggests secreted
44637	**-1,0398**	**0,0007677**	Hypothetical translation initiation factor
40101	**-1,6912**	**0,0007678**	-
54298	**-1,2192**	**0,0007678**	hypothetical. Heterogeneous nuclear ribonucleoproteins A2/B1
204737	**-1,0663**	**0,0007696**	-
37057	**-1,5294**	**0,0007844**	Arginase/agmatinase/formiminoglutamase
55598	**-0,9759**	**0,0007957**	-
203198	**-1,5666**	**0,0007957**	(xdhA) D-xylulose reductase
207411	**-1,3331**	**0,0007957**	Peptidase

55432	**-1,3381**	**0,0008125**	-
57089	**-1,3511**	**0,0008125**	DNA-binding SAP
55324	**-1,324**	**0,0008125**	putative extracellular tyrosinase
199857	**-1,1331**	**0,0008228**	-
171269	**-2,6832**	**0,0008368**	candidate xylanase
56327	**-2,0744**	**0,0008466**	Ubiquitin-conjugating enzyme
51412	**-0,9438**	**0,000863**	-
35944	**-0,8503**	**0,0008637**	hypothetical nitrilase-like protein
200640	**-1,6864**	**0,0008667**	-
38703	**-1,2963**	**0,0008745**	hypothetical carboxylesterase
54140	**-0,9911**	**0,0008745**	Hypothetical myosin assembly protein/sexual cycle protein in A. niger
180923	**-1,2107**	**0,0008745**	Major facilitator superfamily
48684	**-1,5909**	**0,0008755**	(mscA) 2-methylcitrate synthase (citrate synthase family)
198321	**-0,8564**	**0,0008755**	Aldehyde dehydrogenase
211779	**-0,9867**	**0,0008755**	Fungal specific transcription factor
175896	**-1,6995**	**0,0008755**	Glucose-6-phosphate/phosphate and phosphoenolpyruvate/phosphate antiporter
37760	**-2,8048**	**0,000881**	-
175987	**-1,6368**	**0,000881**	Carbon-nitrogen hydrolase
185000	**-1,9208**	**0,000881**	Cytochrome P450
55136	**-2,2117**	**0,000881**	Glycosyl hydrolase family 62
49553	**-1,2804**	**0,000881**	Hypothetical acetyltransferase
48646	**-0,9266**	**0,000881**	Hypothetical enoyl-CoA hydratase (EC 4.2.1.17)
126535	**-2,6674**	**0,000881**	hypothetical protein
46787	**-1,0833**	**0,000881**	Short-chain dehydrogenase/reductase
204476	**-1,34**	**0,000881**	Zinc-containing alcohol dehydrogenase
214624	**-0,7742**	**0,0008843**	Glycosyl transferase, family 8
49420	**-2,0071**	**0,0008908**	-
37856	**-0,9365**	**0,0008908**	Alkyl hydroperoxide reductase/peroxiredoxin
126891	**-0,7979**	**0,0008908**	Molybdopterin cofactor biosynthesis protein
185262	**-1,1505**	**0,0008908**	Zinc-containing alcohol dehydrogenase superfamily
188214	**-1,1119**	**0,000903**	-
197593	**-1,4306**	**0,0009033**	-
126405	**-0,9571**	**0,0009042**	Transcription factor
51633	**-1,8089**	**0,0009058**	(bioA) Biotin synthase
41385	**-1,182**	**0,0009058**	Major facilitator superfamily
42164	**-0,9674**	**0,0009058**	Oxidoreductase, N-terminal
184541	**-0,9227**	**0,0009338**	-
50757	**-1,7114**	**0,0009341**	-
52938	**-0,8728**	**0,0009365**	Esterase/lipase/thioesterase
37923	**-0,7586**	**0,0009439**	-

214517	**-1,0499**	**0,0009439**	Hypothetical COP9 signalosome subunit
52525	**-0,7269**	**0,0009528**	Aminotransferase, class-II
139271	**-2,1402**	**0,000963**	-
39731	**-0,8148**	**0,000963**	-
121695	**-1,5902**	**0,000963**	AMP-dependent synthetase and ligase
210238	**-1,6798**	**0,000963**	#N/A
196874	**-2,8261**	**0,0009638**	Aldehyde dehydrogenase
52415	**-1,7034**	**0,0009638**	Glycoside hydrolase, family 38
213572	**-1,1929**	**0,0009638**	Hypothetical. Related to cell surface antigen spherulin
208272	**-0,9055**	**0,0009638**	Ubiquitin-like protein
53099	**-1,3077**	**0,0009648**	-
210547	**-1,0541**	**0,0009648**	Haloacid dehalogenase-like hydrolase
127436	**-0,9538**	**0,0009692**	Carbohydrate kinase
44666	**-1,3382**	**0,0009707**	-
186422	**-1,4165**	**0,0009707**	Sterol O-acyltransferase/Diacylglycerol O-acyltransferase
205986	**-1,1794**	**0,0009796**	-
214549	**-1,2265**	**0,0009852**	-
38275	**-0,8727**	**0,0009927**	related to 3-ketoacyl-CoA thiolase
212771	**-1,3432**	**0,0009927**	Zinc-binding oxidoreductase
134132	**-0,9123**	**0,0009929**	Peptidase M20
36861	**-1,3906**	**0,0009995**	hypothetical extracellular protein
189206	**-1,1963**	**0,001012**	-
36816	**-0,9671**	**0,0010278**	AMP-dependent synthetase and ligase
40862	**-1,9291**	**0,0010278**	hypothetical protein
180846	**-0,9225**	**0,0010303**	beta-1,6-N-acetylglucosaminyltransferase, contains WSC domain
179532	**-1,5779**	**0,0010303**	Hypothetical GCN5-related N-acetyltransferase
175292	**-2,0387**	**0,0010312**	-
212087	**-0,9912**	**0,0010312**	-
52472	**-0,8548**	**0,0010312**	-
55759	**-1,1393**	**0,0010312**	-
40634	**-1,2894**	**0,0010312**	BTB/POZ domain
56950	**1,5086**	**0,0010312**	Candidate Lysophospholipase precursor (Phospholipase B)
35778	**-1,0005**	**0,0010312**	Hypothetical long chain fatty alcohol oxidase
46311	**-0,7374**	**0,0010317**	Members of tubulin/FtsZ family
51056	**-0,7424**	**0,0010362**	Hypothetical N-(5'-phospho-D-ribosylformimino)-5-amino-1-(5''-phosphoribosyl)-4- imidazole carboxamide isomerase. (EC 5.3.1.16)
200638	**-0,9129**	**0,0010362**	#N/A
208611	**-1,3384**	**0,0010425**	-
128861	**-1,231**	**0,0010425**	Acyl-CoA dehydrogenase

56628	**-2,1847**	**0,0010425**	Dak kinase
214526	**-2,0323**	**0,0010425**	hypothetical protein containing Zn-finger, C2H2 type domain
183088	**-1,9869**	**0,0010425**	hypothetical xylanase
193695	**-0,8286**	**0,0010425**	O-methyltransferase
55964	**-1,6517**	**0,0010425**	Related to alcohol dehydrogenase
177406	**-0,9579**	**0,0010425**	#N/A
54806	**-0,7198**	**0,0010445**	-
123304	**-0,8494**	**0,0010445**	Amino acid/polyamine transporter
55680	**-1,9432**	**0,0010445**	Coenzyme A transferase
38912	**-1,4411**	**0,0010445**	Hypothetical amidase (EC 3.5.1.4)
214837	**-0,8004**	**0,0010445**	Hypothetical GABA permease/amino acid permease
52743	**-1,1006**	**0,0010445**	hypothetical GPI anchor protein
190043	**-0,7676**	**0,0010445**	hypothetical protein with esterase/lipase/thioesterase and membrane anchor motifs
210783	**-1,5813**	**0,0010445**	Hypothetical. Probable peroxisomal membrane. Interpro suggests alkylhydroperoxide reductase
46889	**-0,9512**	**0,0010445**	Inositol monophosphatase
135360	**-0,8698**	**0,0010445**	Lipid phosphate phosphatase and related enzymes of the PAP2 family
55790	**-0,8447**	**0,0010445**	putative allergen produced in response to stress or pathogen infection
193197	**-1,0691**	**0,0010445**	Splicing coactivator SRm160/300, subunit SRm300
52501	**-0,8349**	**0,0010445**	Zinc-containing alcohol dehydrogenase
121852	**-2,3369**	**0,0010445**	#N/A
134644	**-0,8137**	**0,0010445**	#N/A
38152	**-3,1678**	**0,0010474**	-
182373	**-1,1145**	**0,0010517**	Thioesterase superfamily
190884	**-1,1579**	**0,0010523**	Cys/Met metabolism pyridoxal-phosphate-dependent enzymes
54579	**-1,0838**	**0,0010523**	Hypothetical myristoyl-CoA:protein N-myristoyltransferase
170718	**-1,0656**	**0,0010523**	Hypothetical protein with calcium-binding EF-hand domain
55526	**-0,8537**	**0,0010523**	#N/A
38830	**-0,6616**	**0,0010602**	-
127247	**-0,9511**	**0,0010602**	COP9 signalosome, subunit
210944	**-1,0082**	**0,0010602**	Cytochrome P450
122511	**-1,109**	**0,0010602**	Major facilitator superfamily
213261	**-1,0595**	**0,0010675**	Hypothetical aspartic protease
46947	**-0,8161**	**0,0010762**	Hypothetical acetyl-CoA acetyltransferase
199512	**-1,135**	**0,0010762**	Hypothetical proteasome component

213377	**-0,8088**	**0,0010784**	-
38203	**-0,7713**	**0,0010784**	-
38023	**-2,2271**	**0,0010784**	hypothetical Sulfite oxidase, molybdopterin-binding component
118704	**-1,1689**	**0,0010813**	Predicted GYF domain protein
212379	**-1,4192**	**0,0010813**	putative transmembrane GH family 18 endo-chitinase
185582	**-2,0677**	**0,0010887**	putative carboxylesterase, type B
54812	**-1,9688**	**0,0010887**	putative extracellular protein
183653	**-1,1953**	**0,0011043**	-
48257	**-1,3418**	**0,0011048**	#N/A
171196	**-1,0228**	**0,0011079**	-
212884	**-0,75**	**0,0011154**	-
205927	**-0,9492**	**0,0011181**	-
55204	**-1,7561**	**0,0011181**	agsA, one of five alpha-1,3-glucan synthases
53103	**-0,9029**	**0,0011181**	hypothetical protein containing Zn-finger, C2H2 type domain
128447	**-0,8983**	**0,001119**	-
40429	**-0,8115**	**0,001119**	Mpv17 / PMP22 family
46416	**-1,1938**	**0,001119**	Predicted heme/steroid binding protein
52603	**-0,809**	**0,001119**	related to carboxypeptidase Y
126473	**-1,6879**	**0,0011214**	-
209587	**-1,8901**	**0,0011214**	GMC oxidoreductase
174539	**-1,0132**	**0,001133**	-
54649	**-1,0051**	**0,001133**	Hypothetical dehydroquinase
213492	**-1,0634**	**0,0011334**	Glycosyltransferase, family 2
186833	**-0,7479**	**0,0011334**	UBA/THIF-type NAD/FAD binding fold
41014	**-0,8976**	**0,0011392**	Oxidoreductase family
209628	**-1,4219**	**0,0011421**	Hypothetical methyltransferase
52239	**-1,1838**	**0,0011421**	#N/A
50787	**-0,7294**	**0,001147**	-
55651	**-0,7253**	**0,001147**	#N/A
52071	**-3,0449**	**0,001149**	Endo-1,4-beta-xylanase II precursor (Xylanase II) (1,4-beta-D-xylan xylanohydrolase II)
37199	**-2,2503**	**0,00115**	-
207773	**-0,9747**	**0,0011524**	-
185751	**-0,8061**	**0,0011524**	hypothetical lysophospholipase
44329	**-0,7443**	**0,0011617**	Amino acid/polyamine transporter I
187222	**-0,9971**	**0,0011617**	PpiC-type peptidyl-prolyl cis-trans isomerase
51019	**-0,7423**	**0,0011617**	putative GTP binding protein
185306	**-0,8447**	**0,0011617**	Short-chain dehydrogenase/reductase
39658	**-1,2677**	**0,0011637**	AMP-dependent synthetase and ligase
125883	**-1,7205**	**0,0011673**	-
43031	**-1,0257**	**0,0011673**	-

143657	**-1,0804**	**0,0011679**	Hypothetical Zn-finger protein
49344	**-1,1792**	**0,0011733**	putative GH family 76 endo-1,6-alpha-mannanase
211089	**-0,8655**	**0,0011733**	#N/A
122658	**-0,7748**	**0,0011872**	-
184665	**-1,1404**	**0,0011872**	-
55091	**-0,8396**	**0,0011872**	-
198750	**-0,6828**	**0,0011872**	Ammonium transporter
190765	**-0,7479**	**0,0011872**	Fungal transcriptional regulatory protein
188160	**-1,3688**	**0,0011888**	-
54742	**-0,9543**	**0,0011888**	-
210419	**-1,2685**	**0,0011914**	-
45030	**-2,4798**	**0,0011914**	-
213321	**-1,1534**	**0,0011914**	Hypothetical ras1 guanine nucleotide exchange factor
184789	**-1,527**	**0,0011914**	Iron/ascorbate family oxidoreductases
54041	**-1,1709**	**0,0011914**	Tubulin binding cofactor A
205702	**-1,0261**	**0,0011914**	voltage-gated potassium channel activity
132771	**-0,8147**	**0,0012115**	Seems to be two joined proteins, a heat shock protein-like N-terminal and a phosphomannomutase
204445	**-0,8786**	**0,0012127**	Protein kinase
41667	**-0,6667**	**0,001213**	-
46666	**-1,1101**	**0,001213**	Pyridoxal/pyridoxine/pyridoxamine kinase
53191	**-0,8121**	**0,0012165**	-
207694	**-0,7483**	**0,0012233**	-
127124	**-1,0449**	**0,001226**	-
51913	**-0,681**	**0,0012306**	Putative IreA
41890	**-0,9643**	**0,0012306**	Ras-related small GTPase
206238	**-0,6475**	**0,00124**	Na+/dicarboxylate
124352	**-0,7416**	**0,0012431**	-
45070	**-0,7184**	**0,0012431**	-
45993	**-1,1871**	**0,0012431**	-
175174	**-0,7703**	**0,0012431**	Ctr copper transporter family
47116	**-1,2802**	**0,0012431**	Peptidase M14
185392	**-1,0889**	**0,0012431**	#N/A
207710	**-1,1336**	**0,0012576**	MAP kinase
185961	**-1,0582**	**0,0012589**	Hypothetical maltose acetyltransferase. Homology to Bacillus sp. maltose transacetylase
49836	**-0,7133**	**0,0012601**	TAP42-like protein
213067	**-1,1526**	**0,0012837**	SMP30-like protein
188878	**-0,7291**	**0,0012858**	Flavin-containing monooxygenase
56643	**-1,3435**	**0,0012858**	Major facilitator superfamily, putative lactose permease
130008	**-0,9053**	**0,0012874**	(apsB) aminopeptidase B

54651	**-1,4119**	**0,0012874**	hypothetical 3-ketoacyl-CoA-thiolase
53233	**-1,7966**	**0,0012874**	hypothetical short chain dehydrogenase
188125	**-0,6143**	**0,001292**	-
200086	**-0,8374**	**0,001292**	-
38188	**-0,9042**	**0,001292**	N-methyltransferase
54436	**-0,7246**	**0,001292**	Splicing coactivator SRm160
48145	**-1,0007**	**0,0012985**	#N/A
55143	**-1,8783**	**0,0013172**	Hypothetical protein.
212837	**-0,8501**	**0,0013172**	UTP--glucose-1-phosphate uridylyltransferase
40505	**-0,809**	**0,0013196**	-
181551	**-1,0847**	**0,0013196**	GPCR, family 2, secretin-like
46990	**-1,6266**	**0,0013471**	-
50851	**-0,738**	**0,0013497**	Putative prenyltransferase/squalene oxidase
55582	**-0,7395**	**0,0013598**	Arginase family
210481	**-1,6074**	**0,0013598**	Predicted dehydrogenase
42171	**-1,256**	**0,0013634**	Hypothetical isocitrate lyase and phosphorylmutase
212451	**-1,1009**	**0,0013634**	Hypothetical NADH pyrophosphatase I of the Nudix family of hydrolases
44097	**-2,0441**	**0,0013634**	#N/A
213815	**-1,3882**	**0,0013659**	Cytoskeletal protein A
36666	**-0,8369**	**0,0013659**	Fungal specific transcription factor
37636	**-0,7722**	**0,0013659**	Uracil-DNA glycosylase
36119	**-0,6979**	**0,0013716**	-
46133	**-0,687**	**0,0013731**	-
43857	**-0,8869**	**0,0013737**	Amino acid permease
53150	**-3,1593**	**0,0013846**	-
56536	**-0,836**	**0,0013846**	-
41983	**-1,431**	**0,0013889**	Amidohydrolase 2
189390	**-1,1549**	**0,0013889**	Candidate Alanyl-tRNA synthetase
56788	**-1,2026**	**0,0013889**	hypothetical protease that contains peptidase M28 domain
50236	**-1,0378**	**0,0013947**	Hypothetical Esterase/lipase/thioesterase
177847	**-1,114**	**0,0014009**	ABC transporter
52023	**-0,9515**	**0,0014087**	Adenylosuccinate lyase
54083	**-0,9171**	**0,0014131**	Hypothetical. Related to GCN5-related N-acetyltransferase
52371	**-0,7799**	**0,0014256**	hypothetical. Glycolipid transfer protein ?
56846	**0,9928**	**0,0014267**	-
190311	**-1,4121**	**0,0014273**	2-nitropropane dioxygenase
122069	**-0,6589**	**0,0014273**	hypothetical alpha-amylase
209410	**-1,1555**	**0,0014345**	-
130550	**-1,1176**	**0,0014364**	Serine/threonine protein kinase

181655	**-0,6401**	**0,0014445**	Shares amino acid sequence identity with S. cerevisiae DOM34 gene product, a probable RNA-binding protein that functions in protein translation to promote G1 progression and differentiation, required for meiotic cell division.
130814	**1,6387**	**0,0014508**	-
53175	**-0,8617**	**0,0014508**	beta-1,6-N-acetylglucosaminyltransferase, contains WSC domain
182309	**-1,2846**	**0,0014508**	Glycoside hydrolase, family 3
176411	**-0,9718**	**0,0014508**	Haloacid dehalogenase-like hydrolase
210182	**-1,0294**	**0,0014685**	-
187023	**-0,7264**	**0,0014685**	Fungal specific transcription factor
127698	**-2,3084**	**0,0015022**	-
191925	**-0,784**	**0,0015022**	#N/A
171648	**-0,8914**	**0,0015025**	-
137631	**-0,9224**	**0,0015064**	-
57037	**-2,6246**	**0,0015064**	-
136397	**-0,7782**	**0,001524**	-
207626	**-1,3955**	**0,0015395**	-
43941	**-0,6203**	**0,00154**	Haloacid dehalogenase/epoxide hydrolase
45131	**-0,7959**	**0,00154**	Hypothetical aldehyde dehydrogenase (EC 1.2.1.3).
52238	**-1,1206**	**0,00154**	Hypothetical Aromatic aminotransferase, expression is regulated by general control of amino acid biosynthesis, EC 2.6.1.57
54671	**-1,0711**	**0,0015437**	Choline phosphate cytidylyltransferase/Predicted CDP-ethanolamine synthase
48067	**-1,2344**	**0,0015437**	Hydroxyindole-O-methyltransferase and related SAM-dependent methyltransferases
39194	**-0,8269**	**0,001547**	Hypothetical protein kinase
53357	**-1,2222**	**0,001547**	Related to aldehyde dehydrogenase (EC 1.2.1.3). Sequence similarity to ALD2 of C. albicans
46346	**-1,1274**	**0,001547**	#N/A
185667	**-0,8399**	**0,0015534**	-
197060	**-0,9524**	**0,0015547**	Chitin synthase/hyaluronan synthase
129924	**-1,4226**	**0,0015595**	-
184622	**-0,903**	**0,0015595**	-
53140	**-1,4456**	**0,0015595**	FMN-dependent dehydrogenase
43347	**-1,1982**	**0,0015595**	Hypothetical Cytochrome P450 monooxygenase
179933	**-1,2893**	**0,0015719**	#N/A
135973	**-1,005**	**0,001574**	#N/A
35594	**-0,8095**	**0,001574**	#N/A
184233	**1,6902**	**0,0015946**	Amino acid/polyamine transporter
56583	**-0,8071**	**0,0015952**	candidate UDP-glucose 4-epimerase
170910	**-1,196**	**0,0015952**	Glucose/ribitol dehydrogenase

44305	**-0,9545**	**0,0016087**	-
55027	**-0,7703**	**0,0016129**	-
199208	**-0,8673**	**0,0016212**	Hypothetical cysteine peptidase, calpain like
214206	**-0,708**	**0,0016361**	Nucleoside transporter
47549	**-1,3926**	**0,0016388**	#N/A
208912	**-1,2417**	**0,0016564**	Hypothetical bisphosphate nucleotidase
46489	**-0,744**	**0,0016588**	-
171067	**-1,2342**	**0,0016588**	Zn-finger, GATA type
52442	**-0,6797**	**0,0016588**	AAA ATPase
40493	**-0,6387**	**0,001661**	-
194055	**-0,8272**	**0,0016646**	-
41754	**-1,335**	**0,0016818**	-
45282	**-1,0054**	**0,001684**	-
181252	**1,1182**	**0,001684**	#N/A
181362	**-0,7298**	**0,0016855**	#N/A
213350	**-1,13**	**0,0016903**	-
214348	**-0,9232**	**0,0016973**	Acyl-CoA synthetase
55742	**-1,2444**	**0,0016973**	aldA Aldehyde dehydrogenase (aldA) (EC 1.2.1.3)
189001	**-1,2494**	**0,0017046**	-
206445	**-2,8383**	**0,0017178**	hypothetical mixed-linked beta-glucanase
54207	**-1,261**	**0,0017209**	MaoC-like dehydratase
213237	**-1,1767**	**0,0017404**	-
42844	**-0,6886**	**0,0017404**	-
55818	**-1,2337**	**0,0017404**	Predicted inosine-uridine preferring nucleoside hydrolase
191446	**-0,841**	**0,0017424**	-
208123	**-1,0248**	**0,0017424**	Eukaryotic translation initiation factor
189170	**-0,9945**	**0,0017424**	Related to alpha keto acid dehydrogenase complex of Aspergillus fumigatus; EC 2.3.1.12
210233	**-1,5912**	**0,0017424**	#N/A
207011	**-0,6284**	**0,0017496**	Oxysterol-binding protein
214527	**-1,5307**	**0,0017656**	Dihydrodipicolinate synthetase family
141194	**-0,8874**	**0,0017855**	hypothetical protein; KOG Class: Chromatin structure and dynamics; KOG Id: 2510; KOG Description: SWI-SNF chromatin-remodeling complex protein
138062	**-0,6758**	**0,0017855**	hypothetical. Interpro suggests actin-binding, cofilin/tropomyosin type
214453	**-0,8591**	**0,0017855**	#N/A
197132	**-0,901**	**0,0017907**	-
54964	**-1,0778**	**0,0017934**	-
52011	**-3,5103**	**0,0017934**	candidate xyloglucanase
127809	**-0,8834**	**0,0017934**	hypothetical extracellular thaumatin domain protein

188346	**-0,9828**	**0,0017934**	Major facilitator superfamily
209490	**-1,0021**	**0,001797**	GH family 76
130000	**-2,6934**	**0,0018163**	Vacuolar sorting protein VPS1, dynamin, and related proteins
207088	**-0,9874**	**0,0018163**	AAA ATPase
206509	**-1,0786**	**0,0018212**	-
211780	**-0,7157**	**0,0018212**	-
118832	**-0,9125**	**0,0018212**	ABC transporter
214608	**-0,8422**	**0,0018212**	candidate endo-1,4-beta-glucanase; glucan 1,4-beta-glucosidase; glycoside hydrolase, family 5; cellulose-binding region, fungal
43768	**-0,9819**	**0,0018212**	Hypothetical peptidase M20 (based on PFAM information)
209881	**-1,0017**	**0,0018212**	hypothetical protein containing Zn-finger, C2H2 type domain
56776	**-1,418**	**0,0018212**	Predicted NAD-dependent oxidoreductase
211797	**1,5115**	**0,0018265**	Hypothetical aspartic protease
120053	**-1,0723**	**0,0018324**	Fungal specific transcription factor
177071	**-1,0443**	**0,0018511**	Permease of the major facilitator superfamily
126298	**-1,227**	**0,0018547**	Mitochondrial carrier protein
40855	**-0,7844**	**0,0018564**	Ribokinase
205842	**-0,9336**	**0,0018886**	contains WD40 repeats
211749	**-0,7297**	**0,0018908**	Mitochondrial solute carrier protein
57028	**-1,1087**	**0,0018935**	Aldehyde dehydrogenase
174927	**-0,5899**	**0,0018988**	-
54557	**-0,8674**	**0,0018988**	-
55445	**-0,6496**	**0,0018988**	-
39258	**-1,2187**	**0,0018988**	Phenazine biosynthesis PhzC/PhzF protein
206769	**-0,5389**	**0,0018988**	Predicted E3 ubiquitin ligase
55950	**-0,7648**	**0,0018988**	Related to mannose-1-phosphate guanyltransferase. [EC:2.7.7.13]
54934	**-0,8298**	**0,0018995**	-
194208	**-0,7271**	**0,0019067**	Molybdenum cofactor biosynthesis pathway protein
211951	**-0,619**	**0,0019106**	Phenylalanyl-tRNA synthetase, beta subunit archae/euk cytosolic
56576	**-0,9515**	**0,0019134**	Hypothetical glutamine synthase
54633	**-1,1043**	**0,0019181**	hypothetical protein containing Zn-finger, C2H2 type domain
197766	**-1,0318**	**0,0019193**	-
42403	**-0,9296**	**0,0019193**	#N/A
133377	**-0,6239**	**0,0019272**	-
36655	**-0,7572**	**0,0019272**	Hypothetical peptidase (EC 3.5.1.32)
187727	**-1,1472**	**0,0019272**	Hypothetical peptidase aspartic

55214	**-0,5999**	**0,0019272**	Hypothetical, related to kinesin
126639	**-3,3637**	**0,0019272**	Peptidase A4, scytalidopepsin B
50981	**-1,314**	**0,0019272**	putative AMP-dependent synthetase and ligase, Acyl-CoA synthetase
174644	**-1,0014**	**0,0019272**	Ubiquitin-conjugating enzymes
39108	**-0,8855**	**0,001933**	Predicted NUDIX hydrolase FGF-2 and related proteins
207862	**-0,6346**	**0,0019401**	This domain is found in a number of fungal transcription factors. The N-terminal region of a number of fungal transcriptional regulatory proteins contains a Cys-rich motif that is involved in zinc-dependent binding of DNA.
173627	**-0,9817**	**0,0019437**	HypB/UreG, nucleotide-binding
180295	**-0,7698**	**0,0019557**	FAD-dependent oxidoreductase
179916	**-0,8028**	**0,0019699**	-
45652	**-0,8843**	**0,0019935**	Hypothetical Short-chain dehydrogenase/reductase SDR
56247	**-1,219**	**0,0020021**	Phospholipase D. Active site motif
190025	**-1,0352**	**0,0020122**	Major facilitator superfamily
42914	**-0,8494**	**0,0020291**	#N/A
173536	**-1,5014**	**0,0020332**	Glutathione S-transferase
128537	**-0,6726**	**0,0020425**	putative allergen
55693	**-1,0133**	**0,0020469**	-
45989	**-1,6627**	**0,0020473**	hypothetical UDP-glucose 4-epimerase
56475	**-1,4988**	**0,0020564**	Aldo/keto reductase
176347	**-0,8948**	**0,0020564**	#N/A
178166	**-0,9126**	**0,0020584**	-
213288	**-0,9302**	**0,0020584**	-
213970	**-1,5485**	**0,0020584**	#N/A
125764	**-1,1619**	**0,0020655**	-
210048	**-0,9068**	**0,0020787**	-
37736	**-0,7384**	**0,0020787**	(aglA) alpha-galactosidase; extracellular
42642	**-0,6821**	**0,0020862**	Ketopantoate reductase
39069	**-0,5675**	**0,0021045**	-
127683	**-0,7429**	**0,0021045**	Flavoprotein
125584	**-1,1147**	**0,0021045**	hypothetical chitinosanase
137541	**-1,3914**	**0,0021045**	Hypothetical mitochondrial polypeptide chain release factor
205979	**-1,3701**	**0,0021045**	Serine/threonine protein kinase
175387	**-0,7973**	**0,0021084**	-
205376	**-1,0187**	**0,0021084**	-
47870	**-1,0368**	**0,0021084**	-
183042	**-0,8947**	**0,0021093**	-
46275	**-0,8386**	**0,0021093**	-

36773	**-0,9714**	**0,0021093**	Hypothetical enoyl-CoA hydratase. (EC 4.2.1.17) HMM predicts secretion.
199609	**-1,2739**	**0,0021093**	hypothetical protein containing fungal specific transcription factor and fungal transcriptional regulatory protein domains.
47417	**-1,2732**	**0,0021093**	Short-chain dehydrogenase/reductase
46527	**-0,8888**	**0,0021152**	-
207831	**-1,0246**	**0,0021152**	Glucose-methanol-choline oxidoreductase
208663	**-0,7177**	**0,0021229**	-
186253	**-1,2439**	**0,002137**	Predicted transporter (major facilitator superfamily)
131188	**-0,8572**	**0,0021418**	Glucose dehydrogenase/choline dehydrogenase/mandelonitrile lyase (GMC oxidoreductase family)
207187	**-0,8909**	**0,0021686**	hypothetical protein with predicted Appr-1-p domain; KOG Class: Chromatin structure and dynamics; KOG Id: 2633; KOG Description: Hismacro and SEC14 domain-containing proteins
207954	**-0,6501**	**0,0021731**	Spermidine synthase
186207	**-0,6387**	**0,0021788**	Fungal specific transcription factor
211346	**-0,9911**	**0,0021863**	-
48485	**-0,7569**	**0,0021863**	Hypothetical protein
42759	**-0,9889**	**0,0021968**	-
193155	**-1,3224**	**0,0021976**	Amino acid/polyamine transporter I
53896	**-0,6113**	**0,0022017**	ATP-NAD/AcoX kinase
200686	**-1,594**	**0,0022017**	Predicted transporter (major facilitator superfamily)
52517	**-0,8369**	**0,0022152**	Peptidase S10, serine carboxypeptidase
201388	**0,6244**	**0,0022187**	#N/A
52270	**-0,699**	**0,0022218**	#N/A
206457	**-0,7628**	**0,0022244**	-
52585	**-1,4113**	**0,0022364**	Ferric reductase, NADH/NADPH oxidase and related proteins
52452	**-1,0203**	**0,0022364**	hypothetical alpha-amylase; EC 3.2.1.1
212073	**-0,9408**	**0,0022364**	RHO protein GDP dissociation inhibitor
170152	**-1,0659**	**0,0022364**	Zinc-containing alcohol dehydrogenase superfamily
44373	**-1,0309**	**0,0022494**	Mitochondrial carnitine-acylcarnitine carrier protein
198730	**-0,9097**	**0,0022522**	Cell membrane glycoprotein
37942	**-0,9858**	**0,0022527**	Hypothetical Cytochrome P450 monooxygenase
37792	**-0,9933**	**0,0022669**	Haloacid dehalogenase-like hydrolase
51890	**-0,6875**	**0,0023016**	Candidate CotA
186329	**-0,8616**	**0,0023016**	Hypothetical P-type ATPase

202429	**-1,0932**	**0,0023125**	-
35701	**-0,5488**	**0,0023125**	-
210716	**-0,7944**	**0,0023125**	Glycoside hydrolase, family 5
53646	**-0,6951**	**0,0023316**	-
213911	**-1,4**	**0,0023316**	Aldehyde dehydrogenase
172145	**-0,712**	**0,0023316**	#N/A
209514	**-0,7002**	**0,0023423**	Myb, DNA-binding
208264	**-0,848**	**0,0023428**	#N/A
53541	**-3,3902**	**0,0023447**	-
178256	**-0,5953**	**0,0023857**	Related to histidine kinase
186514	**-0,6696**	**0,0023991**	Chitinase
52321	**-1,3669**	**0,0023994**	-
212320	**-0,6763**	**0,002409**	-
53582	**-1,2401**	**0,002409**	-
56296	**-1,1458**	**0,002409**	-
52389	**-1,5163**	**0,002409**	Chloroperoxidase
140623	**-0,6802**	**0,002409**	Cytochrome P450
46302	**-1,0368**	**0,002409**	Serine/threonine protein kinase
197391	**-1,3022**	**0,002409**	#N/A
49546	**-0,6352**	**0,0024094**	-
55501	**-0,7466**	**0,0024218**	Cytochrome P450
42514	**-0,7642**	**0,0024295**	-
181275	**-0,6585**	**0,0024295**	Related to E. nidulans 1-pyrroline-5-carboxylate dehydrogenase (prnC) (EC 1.5.1.12)
52880	**-0,7795**	**0,0024295**	Zn-finger (putative), N-recognin
197415	**-1,3124**	**0,0024314**	putative extracellular proteins sharing 38% amino acid sequence identity with Aspergillus oryzae glutaminase A (PMID: 10952006)
125323	**-2,9343**	**0,0024337**	-
174693	**-0,5986**	**0,0024356**	-
194639	**-2,4072**	**0,002437**	#N/A
43781	**-0,7221**	**0,0024426**	-
185434	**-0,7508**	**0,0024453**	short chain dehydrogenase
54693	**-1,0959**	**0,0024467**	-
38904	**-0,9079**	**0,0024467**	Hypothetical glyoxylase
194112	**-0,8248**	**0,0024566**	lipase essential for autophagy
53315	**-0,9775**	**0,0024824**	related to esterase D
48906	**-0,6809**	**0,0024958**	Hypothetical Cytochrome P450 monooxygenase
52058	**-1,2955**	**0,002507**	Putative Peptidase C1B, bleomycin hydrolases
184312	**-1,624**	**0,0025236**	Glutathione S-transferase
143320	**-0,6207**	**0,0025236**	Hypothetical inosine triphosphate pyrophosphatase
213634	**-0,7285**	**0,002528**	Vesicle coat complex AP-3, delta subunit
205426	**-0,5845**	**0,0025308**	Peptidase

201380	**-0,817**	**0,0025308**	peptidyl-prolyl cis-trans isomerase
36604	**1,3139**	**0,0025308**	There are no hits to identified proteins for this transcript. However, the PFAM indicase and signal peptide predictor indicates an extracellular amidase.
48950	**-0,8181**	**0,0025308**	AAA ATPase
209889	**-0,6227**	**0,0025592**	-
211909	**-0,7073**	**0,002566**	Hypothetical porphobilinogen deaminase
53784	**-0,9214**	**0,0025667**	Ras small GTPase, Rab type
201398	**-1,186**	**0,0025764**	-
43953	**-1,1461**	**0,0025919**	-
214840	**-0,6614**	**0,0026326**	-
127828	**-0,9885**	**0,0026507**	Microtubule-associated protein
214683	**-0,8156**	**0,0026715**	-
56468	**-0,6216**	**0,0026715**	-
194780	**-0,8542**	**0,0026843**	-
41013	**-0,8992**	**0,0026843**	-
55344	**-0,6644**	**0,0026843**	(kexB) proprotein convertase kexB
207169	**-0,5779**	**0,0026843**	Receptor-activated Ca2+-permeable cation channels
205848	**-0,7962**	**0,0026843**	Sulfate/bicarbonate/oxalate exchanger SAT-1 and related transporters (SLC26 family)
56084	**-0,9882**	**0,0026843**	#N/A
209754	**-1,1382**	**0,0026905**	2-nitropropane dioxygenase
205368	**-1,0269**	**0,0026905**	Peptidase
38920	**-1,0485**	**0,0027069**	-
175089	**-0,62**	**0,0027146**	NAD dependent epimerase
54959	**-0,7568**	**0,0027268**	Ubiquitin C-terminal hydrolase
42198	**1,3293**	**0,0027351**	-
40691	**-0,8491**	**0,0027365**	hypothetical Aflatoxin biosynthesis regulatory protein
44761	**-0,7249**	**0,0027494**	-
207660	**-0,6097**	**0,0027494**	Glycosyl transferase, family 48
50504	**-1,4373**	**0,0027494**	Hypothetical alcohol dehydrogenase NADP+ dependent; EC 1.1.1.2
173622	**0,8164**	**0,0027494**	#N/A
189708	**-0,8104**	**0,0027494**	#N/A
53361	**0,8935**	**0,0027494**	#N/A
181700	**-0,6327**	**0,0027616**	Hypothetical 26S proteasome, regulatory subunit
38529	**-1,2927**	**0,002762**	-
46227	**-0,755**	**0,002762**	-
55462	**-0,8901**	**0,002762**	-
210891	**-0,564**	**0,002762**	Amidase
171353	**-1,0057**	**0,002762**	bifunctional deaminase-reductase

39849	**-0,6445**	**0,002762**	Hypothetical Cytochrome P450 monooxygenase
52767	**-0,6754**	**0,002762**	Hypothetical transcription factor containing C2HC type Zn finger
213042	**-0,8182**	**0,002762**	MOSC N-terminal beta barrel domain
189358	**-0,6991**	**0,002762**	Putative hydrolase
137517	**-3,135**	**0,002762**	#N/A
44752	**-0,7445**	**0,0027678**	20S proteasome, regulatory subunit beta type PSMB6/PSMB9/PRE3
50161	**-2,1098**	**0,0027678**	endo-polygalacturonase D [Aspergillus niger, Glycoside hydrolase, family 28
37539	**-0,6658**	**0,0027713**	Related to norsolorinic acid reductase from Aspergillus fumigatus and Aspergillus flavus where it is part of the aflatoxin cluster
38926	**-0,9248**	**0,0027713**	Transcription coactivator
181306	**-0,6928**	**0,0027756**	Basic-leucine zipper (bZIP) transcription factor
197851	**-0,7417**	**0,0027756**	#N/A
193748	**-0,8322**	**0,0027758**	-
212529	**-0,6202**	**0,0027758**	-
120926	**-1,1317**	**0,0027758**	Acyltransferase ChoActase/COT/CPT
193657	**-0,9516**	**0,0027758**	Monocarboxylate transporter
42809	**-1,9307**	**0,0027758**	Thioredoxin
37857	**-0,8288**	**0,0027951**	Heat shock transcription factor
171156	**-0,6734**	**0,0028086**	-
40243	**-0,9721**	**0,0028086**	beta-1,6-N-acetylglucosaminyltransferase, contains WSC domain
128147	**-3,2321**	**0,0028418**	-
44729	**-1,328**	**0,0028418**	Zinc-containing alcohol dehydrogenase superfamily
37730	**-1,1783**	**0,0028509**	-
210724	**-1,2926**	**0,0028509**	GABA/amino acid permease
185118	**-0,8274**	**0,0028509**	Hypothetical N-acetyl transferase, specificity unknown
56336	**-0,7863**	**0,0028509**	Hypothetical peptidase, eukaryotic cysteine peptidase active site
54016	**-0,6458**	**0,0028633**	Hypothetical high-affinity nickel transport protein
199928	**-0,8953**	**0,0028703**	Predicted hydrolase
208525	**-1,1777**	**0,002873**	-
209558	**-0,8234**	**0,0028758**	Phosphoglucomutase/phosphomannomutase
188159	**-2,1548**	**0,0028841**	-
44778	**-0,9395**	**0,0028841**	-
201918	**-0,8299**	**0,0028841**	Synaptic vesicle protein Synapsin
209561	**-1,0804**	**0,0029106**	Fatty acid desaturase
53986	**-0,9223**	**0,0029303**	-
177731	**-0,7445**	**0,0029356**	Major facilitator superfamily

202592	**-0,8902**	**0,0029634**	Predicted gamma-butyrobetaine,2-oxoglutarate dioxygenase
48803	**-0,7258**	**0,0029688**	-
174013	**-4,0419**	**0,0029688**	#N/A
57332	**-0,6808**	**0,0029833**	Galactosyltransferases
124388	**-1,8082**	**0,0030053**	-
36035	**-1,413**	**0,0030058**	-
57320	**-0,6248**	**0,0030058**	Fungal specific transcription factor
207705	**-0,7653**	**0,0030058**	Hypothetical 26S proteasome, regulatory subunit
51199	**-1,1465**	**0,0030058**	UMUC-like DNA-repair protein
205254	**2,3822**	**0,0030137**	-
194806	**-0,8941**	**0,0030351**	Fungal specific transcription factor
47044	**-1,5983**	**0,0030692**	Dihydrodipicolinate synthetase family
214665	**-0,6528**	**0,0030692**	Hypothetical protease
190724	**-0,84**	**0,0030692**	Major facilitator superfamily
213466	**-0,7691**	**0,0030692**	Peptidase
214220	**-1,1573**	**0,0030927**	-
44916	**-0,9618**	**0,0030927**	candidate extracellular phospholipase C
51181	**-1,0721**	**0,0030927**	Cytochrome P450
40260	**-0,8159**	**0,0031008**	Major facilitator superfamily
126433	**-1,525**	**0,0031068**	-
214072	**-0,7597**	**0,0031068**	SCF ubiquitin ligase, Skp1 component
188504	**-0,7566**	**0,0031333**	Cytochrome P450
201083	**-0,5381**	**0,0031335**	Phosphatidylinositol transfer protein SEC14
42606	**-1,713**	**0,0031451**	Generic methyltransferase
120161	**-0,846**	**0,0031451**	May be involved in signal transduction
119885	**-0,7287**	**0,0031485**	Zn-finger, GATA type
42881	**-0,5716**	**0,0031627**	-
213485	**-0,5909**	**0,0031662**	Cytochrome c heme-binding site
205484	**-1,1514**	**0,0031735**	Acyl-CoA dehydrogenase
181136	**-0,6352**	**0,0031735**	Flavoprotein monooxygenase
212567	**-1,0646**	**0,0031735**	Hypothetical aldo/keto reductase
52981	**-0,8391**	**0,0031735**	Metacaspase involved in regulation of apoptosis
208631	**-1,2354**	**0,0031735**	Predicted pyroglutamyl peptidase
174876	**-0,8492**	**0,0031735**	#N/A
213266	**-0,54**	**0,0031769**	-
136694	**-0,6625**	**0,0031784**	Translin family protein
41997	**-0,9282**	**0,0031837**	-
53980	**-1,1507**	**0,0031837**	Amidohydrolase
50744	**1,411**	**0,0031837**	hypothetical glycosyl transferase family 2
46339	**-0,5987**	**0,0031843**	Predicted protein shares amino acid sequence identity to the Saccharomyces cerevisiae THG1 gene product
212624	**-0,6157**	**0,0031936**	-

188691	**-0,986**	**0,0031936**	Hypothetical protein of the glyoxalase family
55287	**-0,6739**	**0,0031936**	Metallophosphoesterase
55113	**-1,0588**	**0,0031936**	#N/A
56736	**-1,4467**	**0,0032042**	Haloacid dehalogenase-like hydrolase
209058	**-0,6306**	**0,0032063**	ATP sulfurylase
214710	**-0,7017**	**0,0032063**	Flavonol reductase/cinnamoyl-CoA reductase
53445	**-0,6122**	**0,0032075**	-
54556	**-0,9232**	**0,0032075**	-
206738	**-0,6142**	**0,003213**	Esterase/lipase/thioesterase
133728	**-1,0149**	**0,0032165**	-
199618	**-0,7128**	**0,0032165**	-
43656	**-0,7534**	**0,0032165**	-
128077	**-1,102**	**0,0032165**	Putative GH family 43
38818	**-0,8449**	**0,0032165**	Ras GTPase
56146	**-1,0891**	**0,0032397**	-
52857	**-0,8037**	**0,0032397**	NEDD8-activating complex, APP-BP1/UBA5 component
56049	**-0,5838**	**0,0032402**	Hypothetical proteasome
210265	**-0,974**	**0,0032602**	Molybdenum cofactor biosynthesis protein
45814	**1,1259**	**0,0032751**	-
53801	**-1,6003**	**0,0032753**	Hypothetical protein. HMMPfam indicates Glucose-methanol-choline oxidoreductase activity
179912	**0,9984**	**0,0032753**	putative extracellular carboxylesterase, type B
207418	**0,8049**	**0,0032753**	#N/A
53661	**2,7912**	**0,0033073**	-
52560	**1,8148**	**0,0033108**	-
47796	**-0,7082**	**0,0033108**	Haloacid dehalogenase-like hydrolase
182516	**-0,74**	**0,0033108**	#N/A
171254	**-0,6282**	**0,0033147**	-
211551	**-0,7902**	**0,0033147**	-
46405	**-1,2241**	**0,0033147**	-
55188	**-1,1487**	**0,0033147**	DP87 protein (prespore protein in Dichostelium)
42722	**-0,9201**	**0,0033147**	Major facilitator superfamily
206534	**-1,1549**	**0,0033147**	Zinc-binding oxidoreductase
44850	**-1,8917**	**0,0033147**	#N/A
38577	**-1,1573**	**0,003316**	Protein kinase
200187	**-0,8713**	**0,00332**	#N/A
55270	**-1,0374**	**0,0033225**	-
180930	**-0,7068**	**0,0033292**	-
46625	**-1,0511**	**0,0033292**	-
56711	**-1,8697**	**0,0033292**	-
53400	**-0,6903**	**0,0033292**	Peptidase
41151	**-0,6001**	**0,0033421**	Hypothetical prefoldin subunit
178388	**-0,6389**	**0,0033555**	Proteasome alpha-subunit

180928	**-1,995**	**0,0033649**	-
49276	**-0,5812**	**0,0033649**	-
52127	**-0,6563**	**0,0033649**	NSF attachment protein
42981	**-1,031**	**0,0033803**	Lanthionine synthetase C-like protein
38532	**-0,8654**	**0,0033973**	-
172390	**-0,5765**	**0,0034078**	Manganese and iron superoxide dismutase
53471	**-0,7219**	**0,0034137**	Fungal transcriptional regulatory protein
207027	**-1,1002**	**0,0034137**	Oxidoreductase, N-terminal
200914	**-0,5602**	**0,0034137**	Predicted GTPase-activating protein
143917	**-0,6848**	**0,0034137**	Upstream transcription factor
43447	**-1,2662**	**0,0034137**	Zinc-containing alcohol dehydrogenase superfamily
35560	**-0,5622**	**0,0034175**	Aromatic amino acid aminotransferase and related proteins
48814	**-1,378**	**0,0034243**	-
47045	**-0,8674**	**0,0034263**	-
36368	**-0,9527**	**0,0034279**	-
173896	**-0,9643**	**0,0034425**	-
197679	**-1,5007**	**0,0034425**	Amino acid/polyamine transporter
190580	**-0,6001**	**0,0034425**	Hypothetical protein prenyltransferase, alpha subunit
134398	**-0,5269**	**0,0034425**	putative GH family 43 protein with 47% sequence identity to an Aspergillus nidulans endo-arabinanase (PMID: 16844780)
37300	**-0,7405**	**0,0034694**	-
189922	**1,906**	**0,0034723**	Cytochrome P450
214598	**-1,7345**	**0,0034765**	extracellular GH family 28 endo-polygalacturonase A
139986	**-0,5596**	**0,0034765**	#N/A
214295	**-0,9544**	**0,0034836**	-
41505	**-0,6902**	**0,0034852**	Permease of the major facilitator superfamily
191956	**2,7101**	**0,0034862**	related to extracellular aspartic protease
186804	**-0,965**	**0,0034871**	-
211544	**-3,6936**	**0,0034871**	(aceA) acetylxylan esterase aceA
209506	**-0,6639**	**0,0035043**	hypothetical alkaline phosphatase
47819	**-1,023**	**0,0035167**	-
55656	**-0,7618**	**0,0035185**	-
44492	**-0,7684**	**0,0035328**	ABC transporter
51782	**-0,8388**	**0,0035591**	Hypothetical protein kinase
212996	**-0,9579**	**0,003561**	-
45662	**-0,5707**	**0,003561**	-
56395	**-1,062**	**0,003561**	2-nitropropane dioxygenase
212091	**-0,791**	**0,0035829**	-
213779	**-1,0934**	**0,0035829**	-

136079	**-0,5157**	**0,0035829**	Hypothetical mitochondrial substrate carrier
214619	**-0,5518**	**0,0035829**	Metallophosphoesterase
205168	**-1,0063**	**0,0036016**	Sulfatase
172413	**-0,7214**	**0,0036051**	-
206611	**-0,7979**	**0,0036115**	hypothetical Acyl-CoA-binding protein
52449	**-1,2098**	**0,0036241**	Candidate pH-response regulator protein pall
54114	**-0,6685**	**0,0036254**	RhoGEF domain
38742	**-0,7104**	**0,0036272**	TPR repeat-containing protein
187256	**-1,2444**	**0,0036466**	Hypothetical phosducin
135741	**-0,5825**	**0,0036878**	-
52079	**-1,3368**	**0,0036878**	-
195023	**-0,5559**	**0,0037001**	-
208879	**-1,0816**	**0,0037001**	Delta-1-pyrroline-5-carboxylate dehydrogenase
42031	**-1,3173**	**0,0037085**	-
207131	**-1,4187**	**0,0037085**	Nucleolar GTPase/ATPase p130
54797	**-0,5715**	**0,0037211**	Predicted proline-serine-threonine phosphatase-interacting protein
54922	**1,0351**	**0,0037464**	Putative alpha 1,2 mannosyltransferase
211010	**-0,6319**	**0,0037498**	Protein kinase
170954	**-0,7451**	**0,0037498**	Transcription factor, MADS-box
172075	**-0,9426**	**0,0037564**	Hypothetical enoyl-CoA hydratase (EC 4.2.1.17)
214715	**-1,0157**	**0,0037606**	Hypothetical protein. KOG suggests chitinase. SignalP suggests secretion
54860	**1,5191**	**0,0037615**	purine nucleoside permease
211472	**-0,8618**	**0,0037708**	Protein kinase
55007	**-1,0531**	**0,0037827**	related to 3-ketoacyl-CoA thiolase
44464	**-0,8338**	**0,0037866**	-
36645	**-3,9883**	**0,0037866**	NRPS
213663	**-0,7219**	**0,0037866**	Putative ubiquitin fusion degradation protein
45354	**-0,8338**	**0,0037899**	Rab6 GTPase activator
213941	**-0,7598**	**0,0038006**	-
43933	**-2,2337**	**0,0038006**	beta-1,6-N-acetylglucosaminyltransferase, contains WSC domain
44193	**-0,735**	**0,0038006**	hypothetical carboxylesterase
194765	**-3,0436**	**0,0038006**	putative GH family 61 endo-1,4-beta-glucanase
199253	**-1,0899**	**0,0038137**	-
41167	**-1,8736**	**0,0038197**	#N/A
136740	**-0,9427**	**0,0038339**	-
142689	**-1,8958**	**0,0039011**	-
37522	**-0,5478**	**0,003919**	Fungal specific transcription factor
57188	**-0,6424**	**0,0039242**	RNA polymerase
208344	**-1,3008**	**0,0039355**	Glycoside hydrolase, family 5
178171	**-0,8027**	**0,0039355**	Serine/threonine protein kinase
132708	**-0,5354**	**0,0039371**	-

45379	**-0,6684**	**0,0039505**	N-acetyltransferase
56196	**-0,7704**	**0,0039622**	related to Candida albicans aspartyl-tRNA synthase
57044	**-1,0851**	**0,0039738**	Hypothetical delta 1-pyrroline-5-carboxylate reductase
50833	**-0,823**	**0,0040168**	-
51373	**-0,672**	**0,0040168**	-
55860	**-1,3248**	**0,0040168**	-
56477	**-1,9493**	**0,0040168**	Epoxide hydrolase
209279	**-0,6313**	**0,0040168**	Fructose-2,6-bisphosphatase
56431	**-0,8117**	**0,0040168**	hypothetical galactokinase
45447	**-0,57**	**0,0040168**	Predicted E3 ubiquitin ligase
53077	**-0,6688**	**0,0040168**	Predicted L-carnitine dehydratase/alpha-methylacyl-CoA racemase
119642	**-0,7512**	**0,0040168**	Rho GTPase activator
132915	**-0,7655**	**0,0040526**	Major facilitator superfamily
42764	**-0,7202**	**0,0040539**	-
188553	**-0,7797**	**0,0040586**	Acyl-CoA dehydrogenase
46582	**-1,1408**	**0,0040586**	D-isomer specific 2-hydroxyacid dehydrogenase, NAD-binding
189002	**-2,247**	**0,0040649**	-
188611	**-0,6166**	**0,0040649**	Hypothetical gamma-cysteine synthetase subunit (EC 6.3.3.2).
170641	**-1,3934**	**0,0040649**	Hypothetical protein with HECT domain
174163	**0,7722**	**0,0040762**	-
53847	**-1,1633**	**0,0040762**	-
51410	**-0,518**	**0,0040762**	candidate a-L-rhamnosidase
119078	**-2,3321**	**0,0040762**	Hypothetical. KOG suggests involvement in RNA processing
190616	**-1,0167**	**0,0040762**	related to GH family 18 endo-chitinase
42657	**-0,7081**	**0,0040826**	-
189693	**-0,6001**	**0,0040863**	-
183753	**-1,3608**	**0,0040863**	Related to Hypocrea jecorina D-galacturonic acid reductase
214857	**-1,1464**	**0,0041009**	Pectinesterase
214897	**-0,947**	**0,0041259**	#N/A
41258	**-0,9452**	**0,0041334**	-
176142	**-0,5886**	**0,0041406**	1-aminocyclopropane-1-carboxylate synthase, and related proteins
125644	**-0,9171**	**0,0041406**	Short-chain dehydrogenase/reductase SDR
175122	**-0,6488**	**0,0041699**	-
46500	**-1,1676**	**0,0041699**	-
187227	**-1,1972**	**0,0041699**	(galA) beta-1,4-endogalactanase A
41815	**-1,0528**	**0,0041699**	(pelA) extracellular pectin lyase A
54678	**-0,9135**	**0,0041699**	Hypothetical heterokaryon incompatibility factor

57294	**-0,7085**	**0,0041704**	glycyl-tRNA synthase
41430	**2,8247**	**0,004185**	-
200255	**-0,657**	**0,0042071**	Hypothetical cation efflux protein
45037	**-0,6267**	**0,0042071**	Major facilitator superfamily
49866	**-0,5966**	**0,0042386**	-
38851	**-1,1697**	**0,0042386**	homogentisate 1,2-dioxygenase
184740	**-0,948**	**0,0042386**	Transcription elongation factor
204035	**-1,2105**	**0,0042396**	Hypothetical monooxygenase. Possible steroid monooxygenase or involved in K+ transport
49232	**-0,9541**	**0,0042405**	-
136394	**-0,5019**	**0,0042405**	#N/A
213766	**-0,749**	**0,0042573**	-
55928	**-1,3539**	**0,0042573**	#N/A
53826	**-0,5485**	**0,0042634**	Glycosyl transferase, family 15
174948	**-1,0425**	**0,0042659**	hypothetical fumarylacetoacetate hydrolase
53301	**-0,8501**	**0,0042741**	-
45320	**-0,7278**	**0,0042826**	-
52154	**1,4057**	**0,004285**	-
41270	**0,9158**	**0,0043099**	hypothetical aspartic protease
54386	**-0,8952**	**0,0043117**	6-phosphogluconate dehydrogenase
40713	**-0,491**	**0,0043151**	Protein kinase
40127	**-0,6177**	**0,004341**	Siroheme synthase
46361	**-3,3564**	**0,0043498**	-
56954	**-0,5602**	**0,0043552**	-
54756	**-0,6014**	**0,0043552**	Sortilin and related receptors
52373	**-0,4853**	**0,0043552**	#N/A
45562	**-0,7962**	**0,0043558**	-
48160	**-1,1985**	**0,0043742**	Hypothetical protein. HMMPfam indicates Acyl-CoA dehydrogenase activity.
171346	**-0,974**	**0,0043811**	-
211565	**-0,7415**	**0,0043811**	extracellular serine protease
141709	**-0,9646**	**0,0043835**	-
179322	**-0,6297**	**0,004388**	Hypothetical protein
208713	**-0,7265**	**0,0043999**	-
52158	**-0,8142**	**0,0043999**	-
55331	**-0,674**	**0,0043999**	Hypothetical. Some relation to Zn-dependent hydrolase/beta-lactamase
204317	**1,6343**	**0,0043999**	Vacuolar H+-ATPase V0 sector, subunits
174315	**-1,3737**	**0,0044212**	-
175036	**-0,7362**	**0,0044212**	-
184563	**-0,8599**	**0,0044212**	-
186792	**-0,9048**	**0,0044212**	-
189463	**-0,8196**	**0,0044212**	-
208069	**-1,2435**	**0,0044212**	-

53410	**-0,5532**	**0,0044212**	-
53658	**-0,797**	**0,0044212**	-
202668	**-1,7024**	**0,0044212**	Glucose/ribitol dehydrogenase
191577	**-1,008**	**0,0044212**	Hypothetical metal dependent terpene synthase
175881	**-0,9593**	**0,0044212**	Hypothetical peptidase
55116	**-0,8236**	**0,0044212**	hypothetical short chain dehydrogenase
205594	**-1,1058**	**0,0044212**	hypothetical. Methionyl aminopeptidase
208685	**2,9733**	**0,0044212**	Phosphoenolpyruvate carboxykinase, N-terminal,
46333	**-0,5152**	**0,0044212**	RNA polymerase II transcription initiation factor TFIIA
205870	**-0,7886**	**0,0044232**	Ubiquitin-conjugating enzyme
40065	**-1,1921**	**0,0044399**	-
181376	**-0,7272**	**0,0044456**	Ferric reductase-like transmembrane component
205518	**1,8694**	**0,0044601**	NADH-dehydrogenase (ubiquinone)
55563	**-0,7056**	**0,0044749**	Uricase (urate oxidase)
129126	**-0,6409**	**0,0044919**	Notchless-like WD40 repeat-containing protein
119984	**3,5353**	**0,0045105**	Hypothetical Potassium transport protein, high-affinity
128744	**-1,1045**	**0,0045126**	-
170134	**-0,7218**	**0,0045126**	-
205095	**-0,9479**	**0,0045178**	Short-chain dehydrogenase/reductase
128404	**-0,5809**	**0,0045187**	-
55683	**-0,7**	**0,0045187**	Glycoside hydrolase, family 47
45912	**-0,7821**	**0,0045282**	FMN-dependent alpha-hydroxy acid dehydrogenase
53797	**-1,6031**	**0,0045282**	related to endoglucanase of Trichoderma reesei; glucan 1,4-beta-glucosidase; cellulose-binding region; glycoside hydrolase, family 61
52211	**-1,1417**	**0,00455**	Hypothetical hydrolase related to dienelactone hydrolase
174873	**-0,7493**	**0,00455**	Hypothetical N-acetyltransferase according to PFam. No supporting sequence information
56053	**1,7904**	**0,00455**	#N/A
137221	**-0,7766**	**0,0045572**	Cytosine deaminase FCY1 and related enzymes
39560	**-0,7485**	**0,0045641**	-
50997	**-0,9654**	**0,0045641**	putative extracellular GH family 3 beta-glucosidase
56252	**-0,7186**	**0,0045942**	Proteasome alpha-subunit
191077	**-0,7243**	**0,0045966**	-
176076	**0,6476**	**0,0046206**	Major facilitator superfamily
129525	**-0,8156**	**0,0046206**	Predicted DHHC-type Zn-finger protein
53173	**1,2808**	**0,004621**	#N/A
194179	**-0,6582**	**0,0046566**	Flavoprotein monooxygenase
48631	**-1,1645**	**0,0046673**	-
51325	**1,0218**	**0,0046739**	Aldehyde dehydrogenase

40514	**-0,4936**	**0,0046777**	Major facilitator superfamily
56457	**-1,0833**	**0,0046856**	(cmkB) calcium/calmodulin dependent protein kinase B - high homology to cmkB in A. nidulans
46255	**-0,9603**	**0,0046878**	Glycoside hydrolase, family 28 (Polygalacturonase)
56409	**-1,1337**	**0,0046878**	Predicted H+-transporting two-sector ATPase, alpha/beta subunit, central region
181057	**-1,2239**	**0,0046959**	-
46629	**-0,6927**	**0,0047214**	-
40623	**-0,6282**	**0,0047214**	#N/A
52460	**-0,5301**	**0,004725**	-
39638	**-0,5773**	**0,004725**	Autophagy protein Apg5
42464	**-1,075**	**0,004725**	candidate Peptidyl-prolyl cis-trans isomerase
180885	**-0,8774**	**0,004725**	Fungal transcriptional regulatory protein
209924	**-0,8188**	**0,004725**	Purine phosphorylase, family 2
187263	**-0,6781**	**0,0047423**	-
55720	**-0,6213**	**0,0047423**	Nonaspanin
48688	**-0,7998**	**0,0047586**	adenosylmethionine-8-amino-7-oxononanoate transaminase
51819	**-0,648**	**0,0047586**	Hypothetical threonyl-tRNA synthetase kinase. HMMPfam indicates Threonyl-tRNA synthetase kinase activity
44861	**-1,7735**	**0,0047586**	#N/A
55956	**-0,7148**	**0,0047635**	Hypothetical subunit of the 26S proteasome regulatory complex
53311	**-0,5859**	**0,0047881**	Longin-like
198787	**-0,5174**	**0,0048044**	-
134257	**-0,5474**	**0,0048087**	-
185810	**-1,3334**	**0,0048087**	-
53655	**-0,5067**	**0,0048087**	-
142899	**1,8789**	**0,0048087**	Protein kinase
56179	**-0,7441**	**0,0048087**	Tyrosine specific protein phosphatase and dual specificity protein phosphatase
38832	**-1,5111**	**0,0048205**	Cytochrome P450
214748	**-1,1161**	**0,0048375**	Acyl-CoA synthetase
55055	**-0,6173**	**0,0048375**	hypothetical protein containing Zn-finger, C2H2 type domain
54843	**-0,6153**	**0,0048375**	Iron/ascorbate family oxidoreductases
53788	**-0,8636**	**0,0048375**	Nucleoside phosphatase
183549	**-0,5135**	**0,0048375**	prolyl-4-hydroxylase
176378	**-0,9492**	**0,0048375**	Short-chain dehydrogenase/reductase
39817	**-1,0966**	**0,0048429**	Hypothetical glutathione-dependent formaldehyde-activating protein
54297	**-1,0741**	**0,0048626**	Predicted L-carnitine dehydratase/alpha-methylacyl-CoA racemase

46707	**-0,6541**	**0,0048626**	TPR Domain
205639	**-0,7161**	**0,0048644**	candidate dihydroorotase/amidohydrolase
209032	**-1,0611**	**0,0048803**	-
142669	**0,5447**	**0,0048845**	#N/A
205050	**-0,5611**	**0,0049154**	Hypothetical thioredoxin-related
55179	**-1,6838**	**0,0049253**	-
188319	**-0,5604**	**0,0049295**	-
214667	**-0,9772**	**0,0049295**	Hypothetical Xanthine dehydrogenase
50148	**4,1793**	**0,0049426**	-
54208	**-0,6099**	**0,0049439**	AAA ATPase
49455	**-0,5558**	**0,0049759**	-
124618	**-1,3751**	**0,0049787**	hypothetical. KOG suggests PHD finger protein AF10
40158	**-0,6075**	**0,0049794**	Cytochrome P450
50197	**-0,8643**	**0,0049794**	Hypothetical protein. PFam suggests a Enoyl-CoA hydratase/isomerase function
182870	**-0,745**	**0,0049794**	Related to A. fumigatus N,N-dimethylglycine oxidase (EC 1.5.99.2)
171548	**-0,7896**	**0,0049794**	#N/A
39105	**2,2532**	**0,0050074**	-
210445	**-1,0235**	**0,0050315**	Cytochrome P450
51764	**-0,604**	**0,0050347**	Glycosyl hydrolases family 35
183029	**-0,6516**	**0,0050556**	Candidate Two-component system protein A
55419	**-0,8242**	**0,0050561**	Hypothetical glycosyl hydrolase (GH family 31)
210364	**1,1015**	**0,0050608**	-
124897	**-0,5373**	**0,0050608**	Golgi reassembly stacking protein GRASP65, contains PDZ domain
53364	**-0,7368**	**0,0050608**	related to aspartic protease
191241	**-0,6033**	**0,0050723**	#N/A
49311	**-1,4533**	**0,0050786**	Hypothetical, similarities to sialidase superfamily
175603	**-0,6945**	**0,0050807**	von Willebrand factor and related coagulation proteins
51997	**-0,8806**	**0,005142**	(xyrA) D-xylose reductase xyrA whose expression requires the xylanolytic transcriptional activator XlnR; involved in pentose and glucuronate interconversions
54362	**-0,6415**	**0,005142**	Cytoplasmic tryptophanyl-tRNA synthetase
40460	**-0,8691**	**0,0051516**	FAD-dependent oxidoreductase
194595	**-0,9153**	**0,0051516**	Flavonol reductase/cinnamoyl-CoA reductase
41165	**-0,8733**	**0,0051779**	putative GH family 16 GPI_glucanosyltransferase
133565	**-0,6954**	**0,0051782**	-
210777	**-0,8562**	**0,0051782**	-
196476	**-0,7734**	**0,0051782**	Phospho-2-dehydro-3-deoxyheptonate aldolase

214740	**-0,9036**	**0,0051782**	Predicted transporter (major facilitator superfamily)
213358	**-0,9938**	**0,0052053**	Fungal specific transcription factor
207331	**-0,6038**	**0,0052053**	Inorganic pyrophosphatase
177723	**-0,5664**	**0,0052067**	-
57073	**-0,6952**	**0,0052173**	proteasome beta-subunit
190247	**-0,8323**	**0,0052205**	SWAP mRNA splicing regulator
55566	**1,3414**	**0,0052311**	Hydroxymethylglutaryl-coenzyme A synthase
171186	**2,6632**	**0,0052429**	-
174230	**-0,5671**	**0,0052512**	-
192625	**-0,5521**	**0,0052512**	-
203267	**-0,9882**	**0,0052512**	-
199777	**-0,7915**	**0,0052512**	Hypothetical ERG4/ERG24 ergosterol biosynthesis protein
212363	**-0,6677**	**0,0052512**	Protein kinase
182955	**-1,0191**	**0,0052536**	-
52947	**-0,6107**	**0,0052564**	Peptidase C19
171092	**-0,7353**	**0,0052616**	Monooxygenase involved in coenzyme Q (ubiquinone) biosynthesis
189022	**-2,293**	**0,0052659**	-
54972	**-0,6167**	**0,0052659**	FAD binding domain
188323	**-0,5797**	**0,0052659**	Fungal specific transcription factor
170119	**-1,0277**	**0,0052659**	Pyridoxal-dependent decarboxylase
37789	**-0,7232**	**0,0052659**	Shares amino acid sequence identity with Saccharomyces cerevisiae GCD1 gene product comprising the gamma subunit of the translation initiation factor eIF2B; the guanine-nucleotide exchange factor for eIF2; activity subsequently regulated by phosphorylated eIF2.
171717	**-0,5711**	**0,0052689**	-
38591	**-0,5547**	**0,0053054**	GCN5-related N-acetyltransferase
180348	**-1,0879**	**0,0053054**	Peptidase S26
46653	**-0,7384**	**0,0053066**	-
52393	**-0,585**	**0,0053222**	Nucleolar GTPase/ATPase p130
135002	**-0,6677**	**0,0053924**	#N/A
182617	**1,6954**	**0,0054272**	Hypothetical secreted iron permease
206645	**-0,5415**	**0,0054272**	related to phosphatidylinositol/phosphatidylglycerol transfer protein
177953	**-0,6721**	**0,0054388**	Hypothetical Zn finger protein with RING domain
55590	**-0,9353**	**0,0054567**	Phosphoglucomutase (Glucose phosphomutase) (PGM)
56312	**-0,744**	**0,005502**	-
43345	**-0,6204**	**0,005506**	Amino acid transporter

201345	**-0,9639**	**0,005506**	#N/A
187292	**-1,1081**	**0,0055576**	Alcohol dehydrogenase
208484	**-0,6557**	**0,0055715**	Signal transduction
56295	**-0,5378**	**0,0055753**	Nuclear export receptor CSE1/CAS (importin beta superfamily)
122575	**-0,5685**	**0,0055923**	-
210814	**-0,4939**	**0,0055923**	Ras-related small GTPase
38924	**-0,5278**	**0,0055923**	#N/A
185464	**-0,5832**	**0,0055941**	DnaJ domain protein
41379	**-0,8464**	**0,0055941**	Fungal transcriptional regulatory protein, N-terminal
205670	**-0,5415**	**0,0055941**	Glycoside hydrolase, family 3
47481	**-0,7029**	**0,0055941**	Protein phosphatase 2C-like
53002	**-0,5219**	**0,005595**	-
214216	**-0,5036**	**0,0056325**	Calmodulin
185606	**-0,7597**	**0,0056384**	-
187028	**-0,5634**	**0,0056384**	-
181153	**-0,5616**	**0,0056409**	-
55604	**-0,5281**	**0,0056409**	-
52783	**-0,7582**	**0,0056409**	Alternative splicing factor SRp55/B52/SRp75 (RRM superfamily)
197480	**-1,2537**	**0,0056409**	Enoyl-CoA hydratase/isomerase
47372	**-1,0828**	**0,0056409**	Peroxidase
37330	**-0,6046**	**0,005646**	-
210842	**-1,399**	**0,0056691**	Cytochrome c heme-binding site
206441	**-3,5891**	**0,0056859**	-
213559	**-0,8479**	**0,0056859**	Arginase/agmatinase/formiminoglutamase
211423	**-0,5021**	**0,0057061**	Actin-related protein
52219	**-1,0389**	**0,005708**	Glycoside hydrolase, family 28
53423	**-1,0196**	**0,005708**	Related to 2-methylcitrate dehydratase of E. coli
55451	**-0,7605**	**0,0057215**	-
207206	**-0,5047**	**0,0057404**	Glycosyl transferase, family 15
51725	**-0,6975**	**0,0057412**	-
45820	**-0,6469**	**0,0057445**	-
51788	**-0,8028**	**0,0057445**	hypothetical protein containing basic-leucine zipper transcription factor domain
180458	**-0,9144**	**0,0057546**	Acetamidase/Formamidase
123165	**-0,6458**	**0,0057546**	Predicted GTP-binding protein
128584	**-1,2566**	**0,0057548**	Non-ribosomal peptide synthetase
53643	**-0,6854**	**0,0057712**	-
182079	**-0,6444**	**0,0057712**	Hypothetical exocyst complex subunit
190033	**-0,9961**	**0,0057712**	putative proline racemase
185579	**-0,6526**	**0,0057874**	-

41345	**-0,8853**	**0,005815**	Peptidase C19, ubiquitin carboxyl-terminal hydrolase 2
197381	**-0,6426**	**0,0058252**	GTPase Rab5/YPT51 and related small G protein superfamily GTPases
179341	**-0,5479**	**0,0058402**	Myb, DNA-binding
37006	**-0,4889**	**0,0058402**	Transferrin receptor and related proteins containing the protease-associated (PA) domain
50998	**-0,712**	**0,0058421**	-
130480	**-0,4708**	**0,0058421**	Predicted RNA binding protein, contains G-patch domain
40780	**-0,6297**	**0,0058621**	-
122901	**-0,6463**	**0,0058669**	#N/A
211517	**1,3517**	**0,0058953**	-
55261	**-0,9446**	**0,0058953**	-
54616	**0,6509**	**0,0058953**	Acetolactate synthase, small subunit
181472	**-0,8846**	**0,0058953**	ER lumen protein retaining receptor
190726	**-0,5129**	**0,0059192**	-
181105	**-0,5317**	**0,0059234**	#N/A
194346	**-0,7141**	**0,0059252**	Esterase/lipase/thioesterase
172633	**-1,1176**	**0,0059295**	-
192901	**-0,6422**	**0,0059398**	-
51753	**-2,4705**	**0,0059398**	-
55813	**-0,5627**	**0,0059543**	hypothetical protein with predicted SH3 domain
214467	**-0,4911**	**0,0059671**	Major facilitator superfamily
193941	**-0,5713**	**0,0059671**	#N/A
54609	**-0,6527**	**0,0059752**	20S proteasome subunits
213343	**0,8235**	**0,0059752**	Predicted 3-hydroxy-3-methylglutaryl-CoA (HMG-CoA) reductase
55163	**-0,665**	**0,0059752**	Zn-finger-like, PHD finger
176418	**-0,9324**	**0,0059794**	-
207067	**0,8965**	**0,0059794**	HAD-superfamily hydrolase,
55077	**-1,034**	**0,0059889**	DNA-binding protein of the nucleobindin family
204025	**-0,608**	**0,0059889**	hypothetical methyl transferase
38054	**-1,2634**	**0,0059889**	Hypothetical Short-chain dehydrogenase/reductase SDR
47390	**-0,7867**	**0,0060096**	-
208716	**-0,7557**	**0,0060096**	Fungal specific transcription factor
203770	**-0,7529**	**0,0060096**	Protein kinase
52816	**-0,7299**	**0,006013**	-
182803	**-0,8504**	**0,006013**	#N/A
206228	**-0,5719**	**0,0060524**	Hypothetical Molecular chaperone (DnaJ superfamily
184329	**-4,4142**	**0,0060524**	putative alkaline lipase
53037	**-0,4966**	**0,0061136**	HEAT repeat-containing protein

48541	**-0,6794**	**0,0061136**	Peptidase S15
128173	**-0,4647**	**0,0061138**	Longin-like
192821	**-0,6614**	**0,0061279**	Helicase-like transcription factor HLTF/DNA helicase RAD5, DEAD-box superfamily
53563	**-0,9755**	**0,0061279**	Mandelate racemase/muconate lactonizing enzyme
188620	**1,284**	**0,006135**	Cation transporting ATPase
194086	**-0,7495**	**0,0061658**	Major facilitator superfamily
209864	**-0,6458**	**0,0061865**	Amidohydrolase 2
40370	**-0,5733**	**0,0061866**	Candidate Calcineurin subint B
180990	**-1,1492**	**0,0061906**	Zinc-binding oxidoreductase
54001	**0,8948**	**0,0062102**	putative Hsp60
47182	**-0,5076**	**0,0062135**	-
47464	**-0,5461**	**0,0062643**	Protein of unknown function DUF6
188492	**-0,6948**	**0,0062655**	Hypothetical RTA1 like protein, mb bound
131431	**-0,4952**	**0,0062655**	Hypothetical. Flavoprotein monooxygenase domain
182968	**-0,503**	**0,0062655**	Possibly related to mitotic and DNA damage checkpoint protein hus
55487	**-0,572**	**0,0063081**	-
57159	**-0,5134**	**0,0063081**	-
185327	**5,4786**	**0,0063081**	Cation transporting ATPase
125768	**-0,5093**	**0,0063081**	Heat shock protein DnaJ
176795	**-0,9376**	**0,0063081**	hypothetical phenylalanine ammonia-lyase
206384	**-1,655**	**0,0063081**	related to aspartic protease
56891	**-0,6041**	**0,0063081**	Shares amino acid sequence identity to Saccharomyces cerevisiae GUS1 gene product comprising a glutamyl-tRNA synthetase (GluRS); forms a complex with methionyl-tRNA synthetase (Mes1p) and Arc1p; complex formation increases the catalytic efficiency of both tRNA synthetases and ensures their correct localization to the cytoplasm.
52040	**-0,815**	**0,0063636**	#N/A
205005	**-1,2836**	**0,0063787**	putative soluble Fumarate reductase/succinate dehydrogenase flavoprotein, N-terminal
37178	**-0,6474**	**0,0063801**	Serine/threonine protein kinase
40948	**-0,6777**	**0,006389**	#N/A
43980	**-0,804**	**0,0064053**	-
38344	**-0,466**	**0,0064053**	hypothetical protein; KOG Class: Chromatin structure and dynamics
54157	**-0,4502**	**0,0064053**	Hypothetical. CREBB binding
52303	**-0,6893**	**0,0065252**	-
56726	**-0,5721**	**0,0065252**	(pyrG) Orotidine 5'-phosphate decarboxylase

37029	**-0,6018**	**0,0065252**	Ferric reductase like transmembrane component
210303	**-0,426**	**0,0065252**	Hypothetical amino acyl-tRNA synthetase complex component.
175181	**-0,7784**	**0,0065252**	Phox-like
120043	**-0,604**	**0,0065252**	RNA-binding protein RBM5 and related proteins, contain G-patch and RRM domains
170627	**-1,0705**	**0,0065503**	-
205396	**-0,5778**	**0,0065503**	-
205517	**-1,0471**	**0,0065503**	msdS, alpha-1,2-mannosidase S
55133	**2,7742**	**0,0065503**	related to extracellular serine protease
45118	**-0,7935**	**0,0065503**	#N/A
119977	**-0,8186**	**0,0065745**	Fungal specific transcription factor
56172	**2,6481**	**0,0065745**	putative GH family 16 GPI-glucanosyltransferase
209331	**-0,5921**	**0,0065954**	-
42277	**-0,5781**	**0,0066072**	-
51602	**-0,5005**	**0,0066072**	-
201939	**-0,9328**	**0,0066072**	Phospholipase/carboxyhydrolase
171965	**-1,8348**	**0,0066072**	#N/A
52126	**-0,5487**	**0,0066359**	Hypothetical endoglucanase
206983	**-0,6927**	**0,0066643**	-
48679	**-0,5315**	**0,0066721**	Glutamine synthetase
211162	**-1,4347**	**0,0067278**	Hypothetical 1,4-alpha-glucan branching enzyme
36285	**-1,0143**	**0,0067369**	-
46681	**-0,5174**	**0,0067369**	#N/A
50676	**-0,5402**	**0,0067706**	putative Inositol polyphosphate related phosphatase
181005	**-0,4442**	**0,0068398**	-
53717	**-0,5125**	**0,0068398**	AAA ATPase
53770	**-0,6135**	**0,0068404**	hypothetical GPI anchor protein
192370	**-0,7121**	**0,0068451**	-
212750	**-0,5665**	**0,0068748**	FAD binding domain
54874	**-0,7326**	**0,0068776**	Predicted oxidoreductase
124587	**-0,5196**	**0,0068776**	#N/A
57344	**-0,5361**	**0,0068977**	Protein prenyltransferase, alpha subunit
207326	**-0,7774**	**0,0069256**	-
209711	**-0,6138**	**0,0069256**	-
47560	**-0,6119**	**0,0069256**	hypothetical protein containing helix-turn-helix, AraC type domain
53811	**-0,6679**	**0,0069256**	Related to profilin an actin bindin protein involved in cytoskeleton dynamics
50166	**-0,7771**	**0,0069334**	Hypothetical glutathione synthase (EC 6.3.2.3). Shows some similarities with S. pombe glutathione synthase
204569	**-0,4637**	**0,0069584**	-

40157	**-0,6081**	**0,0069627**	-
47085	**-0,5502**	**0,0069627**	Hypothetical H+-transporting two-sector ATPase
212664	**1,2164**	**0,0069627**	hypothetical lipase
54513	**-0,5598**	**0,0069627**	hypothetical protein; KOG Class: Chromatin structure and dynamics; KOG Id: 1973; KOG description: Chromatin remodeling protein, contains PHD Zn-finger
185272	**-0,7765**	**0,0069807**	-
51955	**0,4201**	**0,0069807**	-
200205	**-0,5063**	**0,0069902**	-
52144	**-0,5938**	**0,0069923**	Vacuolar H+-ATPase V1 sector
35601	**-0,5423**	**0,0069935**	-
41811	**-0,6364**	**0,0069935**	Molybdopterin synthase sulfurylase
185165	**-0,6488**	**0,0069935**	#N/A
36404	**1,1043**	**0,0069949**	FAD linked oxidase, N-terminal
119946	**-0,7891**	**0,0069949**	AAA ATPase
43321	**0,4527**	**0,0070168**	-
54419	**-0,6704**	**0,0070168**	-
53033	**-1,8503**	**0,0070233**	related to beta-1,3-glucanosyltransferase
57185	**-0,6019**	**0,0070434**	Inositol polyphosphate related phosphatase
54605	**-0,5501**	**0,0071153**	Predicted Zn2+-dependent endopeptidase, insulinase superfamily
195172	**-0,5873**	**0,007133**	hypothetical. N-acetyltransferase activity
40332	**-0,5209**	**0,007133**	MED6 mediator
120082	**-0,6091**	**0,0071455**	Predicted hydrolase involved in interstrand cross-link repair
186700	**-0,6776**	**0,0071535**	-
174666	**-0,7733**	**0,0071566**	-
48560	**-0,8394**	**0,0071566**	Glutathione S-transferase
194526	**-1,3145**	**0,0071566**	putative extracellular HpcH/HpaI aldolase
189790	**1,3168**	**0,0071871**	-
125418	**-0,6785**	**0,0071891**	Short-chain dehydrogenase/reductase SDR
129181	**-0,5822**	**0,0072055**	-
45922	**-2,9747**	**0,0072055**	#N/A
56436	**-0,4712**	**0,0072071**	-
52600	**-0,475**	**0,0072071**	Glutamate decarboxylase
56841	**-0,7218**	**0,0072071**	putative transmembrane GH family 47 mannosyl-oligosaccharide 1,2-alpha-mannosidase
39893	**-0,561**	**0,0072123**	Synaptic vesicle transporter SVOP
212581	**1,0109**	**0,0072426**	Acetohydroxy acid isomeroreductase
209267	**-0,4727**	**0,0072426**	Cytochrome P450
50131	**-0,9279**	**0,0072839**	hypothetical Pyridoxal-5'-phosphate-dependent enzyme, beta subunit

137287	**-0,7841**	**0,007287**	hypothetical. KOG: beta-1,6-N-acetylglucosaminyltransferase
190335	**-0,6766**	**0,0073017**	Protein kinase
52888	**-0,9312**	**0,0073287**	-
48610	**-0,6223**	**0,0073288**	-
50097	**-0,6866**	**0,0073459**	-
51886	**-0,6473**	**0,0073504**	Anthranilate phosphoribosyltransferease, trp biosynthesis, EC 2.4.2.18
37620	**-0,7892**	**0,0073504**	gdhB, NAD dependent glutamate dehydrogenase
121995	**-0,5555**	**0,0073669**	-
121337	**-1,0172**	**0,0073747**	#N/A
42065	**-0,47**	**0,0073764**	-
56242	**-0,6553**	**0,0074052**	-
180608	**-0,8151**	**0,0074186**	-
198250	**-1,0171**	**0,0074186**	2-enoyl-CoA hydratase/3-hydroxyacyl-CoA dehydrogenase/Peroxisomal 3-ketoacyl-CoA-thiolase, sterol-binding domain and related enzymes
46134	**-0,5068**	**0,0074186**	FAD-linked oxidase
194896	**-0,4742**	**0,0074186**	hypothetical amine oxidase
207264	**-1,71**	**0,0074253**	Glycoside hydrolase, family 27
38247	**-0,5221**	**0,0074253**	#N/A
41296	**-0,46**	**0,0074263**	#N/A
124139	**-0,5027**	**0,0074476**	-
57046	**-1,1478**	**0,0074476**	Aldehyde dehydrogenase
213618	**-0,6878**	**0,0074476**	Exocyst subunit - Sec10p
194124	**-0,685**	**0,0074515**	#N/A
179980	**-0,8632**	**0,0074693**	Hypothetical methyltransferase
192380	**-0,6772**	**0,0074854**	-
55148	**-0,5393**	**0,0074854**	-
43726	**0,7066**	**0,0075049**	-
172191	**-0,3992**	**0,0075163**	-
208486	**-0,5523**	**0,0075241**	Peptidase S10
193498	**-0,463**	**0,0075446**	Hypothetical SNARE protein TLG2/Syntaxin 16
40901	**-0,535**	**0,0075446**	Zinc finger protein
189722	**-0,6908**	**0,0075831**	(rghA) extracellular GH family 28 endo-rhamnogalacturonase A
37921	**-0,5934**	**0,007615**	-
53297	**-0,5283**	**0,0076171**	-
134276	**-1,2218**	**0,0076171**	FOG: RRM domain
51860	**-0,478**	**0,0076171**	#N/A
188673	**-0,6714**	**0,0076331**	AMP-dependent synthetase and ligase
192610	**-0,5259**	**0,0076351**	putative cellobiose dehydrogenase (cd00241)
143487	**-0,7649**	**0,0076351**	Serine/threonine protein kinase

198031	**-0,5511**	**0,0076482**	#N/A
206787	**-0,4969**	**0,007655**	Sec1-like protein
47124	**-0,9317**	**0,0076681**	-
210433	**-0,8496**	**0,0076681**	#N/A
56775	**-0,6142**	**0,0076747**	(arp3) implicated in control of actin polymerization
130502	**-1,1303**	**0,0077032**	#N/A
51831	**-0,5477**	**0,007767**	-
54468	**-1,3474**	**0,0077748**	Amidases
176070	**1,0956**	**0,0077748**	ATP-dependent DNA ligase
179405	**-0,5592**	**0,0077748**	Conserved hypothetical ATP binding protein
182977	**-0,5353**	**0,0077748**	related to short-chain alcohol dehydrogenases)
190360	**0,8804**	**0,0077868**	-
41518	**-1,0758**	**0,0077868**	-
55237	**-0,7721**	**0,0077868**	-
125597	**-0,5388**	**0,0077882**	-
57366	**0,7418**	**0,0077882**	-
213937	**-0,5417**	**0,0077882**	26S proteasome subunit
181325	**-0,894**	**0,0077882**	Candidate Peroxisomal phytanoyl-CoA hydroxylase
197735	**-2,3297**	**0,0077882**	Glycoside hydrolase, family 43
207470	**-0,4893**	**0,0077882**	Hypothetical cytosolic asparaginyl-tRNA synthetase
209963	**-0,5019**	**0,0077882**	Hypothetical fructose-2,6-bisphosphatase
207002	**1,2246**	**0,0077882**	Hypothetical. InterPro suggests role in chromosome condensation
53716	**-0,5315**	**0,0077882**	Ribulose kinase and related carbohydrate kinases
171497	**-0,6144**	**0,0077882**	Short-chain dehydrogenase/reductase
188168	**-0,7017**	**0,0078172**	-
129891	**-0,4537**	**0,0078279**	Glycoside hydrolase, family 3
201762	**-0,4282**	**0,0078281**	Predicted ubiquitin-protein ligase/hyperplastic discs protein, HECT superfamily
175678	**-0,843**	**0,0078825**	-
44318	**-0,5709**	**0,0078863**	-
206141	**-0,6898**	**0,0078863**	Predicted RNA-binding protein involved in translational regulation
125526	**-0,8251**	**0,0078952**	-
57012	**-0,6624**	**0,0078952**	Zinc-containing alcohol dehydrogenase
212105	**-0,5843**	**0,0079197**	-
39515	**-0,518**	**0,0079197**	Ras small GTPase, Rab type
38420	**-0,6268**	**0,0079477**	#N/A
211639	**-0,5397**	**0,0079537**	-
39623	**-0,6104**	**0,0079706**	-
50918	**-0,7667**	**0,0079891**	Putative Major facilitator superfamily, Synaptic vesicle transporter SVOP and related transporters
197549	**-0,65**	**0,0079891**	Sugar (ANd other) transporter
206266	**0,7908**	**0,0080025**	Cytochrome P450

52540	**-0,4651**	**0,0080031**	related to UV-endonuclease Uve1p/UVDE
54168	**-0,6257**	**0,0080399**	-
208805	**-0,6066**	**0,0080399**	20S proteasome subunit
40660	**-0,6589**	**0,0080399**	Heterokaryon incompatibility factor
36428	**0,8745**	**0,0080526**	-
182156	**-2,1027**	**0,0080546**	endopolygalacturonase
56770	**-0,8861**	**0,0080569**	Peptidase S16
209757	**-0,5108**	**0,0080943**	-
55881	**-0,4788**	**0,0080943**	-
52528	**-0,492**	**0,0080992**	Fungal transcriptional regulatory protein,
214383	**-0,493**	**0,0080992**	saccharopine dehydrogenase/Lysine-ketoglutarate reductase
54759	**-0,4563**	**0,0081252**	Regulator of Rac1, required for phagocytosis and cell migration
179884	**-0,4554**	**0,0081266**	Protein kinase
212928	**-0,7208**	**0,0081447**	Multidrug/pheromone exporter,
36048	**-1,6906**	**0,0081614**	-
173077	**-0,7185**	**0,0081614**	Dephospho-CoA kinase
212230	**-0,6563**	**0,0081715**	AAA ATPase
175156	**-0,6583**	**0,0081715**	#N/A
214151	**-0,3948**	**0,0081901**	Protein kinase
202206	**-0,5182**	**0,0081929**	Gamma-glutamyl phosphate reductase
137276	**-1,0763**	**0,0082415**	Hypothetical 26S proteasome regulatory complex,
131354	**-0,8097**	**0,0082415**	#N/A
51304	**-0,5081**	**0,0082437**	Might be involved in signal transduction
132816	**1,4498**	**0,0082437**	#N/A
55386	**-0,7056**	**0,0082787**	Sulfatase
183268	**-0,5185**	**0,0083091**	Hypothetical peroxisomal membrane anchor protein
174945	**-1,0837**	**0,0083091**	Major facilitator superfamily
53388	**-0,596**	**0,0083091**	#N/A
49658	**-0,5298**	**0,0083483**	Adenosine/AMP deaminase
56504	**-0,4478**	**0,0083507**	Hypothetical protein with RCC1 domain
207003	**-0,5273**	**0,0083691**	Lysine-ketoglutarate reductase/saccharopine dehydrogenase
205904	**0,5634**	**0,0083871**	Haloacid dehalogenase-like hydrolase
37516	**-0,4506**	**0,0084023**	Hypothetical Cytochrome P450 monooxygenase
206311	**0,5449**	**0,0084024**	-
37580	**-0,5312**	**0,0084024**	-
52883	**-0,6025**	**0,0084024**	Hypothetical subunit of the 20S proteasome
40740	**-0,662**	**0,008419**	Hypothetical Short-chain dehydrogenase
143268	**-0,4912**	**0,008427**	-
54541	**-0,8995**	**0,008427**	Candidate oxidoreductase, Short-chain dehydrogenase/reductase

47288	**-0,4679**	**0,0084301**	putative Translation initiation factor 2B, epsilon subunit (eIF-2Bepsilon/GCD6) Translation, ribosomal structure and biogenesis
173677	**-1,3046**	**0,0084301**	#N/A
57395	**-0,6145**	**0,0084351**	Glycosyl transferase, family 39
52243	**-0,605**	**0,0084351**	Uncharacterized conserved protein
206569	**-0,6175**	**0,0084847**	Hypothetical DNA polymerase alpha, catalytic subunit
36961	**-0,6881**	**0,0084996**	#N/A
42169	**-1,0039**	**0,008529**	-
54665	**-0,556**	**0,0085346**	Splicing coactivator SRm160/300
186504	**-2,081**	**0,0085349**	Hypothetical glyceraldehyde 3-phosphate dehydrogenase; EC 1.2.1.12
52684	**-0,8651**	**0,0085349**	Predicted carbohydrate kinase
175936	**0,4074**	**0,0085451**	Naringenin-chalcone synthase
213924	**-0,4644**	**0,0085534**	-
43391	**-0,4815**	**0,0085534**	Dehydrogenase E1 component
177220	**-1,054**	**0,0085534**	hypothetical protein containing Zn-finger, C2H2 type domain
193097	**-0,571**	**0,0085534**	Major facilitator superfamily
39613	**-1,1182**	**0,0085534**	putative extracellular GH afmily 3 beta-glucosidase
187714	**-0,4415**	**0,0085627**	-
207338	**-0,4749**	**0,0085653**	-
42387	**-0,655**	**0,0085653**	-
44000	**-0,9089**	**0,0085653**	hypothetical Isochorismatase hydrolase
49801	**-0,8008**	**0,0085653**	hypothetical oxidoreductase (qutH A. nidulans)
175768	**-0,9791**	**0,0085677**	HORMA domain
57265	**-1,3576**	**0,0085836**	gatA, 4-aminobutyrate aminotransferase
172548	**-0,5687**	**0,0086135**	-
170122	**0,5536**	**0,0086261**	Predicted BRCT domain protein
54584	**0,7503**	**0,0086734**	Candidate ornithine decarboxylase (EC 4.1.1.17)
35611	**-2,3318**	**0,0086773**	-
37775	**-0,5861**	**0,008691**	hypothetical protein containing Zn-finger, C2H2 type domain
53941	**-0,4662**	**0,0086983**	-
50378	**-1,5044**	**0,0086983**	candidate beta-mannanase, GH family 5 mannan endo-1,4-beta-mannosidase
177314	**-0,5436**	**0,0086983**	Initiation factor 3
48790	**-0,608**	**0,0086983**	Major facilitator superfamily
174810	**-0,5198**	**0,0086983**	putative extracellular protein with glycoside transferase motif
57243	**-0,9047**	**0,0087011**	Hypothetical aldehyde dehydrogenase (EC 1.2.1.3).
44232	**-0,4531**	**0,0087011**	#N/A

172988	**-0,8882**	**0,0087416**	Hypothetical allantoicase. These proteins allow the use of purines as secondary nitrogen sources in nitrogen-limiting conditions through the reaction: allantoate + H(2)0 = (-)-ureidoglycolate + urea.
55991	**-0,5121**	**0,0087513**	papA, Prolyl aminopeptidase papA (EC 3.4.11.5)
43602	**-0,6625**	**0,0088503**	hypothetical endoribonuclease
121960	**-0,4101**	**0,0088619**	Predicted E3 ubiquitin ligase
200706	**-0,6369**	**0,0088674**	-
175143	**0,5451**	**0,0088796**	Transcription factor with Homeobox domains
43932	**-1,6682**	**0,0088805**	-
197291	**-0,5198**	**0,0088896**	SNAP-25 (synaptosome-associated protein) component of SNARE complex
205921	**-0,6154**	**0,0088926**	FKBP-type peptidyl-prolyl cis-trans isomerase
171062	**-0,6144**	**0,0089139**	-
206713	**-0,4832**	**0,0089269**	-
123758	**-0,649**	**0,0089489**	-
127170	**0,8154**	**0,0089489**	-
49473	**-0,4695**	**0,0089489**	-
130344	**-0,4508**	**0,0089489**	Fungal specific transcription factor
134428	**-0,5045**	**0,0089489**	MT3/SUMO-activating complex, AOS1/RAD31 component
51952	**-0,9238**	**0,0090411**	-
170709	**-1,1604**	**0,0090609**	Aldehyde dehydrogenase
208150	**1,1423**	**0,0090609**	FAD-dependent pyridine nucleotide-disulphide oxidoreductase
196499	**-0,8318**	**0,0090609**	Major facilitator superfamily
194059	**-0,5299**	**0,0090609**	related to acetamidase C (EC 3.5.1.4). Looks like it is actually two genes with different activities.
207426	**0,7339**	**0,0090609**	#N/A
53540	**-3,269**	**0,0090854**	putative thioredoxin with signal peptide domain
125165	**0,6386**	**0,0091176**	Hypothetical protein with GAT domain
174132	**-0,9324**	**0,0091283**	#N/A
191974	**-1,2458**	**0,009156**	#N/A
36465	**-0,5559**	**0,0091719**	hypothetical protein with predicted histone-fold; KOG Class: Transcription; KOG Id: 0871; KOG description: Class 2 transcription repressor NC2, beta subunit (Dr1)
210734	**-0,489**	**0,009178**	hypothetical protein with predicted histone deacetylase domain, which catalyses the removal of acetyl group of acetylated lysine residues in histones; KOG Class: Chromatin structure and dynamics; KOG Id: 1343; KOG Description: Histone deacetylase complex, catalytic component HDA1
38906	**-0,6519**	**0,0091804**	-

211661	**2,184**	**0,0091931**	Candidate malic oxidoreductase (EC 1.1.1.40)
49499	**-1,1211**	**0,0091931**	#N/A
53870	**-0,4884**	**0,0091952**	-
209685	**-1,0517**	**0,0092108**	Acyl-CoA dehydrogenase
199877	**-0,5451**	**0,0092108**	hypothetical WD-40 repeat protein and G-protein beta, normally coordinating multi-protein complex assemblies; KOG Class: Chromatin structure and dynamics; KOG Id: 1009; KOG Description: Chromatin assembly complex 1 subunit B/CAC2 (contains WD40 repeats)
118601	**-0,682**	**0,0092108**	Non-ribosomal peptide synthetase
35902	**-0,5433**	**0,0092181**	Fungal specific transcription factor
206802	**-0,5899**	**0,0092181**	Serine/threonine protein kinase
143961	**-0,4405**	**0,0092332**	-
180963	**-0,6911**	**0,0092404**	#N/A
188497	**1,3049**	**0,0092417**	Fungal specific transcription factor
206723	**-0,7247**	**0,0092643**	-
38226	**-0,8083**	**0,0092643**	Related to Geranylgeranyl pyrophosphate synthase
176123	**-0,5478**	**0,0092795**	-
174968	**-0,6503**	**0,0092812**	-
52722	**-0,6453**	**0,0094015**	Predicted membrane protein
202692	**-0,4412**	**0,0094051**	enolase, phosphopyruvate hydratase activity
208481	**-0,4926**	**0,0094093**	Methionyl-tRNA synthetase
51711	**-0,4203**	**0,0094379**	adB. Almost identical to E. nidulans adenylosuccinate synthase (adB) (EC 6.3.4.4)
208323	**-0,4486**	**0,009471**	-
52849	**-0,62**	**0,009471**	-
36513	**-0,5658**	**0,009471**	Peptidase S26B, eukaryotic signal peptidase
187248	**-0,4063**	**0,0094751**	-
190481	**-0,5734**	**0,0094928**	AMP-dependent synthetase and ligase
55412	**-0,6513**	**0,0095368**	F-actin capping protein, beta subunit
123450	**0,7574**	**0,0095368**	hypothetical neutral amino acid permease
208283	**0,689**	**0,0095406**	Candidate S-adenosylmethionine synthetase (metK)
43993	**-0,4326**	**0,0095771**	Fungal specific transcription factor
42106	**-0,7464**	**0,0095942**	Cytochrome P450
142667	**-1,0826**	**0,0096531**	Hypothetical heterokaryon incompatability factor
44808	**-1,2736**	**0,0097099**	Acetyl-CoA acetyltransferase
54610	**-0,912**	**0,0097452**	Histidine kinase
55633	**-0,5102**	**0,0097499**	(gsdA) Glucose 6-phosphate 1-dehydrogenase (EC 1.1.1.49)
36158	**-0,5478**	**0,0097635**	Predicted mitochondrial carrier protein
192623	**-0,6922**	**0,0097687**	Hypothetical DNA helicase
205450	**-0,6408**	**0,0097746**	-

40314	**-0,476**	**0,0097746**	-
213355	**-0,5893**	**0,0097746**	hypothetical protein with cupin region; KOG Class: Chromatin structure and dynamics; KOG Id: 2132; KOG description: Uncharacterized conserved protein, contains JmjC domain
53688	**-0,7044**	**0,0097746**	Zinc-binding oxidoreductase
190111	**-0,6421**	**0,0097751**	-
51685	**0,6101**	**0,0097908**	Related to Schizosaccharomyces pombe asparaginase (EC 3.5.1.1)
54383	**-0,6327**	**0,0097908**	Splicing coactivator SRm160/300, subunit SRm300
53188	**-0,483**	**0,0098037**	#N/A
46769	**-0,5786**	**0,009828**	-
47322	**-0,4688**	**0,0098534**	Clathrin adaptor complex small chain
211276	**-0,6468**	**0,0098534**	Major facilitator superfamily
56137	**-0,3994**	**0,0098534**	#N/A
179474	**-0,3638**	**0,0099051**	Hypothetical RNA lariat debranching enzyme
56389	**-0,9262**	**0,0099636**	alpha/beta hydrolase fold
207689	**-0,5666**	**0,0099636**	Peptidase M20
50103	**-0,8887**	**0,0099701**	Hypothetical, Nucleolar GTPase/ATPase
52545	**-0,4683**	**0,0099701**	RNA recognition motif. (a.k.a. RRM, RBD, or RNP domain)
214261	**0,5719**	**0,0099848**	two-component signal transduction system
35670	**-0,3706**	**0,0099912**	GCN5-related N-acetyltransferase
54817	**0,6842**	**0,0100025**	Hypothetical oligopeptide transporter
40903	**-0,9892**	**0,0100025**	SAM (and some other nucleotide) binding motif
54174	**-1,2612**	**0,0100491**	Dihydroxy-acid dehydratase
207962	**-0,5391**	**0,0100491**	Splicing coactivator SRm160
129033	**-0,5685**	**0,0100491**	Transcription factor MEIS1 and related HOX domain proteins
57100	**-0,443**	**0,0101129**	Mitochondrial carrier protein
185646	**-0,9495**	**0,0101574**	6-phosphogluconate dehydrogenase, NAD-binding
43791	**2,7969**	**0,0101623**	Generic methyltransferase
190965	**-0,6688**	**0,0101753**	-
55306	**-1,053**	**0,0101753**	Aminotransferase class-III
172476	**-0,5712**	**0,0101921**	hypothetical protein containing fungal specific transcription factor domain.
209771	**-0,7669**	**0,0102033**	-
36822	**-0,6444**	**0,0102227**	Hypothetical regulatory subunit of the 20S preoteasome
182862	**-0,8246**	**0,010235**	Zinc-containing alcohol dehydrogenase
180549	**3,8847**	**0,0102356**	-
134215	**-0,484**	**0,0102547**	-
174018	**-0,5009**	**0,0102547**	-
38927	**-0,7197**	**0,0102547**	-

119238	**-0,7684**	**0,0102547**	Fungal Zn(2)-Cys(6) binuclear cluster domain
55665	**1,6107**	**0,0102547**	related to tripeptidyl peptidase
42852	**0,7463**	**0,0102547**	Survival protein SurE
133203	**-1,119**	**0,0102865**	-
47886	**-0,4361**	**0,0103167**	Predicted GTPase-activating protein
201858	**-0,5334**	**0,0103312**	H+-transporting two-sector ATPase
54341	**-1,7371**	**0,0103449**	hypothetical short chain dehydrogenase
38332	**-0,6212**	**0,0103466**	-
52406	**-0,8487**	**0,0103466**	Beta-ketoacyl synthase
49039	**-0,489**	**0,0103518**	Hypothetical protein containing Sec23/Sec24 domains involved in vesicle coating
130463	**-0,6916**	**0,010361**	Histone H3 (Lys9) methyltransferase SUV39H1/Clr4, required for transcriptional silencing
210285	**-0,7883**	**0,010361**	#N/A
55401	**-0,5057**	**0,0103798**	#N/A
52459	**-0,4986**	**0,0104009**	Hypothetical peptidase
204050	**-1,4524**	**0,0104021**	FAD binding domain
210951	**1,8115**	**0,0104228**	Glycine cleavage system P-protein
186686	**-0,5658**	**0,0104228**	hypothetical dihydrofolate reductase
212435	**-0,4088**	**0,0104228**	Nucleoside diphosphate kinase
120955	**-0,6183**	**0,0104318**	-
181202	**-0,5998**	**0,0104671**	-
211236	**-0,404**	**0,0104792**	Cysteinyl-tRNA synthetase
209244	**-0,798**	**0,0105201**	Oxidoreductase
182312	**-0,5867**	**0,0105631**	UreD urease accessory protein
38012	**-0,8713**	**0,0105821**	#N/A
142108	**3,4986**	**0,0105832**	-
46685	**-0,7801**	**0,0106194**	-
202289	**-0,5803**	**0,0106207**	-
53152	**-1,8861**	**0,0106799**	RNA polymerase II, large subunit
45923	**-1,5781**	**0,0106799**	#N/A
36078	**-0,492**	**0,0106822**	#N/A
176272	**-0,9466**	**0,0106886**	Flavin-containing monooxygenase
208837	**-0,4953**	**0,010689**	Aromatic-ring hydroxylase
196058	**-0,4873**	**0,010689**	Transcription factor/CCAAT displacement protein
42949	**1,0194**	**0,0107052**	-
42728	**-0,6316**	**0,0107052**	related to vacuolar ATP synthase subunit D
187949	**-0,6619**	**0,0108122**	Esterase/lipase/thioesterase
212936	**-0,6623**	**0,0108132**	short chain dehydrogenase
207667	**-0,5708**	**0,0108291**	Hypothetical RING finger protein with Zn-finger domain
180387	**-0,5069**	**0,0108339**	-
39667	**1,3407**	**0,0108339**	-
47229	**1,6408**	**0,0108339**	(phyB) phytase B

120468	**-0,584**	**0,0108339**	Fungal specific transcription factor
184932	**-0,7517**	**0,0108339**	hypothetical protein containing ferric reductase-like transmembrane component and helix-turn-helix, Fis-type domain components.
52427	**-0,5306**	**0,0108339**	Mitochondrial carrier proteins
210454	**0,8834**	**0,0108339**	Molecular chaperones mortalin/PBP74/GRP75, HSP70 superfamily
192184	**-0,7663**	**0,0108339**	oxidoreductase, Short-chain dehydrogenase/reductase
182597	**-0,4831**	**0,0108339**	Zn-finger transcription factor
36284	**-0,5871**	**0,0109161**	hypothetical protein containing cytochrome c heme-binding site and Zn-finger, C2H2 type domains
50675	**-0,4874**	**0,0109431**	hypothetical Decapping enzyme complex component
53159	**-2,56**	**0,0109681**	(cbhA) cellobiohydrolase A
37302	**-0,5019**	**0,0109903**	-
209239	**-0,5587**	**0,0109927**	-
38678	**-0,6345**	**0,0110179**	-
51875	**1,1376**	**0,0110482**	#N/A
56871	**0,7644**	**0,0110904**	Mitochondrial carrier proteins
211200	**-0,4429**	**0,0110929**	Snf7 family protein
54712	**-0,5461**	**0,0111142**	Nucleoside diphosphate-sugar hydrolase of the MutT (NUDIX) family
193012	**-0,7867**	**0,0111308**	Ubiquitin-protein ligase
177282	**-0,9401**	**0,0111787**	-
188806	**-0,522**	**0,0112557**	Acyl-CoA synthetase
191206	**-0,7833**	**0,0112557**	Aminoacyl-tRNA synthetase
214441	**-0,4427**	**0,0112557**	hypothetical. KOG: acetyl-CoA acetyltransferase
50680	**-0,4768**	**0,0112617**	hypothetical protein containing Zn-finger, C2H2 type domain
41703	**-0,5637**	**0,0112711**	GH family 88
127635	**-0,5945**	**0,0112912**	-
212507	**0,5614**	**0,0112912**	#N/A
53259	**-0,5111**	**0,0113029**	Hypothetical chitin synthase
40206	**-0,9405**	**0,0113238**	Hypothetical glutathione S-transferase
54380	**-0,8783**	**0,0113764**	-
119138	**-0,8097**	**0,0114389**	-
37044	**-0,4399**	**0,0114397**	Related to anti-silencing protein ASF1
37866	**-0,4291**	**0,0114563**	Predicted membrane protein
38375	**-0,7243**	**0,0114645**	Major facilitator superfamily
201896	**-0,6075**	**0,0114706**	Hypothetical Ubiquitin-specific protease
176012	**-0,7738**	**0,0114721**	-
187815	**-0,7452**	**0,0114721**	Major facilitator superfamily

36647	**-0,7318**	**0,0114938**	Lipocalin-related protein
50029	**-0,5739**	**0,0115131**	-
52629	**-0,7018**	**0,0115131**	-
175257	**-0,9208**	**0,0115171**	hypothetical protein with predicted MT-A70 and N-6 Adenine-specific DNA methylase; KOG Class: Transcription; KOG Id: 2356; KOG description: Transcriptional activator, adenine-specific DNA methyltransferase
194534	**-0,4798**	**0,0115311**	-
212637	**-1,0898**	**0,0115311**	hypothetical protein containing fungal specific transcription factor and fungal transcriptional regulatory protein domains.
36075	**-0,8815**	**0,0115311**	LeaA homologue, regulator of terrequinone A secondary metabolism
214786	**-0,6095**	**0,0115347**	-
35726	**0,7348**	**0,0115347**	-
136869	**-0,4561**	**0,0115347**	hypothetical lysin. Extracellular. Peptidoglycan-binding domain and peptidase-like domain
42779	**-0,4397**	**0,011539**	26S proteasome regulatory complex
210577	**-0,6227**	**0,011539**	#N/A
54258	**-0,5484**	**0,0115466**	-
213757	**-0,6399**	**0,0115466**	Gamma-glutamyltranspeptidase
212893	**-0,979**	**0,0115466**	Glycoside hydrolase
180624	**-0,8703**	**0,011549**	-
170909	**-0,7199**	**0,0115507**	Eukaryotic protein of unknown function DUF846
193056	**-0,4512**	**0,0115659**	-
183145	**-0,5227**	**0,0115659**	Lactate/malate dehydrogenase, NAD dependent
184264	**-2,0293**	**0,0115855**	#N/A
121537	**-0,5399**	**0,0116437**	-
46219	**0,4839**	**0,0116437**	Monooxygenase
52354	**-0,7295**	**0,0116494**	Nucleolar GTPase/ATPase
197907	**-0,4683**	**0,011679**	SNARE protein
173769	**-0,4678**	**0,011698**	-
185285	**-0,897**	**0,0117105**	#N/A
50094	**0,6243**	**0,0117217**	NmrA-like, regulation of nitrogen utilization
211485	**0,9443**	**0,0117641**	Acetylglutamate kinase
56699	**-0,4938**	**0,0117822**	-
179141	**-1,0406**	**0,0118634**	Fungal specific transcription factor
123805	**-0,8413**	**0,0119029**	Predicted seven transmembrane receptor - rhodopsin family
197786	**-0,5892**	**0,0119062**	(dapB) dipeptidylpeptidase
185351	**-0,7158**	**0,0119077**	Flavonol reductase/cinnamoyl-CoA reductase
192461	**-0,6171**	**0,0119203**	#N/A
122612	**-0,5324**	**0,0120081**	Major facilitator superfamily

123645	**-0,579**	**0,0120095**	Hypothetical GCN5-related N-acetyltransferase
209660	**-0,7145**	**0,0120313**	SWI-SNF chromatin-remodeling complex protein
56675	**-0,5686**	**0,0120451**	Ubiquitin-conjugating enzyme
128333	**-0,5853**	**0,0120803**	-
56552	**-0,4335**	**0,0120928**	Protein required for meiotic chromosome segregation
36722	**-0,5431**	**0,0121006**	-
48908	**-0,5713**	**0,0121006**	Fatty acid desaturase
185117	**-0,4757**	**0,0121006**	Hypothetical protein. Electronic annotation suggests pyridine nucleotide-disulphide oxidoreductase
209872	**-0,8519**	**0,0121006**	Peptidase M3A and M3B
54957	**-0,483**	**0,0121006**	Putative GroEL-like chaperone, ATPase
213011	**-0,4489**	**0,0121105**	-
42808	**-1,246**	**0,0121105**	-
184121	**-0,9506**	**0,0121186**	-
183780	**-0,5283**	**0,0121218**	-
193777	**-0,8477**	**0,0121218**	DEAD/DEAH box helicase
55417	**-0,9542**	**0,0121246**	Serine/threonine protein kinase, active site
203669	**0,478**	**0,0121319**	hypothetical 5-methyltetrahydropteroyltriglutamate--homocysteine S-methyltransferase
204514	**-0,5687**	**0,0121319**	Nucleotide excision repair factor NEF2, RAD23 component
184617	**-0,5369**	**0,0121668**	RTA1 like protein
42477	**-0,5971**	**0,0121724**	Peptidase
48719	**-1,0054**	**0,0121724**	Short-chain dehydrogenase/reductase
193822	**-0,4585**	**0,0121956**	-
181867	**-0,5121**	**0,0122407**	Cell division control protein/predicted DNA repair exonuclease
56311	**-1,326**	**0,0122407**	hypothetical Glucose-methanol-choline oxidoreductase
55364	**-0,3909**	**0,0122407**	Molecular chaperone Prefoldin
57291	**0,5999**	**0,0122407**	Serine/threonine protein kinase
173711	**-0,4329**	**0,0122407**	Short-chain dehydrogenase/reductase
187240	**-0,5789**	**0,0122442**	Iron/ascorbate family oxidoreductases
52377	**2,2416**	**0,0122612**	#N/A
47745	**-0,5212**	**0,0122723**	-
56446	**-0,6395**	**0,0123165**	#N/A
43911	**-2,1269**	**0,0123415**	-
46358	**-0,7322**	**0,0123415**	Hypothetical protein. May have catechol dioxygenase activity
202139	**-0,9416**	**0,0123556**	Ubiquitin-like protein
180084	**-0,6187**	**0,0123704**	-

51891	**-0,4933**	**0,0123792**	-
50979	**-0,6122**	**0,0123792**	related to alpha-L-arabinofuranosidase
38952	**-0,6155**	**0,0123939**	-
40181	**-0,4731**	**0,0123959**	-
39908	**0,3603**	**0,0123959**	#N/A
170612	**-0,9362**	**0,0124776**	-
171843	**-0,4588**	**0,012497**	-
48335	**-0,4764**	**0,0125299**	#N/A
49134	**-0,38**	**0,0125369**	Hypothetical hexokinase
47983	**-0,5055**	**0,0125653**	FAD-dependent oxidoreductase
184367	**-0,8645**	**0,012578**	-
212021	**-1,0242**	**0,012578**	Aldehyde dehydrogenase
42654	**-0,6286**	**0,012578**	hypothetical protein containing Zn-finger and Homeobox domains
46606	**-0,4509**	**0,0125987**	hypothetical protein containing glycoside hydrolase, family 76 and helix-turn-helix, AraC type domains
208428	**-0,5336**	**0,0125987**	Metallophosphoesterase
55469	**-0,6269**	**0,0126103**	FAD dependent oxidoreductase
202059	**-0,8448**	**0,0126193**	Isochorismatase hydrolase
202248	**0,6493**	**0,0126299**	-
125804	**-0,5087**	**0,0126599**	-
208898	**1,2031**	**0,0126614**	NADP/FAD dependent oxidoreductase
206461	**-0,7716**	**0,0126614**	Protein kinase
205576	**-0,43**	**0,0126778**	hypothetical. Interpro suggests RNA-binding
121829	**-0,651**	**0,0127091**	-
171442	**-0,8991**	**0,0127091**	-
39391	**-0,4315**	**0,0127091**	-
177726	**-0,5543**	**0,0127164**	-
212502	**1,1854**	**0,0127185**	Hypothetical nucleosome assembly protein
209012	**-1,2025**	**0,0127185**	Proteins containing the FAD binding domain
191298	**-0,4722**	**0,0127442**	Predicted aromatic-ring hydroxylase
189589	**-0,4036**	**0,0127878**	-
211065	**-0,5836**	**0,0127878**	#N/A
181089	**-0,4603**	**0,0127893**	Hypothetical peroxisomal NUDIX hydrolase
45086	**-0,4374**	**0,0128194**	ADP-ribosylation factor GTPase activator
214636	**-0,5029**	**0,0128256**	Metallophosphoesterase
44470	**-0,5957**	**0,0128656**	Fungal specific transcription factor
37157	**1,515**	**0,0128829**	#N/A
51355	**-0,5983**	**0,0128998**	-
135687	**-0,6997**	**0,012988**	-
207539	**-0,6869**	**0,0129892**	UBA/THIF-type NAD/FAD binding fold
212603	**-0,6038**	**0,0130199**	-
130523	**-0,4619**	**0,0130383**	FOG: Zn-finger

43045	**-0,4454**	**0,013054**	related to proteasome subunite beta-like protein
127476	**-0,6674**	**0,0131298**	Serine/threonine protein kinase
133870	**1,1636**	**0,0131318**	hypothetical alpha-1,6-mannanase. GH family 76
55704	**-0,596**	**0,0131412**	(tpsA) trehalose-6-phosphate synthase A
55193	**-0,5471**	**0,0131807**	-
41067	**-0,5313**	**0,0131818**	Predicted tubulin-tyrosine ligase
172596	**-0,4325**	**0,0132269**	-
119631	**-0,5002**	**0,0132269**	hypothetical translation repression protein
204381	**-1,174**	**0,0132269**	Voltage-gated shaker-like K+ channel, subunit beta/KCNAB
52445	**-0,5432**	**0,0132435**	-
52587	**1,2585**	**0,0132918**	related to extracellular acid phosphatase
42307	**1,2319**	**0,0133163**	Inorganic phosphate transporter
37491	**-0,635**	**0,0133406**	Hypothetical heterokaryon incompatibility factor
55560	**1,1092**	**0,0133406**	mannitol-1-phosphate 5-dehydrogenase
36360	**-0,4712**	**0,0133416**	CorA-like Mg2+ transporter protein
53539	**-0,4723**	**0,0133423**	-
213429	**-0,5047**	**0,0133865**	#N/A
56228	**-0,573**	**0,0134116**	-
42726	**-0,415**	**0,0134636**	-
180862	**-1,4063**	**0,0134636**	putative transmembrane GH family 47
141168	**-0,4061**	**0,0134685**	hypothetical protein
197881	**-0,5229**	**0,0134685**	#N/A
38583	**-0,531**	**0,0135384**	-
57253	**-0,829**	**0,0135384**	Ubiquitin-conjugating enzyme
41998	**-0,7619**	**0,0135384**	#N/A
205975	**-0,4074**	**0,0135969**	GTPase Rab11/YPT3, small G protein superfamily
54854	**0,8**	**0,0136037**	Inositol-3-phosphate synthase
194446	**-0,462**	**0,0136075**	GCN5-related N-acetyltransferase
212783	**-0,4392**	**0,0137237**	putative GH family 47 mannosyl-oligosaccharide 1,2-alpha-mannosidase
192050	**-0,602**	**0,0137358**	Hypothetical Na+:Ca2+ antiporter
124948	**-0,62**	**0,0137358**	#N/A
208474	**-0,4491**	**0,0137864**	Phospholipid methyltransferase
49153	**-1,1814**	**0,0138252**	Cytochrome P450
51718	**-0,4814**	**0,0138365**	hypothetical protein with Zn-finger domain
205031	**-0,3773**	**0,0138557**	-
48569	**-0,4035**	**0,0138881**	-
43342	**-0,9091**	**0,0139038**	putative transmembrane GH family 31
135359	**-0,606**	**0,0139052**	-
184568	**0,4679**	**0,0139492**	-
211509	**-0,5706**	**0,0139492**	Fungal specific transcription factor
192658	**-0,6104**	**0,0139492**	#N/A

39581	**-0,8368**	**0,0139715**	Peptidase C19, ubiquitin carboxyl-terminal hydrolase 2
174932	**-0,6089**	**0,0139808**	-
47271	**1,5524**	**0,0139808**	Malonyl-CoA:ACP transacylase
53035	**-0,4575**	**0,0139808**	Phosphoribulokinase/uridine kinase
209919	**-0,4477**	**0,0139808**	Tryptophanyl-tRNA synthetase
51478	**-0,5352**	**0,0140231**	(faeB) feruloyl esterase
129504	**-0,6675**	**0,0140231**	AAA+-type ATPase
214391	**-0,4862**	**0,0140588**	Permease of the major facilitator superfamily
41387	**-0,6792**	**0,014077**	-
52120	**-0,5058**	**0,0141023**	-
194528	**-0,5055**	**0,0141103**	-
207758	**-0,4459**	**0,0141103**	26S proteasome regulatory complex, subunit PSMD9
51189	**-0,6616**	**0,014161**	-
122135	**-0,4442**	**0,0141918**	-
39523	**-0,4802**	**0,0141974**	-
52852	**-1,6378**	**0,0141974**	Flavin-containing monooxygenase
202700	**-0,3894**	**0,0141974**	Multifunctional chaperone (14-3-3 family)
188863	**-0,5888**	**0,0141974**	Related to S. cerevisiae phenylacrylic acid decarboxylase (EC 4.1.1.-)
178744	**-0,8466**	**0,0142075**	Hypothetical Metal-dependent phosphohydrolase, HD region
191589	**-0,6367**	**0,0142155**	-
205944	**-0,3709**	**0,0142155**	-
198713	**-0,5405**	**0,0142155**	Ribonuclease II
213441	**0,8864**	**0,0142155**	Squalene monooxygenase
54682	**-0,5485**	**0,0142806**	-
213502	**5,0109**	**0,014297**	Dihydroxy-acid dehydratase
206308	**-0,6303**	**0,0143251**	Hypothetical molybdenum cofactor biosynthesis protein
37795	**-0,5107**	**0,014341**	-
214849	**-0,9991**	**0,0143508**	FAD-dependent pyridine nucleotide-disulphide oxidoreductase
50815	**-0,4059**	**0,0143669**	Hypothetical UMP-CMP kinase,phosphotransferase activity, phosphate group as acceptor
188780	**-1,2618**	**0,0143924**	Amino acid/polyamine transporter
47261	**-0,421**	**0,0144166**	related to Beta-1,4-mannosyltransferase
185545	**-0,6236**	**0,0144204**	-
52474	**0,9465**	**0,0144441**	FOG: RRM domain
128406	**-0,4357**	**0,0144441**	#N/A
129554	**-0,5048**	**0,0144543**	Translation elongation factor 2
181743	**-0,8426**	**0,0144797**	hypothetical short chain dehydrogenase
172938	**-0,4344**	**0,0144915**	-

190953	**-0,5807**	**0,0144937**	DNA repair protein
38025	**-0,5221**	**0,0144967**	-
206219	**0,5966**	**0,0145058**	ERG2 and sigma1 receptor-like protein
213313	**-0,4984**	**0,0145263**	-
54217	**-0,5908**	**0,0145976**	Conserved Zn-finger protein
202252	**-0,6451**	**0,0146016**	putative extracellular tannase and feruloyl esterase
128109	**-0,5075**	**0,0146022**	-
43621	**-0,5568**	**0,0146039**	SAM (and some other nucleotide) binding motif
37140	**-0,6621**	**0,0146277**	-
52811	**-0,8524**	**0,0146277**	hypothetical glycoside hydrolase, family 5
214305	**-0,5547**	**0,0146277**	Hypothetical Vesicle transport protein (v-SNARE)
57312	**-0,4441**	**0,0146334**	Related to C. albicans seryl-tRNA synthase (EC 6.1.1.11)
51231	**-0,4038**	**0,0146606**	Related to S. cerevisiae alanyl-tRNA synthase (EC 6.1.1.7)
136049	**-0,7996**	**0,0146914**	#N/A
120292	**-0,6098**	**0,0146945**	Fungal specific transcription factor
191505	**-0,4132**	**0,014697**	possible hexose transporter
212473	**-0,4762**	**0,0147432**	ATPase-like
127191	**0,815**	**0,0147772**	-
183086	**-0,5067**	**0,0147772**	-
39803	**-0,8206**	**0,0148068**	Yippee-type zinc-binding protein
211531	**1,4259**	**0,0148212**	#N/A
39128	**-0,4498**	**0,0148487**	hypothetical protein related to cytochrome P450 3A7
190197	**-0,6315**	**0,0148551**	(apsC) aminopeptidase C.
208244	**-0,6136**	**0,0148551**	Protein kinase
193894	**-0,462**	**0,0149297**	-
204333	**0,8477**	**0,0149297**	DUF1275 domain protein
50290	**-0,6722**	**0,0149297**	hypothetical Nicotinate phosphoribosyltransferase
127602	**0,8823**	**0,0149406**	beta-1,6-N-acetylglucosaminyltransferase
54961	**-0,8677**	**0,0149463**	hypothetical cysteine dioxygenase (EC 1.13.11.20)
44376	**-0,7397**	**0,0149481**	-
172591	**-0,6585**	**0,0149887**	Uroporphyrinogen decarboxylase
131182	**-0,424**	**0,0150066**	#N/A
179559	**-0,6062**	**0,0150066**	#N/A
50452	**-0,5049**	**0,0150475**	-
56514	**0,3932**	**0,0151273**	Protein kinase
188245	**-0,8004**	**0,0151273**	#N/A
187977	**-0,6368**	**0,0152073**	Monooxygenase
51255	**-0,741**	**0,0152237**	-
180171	**1,2309**	**0,0152237**	Hypothetical isocitrate lyase and phosphorylmutase

56792	**0,8578**	**0,0152245**	Hypothetical GPI anchor protein
45982	**-0,5487**	**0,0152733**	-
173949	**-0,6117**	**0,0152765**	-
213866	**-0,5831**	**0,015284**	-
41045	**-0,7538**	**0,0152854**	Esterase/lipase/thioesterase
202783	**-0,3657**	**0,0152854**	Ras small GTPase,
125522	**-0,7747**	**0,0152854**	#N/A
175118	**-0,4842**	**0,0152854**	#N/A
184612	**0,7505**	**0,0153408**	Inositol polyphosphate kinase
51267	**-0,5012**	**0,0153674**	Oligosaccharyltransferase subunit
210782	**-0,8393**	**0,0153806**	-
213950	**-0,5393**	**0,0154013**	Peptidase M28
55618	**-0,6467**	**0,0154087**	Related to farnesyl pyrophosphate synthetase
52397	**-0,5031**	**0,0154222**	Hypothetical 20S proteasome, regulatory subunit
185790	**-0,6555**	**0,0154242**	-
124700	**5,2284**	**0,0154666**	Esterase/lipase/thioesterase
210921	**-0,6255**	**0,0154666**	Predicted E3 ubiquitin ligase
177822	**-0,6909**	**0,0154999**	Thioredoxin-like protein
42612	**-0,5635**	**0,0155075**	-
206657	**-0,467**	**0,0155075**	BAR
45641	**-0,4387**	**0,0155075**	Cytochrome P450
213047	**-0,4393**	**0,0155209**	Predicted E3 ubiquitin ligase containing RING finger, subunit of transcription/repair factor TFIIH and CDK-activating kinase assembly factor
128411	**-0,3895**	**0,015528**	#N/A
209716	**-0,6365**	**0,0156341**	Cu2+/Zn2+ superoxide dismutase SOD1
39109	**-0,3787**	**0,0156941**	-
43778	**0,4515**	**0,0156941**	Dehydrogenases with different specificities (related to short-chain alcohol dehydrogenases)
194178	**-0,6061**	**0,0156981**	-
56739	**1,1157**	**0,0156983**	Ornithine-N5-oxygenase
214587	**-1,9862**	**0,0157938**	Acetyl-CoA hydrolase
53262	**-0,4368**	**0,015795**	-
176581	**-0,6841**	**0,0158073**	Predicted haloacid-halidohydrolase and related hydrolases
126898	**-0,342**	**0,0158781**	-
213788	**-0,7505**	**0,0158781**	candidate GABA permease
141605	**-0,6455**	**0,0158793**	Putative signal transduction protein involved in RNA splicing
183896	**-0,4345**	**0,0159011**	Fungal specific transcription factor
40670	**0,3706**	**0,0159746**	#N/A
203804	**-0,5396**	**0,0160006**	Peptidase M49
39990	**-0,9819**	**0,0160357**	Carbamoyl-phosphate synthetase large chain
52146	**-0,5289**	**0,0160396**	(trpB) Tryptophan synthase

191511	**0,9221**	**0,0160726**	related to GH family 12 xyloglucan-specific endo-beta-1,4-glucanase
35899	**-0,4498**	**0,0160981**	hypothetical protein; KOG Class: Chromatin structure and dynamics;
50490	**-0,5143**	**0,0161068**	hypothetical DNA mismatch repair protein
55543	**-0,4473**	**0,0161075**	Metal-dependent phosphohydrolase, HD region
184571	**-0,3674**	**0,0161275**	Pre-mRNA spilicing factor
204276	**-0,5285**	**0,0161392**	Zinc-containing alcohol dehydrogenase
49321	**-0,5105**	**0,0161643**	-
38982	**-0,5225**	**0,0162245**	AAA ATPase
197446	**-0,829**	**0,0163077**	candidate GH family 18 endo-chitinase
178461	**-0,5175**	**0,0163562**	Editing needed. This protein is an artificial hybrid of a purine-nucleoside phosphorylase activity and a 6-phosphogluconate dehydrogenase. In the CBS 513.88 annotation, these are annotated as An11g06110 and An11g06120 respectively.
185698	**-0,8011**	**0,0163651**	-
192720	**-0,5912**	**0,0163651**	-
53082	**0,5989**	**0,0163651**	Related to histone 1 protein, H1, with a predicted H1/H5 domain, histone linker N- terminal, and winged helix DNA binding. The protein is essential for chromatin stucture and links nucleosomes in higher order structures; KOG Class: Chromatin structure and dynamics; KOG Id: 4012; KOG Description: Histone H1
178219	**-0,4059**	**0,0163842**	Hypothetical Metal-dependent phosphohydrolase, HD region
214460	**-0,6372**	**0,0164006**	Serine carboxypeptidase
54525	**-0,6396**	**0,0164829**	Ornithine aminotransferase otaA (EC 2.6.1.13)
53737	**-0,5879**	**0,016488**	Phox-like
206602	**-0,4663**	**0,016615**	Triosephosphate isomerase
184509	**-2,5597**	**0,0166591**	Hypothetical methyltransferase. No sequence similarity is found to identified proteins
209439	**0,7237**	**0,0166747**	candidate HMG-CoA reductase
135107	**-0,5474**	**0,016689**	Hypothetical Actin-binding protein
56298	**-0,8598**	**0,0167382**	Putative mannosyl-oligosaccharide glucosidase, GH family 63
214568	**-0,4849**	**0,0167741**	Extracellular protein SEL-1 and related proteins
43508	**-0,3848**	**0,0167762**	-
126465	**-0,6908**	**0,0167855**	-
211367	**-0,6254**	**0,0167855**	hypothetical protein containing Zn-finger, C2H2 type domain
123018	**-0,5359**	**0,0167922**	-
54489	**1,1435**	**0,0168308**	Hypothetical. Contains aspartic peptidase domain

170972	**-0,6533**	**0,0168367**	-
54558	**-0,5916**	**0,0168481**	Conserved WD40 repeat-containing protein AN11
55916	**-1,3022**	**0,016912**	Hypothetical Acyl-CoA dehydrogenase
170688	**-0,5702**	**0,0169342**	-
170933	**-0,519**	**0,0169342**	FAD binding domain
180300	**-0,5261**	**0,0169498**	Uncharacterized conserved protein, contains WD40 repeats
54717	**0,706**	**0,0169583**	-
213045	**-0,4194**	**0,0169589**	Lipid phosphate phosphatase and related enzymes of the PAP2 family
55218	**-0,8626**	**0,017003**	-
178675	**-0,8719**	**0,0170369**	Autophagy protein Apg4, cystein proteinas
120801	**-0,8532**	**0,0170713**	Fungal specific transcription factor
43221	**1,7789**	**0,0171693**	Amino acid transporters
129315	**-0,725**	**0,0171693**	Protein kinase
57027	**-0,829**	**0,0171881**	(phyA) Multiple inositol polyphosphate phosphatase phyA
208780	**-0,6384**	**0,0172219**	Protein kinase
127358	**-0,492**	**0,0172248**	-
55132	**0,5868**	**0,0172769**	-
183278	**-0,8664**	**0,0172855**	Related to tryptophan synthase. Shows similarity to N. crassa tryptophan synthase of N. crassa
186889	**-0,6038**	**0,0172999**	-
212265	**-1,3601**	**0,0173265**	Hypothetical WW domain protein. Probable involved in signalling cascade
187460	**-0,4392**	**0,0173909**	-
44254	**0,7609**	**0,0174995**	Acyl-CoA thioesterase
38272	**-0,8608**	**0,0174995**	#N/A
126043	**-0,4095**	**0,0175197**	-
175980	**-0,6322**	**0,0175197**	Predicted NUDIX hydrolase FGF-2 and related proteins
209366	**-0,5279**	**0,0175903**	-
41882	**-0,482**	**0,0176167**	-
204610	**0,6762**	**0,0176453**	Ribosomal protein L7/L12
52503	**-0,5996**	**0,0176794**	Peptidase C19
214632	**-1,4904**	**0,0177023**	candidate acetyltransferase
44332	**0,337**	**0,0177156**	-
56903	**-0,4526**	**0,0177619**	Eukaryotic translation initiation factor
210529	**-0,5014**	**0,0177975**	-
52657	**-0,4244**	**0,0177993**	Actin/actin-like
48146	**-0,3855**	**0,0177993**	endonuclease
39592	**-0,3833**	**0,0177993**	Polyadenylate-binding protein (RRM superfamily)
172732	**-0,3433**	**0,0178049**	-

119127	**-0,4264**	**0,0178347**	Putatively involved in growth development in niger
52588	**-1,1627**	**0,0179003**	-
42186	**1,2517**	**0,0179059**	-
49730	**-0,3137**	**0,0179059**	-
205206	**-0,7164**	**0,0179059**	Hypothetical mitochondrial carrier protein
44913	**1,31**	**0,0180295**	hypothetical extracellular mon- and diacylglycerol lipase
196101	**-0,5318**	**0,0180305**	Formyl transferase
183937	**-0,6676**	**0,0180305**	Hypothetical biphenyl-2,3-diol 1,2-dioxygenase III-related protein. Glyoxalase/Bleomycin resistance protein
176433	**-0,7253**	**0,0180594**	Fungal transcriptional regulatory protein
210871	**-0,7246**	**0,0180729**	3-hydroxyacyl-CoA dehydrogenase
48970	**-0,5449**	**0,0180855**	-
187283	**-0,4933**	**0,0180981**	SNF2-related
44497	**0,9995**	**0,0181402**	Hypothetical mitochondrial carrier protein
184331	**-0,5341**	**0,018141**	-
119367	**-0,8086**	**0,018141**	Endoplasmic reticulum protein EP58
208382	**-0,3643**	**0,018141**	Predicted GTP-binding protein (ODN superfamily)
191710	**0,8223**	**0,0181681**	Candidate siderophore iron transporter mirB
193981	**-0,5956**	**0,0181681**	Putative pyruvate decarboxylase joined with TPR repeat containing protein
40489	**-0,3888**	**0,018192**	Related to C. albicans argininosuccinate synthase (EC 6.3.4.5)
174185	**-0,5395**	**0,0182022**	-
48743	**-0,5679**	**0,0182078**	Hypothetical enoyl-CoA hydratase
206200	**-0,4073**	**0,0182083**	-
55395	**0,7414**	**0,0182165**	-
51930	**-0,9942**	**0,0182165**	Gen A8; hypothetical Cyanovirin-N protein
127896	**-0,5679**	**0,0182354**	-
187304	**0,5724**	**0,0183371**	Ergosterol biosynthesis ERG4/ERG24 family
56159	**-0,4881**	**0,018352**	Related to phenylalanine-tRNA ligase of Candida albicans
40161	**-1,463**	**0,0184896**	-
54664	**-0,4923**	**0,0184896**	G-like protein containing WD-40 repeat
44379	**-0,5974**	**0,0184896**	#N/A
45801	**-0,4153**	**0,0185166**	endo-1,6-beta-D-glucanase
203335	**-0,8797**	**0,0185966**	-
193171	**-0,4634**	**0,0186106**	AAA ATPase
185892	**-0,5632**	**0,0186179**	-
52532	**0,8774**	**0,0186179**	-
36527	**-0,3227**	**0,0186946**	Predicted membrane proteins, contain hemolysin III domain

128909	**-0,5092**	**0,0186946**	#N/A
172198	**-0,4235**	**0,0187825**	putative cytochrome P450 monooxygenase
44289	**-0,5742**	**0,0187986**	-
54635	**-0,327**	**0,0188333**	-
54785	**-0,8495**	**0,0188461**	-
56673	**0,3962**	**0,0188461**	Hypothetical fumarate hydratase
121237	**-0,4333**	**0,0188462**	deaminase-reductase
206019	**-0,5403**	**0,0188548**	-
51724	**-0,4152**	**0,0188885**	Hypothetical Molecular chaperone Prefoldin
211094	**1,5383**	**0,0188885**	#N/A
56167	**-0,3566**	**0,018916**	TRIHA 14-3-3 protein homologue, putative kinase regulator
188174	**-0,652**	**0,018916**	#N/A
56880	**-0,5003**	**0,0189391**	srpA, Signal recognition particle, subunit Srp54
42184	**-0,4505**	**0,018984**	pgaX Exopolygalacturonase precursor (ExoPG) (Galacturan 1,4-alpha-galacturonidase)
51703	**-0,3356**	**0,018986**	Serine/threonine protein phosphatase
198703	**-0,5056**	**0,0190072**	Putative cargo transport protein
136823	**1,3165**	**0,0190084**	-
41300	**-0,546**	**0,0190084**	AAA ATPase
126948	**-0,6182**	**0,0190108**	-
40553	**-0,525**	**0,0190108**	-
209252	**-0,5831**	**0,0190108**	Autophagy related protein, involved in membrane trafficking
50444	**-0,9466**	**0,0190108**	Serine/threonine protein kinase Atg1
193909	**-0,6238**	**0,0190971**	Ureidoglycolate hydrolase
49922	**-0,6834**	**0,0191011**	-
37998	**-0,611**	**0,0191109**	Hypothetical protein. Is very likely associated with degradation of aromatic compounds based on Pfam and protein similarity
178353	**-0,5093**	**0,0191167**	Hypothetical N-methyltransferase
211840	**-0,3632**	**0,0192739**	#N/A
129843	**-0,4292**	**0,0193478**	-
189639	**-0,4057**	**0,0193478**	-
53084	**-0,3939**	**0,0193521**	Ubiquitin-conjugating enzymes, 16 kDa
211053	**-1,7665**	**0,0193783**	(eglA) extracellular GH family 12 endo-beta-1,4-glucanase
50499	**-0,3917**	**0,0193783**	related to 2-deoxy-D-gluconate 3-dehydrogenase
170706	**-0,4411**	**0,0194412**	Fungal transcriptional regulatory protein
136701	**-1,4672**	**0,0194819**	SAM-dependent methyltransferases
210722	**-0,3614**	**0,0194953**	Zn-finger, C2H2 type
37368	**-0,5519**	**0,0195868**	#N/A
211085	**0,5882**	**0,0195887**	Got1-like protein
207249	**0,6131**	**0,0196025**	Cysteine synthase

175695	**-0,562**	**0,0196154**	-
174310	**-0,3709**	**0,0196154**	hypothetical protein contains SH3 adaptor domains
127054	**-0,3237**	**0,0196199**	-
206038	**-0,7778**	**0,0196199**	-
52257	**-0,4041**	**0,0196199**	Ankyrin repeat
206503	**-0,4417**	**0,0196199**	Arginyl-tRNA-protein transferase
133108	**-0,5355**	**0,0196199**	Hypothetical phospholipid scramblase
46473	**-0,5608**	**0,0196199**	hypothetical short chain dehydrogenase
214048	**-0,4736**	**0,0196199**	Ribosomal protein S2
187609	**-0,3765**	**0,0196199**	This protein does not have homology with proteins with confirmed asparginase activity
129928	**-0,4027**	**0,0196199**	WD40 repeat-containing protein
182820	**-0,8444**	**0,0196199**	#N/A
40734	**-0,9227**	**0,0196849**	Hypothetical aldehyde dehydrogenase. Specificity towards NAD or NADP is not deducible from sequence data
186933	**-0,3974**	**0,019713**	Inositol polyphosphate kinase
207532	**-0,5739**	**0,019743**	-
208463	**-0,4381**	**0,019743**	-
53949	**-0,4178**	**0,019743**	Major facilitator superfamily
51662	**-0,8535**	**0,019743**	#N/A
56215	**1,5987**	**0,0197749**	Hypothetical Hydroxymethylglutaryl-coenzyme A synthase
197516	**-0,5641**	**0,0198083**	Predicted translation product shares amino acid sequence similarity to the Saccharomyces cerevisiae REX2 gene product; an RNA exonuclease, required for U4 snRNA maturation; functions redundantly with Rnh70p in 5.8S rRNA maturation, and with Rnh70p and Rex3p in processing of U5 snRNA and RNase P RNA (yeast); member of RNase D family of exonucleases.
214458	**-0,533**	**0,019837**	-
213793	**-0,7981**	**0,019837**	candidate succinate-semialdehyde dehydrogenase
207899	**-0,5802**	**0,0198528**	Major facilitator superfamily
186766	**-0,593**	**0,0198579**	-
53856	**-0,671**	**0,0198579**	Protein phosphatase
137748	**-0,7479**	**0,0198666**	-
54260	**-0,449**	**0,0199165**	Hypothetical 20S proteasome, regulatory subunit
44770	**-0,5904**	**0,019925**	-
55578	**-0,4769**	**0,019925**	20S proteasome, A and B subunits
49967	**-0,4819**	**0,019925**	#N/A
181451	**-0,9046**	**0,01993**	Hypothetical 3-methylcrotonyl-CoA carboxylase, subunit beta

212768	**-0,9261**	**0,0199552**	Related to malic oxidoreductase from S. cerevisiae (EC 1.1.1.40). May be the mitochondrial isoenzyme of protein 211661.
48905	**-0,4838**	**0,019972**	Hypothetical biotin holocarboxylase synthetase/biotin-protein ligase
195992	**-0,4654**	**0,0199798**	Hypothetical cyclic-AMP phosphodiesterase
184507	**-0,5847**	**0,0199817**	-
172404	**-0,4279**	**0,0200125**	Predicted fumarylacetoacetate hydralase
40178	**1,2935**	**0,0200367**	#N/A
54960	**-0,463**	**0,020059**	Hypothetical Cyclin D-interacting protein GCIP
43853	**0,4036**	**0,0200718**	Zn-finger, C2H2 type
46716	**-0,6187**	**0,0200852**	-
53510	**-1,1107**	**0,0201071**	Predicted ATPase, nucleotide-binding
49747	**-0,9178**	**0,0201233**	SWI-SNF chromatin-remodeling complex protein
203471	**-0,71**	**0,0201378**	Thioredoxin-like protein
179558	**-0,8629**	**0,0201524**	-
47151	**0,7494**	**0,0201551**	NADP-dependent isocitrate dehydrogenase precursor [Aspergillus niger]
46109	**0,3725**	**0,0201821**	-
47998	**-0,4775**	**0,0201961**	hypothetical phosphotyrosyl phosphatase activator
207429	**-0,3875**	**0,0201962**	-
39998	**-0,5556**	**0,0201962**	Hypothetical subunit of oligosaccharyltransferase
137452	**0,4186**	**0,0203054**	#N/A
211114	**-0,697**	**0,0203358**	-
200589	**-0,8738**	**0,0203424**	8-amino-7-oxononanoate synthase (biotin synthesis)
126001	**-1,0057**	**0,0203748**	-
56715	**0,901**	**0,0203748**	Acetyl-CoA carboxylase
38745	**0,648**	**0,0203748**	Glycosyl transferase, family 28
38373	**0,3847**	**0,0203748**	hypothetical protein; KOG Class: Chromatin structure and dynamics
120610	**-1,2591**	**0,0203748**	#N/A
37444	**-0,5873**	**0,0204995**	Predicted cation transporter
52688	**-1,6459**	**0,0205261**	candidate endoglucanase
39172	**-0,6179**	**0,0205521**	Zinc-containing alcohol dehydrogenase
190278	**-0,4672**	**0,020566**	-
43224	**-0,5227**	**0,0205966**	Fungal transcriptional regulatory protein
210117	**-1,1525**	**0,0206823**	-
120073	**-0,5319**	**0,0207189**	Serine/threonine protein kinase
170638	**-0,6354**	**0,0207556**	-
208544	**-0,6139**	**0,0207706**	Candidate ribose 5-phosphate isomerase
44098	**-0,5136**	**0,0207706**	hypothetical mannose-6-phosphate isomerase
124393	**-0,6861**	**0,0208178**	Peroxisomal NUDIX hydrolase
128213	**-0,4894**	**0,0208569**	-

45715	**-0,6541**	**0,0208569**	#N/A
181698	**-0,4655**	**0,0209694**	Importin-beta
206270	**-0,413**	**0,0209839**	Hypothetical Signal recognition particle, subunit Srp68
184532	**-1,6668**	**0,0210316**	Hypothetical hydroxyacylglutathione hydrolase
50555	**-0,416**	**0,0210316**	Hypothetical Polyadenylate-binding protein (RRM superfamily
36289	**-0,5153**	**0,0210771**	-
57079	**-0,4217**	**0,0210771**	Hypothetical DnaJ domain protein
140813	**-0,3593**	**0,0210771**	Hypothetical. Mannosyltransferase ?
198766	**-0,4708**	**0,0210771**	Putative prefoldin chaperone
39867	**0,7298**	**0,0211713**	-
50689	**0,8918**	**0,0211713**	Arginine biosynthesis protein ArgJ
38587	**1,9312**	**0,0211759**	-
122978	**-1,5876**	**0,0212087**	hypothetical extracellular GH family 43 beta-gaclatosidase, exo-beta-1,3-galactanase
54662	**0,457**	**0,0212087**	hypothetical SNF5/SMARCB1/INI1 protein - a key component of SWI/SNF-class complexes; KOG Class: Chromatin structure and dynamics; KOG Id: 1649; KOG Description: SWI-SNF chromatin remodeling complex, Snf5 subunit
181144	**0,3767**	**0,0212252**	phytoene desaturase
181371	**0,5947**	**0,0212562**	Molecular chaperones HSP70
184712	**-0,3385**	**0,0212873**	-
38433	**0,3292**	**0,0212873**	#N/A
42345	**-0,5953**	**0,0213081**	Fungal transcriptional regulatory protein
47550	**-0,3653**	**0,0213382**	-
174157	**-0,9925**	**0,0213382**	Hypothetical alcohol dehydrogenase; EC 1.1.1.1
50466	**1,0779**	**0,0213382**	putative Prolyl 4-hydroxylase, alpha subunit
40469	**-0,4695**	**0,0213644**	Fungal specific transcription factor
51738	**-0,5057**	**0,0213709**	-
53542	**-0,3726**	**0,021389**	Isopenicillin N synthase
36569	**0,436**	**0,0214562**	-
207656	**0,4442**	**0,021468**	Hypothetical serine palmitoyltransferase
48523	**-0,4544**	**0,0214969**	-
199078	**-1,1955**	**0,0215079**	Atrazine chlorohydrolase/guanine deaminase
214066	**-0,977**	**0,0215449**	ABC transporter
174055	**-0,3888**	**0,0215523**	putative tRNA acetyltransferase,
41055	**-0,3365**	**0,021603**	Ras small GTPase, Ras type
55019	**-0,7163**	**0,021608**	-
201613	**0,5528**	**0,0216117**	pentatricopeptide repeat protein. FOG: PPR repeat
51046	**-0,6437**	**0,0216213**	-
40596	**-1,1438**	**0,0216408**	Aldehyde dehydrogenase

190566	**0,3858**	**0,0216637**	Predicted endoplasmic reticulum membrane protein Lec35
54270	**-0,3997**	**0,0216637**	Predicted translation initiation factor related to eIF-2B alpha/beta/delta subunits (CIG2/IDI2)
190990	**0,6582**	**0,0217121**	Branched-chain amino acid aminotransferase
212036	**0,5145**	**0,0217155**	Tyrosine specific protein phosphatase and dual specificity protein phosphatase
55758	**-0,3904**	**0,0217542**	Zn-finger, AN1-like
57211	**-0,7593**	**0,0218091**	putative cyclin possibly similar to Pcl6 or Pcl7
39106	**0,4601**	**0,0218623**	-
36749	**-0,4294**	**0,0218623**	Collagens (type IV and type XIII), and related proteins
177912	**-0,5443**	**0,0218623**	Protein kinase
35952	**-0,6753**	**0,0218988**	-
44220	**-0,46**	**0,0218988**	Mitochondrial inheritance and actin cytoskeleton organization protein
37719	**-0,6134**	**0,0220667**	Hypothetical aldehyde dehydrogenase (EC 1.2.1.3).
199982	**-0,3994**	**0,0220846**	-
136718	**-0,3386**	**0,0220846**	Protein kinase
174131	**-0,5833**	**0,0221115**	Protein kinase
44033	**-0,3706**	**0,0221857**	(apsA) Peptidase M1
143833	**1,1139**	**0,022201**	#N/A
120986	**-0,436**	**0,0222849**	Fungal specific transcription factor
211800	**-0,733**	**0,0223062**	-
53473	**-0,5852**	**0,0223062**	-
55586	**-0,3466**	**0,0223296**	Hypothetical Ketose/fructose-bisphosphate aldolase. Zn binding ?
51124	**-0,4124**	**0,0223412**	-
171996	**-0,5493**	**0,0223412**	beta-1,6-N-acetylglucosaminyltransferase, contains WSC domain
57101	**0,4291**	**0,0223569**	#N/A
201503	**0,9615**	**0,0223572**	NAD-cytochrome b5 reductase
133134	**-0,6678**	**0,0223593**	#N/A
56528	**-0,6973**	**0,0223702**	Hypothetical histidinol phosphatase. HMMPfam indicates this activity. No homology to confirmed histidinol phosphatases was found
208365	**-0,518**	**0,0224078**	#N/A
56422	**-0,4113**	**0,0225081**	-
179747	**1,2982**	**0,022515**	3-methyl-2-oxobutanoate hydroxymethyltransferase (Ketopantoate hydroxymethyltransferase).
182627	**-0,5469**	**0,0225308**	-

43297	**-1,283**	**0,022567**	Glyoxylate/hydroxypyruvate reductase (D-isomer-specific 2-hydroxy acid dehydrogenase superfamily)
37533	**1,1633**	**0,0225986**	Unknown. SignalP predicts Anchor
38538	**-0,4169**	**0,0226799**	-
207841	**0,7393**	**0,0227867**	-
55738	**0,8672**	**0,0227867**	Multifunctional pyrimidine synthesis protein CAD (pyrABCN)
55058	**0,8709**	**0,0227867**	Putative beta-1,6-N-acetylglucosaminyltransferase, contains WSC domain
189637	**1,0922**	**0,0228226**	-
47279	**-0,6958**	**0,0228226**	Autophagy protein Apg9
184767	**-0,7859**	**0,0228226**	Cystathionine beta-synthase and related enzymes
214413	**-0,5594**	**0,0228303**	Vacuolar protein sorting-associated protein
139245	**0,945**	**0,0228811**	PEP-utilising enzyme
127337	**-0,4401**	**0,0229905**	-
213051	**-0,8411**	**0,0229905**	Hypothetical Aldose 1-epimerase
57172	**-1,2181**	**0,0230294**	-
172234	**-0,3603**	**0,0230707**	#N/A
41359	**0,5048**	**0,0230732**	hypothetical protein; KOG Class: Chromatin structure and dynamics
213512	**-0,7356**	**0,0230958**	Aldo/keto reductase family proteins
132154	**0,8485**	**0,0230958**	Cytochrome P450
56896	**-0,5452**	**0,0230958**	Polyketide synthase
42051	**-0,8331**	**0,0230971**	-
208521	**-1,7243**	**0,0230971**	hypothetical FAD/FMN-containing dehydrogenase (COG0277)with transmembrane motif
138876	**-0,8233**	**0,0231101**	beta-mannosidase A
202801	**0,3676**	**0,0231101**	citA citrate synthase
142878	**0,3424**	**0,0231101**	Esterase/lipase/thioesterase
180383	**-0,4444**	**0,0231101**	Thiamine pyrophosphokinase
35859	**-0,3652**	**0,0231421**	Candidate Porphobilinogen deaminase
38568	**-0,5584**	**0,0231421**	Fungal transcriptional regulatory protei
214644	**-0,5391**	**0,0231421**	Putative phosphoinositide phosphatase
43609	**-0,4171**	**0,0231653**	-
54613	**-0,3754**	**0,0231835**	-
54093	**-0,4693**	**0,0231835**	Phosphofructokinase
39887	**0,4483**	**0,0232083**	-
55847	**-0,5675**	**0,0232175**	hypothetical V-ATP synthase
175113	**-0,412**	**0,0232376**	Predicted Yippee-type zinc-binding protein
175821	**-0,5125**	**0,0232595**	#N/A
181915	**0,3498**	**0,0233587**	NB-ARC / TPR repeat
47753	**-1,0595**	**0,0233661**	Hypothetical Metal dependent protein hydrolase

46369	**-0,5931**	**0,0234282**	hypothetical protein with predicted SET domain & TPR repeat; KOG Class: Chromatin structure and dynamics; KOG Id: 2084; KOG Description: Predicted histone tail methylase containing SET domain
38457	**-0,5049**	**0,0234293**	V-ATPase subunit C
170443	**1,1843**	**0,0234962**	Predicted transporter
181901	**-0,4567**	**0,0236648**	-
203304	**-0,3159**	**0,0236648**	-
188502	**-0,4153**	**0,0236648**	Polyketide synthase
40033	**-0,3335**	**0,0236648**	#N/A
199043	**0,6751**	**0,0238171**	ATP Citrate lyase
53574	**0,5316**	**0,023881**	Candidate carbamoyl-phosphate synthase
211968	**-0,4676**	**0,0239158**	Fungal specific transcription factor
41759	**-0,4618**	**0,0239343**	-
192051	**-0,4661**	**0,0239392**	Putative GTPase activating proteins
38327	**1,1603**	**0,0239742**	-
197079	**0,672**	**0,0240274**	#N/A
205486	**-0,4609**	**0,0240592**	Metallophosphoesterase
208393	**-0,3703**	**0,0240864**	Helix loop helix transcription factor EB
187242	**-0,4401**	**0,0240938**	Phosphoesterases
137793	**-0,7037**	**0,0240938**	Transcription factor, Myb superfamily
170172	**-0,5554**	**0,0241036**	similar to alpha-L-rhamnosidase rhaA of Aspergillus aculeatus
38769	**-0,3359**	**0,0241759**	-
52421	**-0,406**	**0,0242129**	Peptidase M18, aminopeptidase I
53049	**-0,3832**	**0,0242129**	Ras-related small GTPase, Rho type
210321	**-0,4175**	**0,0242131**	#N/A
172796	**-0,8355**	**0,0242547**	Hypothetical urea amidolyase
179878	**-0,6713**	**0,0242914**	Predicted glutamine synthetase
35444	**-0,3922**	**0,0243016**	Hypothetical part of the anaphase-promoting complex
178864	**0,364**	**0,024312**	Protein involved in ubiquinone biosynthesis
194884	**-0,4662**	**0,0244089**	-
41708	**-0,9637**	**0,0244092**	Sensory transduction histidine kinase
56177	**-0,6317**	**0,0244963**	Hypothetical alcohol dehydrogenase
180396	**-0,794**	**0,0246265**	-
209029	**-0,7713**	**0,0246815**	-
39594	**-0,4261**	**0,0246977**	SPRT-like metalloprotease
125004	**0,59**	**0,0246977**	#N/A
42088	**-1,2163**	**0,0247029**	-
173430	**-0,3741**	**0,0247587**	Major facilitator superfamily
198099	**-2,3799**	**0,0248232**	Chloroperoxidase
38774	**-0,7765**	**0,0248922**	Amidohydrolase-like
39196	**-0,5913**	**0,0248924**	Sugar isomerase (SIS)

52818	**-0,561**	**0,0249022**	#N/A
210558	**0,5192**	**0,0249418**	Thiamine pyrophosphate-requiring enzyme
181735	**-0,6312**	**0,0250192**	Fungal specific transcription factor
183511	**-0,4834**	**0,0250192**	Fungal transcriptional regulatory protein
46759	**-0,4833**	**0,0250192**	Hypothetical protein.
50038	**-0,762**	**0,0250192**	Hypothetical, Identity with cerev. Nob 1, nuclear protein involved in proteasome maturation and synthesis of 40S ribosomal subunits
188103	**-0,4888**	**0,0250439**	-
208493	**-0,434**	**0,0251657**	-
37742	**0,9977**	**0,0251657**	Rhodopsin-like GPCR superfamily
40419	**-0,4605**	**0,0251719**	Dolichyl pyrophosphate phosphatase and related acid phosphatases
173432	**-0,4657**	**0,0251829**	-
208263	**0,3592**	**0,0251829**	Tubulin beta-1 chain
42344	**-0,6073**	**0,025184**	Hypothetical esterase/lipase
55954	**-0,3778**	**0,025184**	Peroxisomal biogenesis protein
211385	**-0,4832**	**0,0252604**	-
43035	**-0,5651**	**0,0252695**	-
196729	**-0,5005**	**0,0252695**	Hypothetical Cyclin-like protein
37126	**-0,451**	**0,0252853**	-
119438	**-0,7632**	**0,0252853**	Phosphoprotein involved in cytosol to vacuolar targeting and autophagocytosis
190584	**-0,4334**	**0,0252979**	-
135762	**-0,312**	**0,0252979**	Hypothetical Molecular chaperone (small heat-shock protein Hsp26/Hsp42
207543	**-0,4399**	**0,0252979**	Hypothetical Nuclear division RFT1 protein
209315	**0,4659**	**0,0253231**	#N/A
196275	**0,4369**	**0,0253679**	#N/A
183860	**0,4513**	**0,0253911**	Related to peptidyl-prolyl cis-trans isomerase
37291	**-0,6471**	**0,0254484**	#N/A
196583	**0,3951**	**0,0255614**	Candidate rpl12 gene, component of the large (60S) ribosomal subunit
37344	**-0,544**	**0,0255614**	Inositol polyphosphate 5-phosphatase and related proteins
48002	**-0,4434**	**0,0256004**	Amidohydrolase
174884	**-1,0807**	**0,0257112**	Hypothetical Cytochrome P450 monooxygenase
54046	**-0,6603**	**0,0257316**	Hypothetical beta-1,6-N-acetylglucosaminyltransferase, contains WSC domain
44084	**0,5277**	**0,0257316**	hypothetical. KOG suggests alkyl hydroperoxide reductase/thiol specific antioxidant
130872	**-0,3847**	**0,0257316**	Protein kinase
211948	**-0,3836**	**0,0257406**	Protein kinase

39844	**1,1708**	**0,0258236**	-
40108	**0,3518**	**0,0258855**	FOG: Ankyrin repeat
175034	**-0,4067**	**0,0258921**	#N/A
183269	**-0,3297**	**0,0258975**	-
213733	**-0,5361**	**0,0259326**	Predicted ubiquitin regulatory protein, contains UAS and UBX domains
208006	**0,5353**	**0,025945**	Fungal G-protein, alpha subunit
57437	**-0,8435**	**0,0260352**	Hypothetical protein. PFam suggests oxidoreductase activity.
135788	**-0,4862**	**0,0260817**	#N/A
41410	**0,3833**	**0,0261012**	Hypothetical. GO suggests hydrolase activity, acting on carbon-nitrogen (but not peptide) bonds. Nitrilase/cyanide hydratase and apolipoprotein N-acyltransferase
179677	**-0,7848**	**0,0261144**	Ribosomal protein S2
193642	**-0,7675**	**0,0261596**	-
45023	**-0,4602**	**0,026161**	-
49123	**0,7004**	**0,0263302**	(H2AV/H2A.Z) - histone 2A variant, involved in chromosome stability, and could through chromatin remodeling steps be involved in transcriptional regulation of selected genes and is preventing the propagation of epigenetic silencing into neighboring euchromatin; H2AV also plays a role in efficient DNA repair; H2AV shows a high degree of conservation withing the fungal kingdom; KOG Class: Chromatin structure and dynamics; KOG Id: 1757; KOG Description: Histone 2A
212570	**-0,6313**	**0,0263424**	hypothetical protein; KOG Class: Chromatin structure and dynamics; KOG Id: 1020; KOG Description: Sister chromatid cohesion protein SCC2/Nipped-B
44347	**0,5507**	**0,0263766**	Ribosomal protein L3
138230	**-0,3938**	**0,0264016**	Hypothetical subunit of vacuolar ATPase (EC 3.6.3.6)
52907	**-0,464**	**0,0264112**	Short-chain dehydrogenase/reductase
181098	**-0,326**	**0,0264737**	Peptidyl-prolyl cis-trans isomerase, cyclophilin type
200642	**-0,4942**	**0,026479**	26S proteasome regulatory complex
189770	**-0,8315**	**0,026479**	Short-chain dehydrogenase
38113	**-0,5014**	**0,0265157**	-
50075	**-0,5605**	**0,0265157**	DeoxyUTP pyrophosphatase
170479	**-0,4806**	**0,0265543**	-
130681	**-0,5115**	**0,0265901**	Fungal specific transcription factor domain

57355	**-0,3708**	**0,0266157**	-
42934	**-0,7404**	**0,0266236**	-
52334	**-0,5329**	**0,0266544**	-
45928	**1,9911**	**0,0267021**	-
41947	**-0,8785**	**0,0267021**	hypothetical protein with basic-leucine zipper domain
50766	**1,1871**	**0,0267738**	Hypothetical protein. HMMPfam indicates Zinc-containing alcohol dehydrogenase activity
51797	**-0,6232**	**0,0267738**	Predicted transcription factor
171480	**-0,374**	**0,0267757**	Cys/Met metabolism pyridoxal-phosphate-dependent enzymes
206638	**1,255**	**0,0267797**	Aconitate hydratase
53521	**-0,5195**	**0,0268017**	Hypothetical COP9 signalosome, subunit CSN5
50560	**-0,6899**	**0,0268401**	Predicted ubiquitin regulatory protein
40014	**-0,4077**	**0,0269377**	hypothetical amidase
121949	**-0,5054**	**0,0269741**	-
212427	**-0,3945**	**0,0269807**	#N/A
39673	**0,5191**	**0,0270508**	Nucleolar GTPase/ATPase p130
200242	**-0,4461**	**0,0270596**	Gtr1/RagA G protein
189424	**0,3078**	**0,027135**	putative glycosyl transferase
192093	**-0,7798**	**0,0271819**	Major facilitator superfamily
36609	**-0,5711**	**0,0271898**	#N/A
214844	**0,6355**	**0,0272164**	-
175251	**-0,5467**	**0,0272164**	Hypothetical 3-hydroxyacyl-CoA dehydrogenase
205468	**-0,4524**	**0,0272487**	Hypothetical Sec63, DnaJ like
38013	**-0,3538**	**0,0272758**	#N/A
53338	**0,4413**	**0,0273268**	Related to dihydrolipoamide acetyltransferase, EC 2.3.1.12
198063	**-0,6446**	**0,02734**	(suc1) extracellular GH family 32 beta-fructofuranosidase (invertase)
53518	**-0,449**	**0,02734**	Phosphoribosyltransferase
48817	**-0,4326**	**0,0273481**	Transcription initiation factor IIA, gamma subunit
42044	**-0,7156**	**0,0273933**	-
45754	**-0,3501**	**0,0274393**	hypothetical glutamine tRNA synthetase
55614	**0,8778**	**0,027508**	GNS1/SUR4 membrane protein
52233	**-0,4822**	**0,0275238**	#N/A
210730	**-1,3991**	**0,027539**	related to Thermomyces lanuginosus triacylglycerol lipase
41820	**-0,3314**	**0,0275611**	-
212500	**-0,668**	**0,0275773**	Aromatic amino acid aminotransferase and related proteins
35897	**-0,3574**	**0,0275773**	COP9 signalosome, subunit CSN7

36871	**0,9723**	**0,0275773**	putative midasin, the largest ORF found in yeast that is believed to play a role in nuclear protein folding
143899	**-0,4619**	**0,0275864**	-
173825	**0,5456**	**0,0275864**	Candidate Alpha-1,2 glucosyltransferase alg10
50044	**-0,534**	**0,02761**	related to ubiquitin conjugating enzyme
40762	**-0,3652**	**0,02761**	#N/A
49586	**-0,8563**	**0,0276128**	-
130415	**-0,442**	**0,0276128**	Hypothetical FAD dependent oxidoreductase
36386	**-0,5575**	**0,0276537**	Flavonol reductase/cinnamoyl-CoA reductase
52315	**-0,7026**	**0,0277782**	-
40959	**-0,4736**	**0,0278384**	-
175167	**-0,4654**	**0,0278449**	hypothetical Silent Information regulator protein Sir2p; KOG Class: Chromatin structure and dynamics; KOG Id: 2682; KOG Description:NAD-dependent histone deacetylases and class I sirtuins (SIR2 family)
35589	**-0,4589**	**0,027886**	Flavonol reductase/cinnamoyl-CoA reductase
55668	**-0,3046**	**0,027913**	Sugar transporter
211789	**0,4121**	**0,0280037**	#N/A
51717	**0,3129**	**0,0280299**	hypothetical Mitochondrial phosphate carrier protein
171507	**-0,5194**	**0,0280969**	Related to S. pombe Histidinol-phosphate aminotransferase (EC 2.6.1.9)
191378	**-0,482**	**0,0281089**	-
35485	**-1,0707**	**0,0281089**	Related to saccharopine dehydrogenase (EC 1.5.1.10) from Magnaporthe grisea
194814	**-0,6773**	**0,0281226**	-
46621	**-1,0155**	**0,0281419**	hypothetical amylo-alpha-1,6-glucosidase. Glycogen debranching
39299	**-0,754**	**0,0281792**	Hypothetical. Putative protein kinase domain
179991	**-0,4175**	**0,0282198**	-
197370	**-0,3899**	**0,0282198**	-
210156	**-0,3766**	**0,0282198**	-
36830	**0,633**	**0,0282421**	-
38819	**0,3426**	**0,0282421**	-
55026	**-0,3222**	**0,0282782**	Di-trans-poly-cis-decaprenylcistransferase
51351	**-0,583**	**0,0282782**	Hypothetical phthalate dioxygenase reductase
42698	**-0,4078**	**0,0282878**	-
194162	**0,7726**	**0,0282952**	Amino acid transporters
208547	**0,7437**	**0,0282952**	ATP-citrate lyase
189620	**-1,0901**	**0,0282952**	hypothetical glycoside hydrolase family 2 protein
210597	**-0,5303**	**0,0282952**	#N/A

176339	**-0,4284**	**0,0283058**	hypothetical protein with predicted histone-fold; KOG Class: Transcription; KOG Id: 3902; KOG description: Histone acetyltransferase PCAF/SAGA, subunit SUPT3H/SPT3
212412	**0,6345**	**0,0283314**	#N/A
200704	**-0,7669**	**0,0283344**	Notchless-like WD40 repeat-containing protein
173759	**0,693**	**0,0283344**	#N/A
210108	**-0,6701**	**0,0284065**	AMP-dependent synthetase and ligase
140888	**-0,6359**	**0,0284065**	Glutathione S-transferase
203777	**-0,4854**	**0,0284546**	Hypothetical mitochondrial substrate carrie
185679	**-0,4864**	**0,0284546**	Tyrosine specific protein phosphatase
47102	**-0,3956**	**0,0285008**	Protein phosphatase 2A, regulatory B subunit
139507	**0,4126**	**0,0285008**	Transcription initiation factor TFIID, subunit BDF1 and related bromodomain proteins
171671	**-0,3563**	**0,0285008**	Ubiquitin-conjugating enzymes
42916	**-0,4061**	**0,0285162**	related to alpha-L-rhamnosidase
42079	**-1,0097**	**0,0285177**	-
205259	**-0,97**	**0,0285221**	Short-chain dehydrogenase/reductase SDR
196625	**-0,5774**	**0,0286973**	Hypothetical. KOG: putative COPII vesicle protein
182008	**-0,2914**	**0,0286973**	#N/A
56530	**-0,6154**	**0,0287054**	Fungal specific transcription factor
213612	**-0,913**	**0,0287054**	Nucleolar GTPase
122951	**0,9027**	**0,0287222**	Glycine cleavage system T protein
173212	**-0,8589**	**0,0287618**	Hypothetical 6-phosphogluconate dehydrogenase, NAD-binding
189430	**-0,7523**	**0,0289352**	Hypothetical 2-nitropropane dioxygenase. (EC 1.13.11.32)
56485	**-0,347**	**0,0289605**	GPDA Glyceraldehyde 3-phosphate dehydrogenase
56560	**-0,4481**	**0,028973**	-
54027	**-0,5037**	**0,028973**	Hypothetical pyridoxin synthesis protein/ Imidazoleglycerol-phosphate synthase subunit H-like
35956	**-0,4135**	**0,0292328**	-
40692	**0,6741**	**0,0292374**	Glycosyl hydrolases family 16
137643	**-0,584**	**0,0292374**	Hypothetical copper transporter
47410	**1,4845**	**0,0292374**	hypothetical protein with predicted fungal transcriptional regulatory domain
170270	**-0,5427**	**0,0292374**	Nitrilase/cyanide hydratase and apolipoprotein N-acyltransferase
134131	**0,6389**	**0,0292455**	-
193991	**-0,462**	**0,0293004**	-
51962	**-0,7684**	**0,0293535**	Transcription factor, Myb superfamily
174236	**0,9217**	**0,0295231**	-
135361	**-0,6462**	**0,0295725**	-

55278	**-0,5118**	**0,0295725**	Hypothetical protein containing helix-turn-helix, Fis-type domain
212395	**-0,3952**	**0,0296161**	#N/A
50589	**-0,363**	**0,029649**	Putative Ubiquitin-conjugating enzymes, SUMO
38689	**-0,4624**	**0,0296865**	-
36895	**-0,4615**	**0,0296967**	SAM-dependent methyltransferases
46698	**-0,514**	**0,0296998**	#N/A
211011	**-0,2873**	**0,0297081**	-
214562	**-0,4066**	**0,0297339**	-
52568	**-1,1964**	**0,0297339**	Aconitase/homoaconitase (aconitase superfamily)
192202	**-0,8641**	**0,0297343**	Transketolase, C-terminal domain
133913	**-0,3147**	**0,0297474**	-
201277	**0,6582**	**0,0297704**	Major intrinsic protein
54095	**0,3206**	**0,0298606**	Sugar (ANd other) transporter
48775	**-0,6328**	**0,0299215**	#N/A
51646	**-1,1972**	**0,0300837**	epoxide hydrolase
43191	**-0,4274**	**0,0301201**	Peptidase C48, SUMO/Sentrin/Ubl1
184552	**-0,5094**	**0,0301775**	ABC transporter
130791	**-0,4178**	**0,0301775**	Fungal specific transcription factor
179368	**0,2881**	**0,0301877**	Major facilitator superfamily
37999	**0,3474**	**0,0302296**	-
50333	**-0,4128**	**0,0302296**	putative extracellular phytase
137941	**-0,6216**	**0,0302464**	-
43230	**-0,3657**	**0,0303244**	Hypothetical SNARE protein
203246	**0,3274**	**0,0304833**	40S ribosomal protein S24
53274	**-0,8515**	**0,0305481**	-
39502	**0,3846**	**0,0305564**	#N/A
56641	**0,6788**	**0,0305633**	Glucose/ribitol dehydrogenase
54937	**-0,3831**	**0,0306623**	Hypothetical prephenate hydratase
55707	**-0,3202**	**0,030676**	Nucleotide-sugar transporter
41163	**-0,5138**	**0,030676**	unknown (decarboxylase ?)
180211	**-0,5199**	**0,0307516**	Alpha/beta hydrolase
213414	**0,3557**	**0,0307676**	Predicted transporter (ABC superfamily)
183617	**-0,6785**	**0,0307954**	-
43466	**-0,3391**	**0,0308748**	-
52291	**-0,4273**	**0,0308748**	Anion-transporting ATPase
120585	**-0,3408**	**0,030906**	Tyrosine protein kinase
170230	**-0,6979**	**0,0309189**	-
54758	**-0,3655**	**0,0309189**	Predicted undecaprenyl diphosphate synthase
126448	**-0,4299**	**0,030929**	#N/A
36134	**-0,4304**	**0,0309497**	Myosin regulatory light chain
119101	**0,4636**	**0,0310555**	Nucleolar GTPase/ATPase p130
193846	**-0,4738**	**0,031208**	Hypothetical peptidyl-prolyl cis-trans isomerase, cyclophilin type

203834	**-0,425**	**0,0312188**	Alkyl hydroperoxide reductase, thiol specific antioxidant and related enzymes
54233	**-0,4364**	**0,0312188**	Glycosyl transferases group 1
189097	**-0,7562**	**0,0312188**	Related to pyruvate decarboxylase; EC 4.1.1.1
181931	**-0,4031**	**0,0312188**	Transcription factor with Helix-loop-helix DNA-binding domain
43055	**0,7837**	**0,0312578**	-
171101	**-0,6006**	**0,0312578**	Actin-binding, cofilin/tropomyosin type
48902	**-0,2963**	**0,0313037**	-
133280	**-0,3661**	**0,031383**	#N/A
188804	**-0,3768**	**0,0314612**	-
210760	**1,03**	**0,0314907**	-
48846	**0,5888**	**0,03165**	-
209775	**-0,5895**	**0,0316542**	-
39382	**0,4035**	**0,0316871**	Ca2+/H+ antiporter VCX1 and related proteins
37529	**-0,3958**	**0,0316889**	#N/A
41597	**0,4784**	**0,0317658**	-
47696	**-0,6228**	**0,0317664**	-
170223	**-0,6306**	**0,0317866**	putative GH family 81 endo-1,3-beta-glucanase
52969	**0,9513**	**0,0318069**	Importin-beta, N-terminal
140217	**2,0523**	**0,0318089**	Major facilitator superfamily
172849	**1,1569**	**0,0319005**	-
52839	**-0,381**	**0,031933**	-
39104	**0,5153**	**0,031933**	Metacaspase involved in regulation of apoptosis
171583	**-0,4569**	**0,0319857**	-
57451	**-0,3077**	**0,0319857**	Hypothetical ATP (CTP):tRNA-specific tRNA nucleotidyltransferase.
122948	**-0,4136**	**0,0320188**	-
214434	**-0,3922**	**0,0320188**	Fungal transcriptional regulatory protein
182143	**-0,4008**	**0,0320497**	Cytochrome P450
181888	**-0,5632**	**0,0321869**	Carboxyl transferase
40477	**-1,1629**	**0,0321869**	Hypothetical. Some similarity to alkylhydroperoxidase
41311	**-0,3849**	**0,032191**	Insulinase-like
189528	**-1,1791**	**0,0322381**	-
37193	**-0,4779**	**0,0323455**	#N/A
134514	**0,3357**	**0,0323761**	-
54966	**0,4823**	**0,0324191**	-
213255	**1,1465**	**0,032512**	Zn-finger, C2H2 type
46259	**-0,9682**	**0,0325223**	FMN-dependent alpha-hydroxy acid dehydrogenase, active site
143591	**-0,727**	**0,03264**	#N/A
52387	**-0,4301**	**0,0328567**	Hypothetical H+-transporting two-sector ATPase
42378	**0,4428**	**0,0329652**	Esterase/lipase/thioesterase

202003	**-0,3989**	**0,0329913**	Hypothetical PEP-utilizing enzyme
172245	**-0,2775**	**0,0330027**	Unknown protein product
178324	**-0,4159**	**0,0330027**	#N/A
186407	**-0,4555**	**0,0330283**	Thioesterase superfamily
212968	**-0,6733**	**0,0330283**	Zinc-containing alcohol dehydrogenase
127783	**-0,5436**	**0,0331974**	-
52885	**-0,406**	**0,0332958**	Cullin
54483	**0,3771**	**0,0333375**	Related to squalene synthetase (EC 2.5.1.21). Involved in lipid biosynthesis.
52698	**-0,3872**	**0,0334722**	-
178797	**-0,3606**	**0,0334763**	Peptidase C12, ubiquitin carboxyl-terminal hydrolase 1
175816	**-0,3409**	**0,0334846**	-
35666	**0,4092**	**0,0335411**	FAD linked oxidase
37994	**0,3013**	**0,033559**	Major facilitator superfamily
52326	**-0,4166**	**0,0337193**	Glutathione peroxidase
43477	**0,3743**	**0,0337339**	-
194898	**-0,5426**	**0,0338305**	-
172485	**-0,5763**	**0,0338862**	Predicted membrane protein
183678	**0,3138**	**0,03393**	Major facilitator superfamily
39923	**-0,4443**	**0,0339604**	Arylacetamide deacetylase
173689	**-0,5453**	**0,0339912**	Protein kinase
205291	**-0,682**	**0,0340042**	Isocitrate and isopropylmalate dehydrogenases
36954	**-0,382**	**0,0340799**	-
210525	**-0,4113**	**0,034088**	-
173997	**1,4055**	**0,0340884**	Deduced translation product shares amino acid sequence identity with the Saccharomyces cerevisiae NSR1 gene product; a nucleolar protein that binds nuclear localization sequences, required for pre-rRNA processing and ribosome biogenesis.
52706	**-0,3903**	**0,0341081**	Nucleoside phosphatase
41616	**-0,3616**	**0,0343321**	Proteinase inhibitor I25, cystatin
39869	**-0,6719**	**0,0343361**	RRM domain
127561	**0,5647**	**0,0345911**	-
170758	**-0,8952**	**0,0345944**	-
52997	**-0,5295**	**0,0345944**	E3 ubiquitin protein ligase
179998	**-0,4306**	**0,0345944**	#N/A
209086	**-0,4816**	**0,0346213**	(racA) Ras-related small GTPase, Rho type
53116	**-0,4465**	**0,0346227**	-
204783	**-0,3519**	**0,0346455**	Hypothetical ADAM ("a disintegrin and metalloprotease")family gene
36031	**-0,3401**	**0,0346703**	Putative GroEL-like chaperone, ATPase
54532	**0,975**	**0,0347042**	Amino acid/polyamine transporter I

185870	**-0,3315**	**0,0347277**	No homology to confirmed arginine N-methyltransferases (EC 2.1.1.2)
119741	**-0,3606**	**0,0347666**	Hypothetical Cl- channel, voltage gated
57202	**-0,343**	**0,0347939**	-
137474	**-0,4503**	**0,0348841**	#N/A
47908	**-0,7316**	**0,0349744**	Short-chain dehydrogenase/reductase SDR
183349	**-0,5993**	**0,0350982**	Cytochrome P450
137095	**-0,2855**	**0,0351084**	#N/A
38103	**-0,619**	**0,0351105**	Hypothetical Damage-specific DNA binding protein
41756	**-0,461**	**0,0351471**	Amidohydrolase
40946	**0,925**	**0,035217**	#N/A
175389	**-0,3373**	**0,0352725**	-
46378	**-0,6974**	**0,0352973**	-
56494	**-0,3406**	**0,0352973**	-
35383	**-0,4072**	**0,035446**	-
212533	**-0,3954**	**0,0354569**	#N/A
42282	**0,644**	**0,0354908**	-
136905	**-0,4385**	**0,035536**	Candidate Vps32 homologue
208357	**-0,3701**	**0,0355445**	-
128421	**-0,7126**	**0,035577**	#N/A
195357	**-0,4381**	**0,035577**	#N/A
48811	**-0,6305**	**0,0355801**	(xlnR) Transcriptional activator xlnR
57297	**-0,4276**	**0,0355801**	Hypothetical Mg2+ transporter protein, CorA-like
172690	**-0,3171**	**0,0355801**	Hypothetical protein with Cytochrome c heme-binding site
42644	**-0,4384**	**0,0355801**	Poly(ADP-ribose) polymerase, regulatory region
208699	**0,433**	**0,0355801**	Predicted translation product shares amino acid sequence identity with the Saccharomyces cerevisiae RSC9 gene product; one of 15 subunits of the 'Remodel the Structure of Chromatin' (RSC) complex; DNA-binding protein involved in the synthesis of rRNA and in transcriptional repression and activation of genes regulated by the Target of Rapamycin (TOR) pathway.
209062	**-0,7109**	**0,0355801**	WASP-interacting protein VRP1/WIP
178173	**-0,6258**	**0,0356137**	-
47399	**-0,3696**	**0,0356191**	Aminoacyl-tRNA synthetase, class I
50921	**0,3898**	**0,0356191**	hypothetical Short-chain dehydrogenase/reductase SDR
189889	**0,2725**	**0,0356228**	hypothetical aminotransferase
176315	**-0,56**	**0,0358018**	Carboxymethyl transferase
56063	**-0,4024**	**0,035825**	Rac GTPase-activating protein BCR/ABR
130919	**-0,3746**	**0,0358564**	RING finger protein
175824	**0,3285**	**0,0358881**	#N/A

185842	**-1,1377**	**0,0359584**	cytochrome b5
208917	**-0,4917**	**0,0359875**	Ubiquitin-conjugating enzyme
208535	**-0,6161**	**0,0360031**	-
41915	**-0,4376**	**0,0360031**	-
40329	**-0,442**	**0,0360889**	Hypothetical sec1-like protein
40966	**-0,6354**	**0,03613**	Cu/Zn Superoixide dismutase
37122	**0,3448**	**0,0361862**	Dynactin, subunit p25
137591	**-0,4963**	**0,0362518**	-
53484	**-0,5962**	**0,0362707**	-
194194	**-0,3875**	**0,0362707**	#N/A
39346	**-0,6725**	**0,0363207**	hypothetical protein containing Ada, metal-binding and helix-turn-helix, AraC type domains.
209050	**0,3593**	**0,0367092**	Radical SAM superfamily
47785	**-0,5528**	**0,036937**	hypothetical protein with esterase/lipase/thioesterase motif
130834	**-0,7561**	**0,0369408**	Fungal specific transcription factor
210387	**-0,4478**	**0,0370105**	(pelF) Pectine lyase F. Involved in pectine degradation (EC 4.2.2.10)
179788	**0,6898**	**0,0370105**	Hypothetical DNA-directed DNA polymerase B
41282	**-0,4624**	**0,037036**	-
192778	**-0,5027**	**0,037036**	#N/A
127000	**-0,3235**	**0,0370602**	-
53115	**-0,3255**	**0,0371559**	-
53694	**-0,5109**	**0,0371774**	#N/A
41723	**-0,5632**	**0,0371825**	Hypothetical Cytochrome P450 monooxygenase
131283	**-0,3697**	**0,0371825**	hypothetical lipase
52085	**-0,5441**	**0,0371825**	#N/A
211957	**-0,3434**	**0,0372954**	protein phosphatase
55264	**-0,3302**	**0,0374311**	Putative transcriptional repressor
50257	**-0,377**	**0,0374506**	-
54393	**-0,3165**	**0,0374506**	-
124912	**-0,9294**	**0,0374506**	Choline kinase
50105	**-0,3934**	**0,0374986**	hypothetical glucose transporter
206304	**0,4902**	**0,0374986**	Hypothetical RAS GTPase
45504	**-0,4019**	**0,0375142**	-
119698	**-0,4268**	**0,0375679**	hypothetical protein, related to yeast zds family proteins; KOG Class: Chromatin structure and dynamics; KOG Id: 1472; KOG Description:Histone acetyltransferase SAGA/ADA, catalytic subunit PCAF/GCN5 and related proteins
49598	**-1,1679**	**0,0376503**	Pyridine nucleotide-disulphide oxidoreductase, class-II
133594	**-0,3798**	**0,0376503**	SAM-dependent methyltransferases
182167	**-0,4296**	**0,0377524**	Hypothetical DNA mismatch repair protein

56523	**-0,5325**	**0,0377552**	related to leucine aminopeptidase
38174	**-0,5655**	**0,0377626**	-
199345	**-0,5426**	**0,0377626**	Hypothetical F-actin capping protein, alpha subunit
54077	**-0,9734**	**0,0377626**	Major intrinsic protein
206009	**0,356**	**0,0378572**	Hypothetical Alpha tubulin
212470	**-0,3719**	**0,0380161**	Peptidase C19
178578	**-0,4227**	**0,0380161**	Phospholipase/carboxyhydrolase
208820	**-0,341**	**0,0380753**	Predicted Acyltransferase
54109	**-0,4812**	**0,0380753**	Ras-related GTPase
205776	**-0,3156**	**0,0381211**	Predicted membrane protein
42214	**-0,3452**	**0,038148**	Fungal transcriptional regulatory protein
120396	**-0,3434**	**0,038148**	Splicing coactivator SRm160/300, subunit SRm300
135497	**-0,4177**	**0,0381701**	Alanine racemase
39268	**-0,4868**	**0,0381701**	Fungal specific transcription factor
186516	**0,3326**	**0,038373**	-
45402	**-0,4234**	**0,0384504**	#N/A
208179	**-0,4482**	**0,0384903**	Surf 4 protein . ER to Golgi transport
52215	**-0,4585**	**0,0385006**	-
178895	**-0,4819**	**0,0385006**	#N/A
175854	**0,4436**	**0,0386108**	-
43533	**1,0279**	**0,0386362**	-
177966	**-0,4169**	**0,0386456**	Fungal specific transcription factor
173459	**0,7443**	**0,0386568**	-
38626	**-0,4638**	**0,0386717**	hypothetical DEAH-box helicase; KOG Class: RNA processing and modification; KOG Id: 0922; KOG description: DEAH-box RNA helicase
42073	**0,4027**	**0,0386968**	-
57403	**-0,4055**	**0,0386968**	-
52553	**-0,41**	**0,0387677**	#N/A
56149	**-0,4984**	**0,038838**	Metallophosphoesterase
38958	**-0,3137**	**0,0389349**	Hypothetical Cytochrome P450 monooxygenase
54102	**0,302**	**0,0390236**	#N/A
57417	**-0,3739**	**0,0390236**	#N/A
202763	**-0,4206**	**0,0391261**	Small nuclear ribonucleoprotein
40476	**-0,9734**	**0,0391452**	-
192595	**-0,5008**	**0,0392157**	-
41548	**-0,5373**	**0,0392157**	-
37741	**0,4688**	**0,0392638**	-
183137	**-0,4719**	**0,0393727**	#N/A
57271	**0,6662**	**0,0394936**	#N/A
190324	**-0,442**	**0,0395018**	-
57283	**-0,4494**	**0,0395885**	This protein is involved in sexual reproduction;
50645	**-0,3645**	**0,0396597**	-
183410	**-0,4465**	**0,0396695**	-

214718	**-0,4346**	**0,0398722**	Hypothetical transport protein. Belongs to the major facilitator superfamily and has 11 putative transmembrane domains
52318	**-0,6887**	**0,0398786**	Hypothetical glycosyl transferase. Related to N. crassa clock-controlled gene-9 protein
170145	**1,018**	**0,040052**	-
196617	**-0,385**	**0,0402723**	GCN5-related N-acetyltransferase
56472	**-0,3803**	**0,0403209**	-
42086	**0,4248**	**0,0405716**	-
192770	**0,5084**	**0,0405716**	hypothetical protein with predicted NAP and Poly(A) polymerase domains; KOG Class: Chromatin structure and dynamics; KOG Id: 1507; KOG Description: Nucleosome assembly protein NAP-1
197463	**0,4229**	**0,0405771**	Mitochondrial large ribosomal subunit
55430	**0,3351**	**0,0406452**	#N/A
52539	**-0,5664**	**0,0406467**	-
56378	**-0,6059**	**0,0406467**	-
176865	**-0,3774**	**0,0406467**	Hypothetical GPI anchor protein
212876	**0,2934**	**0,0406646**	Ribosomal protein S5
57352	**0,3315**	**0,0408113**	Ribosomal protein S6e
54389	**0,4783**	**0,0408433**	-
203398	**-1,0573**	**0,041031**	Acyltransferase 3
43416	**0,4572**	**0,0411178**	-
191145	**-0,3185**	**0,0411178**	Esterase/lipase/thioesterase
207276	**-1,2259**	**0,0411755**	UDP-glucose 4-epimerase
211774	**-0,6141**	**0,0412506**	Amino acid/polyamine transporter I
53113	**0,2964**	**0,0412506**	Histone 2A
54765	**-0,3421**	**0,0412584**	-
176254	**0,6722**	**0,0413472**	-
39573	**-0,4147**	**0,0413472**	-
173033	**-0,6882**	**0,0414228**	Translation initiation factor 4F
55897	**0,626**	**0,0414603**	Haem peroxidase, plant/fungal/bacterial
55072	**-0,3654**	**0,0414726**	Fungal transcriptional regulatory protein
131964	**-0,3718**	**0,0414726**	GTP1/OBG subdomain
44367	**-0,2958**	**0,0414771**	-
125380	**-0,5418**	**0,0414771**	Esterase/lipase/thioesterase
186946	**-0,4146**	**0,0414771**	Hypothetical protein. Putative Adenosine deaminase/editase
131319	**0,4482**	**0,0414771**	Major facilitator superfamily
51421	**-0,7198**	**0,0414771**	Major facilitator superfamily
203913	**-0,3339**	**0,0414771**	#N/A
52870	**-0,8222**	**0,0416319**	Sugar (ANd other) transporter
186415	**-0,5261**	**0,0417489**	Short-chain dehydrogenase/reductase
170269	**-0,4424**	**0,0418578**	-

45631	**1,229**	**0,0419134**	Ankyrin
47586	**-0,4107**	**0,0419721**	Fungal specific transcription factor
139052	**-0,3683**	**0,0419721**	hypothetical adaptin gamma subunit
206654	**-0,4169**	**0,0420054**	Fungal transcriptional regulatory protein
44408	**-0,4356**	**0,0420104**	#N/A
119850	**-0,2956**	**0,042045**	-
192427	**-0,3759**	**0,0422399**	-
181231	**-0,3547**	**0,0423021**	#N/A
207006	**-0,3995**	**0,0423562**	-
47885	**-0,5243**	**0,0423562**	-
35358	**0,5591**	**0,0424823**	CCAAT-binding transcription factor,
173111	**-0,4175**	**0,0425819**	Ras small GTPase
55539	**0,5235**	**0,0428745**	Methylenetetrahydrofolate reductase
53849	**-0,3451**	**0,0430017**	-
54071	**0,7774**	**0,0430575**	-
190631	**-0,4218**	**0,0430575**	O-methyltransferase
206764	**0,672**	**0,0430575**	#N/A
44298	**-0,3484**	**0,0430575**	#N/A
171532	**-0,4588**	**0,0433283**	-
52536	**-0,444**	**0,0433744**	Ubiquitin-conjugating enzyme
45134	**0,3388**	**0,0435148**	-
45764	**0,8422**	**0,0435461**	hypothetical aspartate transaminase (EC 2.6.1.1)
48389	**0,6937**	**0,0435461**	Predicted transporter (major facilitator superfamily
45789	**-0,7776**	**0,0436007**	hypothetical copper amine oxidase
54156	**0,6303**	**0,0436427**	putative Heat shock protein DnaJ
202653	**0,2765**	**0,0436482**	putative Ribosomal protein 60S
187232	**0,7088**	**0,0436514**	-
38570	**-0,3747**	**0,0436689**	Fibronectin type III domain
120291	**0,3931**	**0,0437536**	ABC transporter
42805	**-0,4658**	**0,0437858**	-
51721	**-0,3054**	**0,0437874**	-
44378	**-0,5436**	**0,0437989**	-
140013	**-0,9744**	**0,0438088**	Major facilitator superfamily
200072	**0,6188**	**0,0439341**	Hypothetical protein with cytochrome c heme-binding site
43711	**0,5981**	**0,0439511**	beta-1,6-N-acetylglucosaminyltransferase
182707	**0,3811**	**0,0439511**	hypothetical chitin-binding protein
126931	**0,3455**	**0,0439511**	Hypothetical glutathione S-transferase
47218	**-0,4548**	**0,043969**	-
179711	**-0,4074**	**0,043969**	#N/A
56339	**1,9421**	**0,0439698**	Related to sulphate permease. Has 11 transmembrane domains and several sulphate transporter domains.
195459	**-0,4384**	**0,0439746**	#N/A

213660	**-0,4475**	**0,0440082**	Leucine rich repeat protein
52163	**-0,3488**	**0,0440881**	Actin/actin-like
47331	**-0,4292**	**0,0441243**	Eukaryotic protein kinase domain. Related to cell cycle checkpoints
56808	**-0,331**	**0,0441243**	putative translation initiation factor related to the eIF-2B alpha subunit
35727	**-0,5239**	**0,0441333**	-
196638	**0,5394**	**0,0441906**	60S acidic ribosomal protein P0
56013	**-0,4857**	**0,0443746**	Serine/threonine kinase
178649	**-0,4909**	**0,0444781**	Nucleolar GTPase/ATPase p130
36287	**-0,2719**	**0,0444992**	Candidate anbA gene
205494	**0,465**	**0,0446419**	B-cell receptor-associated protein and related proteins
214476	**-0,499**	**0,0446419**	hypothetical protein containing Zn-finger, C2H2 type domain
170319	**-0,412**	**0,0446419**	Major facilitator superfamily
211722	**-0,3485**	**0,0447023**	Ras GTPase
54886	**-0,4152**	**0,0447023**	#N/A
199148	**-0,3995**	**0,0448221**	Candidate Fumarylacetoacetase
182157	**-0,3827**	**0,044889**	-
43260	**0,5596**	**0,0449788**	-
39100	**-0,4363**	**0,0449862**	hypothetical Aflatoxin biosynthesis regulatory protein
192500	**-0,3385**	**0,0449899**	Fungal transcriptional regulatory protein
134242	**-0,418**	**0,0450755**	-
184104	**-0,4628**	**0,0450755**	-
46090	**-0,6373**	**0,0450755**	#N/A
38280	**-0,5651**	**0,0450965**	Oxidosqualene-lanosterol cyclase and related proteins
136363	**-0,3116**	**0,0451594**	#N/A
127827	**-0,4044**	**0,0451725**	Translation initiation factor 1A
138144	**0,5886**	**0,0453278**	Ribosomal L32p protein
41958	**-0,2841**	**0,0453652**	Transport protein particle (TRAPP) complex subunit
52017	**-0,4236**	**0,0454063**	-
42362	**-0,3689**	**0,045441**	Major facilitator superfamily
197123	**-0,3899**	**0,0455715**	Rab GDI protein
47458	**-0,5902**	**0,0455991**	-
52269	**0,7946**	**0,0455991**	-
52755	**0,3997**	**0,0456259**	Hypothetical diacylglycerol kinase
51852	**-0,426**	**0,0456559**	Phox-like
119224	**-0,4686**	**0,0456793**	Transcription coactivator
41900	**-1,8779**	**0,0456813**	-
128800	**-0,6144**	**0,0456813**	ABC superfamily
181530	**-0,4139**	**0,0458866**	#N/A

132538	**-0,8411**	**0,0459361**	Sorbin and SH3 domain-containing protein (signal transduction)
55205	**-0,7097**	**0,0459814**	hypothetical short chain dehydrogenase
135398	**0,2891**	**0,0460661**	-
191172	**-0,525**	**0,0460835**	#N/A
45972	**0,439**	**0,046103**	Hypothetical protein. Induced at pH 2.5.
204315	**-0,5109**	**0,0461465**	Hypothetical. Interpro suggests Cupin domain. Sugar isomerase activity ?
53121	**-0,4029**	**0,0462336**	Choline transporter-like protein
189666	**-0,8837**	**0,0462593**	Aminoacyl-tRNA synthetase
178492	**0,6094**	**0,0464757**	-
53994	**0,447**	**0,0464757**	-
52673	**-0,4059**	**0,0464757**	hogA, osmotic sensitivity mitogen-activated protein (MAP) kinase
213652	**-0,3615**	**0,0464757**	Protein kinase
41401	**-0,3415**	**0,0465505**	#N/A
127816	**-0,3056**	**0,0465731**	SNARE protein
120809	**-0,5989**	**0,0467263**	Flavoprotein monooxygenase
38759	**-0,4213**	**0,0469931**	-
54150	**-0,5073**	**0,0470614**	-
140694	**-0,4958**	**0,047127**	#N/A
181664	**0,4653**	**0,0471281**	Large RNA-binding protein (RRM superfamily)
55911	**-0,43**	**0,0473075**	#N/A
136883	**-0,3977**	**0,0474188**	-
124391	**-0,3376**	**0,0475912**	Glutamate 5-kinase
57068	**-0,296**	**0,0475949**	AICAR transformylase/IMP cyclohydrolase/methylglyoxal synthase
43065	**-0,5122**	**0,0476433**	Ribonuclease III
40412	**-0,4385**	**0,0476433**	Synaptobrevin/VAMP-like protein
55208	**0,978**	**0,0476533**	-
54938	**-0,3473**	**0,0476885**	Polypeptide release factor involved in translation termination.
44465	**-0,4761**	**0,0477122**	#N/A
175546	**-0,5533**	**0,0479056**	Major facilitator superfamily
47529	**-0,4191**	**0,0479307**	-
192619	**-0,3997**	**0,0479734**	Serine carboxypeptidase
41719	**-0,5284**	**0,0480177**	hypothetical FAD/FMN-containing dehydrogenase
195017	**-0,4105**	**0,0480374**	#N/A
186699	**-0,4879**	**0,0480433**	-
207032	**-0,6583**	**0,048052**	-
193151	**-0,5595**	**0,0480525**	-
40867	**-0,2915**	**0,0480525**	-
54593	**-0,3642**	**0,0480525**	Amino acid/polyamine transporter
47812	**0,3315**	**0,0480525**	OPT oligopeptide transporter protein

187673	**-0,4516**	**0,0481734**	Caspase
123330	**-0,4714**	**0,0482092**	#N/A
56901	**-0,2912**	**0,0482538**	-
211829	**-0,3779**	**0,0483527**	#N/A
37080	**-0,4951**	**0,0485079**	pepE, extracellular aspartic protease
40379	**-0,4605**	**0,0485394**	-
55020	**-0,3456**	**0,0485581**	#N/A
55080	**-0,4014**	**0,0486061**	#N/A
56667	**-0,2948**	**0,0486213**	Ankyrin repeat protein
170567	**-0,4657**	**0,0486213**	#N/A
209255	**0,4845**	**0,0486329**	Mitochondrial substrate carrier
213698	**-0,4657**	**0,0486329**	Predicted oxidoreductase
175401	**-0,6317**	**0,0487247**	-
209750	**-0,3864**	**0,0487458**	-
184267	**0,6121**	**0,0487458**	Hypothetical low affinity iron permease
212557	**-0,3376**	**0,0487603**	Sec1-like protein
182540	**-0,4058**	**0,0487639**	-
47636	**-0,3136**	**0,048765**	Hypothetical transcription factor TMF, TATA element modulatory factor
56936	**0,4456**	**0,048765**	#N/A
206626	**-0,6508**	**0,0487799**	Major facilitator superfamily
51112	**-0,4861**	**0,0487923**	Peptidase family M48
186194	**-0,3284**	**0,0488326**	COP9 signalosome, subunit CSN3
44557	**-0,4224**	**0,0488545**	#N/A
44877	**0,471**	**0,0489124**	-
54968	**-0,551**	**0,0489124**	-
212055	**0,4313**	**0,0489124**	40S ribosomal protein S12
56462	**0,4024**	**0,0489124**	Candidate serine hydroxymethyltransferase (EC 2.1.2.1)
45491	**-0,4971**	**0,0489124**	Protein kinase
42733	**1,7466**	**0,0490157**	Dihydroxy-acid dehydratase
125961	**0,3211**	**0,0490157**	Esterase/lipase/thioesterase
132428	**-0,3099**	**0,0490157**	Major facilitator superfamily
129576	**0,7314**	**0,0490295**	-
185022	**-0,3034**	**0,0490856**	FAD linked oxidase
134668	**-0,6153**	**0,049155**	-
47000	**-0,3941**	**0,049155**	-
124595	**-0,8161**	**0,049155**	Possible oxidoreductase
137527	**0,4674**	**0,049155**	#N/A
212180	**-0,3586**	**0,0491802**	Putative GroEL-like chaperone, ATPase
52362	**0,4361**	**0,0493394**	Candidate 40S ribosomal protein S0.
52301	**-0,5233**	**0,0493489**	-
35422	**-0,248**	**0,0493489**	Fungal transcriptional regulatory protein, N-terminal

206767	**0,3732**	**0,0493937**	-
127030	**-0,5034**	**0,049498**	-
208969	**-0,4702**	**0,0495161**	-
205459	**0,495**	**0,0495161**	Alpha-isopropylmalate synthase/homocitrate synthase
40039	**-0,6619**	**0,0496527**	Peptidase, eukaryotic cysteine peptidase active site
56582	**-0,35**	**0,0496575**	-
40885	**-0,5722**	**0,0497276**	beta-1,6-N-acetylglucosaminyltransferase, contains WSC domain

Appendix 2

Significantly regulated proteins of Chapter 4

JGI ID	Fold change	z score	P. Value	Annotation
209700	**-3.385835042**	**-7.91422**	**1.24402E-15**	ABC transporter
119500	**-0.478545405**	**-4.12004**	**1.89406E-05**	-
196714	**-1.585177003**	**-3.88669**	**5.08111E-05**	Ribosomal protein L15e
207954	**-1.612678712**	**-3.70948**	**0.000103841**	Spermidine synthase
40339	**-0.377776332**	**-3.61496**	**0.000150197**	Armadillo/beta-catenin-like repeat-containing protein
172591	**-1.022338571**	**-3.56123**	**0.000184564**	Uroporphyrinogen decarboxylase
172313	**-0.784497614**	**-3.4562**	**0.000273919**	dUTPase
214348	**-0.715486321**	**-3.24401**	**0.000589297**	Acyl-CoA synthetase
55496	**-1.802428541**	**-3.22739**	**0.00062462**	Hypothetical protein with Zn-finger. C-x8-C-x5-C-x3-H type
213572	**-1.135045546**	**-3.18941**	**0.000712811**	Hypothetical. Related to cell surface antigen spherulin
210854	**-0.548847973**	**-3.04577**	**0.001160415**	#N/A
210854	**-0.548847973**	**-3.04577**	**0.001160415**	#N/A
205484	**-1.269481135**	**-2.96573**	**0.00150983**	Acyl-CoA dehydrogenase
207105	**-1.189914083**	**-2.93505**	**0.001667444**	-
207105	**-1.189914083**	**-2.93505**	**0.001667444**	-
55885	**-1.151475213**	**-2.72464**	**0.003218589**	Hypothetical protein with RNA-binding region
53254	**-0.403569693**	**-2.70408**	**0.003424696**	Putative Peptidyl-prolyl cis-trans isomerase. cyclophilin type
50504	**-0.451852835**	**-2.58294**	**0.004898059**	Hypothetical alcohol dehydrogenase NADP+ dependent; EC 1.1.1.2
56152	**-0.526802223**	**-2.48835**	**0.006416847**	related to Asp f4 allergen of Aspergillus fumigatus
47150	**-0.95283337**	**-2.44073**	**0.007328752**	C1-tetrahydrofolate synthase
56395	**-1.092896996**	**-2.35115**	**0.009357792**	2-nitropropane dioxygenase
55680	**-0.403718876**	**-2.3218**	**0.01012196**	Coenzyme A transferase
124867	**-0.78133445**	**-2.24364**	**0.012427795**	putative extracellular protein
207929	**-0.451964892**	**-2.2357**	**0.012685802**	Pentafunctional AROM protein. KOG: Aminoacid transport metabolism
135107	**-0.281503719**	**-2.18535**	**0.014431472**	Hypothetical Actin-binding protein
214549	**-0.32526794**	**-2.13687**	**0.016304255**	-
49515	**-0.616704668**	**-2.12412**	**0.016830085**	-
52865	**-0.726275603**	**-2.11949**	**0.017024355**	Hypothetical. possible DNA binding
47011	**-0.373753061**	**-2.11776**	**0.017097719**	-

56414	**-0.707334822**	**-2.08809**	**0.018394972**	-
205050	**-1.150325936**	**-2.07905**	**0.018806335**	Hypothetical thioredoxin-related
52397	**-0.490319722**	**-2.07641**	**0.018927809**	Hypothetical 20S proteasome. regulatory subunit
209528	**-0.572576853**	**-2.0363**	**0.020860146**	-
171101	**-0.350754961**	**-2.02421**	**0.021474391**	Actin-binding. cofilin/tropomyosin type
55204	**-0.538205414**	**-2.02012**	**0.02168551**	agsA. one of five alpha-1.3-glucan synthases
55011	**-0.282104872**	**-2.01952**	**0.021716503**	51kDa subunit of NADH:ubiquinone reductase (complex I); NADH dehydrogenase [Aspergillus niger]
137182	**-0.283093571**	**-2.00791**	**0.022326571**	60S ribosomal protein L14
51886	**-0.634595269**	**-2.00208**	**0.022638222**	Anthranilate phosphoribosyltransferease. trp biosynthesis. EC 2.4.2.18
190481	**-1.29775914**	**-1.98676**	**0.023474735**	AMP-dependent synthetase and ligase
55741	**-0.663036943**	**-1.96277**	**0.024836254**	Protein import receptor MAS20
213531	**-0.859991044**	**-1.95064**	**0.025549956**	Mitochondrial import translocase. subunit Tom70
187475	**-0.995784443**	**-1.94047**	**0.026161078**	-
37834	**-0.273315543**	**-1.90883**	**0.028142307**	Mitochondrial import inner membrane translocase.
49311	**-0.361556237**	**-1.86774**	**0.030899098**	Hypothetical. similarities to sialidase superfamily
211094	**0.793543577**	**1.988725**	**0.023366**	#N/A
123950	**0.540058013**	**1.990491**	**0.023268**	Protein phosphatase 2C-like
47288	**0.786294568**	**2.033202**	**0.021016**	putative Translation initiation factor 2B. epsilon subunit (eIF-2Bepsilon/GCD6) Translation. ribosomal structure and biogenesis
200642	**0.360452963**	**2.14112**	**0.016132**	26S proteasome regulatory complex
178461	**0.781870132**	**2.287353**	**0.011088**	Editing needed. This protein is an artificial hybrid of a purine-nucleoside phosphorylase activity and a 6-phosphogluconate dehydrogenase. In the CBS 513.88 annotation. these are annotated as An11g06110 and An11g06120 respectively.
54579	**1.699416026**	**3.0448**	**0.001164**	Hypothetical myristoyl-CoA:protein N-myristoyltransferase
201398	**1.603192184**	**3.467571**	**0.000263**	-
211951	**1.434754237**	**3.584087**	**0.000169**	Phenylalanyl-tRNA synthetase. beta subunit archae/euk cytosolic
204505	**0.978022956**	**3.658699**	**0.000127**	Ribosomal protein L39e

Appendix 3 Significantly expressed genes of Chapter 6

pH 2.5

JGI ID	Fold Change	P. Value	Annotation
57241	**-1,64705**	**0,00120173**	oahA, Oxaloacetate acetylhydrolase oahA (EC 3.7.1.1)
139485	**-1,52419**	**0,00767367**	putative lysophospholipase with signal peptide motif
41618	**-1,77389**	**0,00767367**	Hypothetical polyketide synthase
181795	**1,20559**	**0,02352445**	-
184509	**1,67369**	**0,0372688**	Hypothetical methyltransferase. No sequence similarity is found to identified proteins
41394	**-2,05872**	**0,0372688**	-
52588	**-2,5011**	**0,0372688**	-

pH 5.0

JGI ID	Fold change	P. Value	Annotation
206885	**-1,03015**	**0,0050151**	Acetate kinase
184509	**2,29783**	**0,00836649**	Hypothetical methyltransferase. No sequence similarity is found to identified proteins
126194	**-1,52085**	**0,00836649**	#N/A
48286	**-2,2922**	**0,00836649**	hypothetical NADH:flavin oxidoreductase/NADH oxidase
46001	**-2,91785**	**0,00836649**	ConX, conidiation specific protein
55019	**2,20279**	**0,00879326**	-
43792	**1,6298**	**0,0091206**	-
41404	**-2,77815**	**0,0091206**	#N/A
37491	**1,55839**	**0,0091206**	Hypothetical heterokaryon incompatibility factor
37001	**1,58179**	**0,0091206**	#N/A
132624	**1,56452**	**0,00927663**	Fungal specific transcription factor
35697	**-3,73619**	**0,00927663**	#N/A
175986	**1,37566**	**0,00957684**	-
37555	**1,22302**	**0,00957684**	Fungal transcriptional regulatory protein

137491	**1,94443**	**0,00964705**	-
41393	**1,53928**	**0,00964705**	-
45767	**-2,00563**	**0,01069102**	-
173247	**1,68685**	**0,01086467**	Candidate phosphate transporter
182323	**-1,41588**	**0,01245016**	#N/A
188780	**1,02472**	**0,01500038**	Amino acid/polyamine transporter
209625	**2,34947**	**0,01552267**	Generic methyltransferase
54077	**1,30948**	**0,01552267**	Major intrinsic protein
42602	**-1,35272**	**0,01552267**	Cytochrome P450
205518	**-1,3834**	**0,01700634**	NADH-dehydrogenase (ubiquinone)
203979	**-1,75905**	**0,01700634**	-
189162	**-2,49213**	**0,01700634**	RTA1 like protein
189113	**-1,28721**	**0,01700634**	-
184012	**-1,09135**	**0,01700634**	Amino acid transporters
176378	**1,20395**	**0,01700634**	Short-chain dehydrogenase/reductase
141870	**1,09587**	**0,01700634**	#N/A
126826	**-1,84422**	**0,01700634**	#N/A
43431	**1,23656**	**0,01700634**	-
36639	**-1,54513**	**0,01700634**	FAD binding domain
36360	**1,5905**	**0,01700634**	CorA-like Mg2+ transporter protein
198697	**1,12422**	**0,01740326**	Predicted transporter (major facilitator superfamily)
36928	**-1,01876**	**0,01740326**	-
53882	**1,4175**	**0,01756332**	Gene activiation by acetylation of histones
189610	**1,18826**	**0,0184042**	#N/A
48081	**-1,20605**	**0,0184042**	Candidate ornithine aminotransferase (EC 2.6.1.13)
46134	**1,31753**	**0,0184042**	FAD-linked oxidase
189852	**-1,95383**	**0,0187999**	#N/A
57437	**-1,45589**	**0,0187999**	Hypothetical protein. PFam suggests oxidoreductase activity.
53757	**1,04225**	**0,0187999**	-
52588	**-2,16769**	**0,0187999**	-
44917	**-1,25896**	**0,0187999**	Major facilitator superfamily
177916	**1,68692**	**0,01914087**	-
136764	**-1,24869**	**0,01914087**	Chloroperoxidase
42274	**-1,54755**	**0,01914087**	-

36635	**-0,84795**	**0,01914087**	-
172477	**1,78019**	**0,019723**	Short-chain dehydrogenase/reductase
142689	**-1,06022**	**0,019723**	-
52023	**1,24719**	**0,0199321**	Adenylosuccinate lyase
36472	**1,05181**	**0,02014927**	-
37260	**-1,09248**	**0,02016633**	#N/A
212262	**0,85243**	**0,02054418**	-
176483	**-2,00621**	**0,02054418**	#N/A
54305	**-2,65655**	**0,02054418**	Zinc-containing alcohol dehydrogenase
53879	**-2,22291**	**0,02054418**	Zinc-binding oxidoreductase
49768	**0,84686**	**0,02054418**	#N/A
36389	**-1,13891**	**0,02054418**	-
181773	**0,7885**	**0,02096318**	#N/A
197549	**1,2724**	**0,02127836**	Sugar (ANd other) transporter
191511	**-1,48226**	**0,02127836**	related to GH family 12 xyloglucan-specific endo-beta-1,4-glucanase
180844	**-1,46971**	**0,02127836**	Short-chain dehydrogenase/reductase SDR
179042	**1,35939**	**0,02127836**	Zinc-containing alcohol dehydrogenase
126082	**1,89657**	**0,02127836**	Generic methyltransferase
214715	**-1,80392**	**0,02141765**	Hypothetical protein. KOG suggests chitinase. SignalP suggests secretion
123072	**-1,11482**	**0,02159443**	#N/A
40225	**-1,06051**	**0,02247859**	NADH:flavin oxidoreductase/NADH oxidase
42609	**-1,25742**	**0,02284297**	-
43179	**0,78042**	**0,02300214**	-
40273	**-1,31379**	**0,02300214**	#N/A
38052	**-1,39698**	**0,02300214**	#N/A
195091	**-1,85382**	**0,02371474**	Zinc-containing alcohol dehydrogenase
176272	**0,93493**	**0,02388339**	Flavin-containing monooxygenase
185434	**1,00791**	**0,02404571**	short chain dehydrogenase
185386	**-0,99953**	**0,02404571**	#N/A
194896	**1,37699**	**0,02451608**	hypothetical amine oxidase

172934	**1,49915**	**0,02451608**	ABC transporter
131892	**-1,0236**	**0,02499962**	Major facilitator superfamily
45985	**-1,06891**	**0,02530021**	#N/A
129581	**-1,7755**	**0,02669397**	Acyl-CoA synthetase
121842	**-1,67528**	**0,02669397**	Peptidase S28
42689	**-0,83937**	**0,02669397**	-
204317	**1,0105**	**0,0268056**	Vacuolar H+-ATPase V0 sector, subunits
189853	**-2,10166**	**0,0279955**	-
180652	**1,07132**	**0,0279955**	-
54814	**-2,67201**	**0,0279955**	D-xylulose 5-phosphate/D-fructose 6-phosphate phosphoketolase
54811	**-0,99196**	**0,0279955**	Hypothetical cytochrome P450 monooxygenase
42058	**-1,14734**	**0,0279955**	-
41505	**0,85277**	**0,0279955**	Permease of the major facilitator superfamily
38315	**0,9098**	**0,0279955**	#N/A
131747	**0,86511**	**0,02813412**	candidate b-glycosidase related to b-glucosidases
52528	**0,93509**	**0,02813412**	Fungal transcriptional regulatory protein,
52111	**1,09087**	**0,02813412**	hypothetical beta-galactosidase. extracellular GH family 2
36926	**-1,10463**	**0,02813412**	#N/A
36584	**1,69192**	**0,02813412**	Zinc-containing alcohol dehydrogenase superfamily
47677	**0,9167**	**0,02847683**	hypothetical xylosidase/arabinanase. GH family 43
142574	**-1,27533**	**0,02859599**	#N/A
36048	**-0,77714**	**0,02859599**	-
53054	**0,76158**	**0,0286515**	Putative Acyl-CoA synthetase
54838	**1,77718**	**0,02905942**	Major facilitator superfamily
36428	**1,36102**	**0,02959766**	-
208521	**-1,97576**	**0,03147039**	hypothetical FAD/FMN-containing dehydrogenase (COG0277)with transmembrane motif
55139	**2,01189**	**0,03180937**	-
124156	**2,05216**	**0,0319541**	candidate NAD dependent formate dehydrogenase
209012	**1,13324**	**0,0324385**	Proteins containing the FAD binding domain
208129	**-0,82775**	**0,0324385**	Glycine cleavage H-protein
193449	**-1,46896**	**0,0324385**	-

192575	**-2,03986**	**0,0324385**	-
189460	**0,79228**	**0,0324385**	ABC transporter
183137	**1,1747**	**0,0324385**	#N/A
180608	**0,8014**	**0,0324385**	-
179079	**-1,22533**	**0,0324385**	Putative polyketide synthase
176277	**1,01872**	**0,0324385**	RNA-directed RNA polymerase QDE-1 required for posttranscriptional gene silencing and RNA interference
126639	**-2,14383**	**0,0324385**	Peptidase A4, scytalidopepsin B
124657	**-1,26063**	**0,0324385**	FAD-dependent pyridine nucleotide-disulphide oxidoreductase
54375	**-1,25409**	**0,0324385**	catalase
43258	**-0,96493**	**0,0324385**	-
39139	**-1,16013**	**0,0324385**	FAD linked oxidase, N-terminal
36404	**1,01113**	**0,0324385**	FAD linked oxidase, N-terminal
38587	**1,10868**	**0,03306425**	-
209775	**1,01241**	**0,03561154**	-
57037	**1,09256**	**0,03561154**	-
43746	**-1,93172**	**0,03561154**	hypothetical ribonuclease T1
42209	**-1,33526**	**0,03561154**	#N/A
52126	**-0,85005**	**0,03627401**	Hypothetical endoglucanase
39220	**-0,785**	**0,0367867**	#N/A
47922	**-1,77529**	**0,03812475**	-
41351	**0,92007**	**0,03812475**	-
40016	**-1,90396**	**0,03812475**	-
37556	**-0,80632**	**0,03812475**	predicted beta-1,6-N-acetylglucosaminyltransferase, contains WSC domain
194367	**-0,69861**	**0,03832453**	#N/A
35461	**-0,85465**	**0,03832453**	#N/A
38582	**1,18013**	**0,0393887**	FAD-dependent oxidoreductase
171092	**-1,0416**	**0,04008112**	Monooxygenase involved in coenzyme Q (ubiquinone) biosynthesis
44878	**-1,82427**	**0,04008112**	hypothetical cytochrome P450 alkane hydroxylase

41809	**0,81479**	**0,04008112**	Major facilitator superfamily
190025	**1,11801**	**0,04084878**	Major facilitator superfamily
195002	**0,96907**	**0,04124574**	Synaptic vesicle transporter SVOP and related transporters
42235	**-1,24032**	**0,04124574**	-
200723	**-1,16641**	**0,04268402**	Glycosyl transferase, family 28
189708	**1,62514**	**0,04268402**	#N/A
53801	**-0,84711**	**0,04268402**	Hypothetical protein. HMMPfam indicates Glucose-methanol-choline oxidoreductase activity
43969	**-0,89339**	**0,04268402**	hypothetical urea amidolyase (EC 6.3.4.6)
37758	**-0,82256**	**0,04268402**	hypothetical beta-1,6-N-acetylglucosaminyltransferase, contains WSC domain
129269	**0,88389**	**0,04288155**	-
127445	**1,04344**	**0,04308731**	Predicted haloacid-halidohydrolase and related hydrolases
131668	**0,79578**	**0,04320854**	-
35385	**1,11829**	**0,04320854**	-
40159	**-1,16302**	**0,04376242**	-
181283	**0,83558**	**0,044117**	#N/A
135400	**0,6801**	**0,0443291**	-
185855	**-0,95497**	**0,04478906**	-
189424	**0,8642**	**0,04506741**	putative glycosyl transferase
172647	**1,43641**	**0,04506741**	Major facilitator superfamily
44895	**-1,33134**	**0,04506741**	-
205909	**0,92175**	**0,04517196**	ABC transporter associated with fumonisin-like biosyntehetic gene cluster
185038	**-1,13717**	**0,04539719**	#N/A
49482	**-0,95109**	**0,04552901**	Amino acid/polyamine transporter II
38747	**-1,5204**	**0,04628072**	-
172537	**-1,80798**	**0,04656386**	Domain of Unknown function
53901	**-0,89926**	**0,04656386**	-
53539	**0,57514**	**0,04656386**	-
197387	**-1,58982**	**0,04660097**	PHK
199424	**0,64249**	**0,0466086**	-

191395	**0,93314**	**0,0466086**	-
41656	**-0,90789**	**0,0466086**	-
37959	**1,00772**	**0,0466086**	-
185351	**1,00995**	**0,0470042**	Flavonol reductase/cinnamoyl-CoA reductase
177781	**1,08451**	**0,0470042**	GCN5-related N-acetyltransferase
57243	**1,31046**	**0,0470042**	Hypothetical aldehyde dehydrogenase (EC 1.2.1.3).
42523	**0,74635**	**0,0470042**	Hypothetical Inositol monophosphatase
37028	**-0,93162**	**0,0470042**	#N/A
48061	**1,4729**	**0,04712327**	Hypothetical ABC transporter
182447	**0,78813**	**0,04712847**	#N/A
42232	**1,02541**	**0,04712847**	-
39016	**-0,78318**	**0,04712847**	-
118617	**-1,32607**	**0,04728498**	Putative polyketide synthase
45964	**-1,27962**	**0,04728498**	-
207586	**-1,40055**	**0,04739164**	-
171293	**1,48968**	**0,04739164**	Cell adhesin
135939	**0,77037**	**0,04739164**	Hypothetical. Contains Esterase/lipase/thioesterase domain
56930	**0,78601**	**0,04739164**	Hypothetical sexual differentiation process protein ISP4
50375	**0,97126**	**0,04739164**	-
45889	**-0,98913**	**0,04739164**	#N/A
40862	**-1,20591**	**0,04739164**	hypothetical protein
37734	**0,70831**	**0,04739164**	-
36932	**1,05438**	**0,04739164**	-
193672	**0,5613**	**0,04750758**	#N/A
180570	**0,77648**	**0,04750758**	Short-chain dehydrogenase/reductase SDR
173096	**1,22542**	**0,04750758**	-
123557	**-0,9112**	**0,04750758**	Multicopper oxidase, type 1
52995	**1,73775**	**0,04750758**	-
38991	**-1,50058**	**0,04750758**	-
125297	**1,81776**	**0,04760674**	-
50755	**0,87077**	**0,04760674**	putative RTA1 like protein
195023	**-0,66933**	**0,0478762**	-
189676	**0,63474**	**0,04789652**	Malate/L-lactate dehydrogenase
50239	**-2,66889**	**0,04832042**	-
204569	**0,78117**	**0,04839092**	-

181136	**0,84434**	**0,04839092**	Flavoprotein monooxygenase
170237	**1,30069**	**0,04839092**	Arylacetamide deacetylase
144091	**-1,951**	**0,04839092**	#N/A
54095	**1,95798**	**0,04839092**	Sugar (ANd other) transporter
51892	**1,39279**	**0,04839092**	Fungal specific transcription factor
198441	**-2,71564**	**0,04869865**	-
178352	**-0,94167**	**0,04869865**	#N/A
45784	**2,17047**	**0,04869865**	-
41210	**0,91927**	**0,04869865**	Thioesterase superfamily
125829	**-0,83553**	**0,04877012**	Major intrinsic protein
42238	**-1,00296**	**0,04877012**	Guanine-specific ribonuclease N1 and T1
41760	**-1,50325**	**0,04877012**	#N/A
210951	**-1,52228**	**0,04894317**	Glycine cleavage system P-protein
185262	**0,80627**	**0,04894317**	Zinc-containing alcohol dehydrogenase superfamily
181429	**1,20083**	**0,04894317**	-
181275	**0,9252**	**0,04894317**	Related to E. nidulans 1-pyrroline-5-carboxylate dehydrogenase (prnC) (EC 1.5.1.12)
180773	**0,8012**	**0,04894317**	Fungal transcriptional regulatory protein, N-terminal
180730	**0,78696**	**0,04894317**	-
126898	**-0,80603**	**0,04894317**	-
118581	**-1,31038**	**0,04894317**	Putative polyketide synthase
52994	**1,67496**	**0,04894317**	-
44117	**-0,74947**	**0,04894317**	ankyrin-repeat protein
43835	**-0,69884**	**0,04894317**	#N/A
37775	**0,71099**	**0,04894317**	hypothetical protein containing Zn-finger, C2H2 type domain
207689	**0,78657**	**0,04944183**	Peptidase M20
189642	**-0,93506**	**0,04944183**	-
186770	**-0,94032**	**0,04944183**	#N/A
181473	**-1,68096**	**0,04944183**	FMN-dependent alpha-hydroxy acid dehydrogenase
132291	**-2,68041**	**0,04944183**	Sugar (ANd other) transporter
52848	**-1,76481**	**0,04944183**	-

40747	**-1,14461**	**0,04944183**	-
39988	**0,70264**	**0,04944183**	-
39278	**-2,12847**	**0,04944183**	Inorganic ion transport and metabolism
38134	**1,71656**	**0,04944183**	#N/A
212059	**0,81707**	**0,0496284**	-
41769	**1,00626**	**0,0496284**	-
181881	**0,6802**	**0,04993862**	#N/A
126848	**0,70492**	**0,04993862**	Hypothetical Glucose-6-phosphate/phosphate and phosphoenolpyruvate/phosphate antiporter
121874	**-0,9241**	**0,04996624**	putative extracellular carboxylesterase, type B
47967	**-2,82492**	**0,04996624**	Alternative oxidase, mitochondrial precursor

Appendix 4

SDS-page gel pictures of Chapter 7

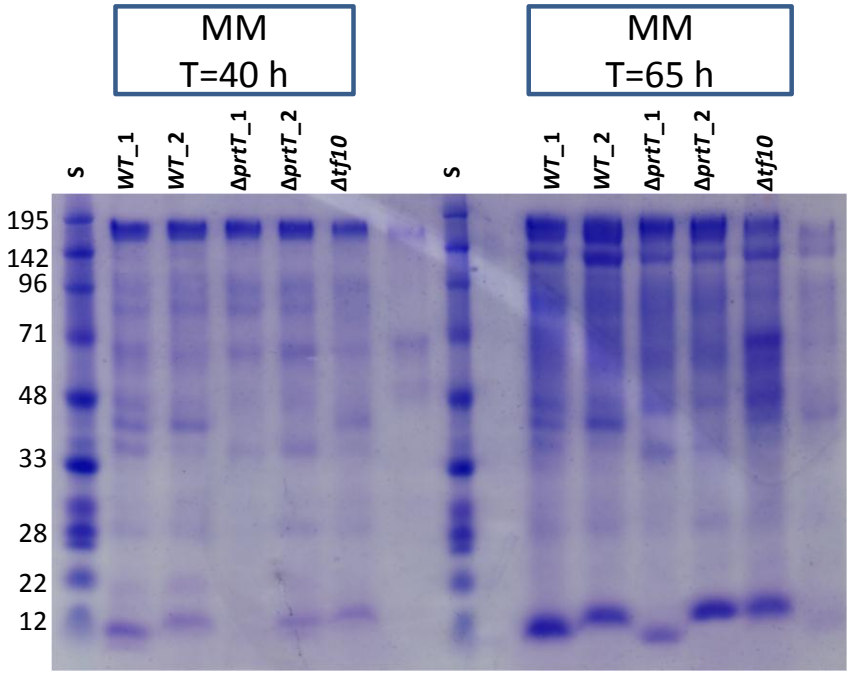

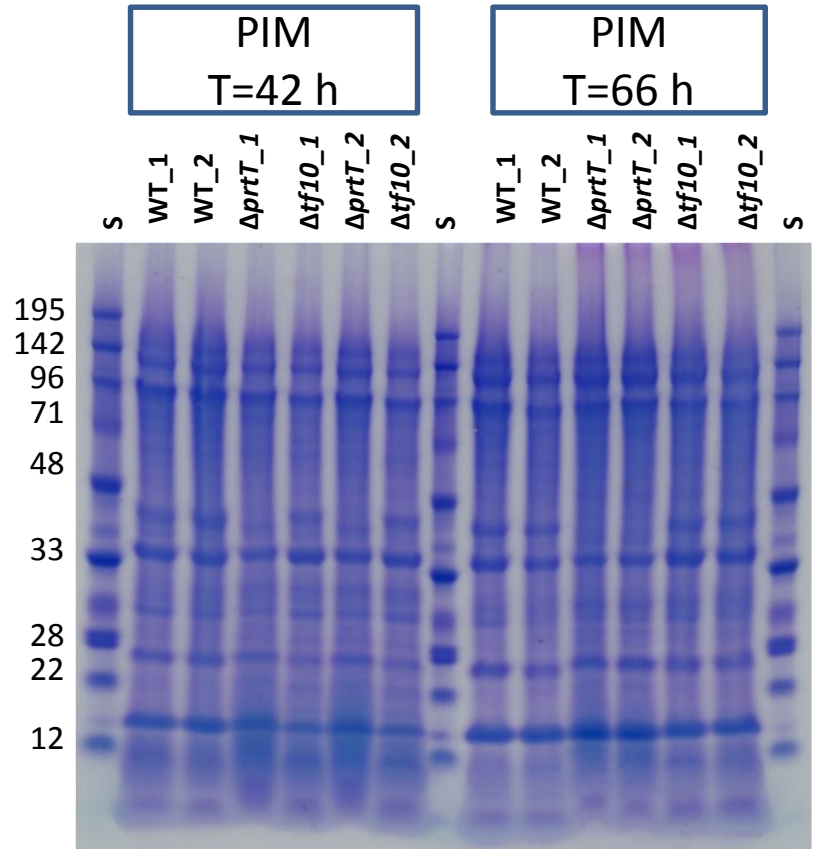

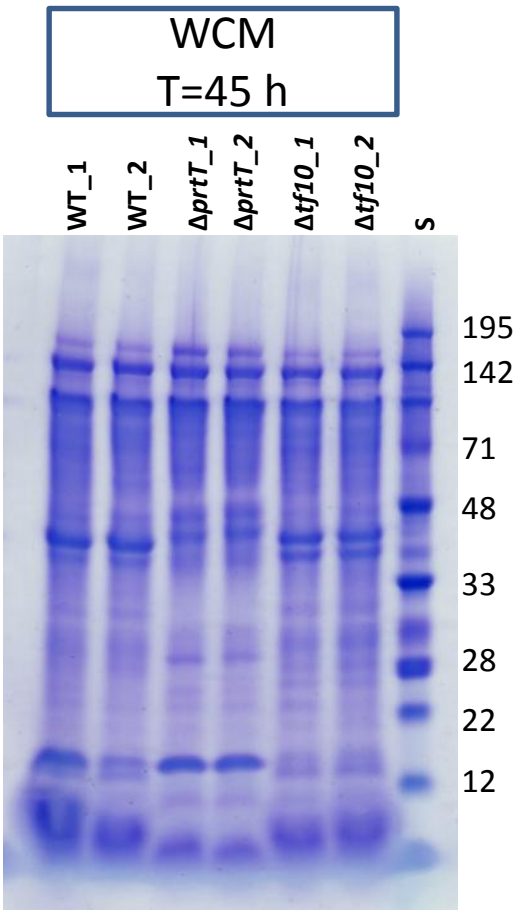
WCM
T=45 h
WT_1
WT_2
ΔprtT_1
ΔprtT_2
Δtf10_1
Δtf10_2
S
195
142
71
48
33
28
22
12

Appendix 5 Integrated Biolog data of Chapter 8

Compound	Plate ID	Source	OD AUC	STD	GFP AUC	STD
Negative Control	PM1	C-Source	0,0	N/A	0,0	N/A
L-Arabinose	PM1	C-Source	33,1	N/A	365,7	N/A
N-Acetyl-D-Glucosamine	PM1	C-Source	65,9	N/A	1466,0	N/A
D-Saccharic Acid	PM1	C-Source	0,1	N/A	0,0	N/A
Succinic Acid	PM1	C-Source	5,1	N/A	759,2	N/A
D-Galactose	PM1	C-Source	10,9	N/A	0,0	N/A
L-Aspartic Acid	PM1	C-Source	0,6	N/A	961,1	N/A
L-Proline	PM1	C-Source	31,0	N/A	2049,6	N/A
D-Alanine	PM1	C-Source	1,1	N/A	2218,8	N/A
D-Trehalose	PM1	C-Source	38,8	N/A	2464,7	N/A
D-Mannose	PM1	C-Source	32,1	N/A	930,8	N/A
Dulcitol	PM1	C-Source	27,2	N/A	32,3	N/A
D-Serine	PM1	C-Source	1,7	N/A	1352,2	N/A
D-Sorbitol	PM1	C-Source	39,5	N/A	0,0	N/A
Glycerol	PM1	C-Source	17,2	N/A	969,6	N/A
L-Fucose	PM1	C-Source	1,8	N/A	148,3	N/A
D-Glucuronic Acid	PM1	C-Source	0,0	N/A	0,0	N/A
D-Gluconic Acid	PM1	C-Source	7,7	N/A	0,0	N/A
D,L-a-Glycerol Phosphate	PM1	C-Source	0,2	N/A	0,0	N/A
D-Xylose	PM1	C-Source	36,3	N/A	0,0	N/A
D,L-Lactic acid	PM1	C-Source	0,0	N/A	0,0	N/A
Formic Acid	PM1	C-Source	0,0	N/A	20,0	N/A
D-Mannitol	PM1	C-Source	1,0	N/A	0,0	N/A
L-Glutamic Acid	PM1	C-Source	0,0	N/A	623,2	N/A
D-Glucose-6-Phosphate	PM1	C-Source	0,5	N/A	0,0	N/A
D-Galactonic Acid-g-Lactone	PM1	C-Source	1,6	N/A	509,5	N/A
D,L-Malic Acid	PM1	C-Source	6,3	N/A	451,9	N/A
D-Ribose	PM1	C-Source	10,0	N/A	2517,6	N/A
Tween 20	PM1	C-Source	5,6	N/A	302,9	N/A
L-Rhamnose	PM1	C-Source	32,8	N/A	1187,7	N/A
D-Fructose	PM1	C-Source	52,2	N/A	189,7	N/A
Acetic Acid	PM1	C-Source	6,0	N/A	0,0	N/A
a-D-Glucose	PM1	C-Source	57,5	N/A	2750,3	N/A
Maltose	PM1	C-Source	26,3	N/A	710,4	N/A
D-Melibiose	PM1	C-Source	26,0	N/A	0,0	N/A
Thymidine	PM1	C-Source	0,0	N/A	912,6	N/A
L-Asparagine	PM1	C-Source	10,7	N/A	432,3	N/A
D-Aspartic Acid	PM1	C-Source	0,6	N/A	0,0	N/A
D-Glucosaminic Acid	PM1	C-Source	0,0	N/A	0,0	N/A
1,2-Propanediol	PM1	C-Source	0,2	N/A	1035,5	N/A
Tween 40	PM1	C-Source	4,7	N/A	1122,3	N/A
a-Ketoglutaric Acid	PM1	C-Source	3,4	N/A	0,0	N/A
a-Ketobutyric Acid	PM1	C-Source	2,0	N/A	487,4	N/A
a-Methyl-D-Galactoside	PM1	C-Source	3,2	N/A	0,0	N/A
a-D-Lactose	PM1	C-Source	0,0	N/A	0,0	N/A
Lactulose	PM1	C-Source	0,0	N/A	1402,5	N/A
Sucrose	PM1	C-Source	38,0	N/A	82,0	N/A
Uridine	PM1	C-Source	0,0	N/A	123,9	N/A

L-Glutamine	PM1	C-Source	11,5	N/A	0,0	N/A
m-Tartaric Acid	PM1	C-Source	0,0	N/A	0,0	N/A
D-Glucose-1-Phosphate	PM1	C-Source	0,0	N/A	0,0	N/A
D-Fructose-6-Phosphate	PM1	C-Source	0,0	N/A	0,0	N/A
Tween 80	PM1	C-Source	7,6	N/A	0,0	N/A
a-Hydroxyglutaric Acid-g-Lactone	PM1	C-Source	3,6	N/A	1026,8	N/A
a-Hydroxybutyric Acid	PM1	C-Source	3,5	N/A	967,2	N/A
b-Methyl-D-Glucoside	PM1	C-Source	43,0	N/A	0,0	N/A
Adonitol	PM1	C-Source	6,6	N/A	0,0	N/A
Maltotriose	PM1	C-Source	51,7	N/A	0,0	N/A
2'-Deoxyadenosine	PM1	C-Source	0,0	N/A	0,0	N/A
Adenosine	PM1	C-Source	0,0	N/A	355,2	N/A
Gly-Asp	PM1	C-Source	4,8	N/A	0,0	N/A
Citric Acid	PM1	C-Source	7,1	N/A	0,0	N/A
m-Inositol	PM1	C-Source	19,9	N/A	635,4	N/A
D-Threonine	PM1	C-Source	1,4	N/A	2454,6	N/A
Fumaric Acid	PM1	C-Source	2,3	N/A	0,0	N/A
Bromosuccinic Acid	PM1	C-Source	2,3	N/A	391,1	N/A
Propionic Acid	PM1	C-Source	6,1	N/A	0,0	N/A
Mucic Acid	PM1	C-Source	0,3	N/A	0,0	N/A
Glycolic Acid	PM1	C-Source	0,9	N/A	0,0	N/A
Glyoxylic Acid	PM1	C-Source	7,2	N/A	1764,7	N/A
D-Cellobiose	PM1	C-Source	42,2	N/A	0,0	N/A
Inosine	PM1	C-Source	0,0	N/A	0,0	N/A
Gly-Glu	PM1	C-Source	3,3	N/A	539,9	N/A
Tricarballylic Acid	PM1	C-Source	0,0	N/A	0,0	N/A
L-Serine	PM1	C-Source	3,7	N/A	0,0	N/A
L-Threonine	PM1	C-Source	4,0	N/A	0,0	N/A
L-Alanine	PM1	C-Source	16,9	N/A	0,0	N/A
Ala-Gly	PM1	C-Source	4,2	N/A	0,0	N/A
Acetoacetic Acid	PM1	C-Source	0,0	N/A	0,0	N/A
N-Acetyl-D-Mannosamine	PM1	C-Source	0,0	N/A	306,0	N/A
Mono-Methylsuccinate	PM1	C-Source	3,2	N/A	805,3	N/A
Methylpyruvate	PM1	C-Source	1,3	N/A	0,0	N/A
D-Malic Acid	PM1	C-Source	4,4	N/A	254,5	N/A
L-Malic Acid	PM1	C-Source	0,0	N/A	227,3	N/A
Gly-Pro	PM1	C-Source	11,1	N/A	177,3	N/A
p-Hydroxyphenyl Acetic Acid	PM1	C-Source	8,5	N/A	309,5	N/A
m-Hydroxyphenyl Acetic Acid	PM1	C-Source	3,5	N/A	0,0	N/A
Tyramine	PM1	C-Source	15,3	N/A	919,6	N/A
D-Psicose	PM1	C-Source	7,2	N/A	0,0	N/A
L-Lyxose	PM1	C-Source	10,1	N/A	3109,0	N/A
Glucuronamide	PM1	C-Source	0,0	N/A	826,3	N/A
Pyruvic Acid	PM1	C-Source	0,0	N/A	0,0	N/A
L-Galactonic Acid-g-Lactone	PM1	C-Source	5,8	N/A	785,8	N/A
D-Galacturonic Acid	PM1	C-Source	7,0	N/A	1643,4	N/A
b-Phenylethylamine	PM1	C-Source	0,0	N/A	0,0	N/A
2-Aminoethanol	PM1	C-Source	0,7	N/A	257,2	N/A
Negative Control	PM2A	C-Source	0,0	0,0	0,0	0,0
Chondroitin Sulfate C	PM2A	C-Source	0,7	0,0	43,5	61,6
a-Cyclodextrin	PM2A	C-Source	1,7	1,8	904,6	1279,3
b-Cyclodextrin	PM2A	C-Source	1,5	2,1	0,0	0,0

g-Cyclodextrin	PM2A	C-Source	13,4	15,1	79,5	112,4
Dextrin	PM2A	C-Source	17,1	0,9	0,5	0,7
Gelatin	PM2A	C-Source	2,1	2,7	732,9	84,0
Glycogen	PM2A	C-Source	13,6	6,9	1071,8	1515,7
Inulin	PM2A	C-Source	9,5	3,0	28,4	40,1
Laminarin	PM2A	C-Source	18,9	2,7	569,7	805,7
Mannan	PM2A	C-Source	3,0	4,2	65,2	92,2
Pectin	PM2A	C-Source	1,2	1,7	593,6	839,4
N-Acetyl-D-Galactosamine	PM2A	C-Source	0,0	0,0	41,8	59,1
N-Acetyl-Neuraminic Acid	PM2A	C-Source	0,0	0,0	146,1	206,5
b-D-Allose	PM2A	C-Source	0,8	1,2	678,5	792,8
Amygdalin	PM2A	C-Source	23,0	2,0	863,7	725,5
D-Arabinose	PM2A	C-Source	3,9	0,5	1723,8	2437,8
D-Arabitol	PM2A	C-Source	9,4	0,8	91,7	129,7
L-Arabitol	PM2A	C-Source	9,7	3,6	374,0	528,8
Arbutin	PM2A	C-Source	19,5	0,8	6278,0	2453,0
2-Deoxy-D-Ribose	PM2A	C-Source	6,8	2,0	2489,6	1520,8
i-Erythritol	PM2A	C-Source	16,0	6,8	679,0	960,2
D-Fucose	PM2A	C-Source	7,9	4,2	1012,0	167,1
3-0-?-D-Galactopyranosyl-D-Arabinose	PM2A	C-Source	10,9	13,8	1609,3	2275,9
Gentiobiose	PM2A	C-Source	31,1	0,9	681,0	317,7
L-Glucose	PM2A	C-Source	0,0	0,0	164,8	57,4
D-Lactitol	PM2A	C-Source	0,0	0,0	1507,6	2132,0
D-Melezitose	PM2A	C-Source	15,3	8,8	986,5	1395,1
Maltitol	PM2A	C-Source	1,8	1,3	29,7	41,9
a-Methyl-D-Glucoside	PM2A	C-Source	0,7	1,0	120,2	169,9
b-Methyl-D-Galactoside	PM2A	C-Source	3,1	4,4	846,8	151,0
3-Methylglucose	PM2A	C-Source	3,5	3,1	259,5	367,0
b-Methyl-D-Glucuronic Acid	PM2A	C-Source	0,0	0,0	544,7	168,0
a-Methyl-D-Mannoside	PM2A	C-Source	3,3	4,6	114,5	162,0
b-Methyl-D-Xyloside	PM2A	C-Source	0,2	0,2	418,5	301,5
Palatinose	PM2A	C-Source	28,5	9,7	563,3	355,7
D-Raffinose	PM2A	C-Source	41,8	4,0	441,1	623,8
Salicin	PM2A	C-Source	14,4	0,6	1491,8	14,8
Sedoheptulosan	PM2A	C-Source	2,7	3,9	733,8	305,2
L-Sorbose	PM2A	C-Source	9,7	1,7	328,0	70,4
Stachyose	PM2A	C-Source	44,5	4,1	121,7	172,1
D-Tagatose	PM2A	C-Source	2,1	2,9	242,6	47,7
Turanose	PM2A	C-Source	14,5	0,8	220,5	154,0
Xylitol	PM2A	C-Source	8,3	2,6	217,2	307,1
N-Acetyl-D-glucosaminitol	PM2A	C-Source	0,0	0,0	1052,6	604,2
g-Amino-N-Butyric Acid	PM2A	C-Source	11,8	1,7	967,2	87,6
d-Amino Valeric Acid	PM2A	C-Source	1,9	0,4	700,2	151,1
Sodium butyrate	PM2A	C-Source	1,1	1,5	93,9	132,8
Capric Acid	PM2A	C-Source	0,0	0,0	1257,7	156,9
Caproic Acid	PM2A	C-Source	7,7	1,7	1,4	2,0
Citraconic Acid	PM2A	C-Source	2,6	3,7	445,0	629,3
D,L-Citramalic Acid	PM2A	C-Source	1,0	1,3	251,2	84,8
D-Glucosamine	PM2A	C-Source	19,1	9,1	2432,1	1204,5
2-Hydroxybenzoic acid	PM2A	C-Source	19,3	3,2	102,0	144,3
4-Hydroxybenzoic Acid	PM2A	C-Source	10,3	0,3	7,1	10,1

b-Hydroxybutyric Acid	PM2A	C-Source	0,0	0,0	144,6	204,5
g-Hydroxybutyric Acid	PM2A	C-Source	2,8	2,2	242,7	110,8
2-Oxovaleric acid	PM2A	C-Source	0,0	0,0	38,5	54,4
Itaconic Acid	PM2A	C-Source	0,6	0,8	352,1	498,0
5-Keto-D-Gluconic Acid	PM2A	C-Source	0,0	0,0	701,9	992,7
D-Lactic Acid Methyl Ester	PM2A	C-Source	0,6	0,7	185,4	262,2
Malonic Acid	PM2A	C-Source	0,0	0,0	560,5	163,8
Melibionic Acid	PM2A	C-Source	0,5	0,7	318,3	450,1
Oxalic Acid	PM2A	C-Source	0,1	0,1	93,2	131,7
Oxalomalic Acid	PM2A	C-Source	0,4	0,6	983,8	169,0
Quinic Acid	PM2A	C-Source	9,7	0,7	1219,6	1724,8
D-Ribono-1,4-Lactone	PM2A	C-Source	0,0	0,0	6,1	8,6
Sebacic Acid	PM2A	C-Source	7,7	2,8	368,1	520,6
Sorbic Acid	PM2A	C-Source	5,0	7,0	1370,2	1382,8
Succinamic Acid	PM2A	C-Source	1,3	1,8	99,7	141,0
D-Tartaric Acid	PM2A	C-Source	0,1	0,2	545,4	771,3
L-Tartaric Acid	PM2A	C-Source	1,6	2,3	689,6	246,0
Acetamide	PM2A	C-Source	0,0	0,0	94,2	133,1
L-Alaninamide	PM2A	C-Source	0,0	0,0	72,2	102,0
N-Acetyl-L-Glutamic Acid	PM2A	C-Source	0,0	0,0	0,0	0,0
L-Arginine	PM2A	C-Source	7,1	1,2	1721,5	68,7
Glycine	PM2A	C-Source	1,5	1,8	0,0	0,0
L-Histidine	PM2A	C-Source	1,8	0,4	1018,9	95,5
L-Homoserine	PM2A	C-Source	0,4	0,5	853,6	1207,1
Hydroxy-L-Proline	PM2A	C-Source	0,0	0,0	784,2	304,2
L-Isoleucine	PM2A	C-Source	0,0	0,0	543,6	768,8
L-Leucine	PM2A	C-Source	0,0	0,0	179,5	201,2
L-Lysine	PM2A	C-Source	0,0	0,0	176,9	250,2
L-Methionine	PM2A	C-Source	0,0	0,0	155,2	219,4
L-Ornithine	PM2A	C-Source	5,5	0,9	0,5	0,7
L-Phenylalanine	PM2A	C-Source	3,2	0,3	148,0	209,3
L-Pyroglutamic Acid	PM2A	C-Source	5,2	2,1	1442,0	370,7
L-Valine	PM2A	C-Source	0,0	0,0	256,2	362,3
D,L-Carnitine	PM2A	C-Source	0,0	0,0	97,4	137,7
Sec-Butylamine	PM2A	C-Source	0,2	0,3	287,3	406,2
D,L-Octopamine	PM2A	C-Source	0,0	0,0	567,4	802,4
Putrescine	PM2A	C-Source	2,9	2,0	116,5	164,8
Dihydroxyacetone	PM2A	C-Source	5,3	1,5	4602,8	245,0
2,3-Butanediol	PM2A	C-Source	0,0	0,0	520,2	735,6
2,3-Butanone	PM2A	C-Source	0,3	0,5	299,6	423,7
3-Hydroxy 2-Butanone	PM2A	C-Source	0,0	0,0	805,7	903,4
Negative Control	PM3B	N-Source	0,0	N/A	0	N/A
Ammonia	PM3B	N-Source	21,5	N/A	0	N/A
Nitrite	PM3B	N-Source	33,7	N/A	0	N/A
Nitrate	PM3B	N-Source	42,2	N/A	0	N/A
Urea	PM3B	N-Source	61,6	N/A	362,3	N/A
Biuret	PM3B	N-Source	0,0	N/A	0	N/A
L-Alanine	PM3B	N-Source	58,7	N/A	0	N/A
L-Arginine	PM3B	N-Source	60,3	N/A	643,1	N/A
L-Asparagine	PM3B	N-Source	58,7	N/A	1008,05	N/A
L-Aspartic Acid	PM3B	N-Source	45,5	N/A	0	N/A
L-Cysteine	PM3B	N-Source	17,3	N/A	165,4	N/A

L-Glutamic Acid	PM3B	N-Source	48,1	N/A	567,95	N/A
L-Glutamine	PM3B	N-Source	56,9	N/A	0	N/A
Glycine	PM3B	N-Source	71,3	N/A	0	N/A
L-Histidine	PM3B	N-Source	33,2	N/A	427,35	N/A
L-Isoleucine	PM3B	N-Source	18,5	N/A	0	N/A
L-Leucine	PM3B	N-Source	22,8	N/A	0	N/A
L-Lysine	PM3B	N-Source	5,9	N/A	0	N/A
L-Methionine	PM3B	N-Source	61,9	N/A	0	N/A
L-Phenylalanine	PM3B	N-Source	22,9	N/A	322,55	N/A
L-Proline	PM3B	N-Source	37,3	N/A	0	N/A
L-Serine	PM3B	N-Source	43,4	N/A	218	N/A
L-Threonine	PM3B	N-Source	55,8	N/A	420,25	N/A
L-Tryptophan	PM3B	N-Source	39,2	N/A	1882,05	N/A
L-Tyrosine	PM3B	N-Source	0,0	N/A	544,85	N/A
L-Valine	PM3B	N-Source	38,1	N/A	0	N/A
D-Alanine	PM3B	N-Source	17,3	N/A	0	N/A
D-Asparagine	PM3B	N-Source	27,8	N/A	21,3	N/A
D-Aspartic Acid	PM3B	N-Source	2,8	N/A	137,2	N/A
D-Glutamic Acid	PM3B	N-Source	0,0	N/A	606,25	N/A
D-Lysine	PM3B	N-Source	9,3	N/A	0	N/A
D-Serine	PM3B	N-Source	0,0	N/A	0	N/A
D-Valine	PM3B	N-Source	0,1	N/A	0	N/A
L-Citrulline	PM3B	N-Source	45,5	N/A	365,15	N/A
L-Homoserine	PM3B	N-Source	23,3	N/A	0	N/A
L-Ornithine	PM3B	N-Source	83,4	N/A	0	N/A
N-Acetyl-L-Glutamic Acid	PM3B	N-Source	7,4	N/A	0	N/A
N-Phthaloyl-L-Glutamic Acid	PM3B	N-Source	7,4	N/A	0	N/A
L-Pyroglutamic Acid	PM3B	N-Source	58,0	N/A	0	N/A
Hydroxylamine	PM3B	N-Source	0,0	N/A	292,2	N/A
Methylamine	PM3B	N-Source	73,7	N/A	0	N/A
N-Amylamine	PM3B	N-Source	12,9	N/A	0	N/A
N-Butylamine	PM3B	N-Source	20,3	N/A	0	N/A
Ethylamine	PM3B	N-Source	15,1	N/A	0	N/A
Ethanolamine	PM3B	N-Source	40,9	N/A	0	N/A
Ethylenediamine	PM3B	N-Source	6,7	N/A	0	N/A
Putrescine	PM3B	N-Source	32,0	N/A	0	N/A
Agmatine	PM3B	N-Source	45,0	N/A	538,8	N/A
Histamine	PM3B	N-Source	12,5	N/A	0	N/A
b-Phenylethylamine	PM3B	N-Source	41,0	N/A	68,35	N/A
Tyramine	PM3B	N-Source	36,0	N/A	1272,9	N/A
Acetamide	PM3B	N-Source	8,6	N/A	0	N/A
Formamide	PM3B	N-Source	0,0	N/A	0	N/A
Glucuronamide	PM3B	N-Source	6,7	N/A	0	N/A
D,L-Lactamide	PM3B	N-Source	9,8	N/A	98,85	N/A
D-Glucosamine	PM3B	N-Source	23,3	N/A	0	N/A
D-Galactosamine	PM3B	N-Source	1,9	N/A	0	N/A
D-Mannosamine	PM3B	N-Source	8,0	N/A	5,75	N/A
N-Acetyl-D-Glucosamine	PM3B	N-Source	68,1	N/A	835,2	N/A
N-Acetyl-D-Galactosamine	PM3B	N-Source	0,0	N/A	0	N/A
N-Acetyl-D-Mannosamine	PM3B	N-Source	0,0	N/A	0	N/A
Adenine	PM3B	N-Source	33,4	N/A	0	N/A
Adenosine	PM3B	N-Source	76,8	N/A	0	N/A

Cytidine	PM3B	N-Source	12,7	N/A	0	N/A
Cytosine	PM3B	N-Source	37,9	N/A	0	N/A
Guanine	PM3B	N-Source	42,6	N/A	0	N/A
Guanosine	PM3B	N-Source	26,2	N/A	0	N/A
Thymine	PM3B	N-Source	0,0	N/A	0	N/A
Thymidine	PM3B	N-Source	0,0	N/A	0	N/A
Uracil	PM3B	N-Source	26,6	N/A	0	N/A
Uridine	PM3B	N-Source	6,2	N/A	561,5	N/A
Inosine	PM3B	N-Source	88,6	N/A	0	N/A
Xanthine	PM3B	N-Source	35,4	N/A	0	N/A
Xanthosine	PM3B	N-Source	12,1	N/A	0	N/A
Uric Acid	PM3B	N-Source	90,7	N/A	0	N/A
Alloxan	PM3B	N-Source	1,0	N/A	0	N/A
Allantoin	PM3B	N-Source	43,1	N/A	0	N/A
Parabanic Acid	PM3B	N-Source	17,1	N/A	0	N/A
D,L-a-Amino-N-Butyric Acid	PM3B	N-Source	23,4	N/A	0	N/A
g-Amino-N-Butyric Acid	PM3B	N-Source	60,2	N/A	0	N/A
e-Amino-N-Caproic Acid	PM3B	N-Source	13,0	N/A	883,6	N/A
D,L-a-Amino-Caprylic Acid	PM3B	N-Source	0,0	N/A	54,1	N/A
d-Amino-N-Valeric Acid	PM3B	N-Source	24,4	N/A	101,35	N/A
a-Amino-N-Valeric Acid	PM3B	N-Source	25,5	N/A	877,75	N/A
Ala-Asp	PM3B	N-Source	81,2	N/A	0	N/A
Ala-Gln	PM3B	N-Source	112,4	N/A	0	N/A
Ala-Glu	PM3B	N-Source	68,8	N/A	0	N/A
Ala-Gly	PM3B	N-Source	73,0	N/A	0	N/A
Ala-His	PM3B	N-Source	12,4	N/A	977,95	N/A
Ala-Leu	PM3B	N-Source	34,6	N/A	974,1	N/A
Ala-Thr	PM3B	N-Source	58,9	N/A	60,5	N/A
Gly-Asn	PM3B	N-Source	55,9	N/A	812,1	N/A
Gly-Gln	PM3B	N-Source	52,9	N/A	0	N/A
Gly-Glu	PM3B	N-Source	29,5	N/A	0	N/A
Gly-Met	PM3B	N-Source	51,9	N/A	0	N/A
Met-Ala	PM3B	N-Source	78,8	N/A	0	N/A
Negative Control	PM4A	P-Source	0,0	0,0	0,0	0,0
Phosphate	PM4A	P-Source	15,5	10,6	0,0	0,0
Pyrophosphate	PM4A	P-Source	0,1	0,2	609,4	861,9
Trimetaphosphate	PM4A	P-Source	14,7	4,8	1119,2	382,0
Tripolyphosphate	PM4A	P-Source	14,6	20,6	1022,2	1445,5
Triethyl Phosphate	PM4A	P-Source	0,0	0,0	0,0	0,0
Hypophosphite	PM4A	P-Source	0,0	0,0	287,6	174,7
Adenosine 2'-Monophosphate	PM4A	P-Source	15,0	10,3	877,7	1241,3
Adenosine 3'-Monophosphate	PM4A	P-Source	19,2	0,9	0,0	0,0
Adenosine 5'-Monophosphate	PM4A	P-Source	9,5	13,4	0,0	0,0
Adenosine 2',3'-Cyclic Monophosphate	PM4A	P-Source	21,6	0,5	0,0	0,0
Adenosine 3',5'-Cyclic Monophosphate	PM4A	P-Source	25,4	8,9	0,0	0,0
Thiophosphate	PM4A	P-Source	23,3	11,0	0,0	0,0
Dithiophosphate	PM4A	P-Source	26,5	12,6	185,7	262,7
D,L-a-Glycerol Phosphate	PM4A	P-Source	7,1	7,8	936,9	1324,9
b-Glycerol Phosphate	PM4A	P-Source	6,2	8,7	0,0	0,0
Carbamyl Phosphate	PM4A	P-Source	13,5	4,1	337,4	477,2

D-2-Phospho-Glyceric Acid	PM4A	P-Source	16,1	7,4	92,2	130,4
D-3-Phospho-Glyceric Acid	PM4A	P-Source	45,6	4,8	0,0	0,0
Guanosine 2'-Monophosphate	PM4A	P-Source	12,1	4,0	0,0	0,0
Guanosine 3'-Monophosphate	PM4A	P-Source	22,2	5,6	0,0	0,0
Guanosine 5'-Monophosphate	PM4A	P-Source	11,4	1,1	660,4	495,0
Guanosine 2',3'-Cyclic Monophosphate	PM4A	P-Source	20,2	1,6	464,0	1,7
Guanosine 3',5'-Cyclic Monophosphate	PM4A	P-Source	23,4	3,4	901,6	558,9
Phosphoenol Pyruvate	PM4A	P-Source	16,0	18,7	92,9	131,3
Phospho-Glycolic Acid	PM4A	P-Source	11,0	2,2	0,0	0,0
D-Glucose-1-Phosphate	PM4A	P-Source	14,6	10,6	647,0	915,0
D-Glucose-6-Phosphate	PM4A	P-Source	0,0	0,0	0,0	0,0
2-Deoxy-D-Glucose 6-Phosphate	PM4A	P-Source	0,0	0,0	239,9	339,3
D-Glucosamine-6-Phosphate	PM4A	P-Source	45,0	2,9	166,9	236,0
6-Phospho-Gluconic Acid	PM4A	P-Source	20,3	12,8	0,0	0,0
Cytidine 2'-Monophosphate	PM4A	P-Source	13,2	5,0	675,7	955,5
Cytidine 3'-Monophosphate	PM4A	P-Source	11,6	12,0	333,3	471,4
Cytidine 5'-Monophosphate	PM4A	P-Source	13,0	7,3	0,0	0,0
Cytidine 2',3'-Cyclic Monophosphate	PM4A	P-Source	12,3	17,4	475,6	672,6
Cytidine 3',5'-Cyclic Monophosphate	PM4A	P-Source	20,8	9,0	111,3	157,4
D-Mannose-1-Phosphate	PM4A	P-Source	4,4	6,2	462,0	144,7
D-Mannose-6-Phosphate	PM4A	P-Source	9,6	13,5	741,6	1048,8
Cysteamine-S-Phosphate	PM4A	P-Source	21,2	17,3	323,5	457,4
Phospho-L-Arginine	PM4A	P-Source	21,1	9,7	524,0	110,6
O-Phospho-D-Serine	PM4A	P-Source	0,7	1,0	806,6	1140,7
O-Phospho-L-Serine	PM4A	P-Source	40,9	25,0	287,0	405,9
O-Phospho-L-Threonine	PM4A	P-Source	31,3	2,4	176,9	250,1
Uridine 2'-Monophosphate	PM4A	P-Source	19,6	27,8	196,6	278,0
Uridine 3'-Monophosphate	PM4A	P-Source	17,7	1,5	412,8	583,8
Uridine 5'-Monophosphate	PM4A	P-Source	5,0	7,1	519,6	95,0
Uridine 2',3'-Cyclic Monophosphate	PM4A	P-Source	11,8	0,3	610,5	863,4
Uridine 3',5'-Cyclic Monophosphate	PM4A	P-Source	10,9	10,2	1146,7	671,2
O-Phospho-D-Tyrosine	PM4A	P-Source	12,3	3,3	163,7	54,4
O-Phospho-L-Tyrosine	PM4A	P-Source	5,1	7,3	0,0	0,0
Phosphocreatine	PM4A	P-Source	10,5	11,3	779,9	1102,9
Phosphoryl Choline	PM4A	P-Source	22,2	7,5	449,1	306,7
O-Phosphoryl-Ethanolamine	PM4A	P-Source	14,1	9,1	0,0	0,0
Phosphono Acetic Acid	PM4A	P-Source	3,4	4,9	362,6	512,7
2-Aminoethyl Phosphonic Acid	PM4A	P-Source	6,2	7,0	93,9	132,7
Methylene Diphosphonic Acid	PM4A	P-Source	1,9	2,7	0,0	0,0
Thymidine 3'-Monophosphate	PM4A	P-Source	17,7	8,7	251,8	356,1
Thymidine 5'-Monophosphate	PM4A	P-Source	41,2	5,5	0,0	0,0
Inositol Hexaphosphate	PM4A	P-Source	3,6	3,7	327,0	266,9
Thymidine 3',5'-Cyclic Monophosphate	PM4A	P-Source	20,0	4,7	26,1	36,9
Negative Control	PM4A	S-Source	21,8	1,4	511,6	472,7
Sulfate	PM4A	S-Source	13,2	8,3	0,0	0,0
Thiosulfate	PM4A	S-Source	25,7	15,6	378,0	534,5
Tetrathionate	PM4A	S-Source	15,9	11,9	361,6	511,4
Thiophosphate	PM4A	S-Source	27,6	24,4	547,2	96,5
Dithiophosphate	PM4A	S-Source	13,1	6,0	295,8	418,3

L-Cysteine	PM4A	S-Source	20,4	7,9	847,3	1198,2
D-Cysteine	PM4A	S-Source	12,9	2,3	488,8	691,3
Cys-Gly	PM4A	S-Source	19,5	12,9	451,7	613,2
L-Cysteic Acid	PM4A	S-Source	9,7	3,7	0,0	0,0
Cysteamine	PM4A	S-Source	11,3	12,8	0,0	0,0
L-Cysteine Sulfinic Acid	PM4A	S-Source	22,8	7,4	432,0	611,0
N-Acetyl-L-Cysteine	PM4A	S-Source	20,0	7,6	373,2	527,7
S-Methyl-L-Cysteine	PM4A	S-Source	26,9	20,2	150,4	212,7
Cystathionine	PM4A	S-Source	32,1	11,3	290,6	410,9
Lanthionine	PM4A	S-Source	14,7	5,5	296,6	419,5
Glutathione	PM4A	S-Source	20,9	11,5	48,6	68,7
D,L-Ethionine	PM4A	S-Source	5,9	7,4	1163,9	135,0
L-Methionine	PM4A	S-Source	26,8	19,7	0,0	0,0
D-Methionine	PM4A	S-Source	14,3	10,9	344,2	486,7
Gly-Met	PM4A	S-Source	28,6	10,2	245,6	347,4
N-Acetyl-D,L-Methionine	PM4A	S-Source	33,3	15,8	449,1	635,2
L-Methionine Sulfoxide	PM4A	S-Source	19,8	2,0	35,1	49,6
L-Methionine Sulfone	PM4A	S-Source	16,6	6,3	0,0	0,0
L-Djenkolic Acid	PM4A	S-Source	14,5	4,1	1179,0	1598,5
Thiourea	PM4A	S-Source	32,7	19,4	363,4	201,7
1-Thio-b-D-Glucose	PM4A	S-Source	32,4	7,9	423,2	598,4
D,L-Lipoamide	PM4A	S-Source	16,4	6,6	729,7	1032,0
Taurocholic Acid	PM4A	S-Source	17,1	2,9	34,2	48,4
Taurine	PM4A	S-Source	20,3	8,0	206,8	292,5
Hypotaurine	PM4A	S-Source	24,3	4,9	391,5	440,7
p-Aminobenzene Sulfonic Acid	PM4A	S-Source	19,0	0,6	262,6	371,4
Butane Sulfonic Acid	PM4A	S-Source	26,8	13,0	888,8	1256,9
2-Hydroxyethane Sulfonic Acid	PM4A	S-Source	21,6	6,8	745,8	2,9
Methane Sulfonic Acid	PM4A	S-Source	24,1	7,1	0,0	0,0
Tetramethylene Sulfone	PM4A	S-Source	27,4	0,8	544,9	770,6
1% NaCl	PM9	osmotic sensitivity	264,4	7,4	2006,0	79,9
2% NaCl	PM9	osmotic sensitivity	246,6	3,6	4066,3	314,1
3% NaCl	PM9	osmotic sensitivity	204,6	52,3	2710,4	691,7
4% NaCl	PM9	osmotic sensitivity	200,0	24,8	3971,8	3293,5
5% NaCl	PM9	osmotic sensitivity	204,3	15,6	6523,2	1196,9
5.5% NaCl	PM9	osmotic sensitivity	193,7	1,2	6283,4	4098,3
6% NaCl	PM9	osmotic sensitivity	181,8	37,6	3874,9	1994,9
6.5% NaCl	PM9	osmotic sensitivity	195,8	7,4	5639,4	666,2
7% NaCl	PM9	osmotic sensitivity	190,9	1,8	7805,4	3879,6
8% NaCl	PM9	osmotic sensitivity	179,4	5,8	11371,8	471,1
9% NaCl	PM9	osmotic sensitivity	172,7	3,7	13814,8	4118,1
10% NaCl	PM9	osmotic	161,9	11,3	10377,5	9387,4

		sensitivity				
6% NaCl	PM9	osmotic sensitivity	181,4	32,8	4025,8	1000,6
6% NaCl + Betaine	PM9	osmolyte	202,5	9,2	5548,0	171,1
6% NaCl + N-N Dimethyl glycine	PM9	osmolyte	200,0	2,8	5997,2	1603,4
6% NaCl + Sarcosine	PM9	osmolyte	179,8	5,4	9502,2	5327,2
6% NaCl + Dimethyl sulphonyl propionate	PM9	osmolyte	202,4	3,3	9281,6	181,3
6% NaCl + MOPS	PM9	osmolyte	188,7	28,8	3084,2	1671,1
6% NaCl + Ectoine	PM9	osmolyte	205,3	5,8	5210,3	595,5
6% NaCl + Choline	PM9	osmolyte	201,5	0,6	5511,6	1184,4
6% NaCl + Phosphorylcholine	PM9	osmolyte	202,9	7,2	6167,1	307,3
6% NaCl + Creatine	PM9	osmolyte	196,1	4,4	3374,9	2876,8
6% NaCl + Creatinine	PM9	osmolyte	206,8	1,5	5072,6	1167,1
6% NaCl + L-Carnitine	PM9	osmolyte	217,4	4,7	2082,0	1318,8
6% NaCl + KCl	PM9	osmolyte	210,4	5,4	5228,9	2114,6
6% NaCl + L-Proline	PM9	osmolyte	211,1	8,5	4969,7	2509,7
6% NaCl + N-Acetyl-L-glutamine	PM9	osmolyte	200,9	4,1	3583,6	3167,7
6% NaCl + ?-Glutamic acid	PM9	osmolyte	162,3	68,9	5699,8	636,4
6% NaCl + ?–Amino-N-butyric acid	PM9	osmolyte	176,2	47,4	3713,0	3956,7
6% NaCl + Glutathione	PM9	osmolyte	216,2	10,1	6295,5	2836,7
6% NaCl + Glycerol	PM9	osmolyte	183,6	42,6	2987,8	2582,8
6% NaCl + Trehalose	PM9	osmolyte	208,2	7,2	4725,3	1463,9
6% NaCl + Trimethylamine-N-oxide	PM9	osmolyte	211,4	1,7	5301,9	1291,3
6% NaCl + Trimethylamine	PM9	osmolyte	164,9	48,2	3630,4	4409,2
6% NaCl + Octopine	PM9	osmolyte	200,8	5,9	6433,5	1729,9
6% NaCl + Trigonelline	PM9	osmolyte	217,1	6,4	4570,1	4354,4
3% Potassium Chloride	PM9	osmotic sensitivity	240,5	6,7	5631,8	739,0
4% Potassium Chloride	PM9	osmotic sensitivity	234,5	4,3	4727,3	719,3
5% Potassium Chloride	PM9	osmotic sensitivity	222,1	9,4	5625,0	1191,8
6% Potassium Chloride	PM9	osmotic sensitivity	206,8	0,1	4771,9	400,3
2% Sodium Sulfate	PM9	osmotic sensitivity	266,7	5,9	2967,5	574,1
3% Sodium Sulfate	PM9	osmotic sensitivity	253,4	11,3	2055,4	850,9
4% Sodium Sulfate	PM9	osmotic sensitivity	243,5	2,4	3121,7	532,4
5% Sodium Sulfate	PM9	osmotic sensitivity	223,6	3,0	4624,2	1643,3
5% Ethylene Glycol	PM9	osmotic sensitivity	266,6	5,5	2239,6	1555,4
10% Ethylene Glycol	PM9	osmotic sensitivity	267,9	6,0	2278,5	1684,5
15% Ethylene Glycol	PM9	osmotic sensitivity	253,4	32,4	898,1	1228,5
20% Ethylene Glycol	PM9	osmotic sensitivity	243,9	18,7	513,2	725,7
1% Sodium Formate	PM9	osmotic sensitivity	285,9	0,4	12346,6	2060,2

2% Sodium Formate	PM9	osmotic sensitivity	245,6	20,6	5017,0	1161,1
3% Sodium Formate	PM9	osmotic sensitivity	208,9	2,1	3024,3	1165,7
4% Sodium Formate	PM9	osmotic sensitivity	178,1	4,9	4764,9	1037,2
5% Sodium Formate	PM9	osmotic sensitivity	159,0	5,8	5143,7	832,9
6% Sodium Formate	PM9	osmotic sensitivity	147,4	1,9	5091,8	1259,7
2% Urea	PM9	osmotic sensitivity	299,7	3,2	1036,9	195,1
3% Urea	PM9	osmotic sensitivity	287,9	0,2	2334,3	1570,3
4% Urea	PM9	osmotic sensitivity	268,3	2,1	5798,5	1652,2
5% Urea	PM9	osmotic sensitivity	250,1	7,2	5625,4	631,9
6% Urea	PM9	osmotic sensitivity	225,0	13,5	12828,8	9128,8
7% Urea	PM9	osmotic sensitivity	201,8	43,1	15122,2	13273,2
1% Sodium Lactate	PM9	osmotic sensitivity	285,2	2,8	13459,0	4170,6
2% Sodium Lactate	PM9	osmotic sensitivity	266,9	5,5	32607,3	6928,9
3% Sodium Lactate	PM9	osmotic sensitivity	254,2	1,5	34193,1	4335,3
4% Sodium Lactate	PM9	osmotic sensitivity	256,8	1,7	31059,8	5977,2
5% Sodium Lactate	PM9	osmotic sensitivity	232,8	19,9	36908,5	1008,1
6% Sodium Lactate	PM9	osmotic sensitivity	250,3	4,7	33989,6	1030,0
7% Sodium Lactate	PM9	osmotic sensitivity	245,0	3,0	35704,4	7802,4
8% Sodium Lactate	PM9	osmotic sensitivity	251,1	5,0	29775,7	2999,0
9% Sodium Lactate	PM9	osmotic sensitivity	249,0	2,8	33669,6	5301,6
10% Sodium Lactate	PM9	osmotic sensitivity	236,3	0,5	29839,1	834,9
11% Sodium Lactate	PM9	osmotic sensitivity	224,8	20,5	39618,9	3232,0
12% Sodium Lactate	PM9	osmotic sensitivity	238,7	14,2	29764,7	1380,1
20mM Sodium Phosphate pH 7	PM9	toxicity	275,5	3,8	3044,1	50,4
50mM Sodium Phosphate pH 7	PM9	toxicity	267,6	3,7	6880,0	1081,4
100mM Sodium Phosphate pH 7	PM9	toxicity	257,1	1,2	13857,1	1565,8
200mM Sodium Phosphate pH 7	PM9	toxicity	220,9	2,8	17945,7	2974,0
20mM Sodium Benzoate pH 5.2	PM9	toxicity	183,2	6,1	11286,8	2862,6
50mM Sodium Benzoate pH 5.2	PM9	toxicity	0,0	0,0	3791,9	2417,6
100mM Sodium Benzoate pH 5.2	PM9	toxicity	0,0	0,0	3582,9	2093,6
200mM Sodium Benzoate pH 5.2	PM9	toxicity	0,1	0,2	2906,0	2203,2

10mM Ammonium Sulfate pH 8	PM9	toxicity	257,3	5,6	619,0	401,8
20mM Ammonium Sulfate pH 8	PM9	toxicity	259,6	7,4	228,5	243,4
50mM Ammonium Sulfate pH 8	PM9	toxicity	265,5	2,3	1194,4	272,8
100mM Ammonium Sulfate pH 8	PM9	toxicity	262,8	3,5	782,4	280,8
10mM Sodium Nitrate	PM9	toxicity	278,4	12,2	950,6	143,1
20mM Sodium Nitrate	PM9	toxicity	278,9	3,6	3269,2	992,9
40mM Sodium Nitrate	PM9	toxicity	274,3	1,0	3871,3	99,1
60mM Sodium Nitrate	PM9	toxicity	270,7	6,9	3243,9	133,5
80mM Sodium Nitrate	PM9	toxicity	274,0	1,2	4994,1	1148,4
100mM Sodium Nitrate	PM9	toxicity	265,3	5,3	3472,5	2146,8
10mM Sodium Nitrite	PM9	toxicity	209,0	0,2	3025,2	125,1
20mM Sodium Nitrite	PM9	toxicity	103,6	10,4	8829,8	208,3
40mM Sodium Nitrite	PM9	toxicity	12,6	2,6	5641,9	640,1
60mM Sodium Nitrite	PM9	toxicity	28,8	16,8	1393,1	1610,5
80mM Sodium Nitrite	PM9	toxicity	22,5	0,0	1239,4	222,5
100mM Sodium Nitrite	PM9	toxicity	34,2	12,3	435,1	36,6